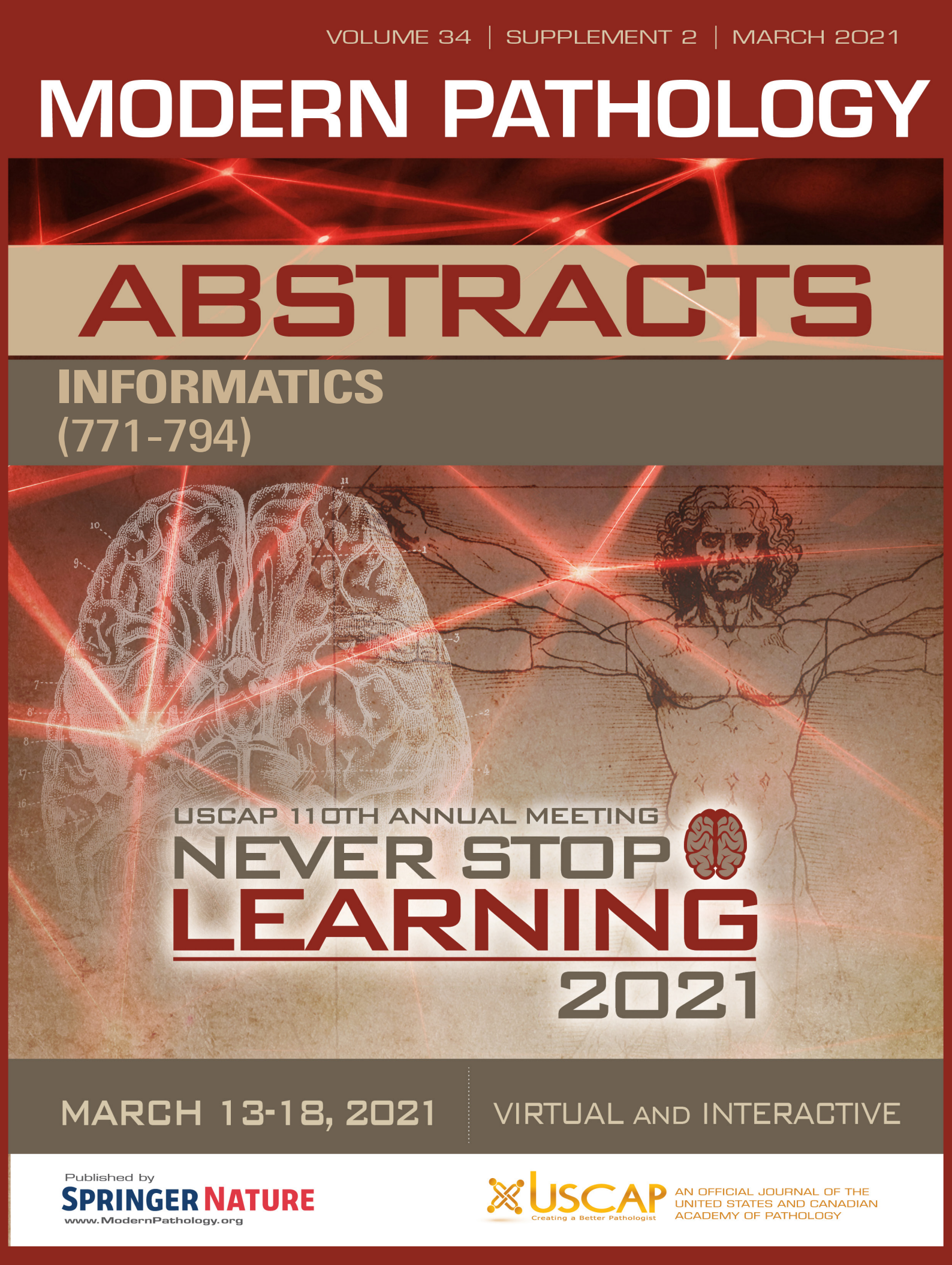# ABSTRACTS

## GASTROINTESTINAL PATHOLOGY (311-404)

USCAP 110TH ANNUAL MEETING

NEVER STOP
LEARNING
2021

MARCH 13-18, 2021 | VIRTUAL AND INTERACTIVE

## EDUCATION COMMITTEE

## ABSTRACT REVIEW BOARD

## 311 Histology of Distal Esophageal and Gastroesophageal Junction Adenocarcinomas Correlate with Overexpression of HER2/neu

Ashna Aggarwal[1], Deyali Chatterjee[2]
[1]Barnes-Jewish Hospital/Washington University, St. Louis, MO, [2]Washington University in St. Louis, St. Louis, MO

**Disclosures:** Ashna Aggarwal: None; Deyali Chatterjee: None

**Background:** Biomarkers currently used to guide targeted therapy in advanced gastric and esophageal carcinomas include HER2, MMR, and PD-L1. Recent studies have shown the association of HER2 non-expression with signet ring cell morphology in gastric and gastroesophageal junction adenocarcinomas. The purpose of our study is to systematically evaluate the histology of distal esophageal and gastroesophageal junction (GEJ) adenocarcinomas and correlate with the expression of these pertinent biomarkers.

**Design:** All available archival biopsy slides of distal esophageal and GEJ adenocarcinomas diagnosed at our institution is reviewed, which have a complete workup for HER-2, MMR, and PD-L1 already performed. Histologic subtype was correlated with expression of these biomarkers using standard statistical software (2 tailed z-score test for two population proportions).

**Results:** A total of 88 adenocarcinomas were available for review. Tumors were categorized into the following subtypes: Intestinal (tubular, papillary, or tubulopapillary) = 53 cases; poorly cohesive, non-signet ring cell type = 14 cases; mixed signet ring and non- signet ring cell type = 4 cases; pure signet ring cell type (invariably associated with extracellular pools of mucin) = 3 cases; poorly cohesive carcinoma with lymphoid stroma = 1 case, mixed intestinal and poorly cohesive carcinoma = 6 cases, and intestinal with mucinous features = 7 cases.

HER2 overexpression was noted in 39.6% (21/53 cases) of intestinal subtype irrespective of tumor differentiation, but were not expressed in any of the other histologic subtypes, including tumors showing intestinal differentiation, but with a mucinous component. There was no statistical difference between the groups in terms of MMR expression (p=0.24) or PD-L1 expression (p=0.98).

**Conclusions:** The histology of distal esophageal and GEJ adenocarcinomas correlate with HER2 overexpression. In particular, no cases of poorly cohesive (signet ring cell type as well as non-signet ring type) or mucinous adenocarcinomas show HER2 overexpression in our cohort. Tumor morphology does not correlate with MMR or PD-L1 expression.

## 312 The Histopathologic Characteristics of the Gastrointestinal System in SARS-CoV-2 Infected Patients Who Underwent Biopsy or Resection

Sunjida Ahmed[1], Deepthi Hoskoppal[2], Lawrence Lin[1], Yvelisse Suarez[3], Weiguo Liu, Margaret Cho[1], Kristen Thomas[1], Melissa Guzzetta[4], Cristina Hajdu[5], Neil Theise[6], George Jour[7], Suparna Sarkar[1], Wenqing (Wendy) Cao[1]
[1]NYU Langone Health, New York, NY, [2]New York University Langone Medical Center, New York, NY, [3]NYU Medical Center, New York, NY, [4]NYU Langone Health, Westfield, [5]New York University School of Medicine, New York, NY, [6]NYU Grossman School of Medicine, New York, NY, [7]New York University, New York, NY

**Disclosures:** Sunjida Ahmed: None; Deepthi Hoskoppal: None; Lawrence Lin: None; Yvelisse Suarez: None; Weiguo Liu: None; Margaret Cho: None; Kristen Thomas: None; Melissa Guzzetta: None; Neil Theise: None; George Jour: None; Suparna Sarkar: None; Wenqing (Wendy) Cao: None

**Background:** In addition to respiratory distress, GI symptoms have been reported in COVID-19 patients at various stages of the disease. Among the GI symptoms that have been reported, diarrhea, nausea, vomiting, abdominal pain and GI bleeding were often seen. Age and comorbid conditions such as obesity, HTN, DM and/or CAD have been considered as risk factors for COVID-19 patients for severe disease. GI manifestations in COVID-19 patients appeared to act as a sign for a serious condition. The virus has been identified in the stool and in rectal swabs of

some infected patients, even after a negative nasopharyngeal test. There is a lack of reports on pathological alterations of the GI tract in COVID-19 infected patients.

**Design:** 16 PCR confirmed COVID-19 patients (11 males and 5 females) were included in the study. Biopsy or resection specimens were taken from the esophagus (4), stomach (6), small intestine (5), appendix (3), colon (5) and gallbladder (3). Clinical information including demographics, comorbidities, GI symptoms, related laboratory tests were collected. Histopathologic evaluation was performed and correlated with clinical properties.

**Results:** The age of the patients ranged from 10 to 84 years old, with an average of 47 years. Eight (50%) patients had at least one comorbid condition, two patients (12.5%) had prior history of cancer, and six patients had no significant medical history. Abdominal pain and GI bleeding were the most common presenting symptoms. Histologically, acute and chronic inflammation was seen in 14 of 16, and 15 of 16 cases, respectively. Eight cases showed severe acute inflammation with ulceration. The mucosal changes included nonspecific reactive change, hypermucinous, atrophic/ischemic changes, and necrosis, were indiscriminately noticed in these cases. Four cases showed intraepithelial lymphocytosis. Viral like inclusions were found in four cases. Microthrombi were identified in 5 cases with an average patient age of 60 years. Notably, microthrombi were seen in about 5 out of 8 (62%) patients with comorbidities. The patients with microthrombi had a higher D dimer test value than those without thrombus. Three patients died shortly after operation, and two of them showed microthrombi in the tissue specimens.

**Conclusions:** Acute and chronic inflammation were indiscriminately seen in these cases. Microthrombi were dominantly found in aging patients with comorbidities, suggesting microthrombi in the GI tract may be a histologic indication for severe COVID-19 patients with GI symptoms.

---

**313 Microscopic Incidentally Identified Gastrointestinal Malakoplakia During Screening Colonoscopy is Neither Associated with Malignancy or Immunodeficiency**

Ali Aldawood[1], Iván González[1], Andrea Barbieri[2], Dhanpat Jain[3]
[1]Yale New Haven Hospital, New Haven, CT, [2]Yale University, New Haven, CT, [3]Yale School of Medicine, New Haven, CT

**Disclosures:** Ali Aldawood: None; Iván González: None; Andrea Barbieri: None; Dhanpat Jain: None

**Background:** Malakoplakia is a rare inflammatory disease characterized by impaired bactericidal capability of macrophages that leads to accumulation of characteristic intra-cytoplasmic Michaelis-Gutmann (MG) bodies. Gastrointestinal (GI) tract is the second most commonly involved site after genitourinary tract. Prior studies of GI malakoplakia have shown that about 39% are associated with malignancies and 91% with underlying immunodeficiencies We have identified cases of malakoplakia presenting as mucosal polyps as incidental finding during screening coloscopy and goal of this study was to characterize the clinicopathologic features of malakoplakia in such cases.

**Design:** The pathology department archives were retrospectively searched for a diagnosis of malakoplakia in GI tract between 1985-2020. From these cases, malakoplakia diagnosed in colonic biopsies during screening colonoscopy were selected for the study. Hematoxylin and eosin (H&E) stain and special stains (PAS, iron and Von-Kossa) were performed on all cases and reviewed. Medical records were reviewed for clinical information, especially any endoscopic/macroscopic appearance and associated diagnosis.

**Results:** A total of sixteen cases of GI malakoplakia were identified, of which 5 cases met the inclusion criteria. All were women, with mean age of 61 years (range 51-73). All cases showed typical histologic features comprising of aggregation of histiocytes with pinkish, fine granular cytoplasm on H&E slides and presence of round concentric lamellated cytoplasmic calcified body MG bodies (Fig.1). Four of the 5 lesions occurred within benign lymphoid aggregate which showed tiny clusters of plum histiocytes. Smallest lesion measured < 0.3cm within such a lymphoid aggregate (Fig.2). The lesions endoscopically appeared as mucosal polyps (0.3-1.3cm) and were distributed throughout large bowel including cecum, appendiceal orifice and rectum. One patient had *H.pylori* gastritis diagnosed at the same time and presented with dyspepsia. All other patients were asymptomatic. Follow-up was available in all cases range from 1 day to 151 months. One patient developed

squamous cell carcinoma of the uterine cervix after 12 years of the diagnosis of malakoplakia. None of the patients had or developed any associated GI malignancy or immunodeficiency.

Figure 1 - 313
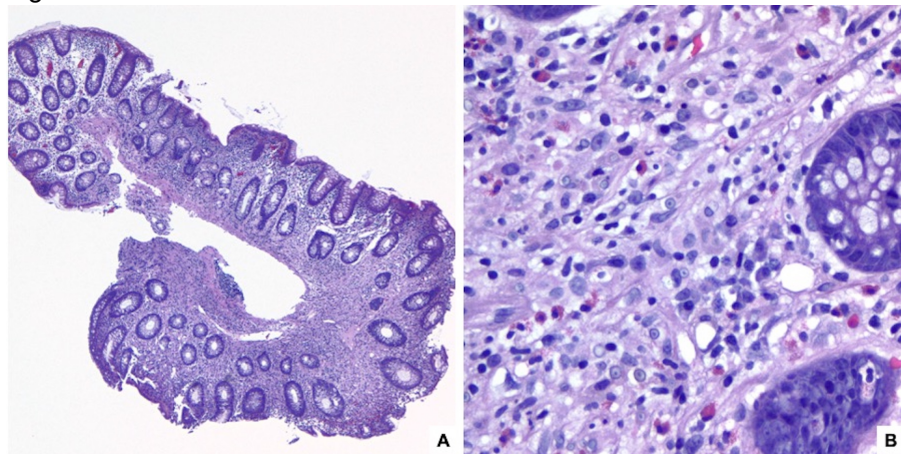


**Fig1.** Colonic crypts distortion with lamina propria histiocytic infiltration, H&E 100x **(a)**. Intracytoplasmic lamellated and targetoid inclusions. H&E 400x magnification **(b)**

Figure 2 - 313
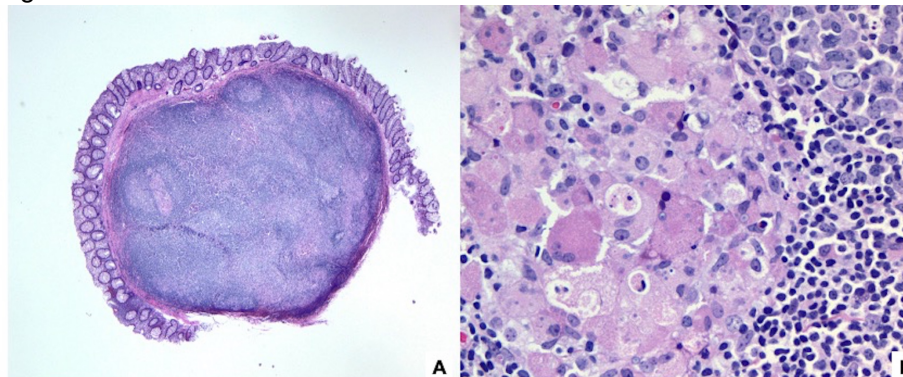


**Fig2.** Appendiceal orifice polyp with submucosal dense lymphoid aggregate with germinal centers and focal aggregate of few histocytes, H&E 100x **(A)**. Histocytes reveal inclusion that are typical of Mikulicz-Gutmann bodies. H&E 400x magnification **(B)**

**Conclusions:** Incidental microscopic GI malakoplakia is occasionally identified during screening colonoscopy and constitutes approximately 1/3rd of all GI malakoplakia. Unlike most cases of GI malakoplakia such cases are very tiny, localized, potentially easily missed and are not associated with any underlying predisposing causes. Association of such lesions with any specific microorganism and long-term consequences need further study.

### 314 Correlation of Unique Histologic Features of Colorectal Adenocarcinoma with Clinical and Molecular Outcomes, an Exploration of the TCGA Dataset

Joshua Anderson[1], Zaid Mahdi[2], Alyssa Krasinskas[1], Brian Robinson[1]
[1]Emory University, Atlanta, GA, [2]Emory University Hospital, Atlanta, GA

**Disclosures:** Joshua Anderson: None; Zaid Mahdi: None; Alyssa Krasinskas: None; Brian Robinson: None

**Background:** With the emergence of molecular oncology, colorectal adenocarcinoma (CRC) is now defined on a molecular level by microsatellite instability status, the presence of CpG island methylator phenotype, and mutations in major driver genes, such as KRAS. CRCs display a wide variety of histologic features and subtypes, yet the connection between these morphologic features and the somatic alterations they are associated with is less clear. The aim of this study is to utilize The Cancer Genome Atlas to determine which unique histologic subtype(s) and/or features of CRC are linked to different clinical or molecular outcomes.

**Design:** Using the TCGA PanCancer Atlas dataset, we analyzed the morphologic features of 462 H&E digital slides. Samples were classified into major subtypes and then assessed for additional features, including extensive necrosis, mucin vacuole formation, cribriform growth, expansile growth, mucinous features, single cell growth, medullary features, rosette, villous features, neuroendocrine features, corded growth, squamoid features, and desmoplasia. Clinical outcomes and DNA mutational data were correlated with histologic findings.

**Results:** Five major histologic subtypes including solid (38 cases), mucinous (36 cases), villous (12 cases), micropapillary (2 cases), and not otherwise specified (NOS, 374 cases) were identified (Figure 1). Other prominent morphologic features included extensive necrosis (8%), mucin vacuole formation (8.4%), and cribriform growth (8%). Overall and progression free survival were worse in the solid and micropapillary subtypes (Figure 1). The solid group is significantly enriched for mutations in BRAF (50%), FBXW7 (43%), ARID1A or ARID2 (33 and 36%), and RB1 (16.7%) (Figure 2). The mucinous subgroup is enriched for mutations in BRAF (31%), while the villous group is enriched for mutations in KRAS/NRAS (100%) and FBXW7 (44%). Both solid and mucinous groups are enriched for mutations in mismatch repair proteins (MLH1, PMS2, MSH2, MSH6) and POLE. 61% of solid adenocarcinomas were MSI-H while the remaining were MSS; amongst solid MSS adenocarcinomas, TP53 was significantly enriched when compared to MSI-H (91% vs 32%). Extensive necrosis is associated with TP53 mutations (79% vs 52%, p< .05), mucin vacuole formation is associated with KRAS (67% vs 42%) and reduced TP53 mutations (28% vs 54%), cribriform growth is associated with RB1 (14% vs 1%) and MMR-protein alterations (46% vs 24%), and expansile growth is associated with APC mutation (98% vs 70%). For the solid adenocarcinomas, MSS tumors showed enrichment for cribriform growth (60% vs 17%), while MSI-H were linked to neuroendocrine and medullary features. No medullary features were present in the MSS solid tumors.

Figure 1 - 314



**NOS (n=374)**    **Solid (n=38)**    **Mucinous (n=36)**
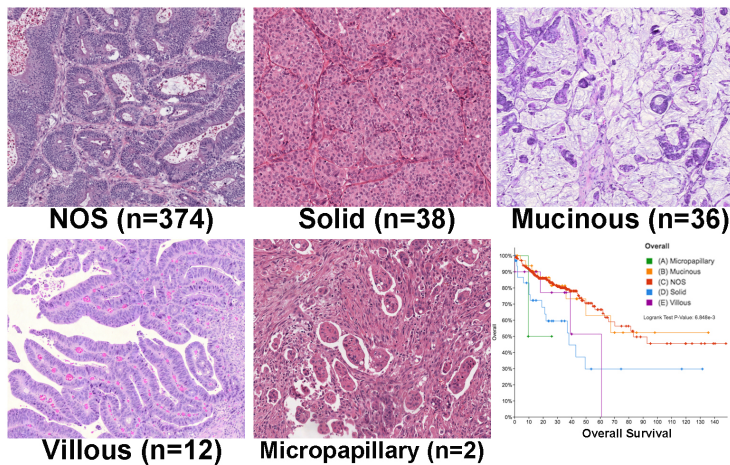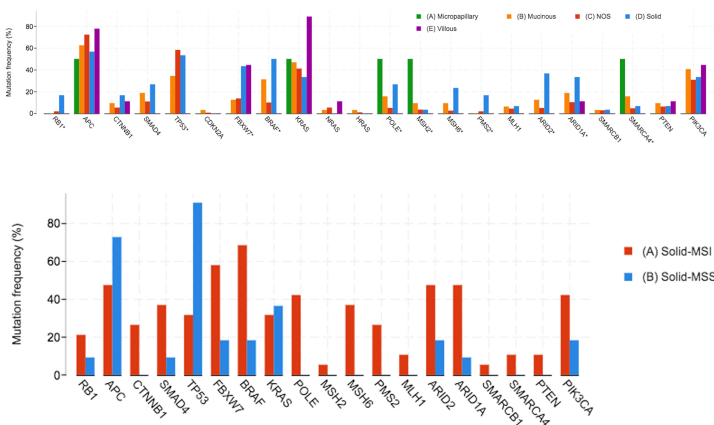
**Villous (n=12)**    **Micropapillary (n=2)**

Figure 2 - 314



**Conclusions:** We identified several histologic subtypes and features in CRC that were correlated with distinct clinical and molecular characteristics. These data could influence prognosis and treatment.

### 315 Appendiceal Inflammation in Colectomy Predicts Early Pouchitis Following Ileal Pouch Anal Anastomosis in Ulcerative Colitis and Indeterminate Colitis

Soe Htet Arker[1], Adam Petchers[1], Georgi Lukose[1], Edward Lee[2], Cary Qualia[1], Hua Li[1], Mustafa E Arslan[1], Hwa Lee[1]
[1]Albany Medical Center, Albany, NY, [2]Albany Medical College, Albany, NY

**Background:** Pouchitis is a common, but significant inflammatory condition complicating Ileal Pouch Anal Anastomosis (IPAA). Appendiceal inflammation in colectomy is one of the histologic predictors of pouchitis in ulcerative colitis (UC). A recent study of IPAA patients suggests fecal calprotectin level increases 2 months prior to the onset of pouchitis. We evaluated whether inflammation and calprotectin expression in appendiceal specimens predicts early-onset pouchitis in UC and indeterminate colitis (IC).

**Design:** IPAA (2000-2018) cases with appendix blocks available in colectomy specimens were identified (n=93). Histologic features thought to predict pouchitis were evaluated. The degree of appendiceal inflammation was scored: fibrous obliteration=1, no =2, mild =3, moderate =4, severe activity with ulcer <50%=5 and ulcer >50%=6. Calprotectin immunostain was performed on the appendix blocks and the extent of mucosal staining was quantified. Electronic medical records were reviewed for demographics, underlying disease, smoking history, clinical pouchitis, time of onset of pouchitis, and clinical and endoscopic components of the Pouchitis Disease Activity Index (PDAI) score. Follow-up pouch biopsies were reviewed and scored to generate histologic PDAI score, when available. Chi-square test, Fisher's exact test, Mann-Whitney U test, Kaplan-Meier Log rank and Spearman's rho were performed when appropriate, with significance at p<0.05.

**Results:** The indications for IPAA were UC (n=90) and IC (n=3). Among the patients with clinical pouchitis (n=73), appendiceal inflammatory scores ≥4 predicted earlier pouchitis compared to scores <4 (median time to pouchitis 12.0 vs. 23.8, log rank p=0.016). Calprotectin staining correlated with inflammatory scores of the appendix (Spearman's rho, r=0.630, p<0.001). The remaining clinicopathologic parameters including calprotectin staining did not predict early pouchitis (p>0.05). No parameter, including appendiceal inflammation, predicted the development of pouchitis (p>0.05). [Table 1].

| | Overall | Pouchitis (n=73) | No pouchitis (n=20) | p- value |
|---|---|---|---|---|
| Age, years (mean, median) | 6-62 (33.5, 32.0) | 6-61 (32.6, 32.0) | 12-62 (36.6, 40.0) | 0.372[†] |
| Sex, male (%) | 48/93 (51.6) | 34/73 (46.6) | 14/20 (70.0) | 0.079 |
| Follow-up following ileoanal anastomosis, months (mean, median) | 1-227 (78.4, 61.0) | 2-227 (84.5, 68.0) | 1-219 (56.0, 35.0) | 0.041[†] |
| Smoking history (%) | 20/93 (21.5) | 17/73 (23.3) | 3/20 (15.0) | 0.548** |
| Pancolitis (%) | 42/93 (45.2) | 33/73 (35.2) | 9/20 (45.0) | 1.000 |
| Fissuring ulcer (%) | 11/93 (11.8) | 7/73 (9.6) | 4/20 (20.0) | 0.242** |
| Backwash ileitis (%) | 12/89 (13.5) | 11/70 (15.7) | 1/19 (5.3) | 0.449** |
| No/mild appendiceal inflammation [inflammation score <4] (%) | 76/93 (81.7) | 58/73 (79.5) | 18/20 (90.0) | 0.348** |
| Moderate to severe appendiceal inflammation [inflammation score ≥ 4] (%) | 17/93 (18.3) | 15/73 (20.5) | 2/20 (10.0) | |
| Calprotectin ≥10% (%) | 49/93 952.7) | 39/73 (53.4) | 10/20 (50.0) | 0.806 |
| Calprotectin ≥50% (%) | 27/93 (29.0) | 21/73 (28.8) | 6/20 (30.0) | 1.000 |
| Complete PDAI (%) | 52/93 (55.9) | 50/73 (71.2) | 2/20 (10.0) | |
| PDAI ≥ 7 | 41/52 (78.8) | 41/50 (80.0) | 0/2 (0) | |
| Time to pouchitis, months (mean, median) | | 1.4-175 (41.6, 22.0) | | |

Table 1. PDAI: pouch disease activity index; ≥ 7 is considered pouchitis. [†]Mann-Whitney U test p-value; **Fisher's Exact p-value

**Conclusions:** The presence of moderate to severe appendiceal inflammation at the time of colectomy was associated with a shorter time to pouchitis following IPAA. Calprotectin immunostain may be used to demonstrate the presence of inflammation in the appendix but the staining extent did not predict early pouchitis. No other histologic or clinical parameters predicted pouchitis development, likely due to the relatively high frequency of pouchitis in our cohort.

### 316     Assessment of Zoom in Grading of Inflammatory Bowel Disease (IBD) Dysplasia

Christina Arnold[1], Michael Arnold[2], Toby Cornish[3], Patrick Henn[4], Linh Ho[4], Jeffrey Kaplan[1], Antonio Galvao Neto[5], Erin Rubin[4], Cassie Xu[3], Lindsey Westbrook[4]
[1]University of Colorado, Aurora, CO, [2]Children's Hospital Colorado, Aurora, CO, [3]University of Colorado School of Medicine, Aurora, CO, [4]University of Colorado Anschutz Medical Campus, Aurora, CO, [5]UCHealth University of Colorado Hospital, Aurora, CO

**Disclosures:** Christina Arnold: None; Michael Arnold: None; Toby Cornish: *Advisory Board Member*, Leica, Inc; Patrick Henn: None; Linh Ho: None; Jeffrey Kaplan: None; Antonio Galvao Neto: None; Erin Rubin: None; Cassie Xu: None; Lindsey Westbrook: None

**Background:** The SARS-CoV-2 pandemic required social distancing, which disrupted our usual peer review at a multiheaded microscope and led to Zoom-based review. This study assesses the diagnostic utility of Zoom.

**Design:** A computer-based search identified 791 consecutive IBD cases from 2010-2020. Of these cases, 12 unique parts per dysplasia category were retrieved: negative for dysplasia (NFD), indefinite for dysplasia (IFD), low-grade dysplasia (LGD), high-grade dysplasia (HGD), and adenocarcinoma. The most representative 4x field was circled on each slide.  A random case order was generated using Microsoft Excel, and then the cases were shared on Zoom. After >3 week washout period, the cases were re-randomized, and shown at the multi-headed microscope. Participants self-recorded their diagnoses, confidence, and time to diagnosis. The following were excluded from review: areas outside of the circled 4x field, polyps, p53, deepers, additional parts, and prior cases.

**Results:** Overall, 1,080 diagnoses were collected (9 pathologists scored 60 cases on Zoom and then in person).  When comparing Zoom vs in person review, the average intraobserver concordance was 64.4% (range 56.7-80%). Of the diagnostic categories selected for the study, the highest intraobserver concordance was seen in adenocarcinoma (99.1%; all other categories= 55.8%)(P=0.0001). Concordance tended to track with years of experience grading dysplasia in adult IBD, although this was not statistically significant: residents=57.5%, junior faculty/non-adult GI= 63.3%, senior GI faculty=68.8%.  The overall concordance with the original rendered diagnoses was similar for Zoom and in person (65.7% vs 61.1%, P=0.129). For cases with an original diagnosis of LGD and HGD, Zoom was more often concordant with the original diagnosis than in person (LGD 72.2% vs. 58.3%, P=0.045; HGD 65.7% vs. 50.9%, P=0.038). Self-reported diagnostic confidence was not significantly different between Zoom and in person  (Zoom=2.93 vs in person=2.86, P=0.320). Average time to diagnosis was statistically significantly longer for Zoom than in person (Zoom=20.77 vs in person=17.48 seconds, P= 0.0001). Post-study surveys identified that important Zoom advantages included reducing the risk of SARS-CoV-2 and eliminating the time to walk to the multiheaded scope room (> 30 min walk/visit for 3 faculty).

**Conclusions:** This study demonstrates that Zoom is slightly more effective than in person review based on slightly higher concordance with the original diagnosis, slightly higher confidence, and similar time to diagnosis, while reducing SARS-CoV-2 risk and eliminating time to walk to the multiheaded scope room.

### 317    Normal Duodenal Histology in Cases with Abnormal Celiac Serology: Dilemma in Gastroenterology Practices

Juwairiya Arshi[1], Feng Yin[1]
[1]University of Missouri, Columbia, MO

**Disclosures:** Juwairiya Arshi: None; Feng Yin: None

**Background:** Celiac disease (CD) is an autoimmune disorder presented with malabsorption following gluten-containing diet. Celiac serology panel, including tissue transglutaminase antibody (TTG), endomysial antibody (EMA), deamidated gliadin peptide antibody (DGP) IgG and IgA, has been reported to be highly sensitive and specific for the clinical diagnosis of CD. However, duodenal biopsy, with the hallmark characteristics of intraepithelial lymphocytosis (IEL) and villous architectural changes, is considered the "gold standard" for the initial diagnostic confirmation and subsequent treatment response monitoring. In this study, we aim to perform a retrospective clinicopathologic evaluation in cases with abnormal Celiac serology panel and unremarkable duodenal histology.

**Design:** A retrospective search for patients with abnormal celiac serology panel and normal duodenal biopsy was performed in our pathology database from January 2010 to September 2020. A total of 20 cases were identified. The clinical, demographic and histopathologic information was reviewed.

**Results:** The study group consisted of 20 patient (M:F 1:3; mean age 13.1). Abdominal pain was the most common clinical presentation (50%). Serum TTG (60%) and DGP IgG (50%) were among the most common positive antibodies, followed by DGP IgA (30%) and EMA (25%). All the upper endoscopy and duodenal biopsies showed unremarkable findings with no evidence of IEL. Interestingly, only one patient (5%) had final clinical diagnosis of CD two years later through follow-up biopsy showing duodenal IEL and villous atrophy. On follow-up testing, Celiac serology returned to normal in 3 patients. In contrast, 2 patients had persistent abnormal Celiac serology testing. Of note, 18 patients (90%) had comorbid medical conditions, with Diabetes mellitus type 1 being the most common (30%), followed by development delay/poor growth (25%) and hypothyroidism (15%). Four patients (20%) had strong family history of autoimmune diseases. Twelve patients (60%) were on medication at the time of biopsy.

**Conclusions:** A unique Celiac testing pattern (abnormal celiac serology and normal duodenal biopsy) has been identified in a specific patient population characterized by younger age and female predominance. Our study highlights its strong association with various autoimmune disorders, especially Diabetes mellitus type 1 and hypothyroidism. Our study suggests that the Celiac serology panel alone is not sufficient for the clinical diagnosis of CD. Concurrent duodenal biopsy is able to confirm the initial diagnosis, as well as to identify false positive serology testing.

### 318    Inflammation and Telocyte Activation Contribute to Fibrosis Progression and Obstruction in Stricturing Crohn's Disease: Image Processing and Analysis Study

Mustafa E Arslan[1], Rupinder Brar[1], Lianna Goetz[2], Dipti Karamchandani[2], Kyle Hodge[1], Hua Li[1], Sangtae Ahn, Hwajeong Lee[1]
[1]Albany Medical Center, Albany, NY, [2]Penn State Health Milton S. Hershey Medical Center, Hershey, PA

**Disclosures:** Mustafa E Arslan: None; Rupinder Brar: None; Lianna Goetz: None; Dipti Karamchandani: None; Kyle Hodge: None; Hua Li: None; Sangtae Ahn: None; Hwajeong Lee: None

**Background:** Crohn's disease (CD) can manifest as variable clinical phenotypes such as inflammatory, stricturing, or penetrating. It is hypothesized that inflammation and structural remodeling contribute to fibrosis progression in CD. We quantified the immunoexpression of calretinin, CD34 and calprotectin as a surrogate for mucosal innervation, telocytes (interstitial cells playing a role in networking) and inflammation, respectively, and correlated them with submucosal thickness in stricturing CD.

**Design:** Primary ileocecal resection specimens for structuring CD (n=31) were identified.  The blocks with proximal and distal margins were stained with calretinin, and stricture site with CD34 and calprotectin. Microscopic images (6 images/slide, x200, JPEG) were captured from the mucosa (calretinin), submucosa (calprotectin) and myenteric

plexus (CD34). Pixel count (PC; the percentage of stained pixels) was generated for each image by image processing and analysis (IPA) using MATLAB. Submucosal thickness was measured at the resection margins and stricture site, and correlated with PC (r, Pearson's correlation coefficient, significance p<0.05). The control group comprised ileocecal resections for inflammatory CD (n=16) and ileocolonic resections for non-CD (left-sided ulcerative colitis or trauma, calretinin only, proximal right colon section used in lieu of distal margin; n=20). Demographics and >1- year follow-up data (n=40) were collected. Student's t-test was used when indicated.

**Results:** The stricturing CD cases comprised of 14 males and 17 females (mean age 34 years, range 12-65). A total of 1368 images were analyzed. The submucosal thickness at the stricture site correlated with calprotectin-PC (r=0.39) and correlated inversely with calretinin-PC at the proximal margin (r=-0.38). **[Figure 1, an example image of calprotectin IPA].** Both proximal and distal submucosal thickness inversely correlated with CD34-PC (prox. r=-0.45, dist. r=-0.31). The submucosal thickness at proximal margin correlated with proximal calretinin-PC in both stricturing (r=0.37) and inflammatory CD (r=0.53). Distal calretinin-PC of non-CD was significantly lower than that in stricturing/inflammatory CD (1.43% vs. 2.42%, p<0.0001). No parameter predicted CD recurrence at the end of the follow-up.

Figure 1 - 318
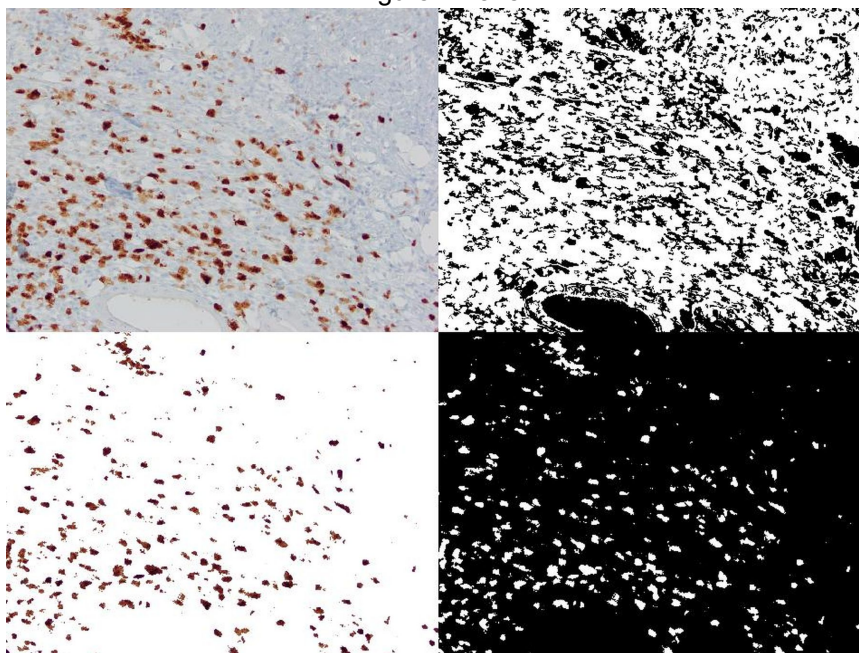


**Conclusions:** Inflammation and tissue remodeling via telocyte activation contribute to fibrosis progression in stricturing CD. However, this process appears to attenuate fibrosis at proximal/distal segments, resulting in localized obstruction. Distal calretinin-PC may be used as a biomarker for CD in the right context.

**319    Gastric Metaplasia and Paneth Cell Hyperplasia in the Biopsy Diagnosis of Chronic Ileitis: Neglected Histological Features of Crohn's Disease**
Agnes Bathori[1], Anita Sejben[2], Fanni Hegedűs[2], Bela Vasas[3], Gregory Lauwers[4], Bence Kővári[1]
[1]H. Lee Moffitt Cancer Center & Research Institute, Tampa, FL, [2]University of Szeged Faculty of Medicine, Szeged, Hungary, [3]University of Szeged, Szeged, Hungary, [4]H. Lee Moffitt Cancer Center & Research Institute, University of South Florida, Tampa, FL

**Disclosures:** Agnes Bathori: None; Anita Sejben: None; Fanni Hegedűs: None; Bela Vasas: None; Gregory Lauwers: None; Bence Kővári: None

**Background:** In the typical clinical setting, the histologic diagnosis of Crohn's disease (CD) relies on the recognition of the chronic ileitis/colitis pattern, with or without granuloma(s). However, other etiologies can induce a

similar morphology. The classic features of chronic ileitis are crypt architectural distortion and basal plasmacytosis. Nevertheless, given the discontinuity of CD, these classic alterations are not always present in biopsy material, especially in small, poorly-oriented, or superficial fragments. Other features of chronicity, including (pseudo)pyloric–gastric metaplasia (PY-GM), foveolar–gastric metaplasia (FO-GM), and Paneth cell hyperplasia (PCH), are less commonly reported in the literature; however, their detection may improve the diagnosis of CD.

**Design:** The presence of PY-GM, FO-GM, and PCH was evaluated in biopsy specimens of clinically confirmed ileal CD cases (n=47) and in two groups of clinically confirmed ulcerative colitis (UC) patients, one with normal terminal ileum (n=20) and one with backwash ileitis (n=20). The association of PY-GM, FO-GM, and PCH to active inflammation, crypt architectural distortion, and basal plasmacytosis was also investigated.

**Results:** Eleven (23%) of 47 CD cases showed gastric metaplasia, whereas it was absent in all ileal samples of UC cases, including those with backwash ileitis. Gastric metaplasia included both PY-GM and FO-GM in 4 (9%) cases, while 6 (13%) and 1 (2%) cases showed exclusively PY-GM and FO-GM, respectively. Altogether, FO-GM was present in 11%, while PY-GM was detected in 21% of CD cases. Both types of gastric metaplasia frequently coexisted with active inflammation, especially erosion and ulceration. PCH was identified in 20 (43%) CD cases, whereas it was present in a single case (5%) of backwash ileitis and absent in all the other UC cases. The presence of PCH was not related to active inflammation.

**Conclusions:** PY-GM, FO-GM, and PCH are features of chronicity not uncommonly detected in ileal CD. Their recognition may be useful in suggesting a diagnosis of ileal CD since these features are infrequent in backwash ileitis. Although not a single case showed gastric metaplasia as the sole feature of chronicity in this series, the surface localization of FO-GM can be particularly helpful in ill-oriented or superficial samples. PY-GM and FO-GM are two sides of the same coin, and the term gastric metaplasia should be promoted to represent both subtypes better.

## 320 Image Analysis of Intratumoral Budding in Colorectal Carcinoma is Prognostically Significant Across All Stage Groups and Histologic Grades

Phoenix Bell[1], Amitabh Srivastava[1], Michael Drage[2]
[1]Brigham and Women's Hospital, Harvard Medical School, Boston, MA, [2]University of Rochester Medical Center, Rochester, NY

**Background:** High tumor budding in colorectal carcinoma (CRC) predicts lymph node involvement and overall survival (OS) in stage II tumors. However, reporting tumor budding remains an optional criterion in current practice due to concerns around accuracy and interobserver variability. We used a machine learning approach to measure the density of intratumoral budding (ITB) and determined its prognostic significance in a large series of CRC.

**Design:** One representative block from 304 CRC resections was stained with H&E and AE1/AE3. H&E slides were scored manually for tumor budding according to ITBCC consensus guidelines. Whole slide AE1/AE3 images were scanned (0.173 μm/pixel) and regions of interest (ROI) manually annotated, including "margin" (advancing front +/- 500 μm) and "center" (area >1000 μm from advancing front and tissue edge). A random forest classifier was used at 1.04 μm/pixel resolution to classify Keratin-positive tissue as tumor and keratin-negative tissue as stroma, and area, perimeter, and number of nuclei were collected for each keratin-positive object. "Tumor buds" were defined as keratin positive objects containing 1-4 nuclei with an area of 50-500 $\mu m^2$ and compactness > 0.5. The number of tumor buds divided by the area of the ROI yielded ITB density. Potential correlation of ITB density with clinicopathologic features was assessed with Fisher's Exact Test, and prognosis with Log-Rank test and Cox regression analysis.

**Results:** The mean patient age was 64 years (M:F; 0.99); 157 (49.1%) CRC were in right colon, 111 (34.7%) in left colon, and 52 (16.3%) in rectum; 58 (18.1%) were MMR-deficient. 58 (18.1%) CRC were stage I; 96 (30.0%) stage II, 117 (36.6%) stage III, and 47 (14.7%) stage IV; mean followup duration was 45.28 months (range 1-162). A bell curve distribution was present below 30 buds/$mm^2$ on the keratin images, and CRC with ≥30 buds/$mm^2$ were classified as high "intratumoral budding" (ITB). Univariate analysis revealed that high ITB correlated with manually classified high tumor budding (p=0.019), patient age $\geq$ 65y (p=0.016), right-sided location

(p=0.017), high tumor grade (p<0.001), IEL> 20 per HPF (p=0.005), and overall mortality (p=0.001), but not MMR deficiency (p=0.841). In multivariate Cox regression, factors which showed prognostic impact included age $\geq$ 65 (p=0.035), overall AJCC stage (p<0.001), and ITB > 30/mm$^2$ (p=0.017). Importantly, the prognostic association of high ITB was maintained in multivariate cox regression in subset analysis restricted to either stage II CRC (p=0.008) or to low grade tumors (p=0.047).

**Table 2: Clinicopathologic Correlates and Prognostic Significance of High Intratumoral Budding in Colorectal Carcinoma**

| Variable | Low ITB (n=256) (n;%) | High ITB (n=47)(n;%) | Total (n=303)(n;%) | *OR | *P |
|---|---|---|---|---|---|
| Age 65 or greater (y) | 134 (52.3) | 34 (72.3) | 168 (55.4) | 2.381 | **0.016** |
| Male | 125 (48.6) | 24 (51.1) | 149 (49.0) | 1.102 | 0.874 |
| Right Colon | 118 (45.9) | 31 (66.0) | 149 (49.0) | 2.282 | **0.017** |
| Size $\geq$ 4.0 cm | 162 (63.5) | 25 (55.6) | 187 (62.3) | 0.321 | 0.718 |
| High Tumor Grade | 70 (27.2) | 26 (55.3) | 96 (31.6) | 3.307 | **<0.001** |
| LVI | 103 (40.1) | 22 (48.9) | 125 (41.4) | 1.430 | 0.325 |
| PNI | 50 (19.5) | 11 (25.6) | 61 (20.4) | 1.416 | 0.413 |
| High tumor budding | 10 (4.0) | 6 (14.0) | 16 (5.5) | 3.843 | **0.019** |
| Stage II-IV | 207 (81.2) | 39 (84.8) | 246 (81.7) | 1.292 | 0.681 |
| IEL $\geq$ 20 per HPF | 97 (40.4) | 28 (63.6) | 125 (44.0) | 2.580 | **0.005** |
| PTLA (CD8) | 177 (73.8) | 26 (59.1) | 203 (71.5) | 0.514 | 0.068 |
| Crohn's-like | 53 (22.1) | 7 (15.9) | 60 (21.1) | 0.668 | 0.426 |
| MSI | 46 (19.2) | 10 (21.3) | 56 (19.6) | 1.134 | 0.841 |
| Overall Mortality | 56 (21.9) | 22 (46.8) | 78 (25.7) | 3.143 | **0.001** |

ITB=Intratumoral Budding; LVI=Lymphovascular invasion; PNI=Perineural invasion; IEL=Intraepithelial lymphocytes; HPF=high power field; PTLA=Peritumoral lymphoid aggregates (CD8-positive); MSI=Microsatellite instable (MMR deficient by IHC). High ITB >=30 buds/mm$^2$ in the tumor center.

*Fisher Exact Test for univariate comparison between tumors with low and high intratumoral budding (2-sided).

Cox Proportional Hazards (overall model p<0.001)

| | B | SE | Wald | df | Sig. | Exp(B) | 95.0% CI for Exp(B) Lower | Upper |
|---|---|---|---|---|---|---|---|---|
| Age (y) | 0.035 | 0.011 | 11.158 | 1 | 0.001 | 1.036 | 1.015 | 1.058 |
| Male | -0.051 | 0.271 | 0.036 | 1 | 0.850 | 0.950 | 0.559 | 1.616 |
| Right Colon | 0.047 | 0.291 | 0.026 | 1 | 0.872 | 1.048 | 0.592 | 1.855 |
| Size (cm) | 0.010 | 0.068 | 0.020 | 1 | 0.889 | 1.010 | 0.883 | 1.154 |
| LVI | -0.015 | 0.341 | 0.002 | 1 | 0.965 | 0.985 | 0.505 | 1.923 |
| PNI | -0.132 | 0.352 | 0.141 | 1 | 0.707 | 0.876 | 0.440 | 1.746 |
| High Tumor budding | -0.095 | 0.568 | 0.028 | 1 | 0.867 | 0.910 | 0.299 | 2.769 |
| Overall stage grouping | | | 18.826 | 4 | 0.001 | | | |
| Stage I | 1.147 | 1.199 | 0.914 | 1 | 0.339 | 3.148 | 0.300 | 33.029 |
| Stage II | -1.486 | 0.573 | 6.717 | 1 | 0.010 | 0.226 | 0.074 | 0.696 |
| Stage III | -1.329 | 0.409 | 10.532 | 1 | 0.001 | 0.265 | 0.119 | 0.591 |
| Stage IV | -1.131 | 0.364 | 9.654 | 1 | 0.002 | 0.323 | 0.158 | 0.659 |
| PTLA | 0.408 | 0.298 | 1.877 | 1 | 0.171 | 1.504 | 0.839 | 2.696 |
| Crohns-like Infiltrate | -0.161 | 0.379 | 0.182 | 1 | 0.670 | 0.851 | 0.405 | 1.788 |
| MSI (IHC) | 0.389 | 0.515 | 0.572 | 1 | 0.449 | 1.476 | 0.538 | 4.050 |
| Maximum IEL/HPF | -0.027 | 0.020 | 1.933 | 1 | 0.164 | 0.973 | 0.937 | 1.011 |
| High ITB (>30/mm2) | -0.831 | 0.330 | 6.345 | 1 | 0.012 | 0.436 | 0.228 | 0.832 |

**Conclusions:** Our findings suggest that a machine learning approach can be easily applied to score ITB, a prognostically significant parameter in CRC that is challenging on manual quantitation.

**321  Persistent or Recurrent Barrett's Neoplasia After Endoscopic Therapy is Associated with DNA Content Abnormality Detected by DNA Flow Cytometric Analysis of Paraffin-Embedded Tissue**

Christopher Bowman[1], Ruth Zhang[1], Dana Balitzer[2], Dongliang Wang[3], Peter Rabinovitch[4], Bence Kővári[5], Aras Mattis[1], Sanjay Kakar[1], Gregory Lauwers[6], Won-Tak Choi[1]
[1]University of California, San Francisco, San Francisco, CA, [2]San Francisco VA Health Care System, San Francisco, CA, [3]SUNY Upstate Medical University, Syracuse, NY, [4]University of Washington, Seattle, WA, [5]H. Lee Moffitt Cancer Center & Research Institute, Tampa, FL, [6]H. Lee Moffitt Cancer Center & Research Institute, University of South Florida, Tampa, FL

**Disclosures:** Christopher Bowman: None; Ruth Zhang: None; Dana Balitzer: None; Dongliang Wang: None; Peter Rabinovitch: None; Bence Kővári: None; Aras Mattis: None; Sanjay Kakar: None; Gregory Lauwers: None; Won-Tak Choi: None

**Background:** Endoscopic therapy (ET) represents the standard of care for the treatment of dysplasia (in particular high-grade dysplasia [HGD]) and intramucosal adenocarcinoma (IMC) in patients with Barrett's esophagus (BE). Visible lesions are typically treated with endoscopic mucosal resection (EMR) coupled with radiofrequency ablation (RFA). However, ET may require multiple sessions and does not always result in complete remission of neoplasia. Recurrences are also common. This study aims to assess which potential risk factors can predict a poor response to ET.

**Design:** Forty-five BE patients who underwent ET were analyzed. DNA flow cytometry was performed on 82 paraffin-embedded, pre-ET biopsies/EMR specimens from the 45 patients, including 78 HGD/IMC, 2 low-grade dysplasia, and 2 indefinite for dysplasia.

**Results:** Sixty (73%) of the 82 pre-ET biopsies/EMR specimens showed abnormal DNA content (aneuploidy or elevated 4N fraction). They were all HGD/IMC samples (representing 77% of that group). Forty-two (70%) of the 60 HGD/IMC cases with abnormal DNA content demonstrated persistence/recurrence following ET, whereas only 6 (27%, all HGD/IMC) of the 22 remaining cases with normal DNA content showed persistence/recurrence within a mean follow-up time of 16 months (range: 1 month to 9.5 years). In the multivariate Cox model, abnormal DNA content (HR = 7.8, p = 0.001) and BE segment ≥ 3 cm (HR = 2.6, p = 0.026) were significantly associated with an increased risk for persistent/recurrent neoplasia. Combined endoscopic modalities (i.e., EMR with RFA) were associated with 60% reduction in risk (HR = 0.4, p = 0.031) compared with EMR alone. Age, gender, BMI, ethnicity, and hiatal hernia were not significant risk factors (p > 0.05). Three-month, 6-month, 1-year, and 3-year probabilities of persistent/recurrent neoplasia in the setting of abnormal DNA content were 31%, 56%, 67%, and 79%, respectively, whereas 3-month, 6-month, 1-year, and 3-year probabilities in the setting of normal DNA content were 10%, 21%, 28%, and 38%, respectively.

**Conclusions:** Not only can DNA content abnormality detected by DNA flow cytometry serve as a diagnostic marker of HGD/IMC (with the estimated sensitivity of 77%), but it can also facilitate identification of patients at high risk for persistent/recurrent neoplasia. The diagnosis of HGD/IMC in the setting of abnormal DNA content may warrant more aggressive therapeutic and surveillance strategies with shorter surveillance intervals and long-term follow-up after ET.

**322  Gastrointestinal Polyps and Polyposes in Individuals Harboring CHEK2 Germline Mutations**

Corey Chang[1], John Lee[1], Kevin Waters[1], Brent Larson[1]
[1]Cedars-Sinai Medical Center, Los Angeles, CA

**Disclosures:** Corey Chang: None; John Lee: *Advisory Board Member*, Invitae; Kevin Waters: None; Brent Larson: None

**Background:** Checkpoint kinase 2 (CHEK2) is a tumor suppressor gene which plays a critical role in the DNA damage checkpoint system and may be mutated in a number of cancers. Several patients with germline CHEK2 mutations and colon polyps were noted in our GI clinics, and some sources advocate genetic testing for patients

with ≥10 lifetime polyps. This study was undertaken to assess whether CHEK2 might be associated with low-level polyposis, and to characterize the GI clinicopathologic profile of these patients.

**Design:** A retrospective analysis was performed from a database of patients harboring germline CHEK2 mutations. Available slides of polyps were retrieved from departmental archives and reviewed by two pathologists at a multiheaded microscope. Clinical notes, endoscopic reports, pathology reports, and genetic testing reports were reviewed, and the findings correlated.

**Results:** From a database of 107 patients, 39 patients had documented endoscopic examination and were included in this study. Twenty-five patients (19 females, 6 males) had documented polyps within the GI tract: 4 with only upper GI polyps, 4 with only lower GI polyps and 17 with both upper and lower GI polyps. The median age at initial detection of a GI polyp was 54 years (range: 40-72 years). Among patients with lower GI polyps, 9 had adenomas, 6 had serrated polyps, 1 had an inflammatory polyp and 5 had both adenomatous and serrated polyps. Fourteen patients had negative colonoscopies. The average number of cumulative polyps was 6; 22 patients had <10 cumulative polyps, 2 patients had 10-30 polyps, and 1 patient developed >40 polyps. Five patients (11.4%) developed colonic adenocarcinoma. The most common germline CHEK2 mutations in patients with GI polyps were p.S248F (n=10 patients) and p.I157T (n=4 patients) with other mutations present in 1 patient each. Six out of 10 patients with p.S248F were found to have isolated polyps in the right colon. One patient with a CHEK2 p.I157T mutation developed 13 adenomas (1 in the stomach and 12 in the ascending colon). The patient with >40 polyps had a CHEK2 p.I157T germline mutation and a concurrent germline POLE p.L424V mutation.  One patient with a possible mosaic CHEK2 c.776del mutation developed 1 adenoma in the cecum and 20 hyperplastic polyps in the rectosigmoid and descending colon, fulfilling the WHO 2019 criteria for serrated polyposis syndrome. One additional patient with a likely pathogenic CHEK2 p.R117G mutation developed 9 adenomas (1 in the cecum, 3 in the ascending colon, 1 in the descending colon and 4 in the sigmoid).

**Conclusions:** The majority of patients harboring germline CHEK2 p.S248F mutations were found to have right-sided polyps, indicating the importance of right-sided colonoscopic exam in these patients. A minority (6.8%) of patients with germline CHEK2 mutations may present with polyposis phenotypes, and these germline mutations should be considered when testing patients with >10 polyps for polyposis syndromes.

### 323 A Multi-Institutional Study of Large B-Cell Lymphomas of the Stomach Demonstrates a Male Predominance and Low Incidence of MYC Gene Rearrangements Despite Double-Expressor Phenotype

Jigisha Chaudhari[1], Eric Gars[2], Kwun Wah Wen[3], Mitul Modi[4], Robert Ohgami[3], Rifat Mannan[5]
[1]Pennsylvania Hospital, Philadelphia, NJ, [2]Stanford Medicine/Stanford University, CA, [3]University of California, San Francisco, San Francisco, CA, [4]Pennsylvania Hospital of the University of Pennsylvania Health System, Philadelphia, PA, [5]Perelman School of Medicine at the University of Pennsylvania, Philadelphia, PA

**Disclosures:** Jigisha Chaudhari: None; Eric Gars: None; Kwun Wah Wen: None; Mitul Modi: None; Robert Ohgami: None; Rifat Mannan: None

**Background:** Gastric lymphomas account for 30-40% of all extra-nodal lymphomas and 55-65% of all lymphomas involving gastro-intestinal(GI) tract. Of these large B-cell lymphomas (LBCL) and marginal zone lymphomas are the most common.  While the significance of myc protein expression and *MYC* gene rearrangements is well established in nodal large B-cell lymphomas, these and other prognostic markers have not been well studied in primary gastric large B-cell lymphomas.

**Design:** We searched the pathology tissue and slide archives of 3 major hospitals for cases of large B-cell lymphomas primary to the stomach. We retrospectively analyzed clinical, histopathological, immunophenotypic and molecular features.

**Results:** Nineteen cases (13 M and 6 F) were identified over a period of 5 years. The overall median age was 66 years (range, 26-88). Using the Hans algorithm , 54% (7/13) were classified as germinal center B type (GCB) and 46% (6/13) as Activated B-Cell (ABC) type. The characteristics of GCB and ABC subtypes,  were : median age (GCB 69 vs ABC 67.5); M:F (GCB 6:1 vs ABC 3:3); and Ki-67 labeling index (GCB 92% vs ABC 70%) Of all cases,

4 were classified as "double expressor" subtypes (co-expressing c-myc and bcl-2) which had a male predominance (3:1), median age of 66, median Ki-67 proliferation index 67.5% ; 2 were GCB type and 2 ABC type. No "double hit" lymphomas were identified though one case had a *MYC* gene rearrangement (71 year old, female, Ki-67 proliferation index 99%  and GCB subtype).

Clinicopathologic details of Large B-Cell Lymphoma of stomach

| | All Cases | Double Expressor (n=4) | Double Hit (n=0) | GCB subtype (n=7) | ABC  subtype (n=6) |
|---|---|---|---|---|---|
| Sex (M:F) | 13:6 | 3:1 | NA | 6:1 | 3:3 |
| Age (years) (medan;range) | 66 (26-88) | 66 (55-86) | NA | 69 (39-78) | 67.5 (26-88) |
| Ki67 (%) (median;range) | 79 (40-100) | 67.5 (40-80) | NA | 92 (85-99) | 70 (40-80) |
| GCB subtype | 7/13 | 2 | NA | | |
| ABC Subtype | 6/13 | 2 | NA | | |

GCB - germinal center B; ABC - activated B-cell; NA - not available

**Conclusions:** LBCL of the stomach present at a relatively older age group with male preponderance, show a high proliferation index with a similar incidence of GCB and ABC subtypes. While double expressor subtypes are present in a significant portion of these cases, *MYC* gene rearrangements are infrequent.

**324    Clinicopathologic and Immunohistochemical Characterization of Primary Gastrointestinal Tract Neuroendocrine Carcinomas**
Irene Chen[1], Dongwei Zhang[1], Moises Velez[2], Sierra Kovar[1], Xiaoyan Liao[1]
[1]University of Rochester Medical Center, Rochester, NY, [2]University of Rochester, Rochester, NY

**Disclosures:** Irene Chen: None; Dongwei Zhang: None; Moises Velez: None; Sierra Kovar: None; Xiaoyan Liao: None

**Background:** Primary gastrointestinal tract neuroendocrine carcinomas (GI-NECs) are malignant neoplasms that can be divided into small cell NEC (SCNEC), large cell NEC (LCNEC), and mixed adenoneuroendocrine carcinoma (MANEC) when both components are high grade and comprise ≥30% of the neoplasm. GI-NECs are rare and the clinicopathologic features are not well understood.

**Design:** A total of 43 patients diagnosed with primary GI-NECs (21 resections, 22 biopsies) were identified and reassessed based on the World Health Organization 2019 classification and grading criteria.

**Results:** The cohort included 27 men and 16 women, with a median age of 66 years. Six (14%) patients had a history of inflammatory bowel disease. Histologically, 19 (44%) were LCNEC, 12 (28%) SCNEC, and 4 (9%) combined SC/LC NEC. Eight (19%) were MANECs, in which the neuroendocrine components were all LCNEC. Tumor sites included colon (n=14, 33%), rectum (n=13, 30%), esophagus (n=9, 21%), stomach (n=3), small bowel (n=2) and ileocolonic junction (n=2). Immunohistochemically, INSM1 was the most sensitive marker for

neuroendocrine expression, detected in all 28 (100%) tested cases, followed by synaptophysin (40/43, 93%), CD56 (22/35, 63%), and chromogranin (18/40, 45%). SATB2, CDX2, CK20 and CK7 were positive in 21/26 (81%), 26/37 (70%), 11/35 (31%), and 10/35 (29%) cases, respectively. Three of 25 cases (11%) were mismatch repair deficient with loss of MLH1/PMS2. The expression of transcription factors, neuroendocrine and cytokeratin markers were not associated with a specific tumor location or NEC type. Molecular analysis showed 4/6 (67%) cases harbored *TP53*, 2 (33%) *KRAS,* and 2 (33%) *PTEN* mutations. Of 21 resected tumors, 19 (90%) were pT3 and above, while 13 (62%) had nodal metastasis. Ten cases had biopsy-proven liver metastasis. Treatment modalities included chemotherapy (20 NEC-based/10 adenocarcinoma-based, 70%), radiation (n=6, 14%), or immunomodulators (n=8, 19%). On follow-up, 26 (60%) patients died after a median survival of 9 months. By Kaplan-Meier analysis, the 5-year survival rate was 20% and the prognosis was tumor stage dependent (P<0.05). NECs in colon had slightly better survival than other sites, while age, sex, tumor type and treatment were not significant prognostic factors.

**Conclusions:** Primary GI-NECs are aggressive neoplasms with poor prognosis associated with tumor stage and location. INSM1, synaptophysin, and SATB2 are sensitive markers, but not site or tumor type specific.

**325    Combined Histologic Risk Score Using TP53 Protein Expression, CD8 T-cell Density, and Tumor Budding is an Independent Predictor of Survival in Colon Cancer**
Wei Chen[1], Douglas Hartman[1], Reetesh Pai[2]
[1]University of Pittsburgh Medical Center, Pittsburgh, PA, [2]UPMC Presbyterian Hospital, Pittsburgh, PA

**Disclosures:** Wei Chen: None; Douglas Hartman: None; Reetesh Pai: None

**Background:** Recent evidence indicates that immune cell density and tumor budding are prognostic factors in colon cancer. TP53 expression has also been associated with survival in colon cancer in some, but not all, studies. We investigated the prognostic effect of TP53 expression and its association with immune cell density and tumor budding in colon cancer.

**Design:** A series of 261 patients with resected colon cancer were analyzed for TP53 expression, CD8 T-cell density, MMR protein expression, KRAS/BRAF mutation, and histologic features.  TP53 immunohistochemistry was evaluated on tissue microarrays with aberrant TP53 expression defined as either (1) strong, diffuse positive nuclear expression easily visualized at low-power (2x or 4x objective) magnification or (2) complete loss of nuclear expression within the tumor cells using tumor associated stroma as an internal control. All other TP53 expression patterns were scored as wild-type. Disease-free survival (DFS) was the primary endpoint.

**Results:** 46% of colonic adenocarcinomas had aberrant TP53 expression. Compared to wild-type tumors, aberrant TP53 was more often identified in the left colon (43% vs. 24%); had lymphatic (66% vs. 46%), venous (41% vs. 17%), and perineural (33% vs. 18%) invasion (all with p<0.01); and demonstrated high tumor budding (27% vs. 14%, p=0.01). Tumors with aberrant TP53 expression were infrequently MMR protein deficient or BRAF mutation positive (both with p<0.001). Features associated with DFS on univariate analysis included aberrant TP53 expression (Figure 1), tumor budding, CD8 T-cell density, venous invasion, perineural invasion, and MMR status (all with p<0.05). A combined histopathologic risk score was created using TP53 expression, CD8 T-cell density, and tumor budding as adverse risk factors; patients were separated into low-risk (0-1 factors) and high risk (2-3 factors) categories.  In the multivariable model, patients in the high risk category were 4.71-fold more likely to develop tumor recurrence (95% CI 1.69-13.08, p=0.003) (Figure 2).  Stage III tumors (HR 2.80, p=0.03) and venous invasion (HR 3.92, p=0.006) were also independent predictors of recurrence.

**Table 1. Clinicopathologic features of patients with colonic adenocarcinoma stratified by TP53 expression**

| Clinicopathologic Feature | Wild-type TP53 Expression | Aberrant TP53 Expression | P-value |
|---|---|---|---|
| Number of patients (%) | 140 (54) | 121 (46) | |
| Median age in years (range) | 73 (30-93) | 69 (32-93) | 0.02 |
| Gender, male/female | 59 (42) / 81 (58) | 64 (53) / 57 (47) | 0.08 |
| Location | | | |
| Left | 34 (24) | 52 (43) | 0.001 |
| Right | 106 (76) | 69 (57) | |
| Tumor size in cm (median, range) | 5.0 (0.5-13.5) | 4.0 (1was-12) | 0.001 |
| Lymphatic invasion present | 64 (46) | 80 (66) | 0.001 |
| Venous invasion present | 24 (17) | 50 (41) | <0.001 |
| Perineural invasion present | 25 (18) | 40 (33) | 0.005 |
| High tumor grade | 34 (24) | 13 (11) | 0.005 |
| BRAF mutation | | | <0.001 |
| Number tested | 134 | 118 | |
| Number positive | 57 (43) | 13 (11) | |
| CDX2 expression | | | 0.005 |
| Number evaluated | 140 | 120 | |
| Number positive | 116 (83) | 113 (94) | |
| SATB2 expression | | | 0.07 |
| Number evaluated | 136 | 118 | |
| Number positive | 126 (93) | 101 (86) | |
| KRAS mutation | | | 0.63 |
| Number tested | 90 | 115 | |
| Number positive | 35 (39) | 41 (36) | |
| MMR status | | | <0.001 |
| Proficient | 52 (37) | 110 (91) | |
| Deficient | 88 (63) | 11 (9) | |
| Stage | | | 0.36 |
| 1 | 21 (15) | 13 (11) | |
| 2 | 62 (44) | 46 (38) | |
| 3 | 39 (28) | 44 (36) | |
| 4 | 18 (13) | 18 (15) | |
| Tumor budding (per 0.785 mm$^2$) | | | 0.01 |
| 0-9 | 120 (86) | 88 (73) | |
| ≥10 | 20 (14) | 33 (27) | |
| Combined CD8+ T-cell Density Score* | | | 0.09 |
| Number tested | 132 | 118 | |
| Low | 35 (27) | 43 (36) | |
| Intermediate or High | 97 (73) | 75 (64) | |

\* High = high CD8 in both the tumor center and invasive front, Low = low CD8 in both the tumor center and invasive front and Intermediate = high CD8 in either tumor center or invasive front.
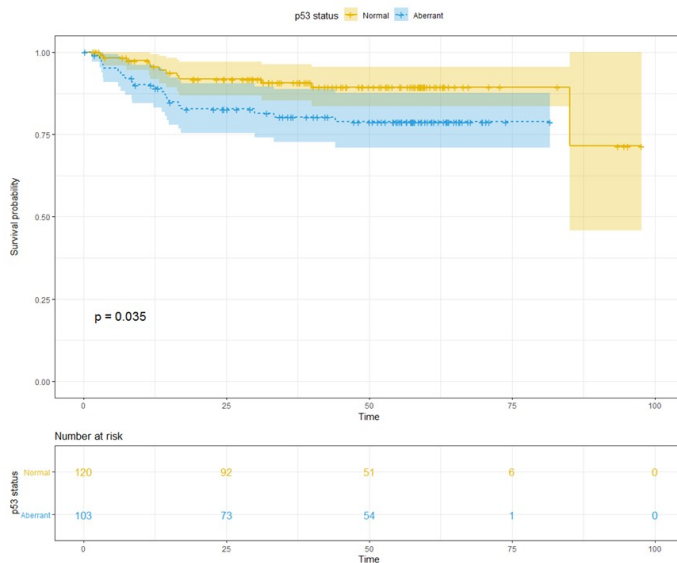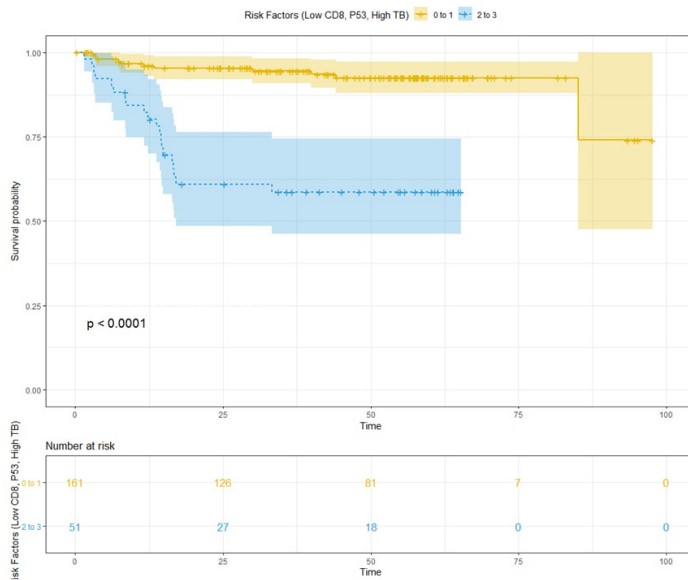
Figure 1 - 325

Figure 2 - 325



**Conclusions:** A combined histopathologic risk score including TP53 expression, CD8 T-cell density, and tumor budding is an independent predictor of disease-free survival in colon cancer. Incorporation of these biomarkers may be helpful in identifying patients at risk for recurrence following resection.

**326 Combined Histologic Risk Score using TP53 protein expression, CD8 T-cell Density, and Intratumoral Budding is an Independent Predictor of Neoadjuvant Therapy Response in Rectal Cancer**

Wei Chen[1], Douglas Hartman[1], Reetesh Pai[2]
[1]University of Pittsburgh Medical Center, Pittsburgh, PA, [2]UPMC Presbyterian Hospital, Pittsburgh, PA

**Disclosures:** Wei Chen: None; Douglas Hartman: None; Reetesh Pai: None

**Background:** Neoadjuvant therapy is the recommended treatment for locally advanced rectal adenocarcinoma; however, there remains significant variability in response to therapy. TP53 has been associated with therapy response and patient prognosis, but the data are not consistent. Recently, we demonstrated that immune cell density and intratumoral budding (ITB) are prognostic factors in rectal cancer. Here we investigated predictive value of TP53 with CD8+ T-cell density and ITB for therapy response and disease free survival (DFS).

**Design:** Biopsies of rectal adenocarcinoma from 117 patients with neoadjuvant therapy were analyzed for TP53 expression, ITB, CD8+ T-cell density, and MMR protein expression. Aberrant TP53 expression was defined as either (1) strong, diffuse positive nuclear expression easily visualized at low-power (2x or 4x objective) magnification or (2) complete loss of nuclear expression within the tumor cells using tumor associated stroma as an internal control. All other TP53 expression patterns were scored as wild-type. Therapy response and DFS were the primary endpoints.

**Results:** TP53 status included 34 wild-type cases (29%) and 83 aberrant cases (71%). Compared to TP53 wild type, aberrant TP53 expression was associated with proficient MMR status (100%, $p=0.006$), low CD8+ T-cell density (<157 / mm$^2$, $p=0.009$), and is borderline associated with high ITB (=6 or more per 0.785 mm$^2$, $p=0.08$) (Table 1). High CD8+ T-cell density was associated with a higher likelihood of achieving complete/near complete response (odds ratio (OR) 3.94, $p=0.001$). ITB (OR 0.36, $p=0.04$) and aberrant TP53 expression (OR 0.55, $p=0.1$) were associated with reduced likelihood of achieving complete/near complete response, although TP53 expression had borderline significance. A combined histopathologic risk score was created using CD8 T-cell density, ITB, and TP53 expression, as risk factors. Patients were separated into low-risk (0-1 factors) and high risk (2-3 factors) categories. In the multivariable model, patients in the low-risk category were 2.64-fold more likely to achieve

complete/near complete therapy response (95% CI 1.22-5.71, p=0.02). Patients with a high risk score had a trend for poor disease-free survival compare to patients with a low-risk score (HR 2.09, p=0.08) (Figure 1).

**Table 1. Clinicopathologic features of rectal adenocarcinoma stratified by TP53 expression**

| Clinicopathologic Feature | | TP53 Expression in biopsy (%) | | p-value |
|---|---|---|---|---|
| | | Aberrant | Wild-type | |
| Number of patients (%) | | 83 (71) | 34(29) | |
| Number with resection | | 75(71) | 30(29) | |
| Median age in years (IQR) | | 60 (18) | 63 (12) | 0.3 |
| Gender, male/female | | 45(54)/38(46) | 24(71)/10(29) | 0.1 |
| Location | | | | |
|    Mid rectum | | 37(45) | 16(47) | 0.81 |
|    Distal rectum | | 46(55) | 18(53) | |
| Median tumor size in cm (IQR) | | 5.0 (2.5) | 5.1 (4.2) | 0.5 |
| Neoadjuvant therapy | | | | |
|    Chemoradiotherapy | | 68(82) | 27(79) | 0.8 |
|    TNT | | 15(18) | 7(21) | |
| MMR status | | | | |
|    MMR deficient | | 0 | 3(9) | 0.006 |
|    MMR proficient | | 83(100) | 31(91) | |
| High tumor grade on biopsy | | 5(62) | 3(38) | 0.6 |
| Stage (ypTNM) | | | | |
| | 0 | 18(22) | 9(26) | 0.8** |
| | 1 | 16(19) | 6(18) | |
| | 2 | 18(22) | 12(35) | |
| | 3 | 31(37) | 7(21) | |
| Recurrence Pattern | | | | |
|    No recurrence | | 70(84) | 30(88) | 0.5 |
|    Local recurrence | | 3(4) | 0 | |
|    Systemic recurrence | | 10(12) | 4(12) | |
| Intratumoral budding present in biopsy | | 22(85) | 4(15) | 0.08 |
| CD8+ T-cell Density in biopsy | | | | |
|    Low (<157 / mm$^2$) | | 58(70) | 15(44) | 0.009 |
|    High (≥157 / mm$^2$) | | 25(30) | 19(56) | |
| Tumor regression score | | | | |
| | 0 | 17(20) | 10(29) | 0.1* |
| | 1 | 17(20) | 9(26) | |
| | 2 | 31(37) | 8(24) | |
| | 3 | 18(23) | 7(21) | |
| IQR, interquartile range; CR, clinical response; TNT, total neoadjuvant therapy. | | | | |
| *p-value is for tumor regression score 0 or 1 vs. 2 or 3. | | | | |
| **p-value is for stage 0 or 1 vs. 2 or 3 | | | | |
| | | | | |

Figure 1 - 326
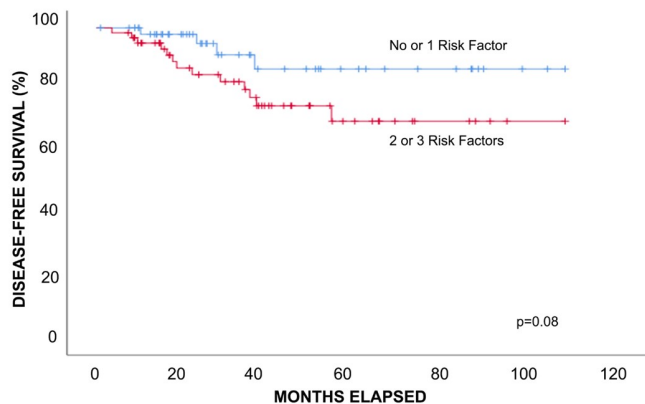
**Conclusions:** A combined histopathologic risk score based on aberrant TP53 expression, high ITB, and low CD8+ T-cell density is predictive of response to neoadjuvant therapy and is associated with DFS. These biomarkers may be helpful in identifying patients at risk for therapy resistance and disease recurrence.

## 327 Hypermucinous, Goblet Cell Deficient, and Crypt Cell Dysplasias in Inflammatory Bowel Disease: A Multicenter Clinicopathologic Study of 126 Cases

Won-Tak Choi[1], Marcela Salomao[2], Lei Zhao[3], Lindsay Alpert[4], Namrata Setia[4], Xiaoyan Liao[5], Michael Drage[5], Maria Westerhoff[6], Jerome Cheng[6], Gregory Lauwers[7], Huaibin Mabel Ko[8]
[1]University of California, San Francisco, San Francisco, CA, [2]Mayo Clinic, Scottsdale, AZ, [3]Brigham and Women's Hospital, Harvard Medical School, Boston, MA, [4]University of Chicago, Chicago, IL, [5]University of Rochester Medical Center, Rochester, NY, [6]University of Michigan, Ann Arbor, MI, [7]H. Lee Moffitt Cancer Center & Research Institute, University of South Florida, Tampa, FL, [8]Columbia University Irving Medical Center, New York-Presbyterian Hospital, New York, NY

**Disclosures:** Won-Tak Choi: None; Marcela Salomao: None; Lei Zhao: None; Lindsay Alpert: None; Namrata Setia: None; Xiaoyan Liao: None; Michael Drage: None; Maria Westerhoff: None; Jerome Cheng: None; Gregory Lauwers: None; Huaibin Mabel Ko: None

**Background:** Several types of non-conventional dysplasia (NCD) have been described in IBD. Although hypermucinous, goblet cell deficient (GCD), and crypt cell dysplasias (CCD) have received more attention, there is limited information regarding their clinicopathologic features.

**Design:** A total of 126 hypermucinous (n = 55), GCD (n = 26), and CCD (n = 45) cases from 97 IBD patients were collected from 7 different institutions and analyzed.

**Results:** The cohort included 62 (64%) men and 35 (36%) women with a mean age of 49 years and a long history of IBD (mean: 18 years). Sixty-eight patients (70%) had ulcerative colitis (UC), 25 (26%) Crohn's disease (CD), and 4 (4%) indeterminate colitis. NCD was predominantly found in UC patients (70%) and in the left colon (63%); however, in CD patients, hypermucinous (34%) or GCD (26%) dysplasia was more common than CCD (11%) (p = 0.016). While hypermucinous dysplasia often had a polypoid endoscopic appearance (58%), CCD and GCD variants more frequently presented as an invisible lesion (89% and 54%, respectively) (p = < 0.001). Hypermucinous dysplasia often demonstrated tubulovillous architecture (75%), whereas GCD dysplasia was predominantly tubular (92%) (p < 0.001). Follow-up information was available for 92 cases, of which 55 cases (60%, including 19 [49%] of 39 for hypermucinous, 10 [59%] of 17 GCD, and 26 [72%] of 36 CCD; p = 0.116) were found to have advanced neoplasia (34 [62%] high-grade dysplasia and 21 [38%] adenocarcinoma) in the same colonic segment within a mean follow-up time of 12 months. Greater than half of the patients (52%) had a history of conventional dysplasia, which was detected in the same colonic segment as NCD at a rate of 33%. GCD dysplasia (74%) was more frequently associated with a history of conventional dysplasia than hypermucinous dysplasia (43%) or CCD (48%) (p = 0.044). Six patients (6%) also had a history of adenocarcinoma in a different colonic segment away from NCD.

**Conclusions:** Hypermucinous, GCD, and CCD variants have distinct clinicopathologic features but appear to have a similar high risk of association with advanced neoplasia. Greater than half of the cases (55%) presented as an invisible lesion, suggesting that random biopsy sampling may be needed in IBD patients in addition to targeted biopsies. Although not uncommonly associated with conventional dysplasia, they may develop in a separate field of carcinomatous development and may be the only dysplastic subtype identified in IBD patients.

## 328 Molecular Profiling of Polyploid Dysplasia Within and Outside Areas of Colitis in IBD Patients: A Comparative Analysis with Sporadic Adenomas in Non-IBD Patients

Alexander Christakis[1], Jonathan Nowak[1], Robert Odze, Matthew Hamilton[1], Paige Parrack[1], John Goldblum[2], Amaya Pankaj[3], Vikram Deshpande[4], Neal Lindeman[5], Deepa Patil[5]

[1]Brigham and Women's Hospital, Boston, MA, [2]Cleveland Clinic, Cleveland, OH, [3]Massachusetts General Hospital, Boston, MA, [4]Massachusetts General Hospital, Harvard Medical School, Boston, MA, [5]Harvard Medical School, Brigham and Women's Hospital, Boston, MA\

**Disclosures:** Alexander Christakis: None; Jonathan Nowak: None; Robert Odze: *Consultant*, CDX Diagnostics; Matthew Hamilton: None; Paige Parrack: None; John Goldblum: None; Amaya Pankaj: None; Vikram Deshpande: None; Neal Lindeman: None; Deepa Patil: None

**Background:** Recent studies indicate that inflammatory bowel disease (IBD)-associated dysplastic lesions have greater chromosomal instability and more frequently harbor *TP53* and *FBXW7* mutations as compared to sporadic adenomas in non-IBD patients. However, little is known about the molecular features of polypoid dysplastic lesions that arise outside the areas of colitis in IBD patients. Therefore, we sought to genomically profile polypoid low-grade dysplastic lesions (all intestinal-type), both within and outside areas of known inflammation in ulcerative colitis (UC) patients and to compare the features with known sporadic adenomas in non-IBD patients.

**Design:** Cohort 1 consisted of 14 polypoid low-grade dysplastic lesions *within* areas of known colitis from 13 UC patients (mean age: 58y; 8M; 7F; 9 with pancolitis); cohort 2 consisted of 8 polypoid low-grade dysplastic lesions *outside* areas of colitis from 6 UC patients (mean age; 56y; 4M; 2F; 5 with left sided colitis, 1 with UC proctitis) and cohort 3 consisted of 5 sporadic adenomas from 3 non-IBD patients (mean age; 66y; 3M). DNA from macrodissected FFPE tissue was analyzed using the OncoPanel assay (version 3.1), interrogating 447 cancer-associated genes for mutations and copy number alterations. Categorical variables were analyzed using Fisher's exact test or chi2 test; student's T test was used for continuous variables.

**Results:** Polypoid dysplastic lesions located within area of colitis (mean: 1.7 cm; range 0.1-4.3) were significantly larger compared to those outside of colitis in UC patients (mean: 0.3 cm; range: 0.2-0.5; p=0.004) and sporadic adenomas in non-IBD patients (mean: 0.5 cm; range: 0.3-0.6; p=0.02). Alterations in *APC* (64%, 88%, 80%) and *CTNNB1* (7%, 38%, 40%) were seen in all three cohorts, respectively. Mutations in additional known colorectal cancer genes, including *TP53*, *ARID1A*, *TCF7L12*, *TCF7* and *RNF43* were only seen in polypoid lesions within areas of known colitis; although at low individual frequencies (Table 1). *FBXW7* mutation was seen in 21% of polypoid lesions within areas of known colitis, 13% of lesions outside areas of colitis, and in none of the sporadic adenoma cases. There were no significant differences between polypoid lesions located outside the areas of colitis in IBD patients and sporadic adenomas in non-IBD patients. Activating mutations in *KRAS* and *BRAF* (p=0.005) and *ARID1A* (p=0.05) were found exclusively in polypoid lesions within areas of colitis.

**Table 1**: Mutation incidence for key colorectal adenocarcinoma genes across cohorts.

| Genes analyzed | Cohort 1 (Polypoid dysplasia within areas of known colitis in IBD patients) (n=14) | Cohort 2 (Polypoid dysplasia outside areas of colitis in IBD patients) (n= 8) | Cohort 3 (Sporadic adenomas in non-IBD patients) (n=5) | Cohort 2 vs 3 P value | Cohort 1 vs Cohorts 2 + 3 P value |
|---|---|---|---|---|---|
| *APC* | 9 (64%) | 7 (88%) | 4 (80%) | 0.6 | 0.38 |
| *KRAS* | 6 (43%) | 0 | 0 | 1 | **0.015** |
| *BRAF* | 1 (7%) | 0 | 0 | 1 | 0.5 |
| *KRAS+BRAF* | 7 (50%) | 0 | 0 | 1 | **0.005** |
| *CTNNB1* | 1 (7%) | 3 (38%) | 2 (40%) | 0.68 | 0.06 |
| *FBXW7* | 3 (21%) | 1 (13%) | 0 | 0.61 | 0.6 |
| *TP53* | 2 (14%) | 0 | 0 | 1 | 0.48 |
| *TCF7* | 1 (7%) | 0 | 0 | 1 | 0.5 |
| *TCF7L12* | 1 (7%) | 0 | 0 | 1 | 0.5 |
| *RNF43* | 1 (7%) | 0 | 0 | 1 | 0.5 |
| *ARID1A* | 4 (29%) | 0 | 0 | 1 | **0.05** |

**Conclusions:** Polypoid dysplastic lesions that arise outside areas of known colitis in UC patients are molecularly similar to sporadic adenomas arising in non-IBD patients. Polypoid dysplastic lesions arising within a field of IBD

are more likely to harbor *KRAS/BRAF* driver alterations and *ARID1A* mutations suggesting that these lesions develop via different molecular pathways than sporadic adenomas.

### 329 Clinical, Histological, and Molecular Features of Cribriform Morphology in Colorectal Cancers from The Cancer Genome Atlas

Philippe Echelard[1], Anne Xuan-Lan Nguyen[2], Vincent Quoc-Huy Trinh[3]
[1]Université de Sherbrooke, Sherbrooke, Canada, [2]McGill University, Montréal, Canada, [3]Vanderbilt University Medical Center, Nashville, TN

**Disclosures:** Philippe Echelard: None; Anne Xuan-Lan Nguyen: None; Vincent Quoc-Huy Trinh: None

**Background:** Cribriform comedo-type is a newly included colorectal adenocarcinoma (CRC) subtype in the WHO. Per the AJCC grading system, CRC with cribriform morphology are graded as well to moderately differentiated adenocarcinomas despite some colorectal studies suggesting a worst. This morphology has been shown in other organs, such as the prostate, the lung, and breast, to have significantly different outcomes and molecular features. Our goal is to use the digital slides and the genomic data from the Cancer Genome Atlas (TCGA) to clarify the molecular and prognostic factors associated with cribriform morphology in CRC.

**Design:** 594 CRC are available in the TCGA. Clinical, pathological, histological, digital slides, and molecular data were extracted using different programs in R and from web-based platforms: R, cBioPortal, GDC Legacy Archive, GDC Data Transfer Tool v1.6.0. Cases with insufficient clinical data, no diagnostic slides, or poor slide quality were excluded. Cases were separated into 5 groups based on cribriform studies from the prostate: no-cribriform, loose cribriform, small cribriform glands, diffuse large cribriform, and intraductal carcinoma of the prostate-like (IDCP-like, Figure 1). TCGA coded data, pathology reports, and digital diagnostic slides were reassessed by one GI-liver pathologist and a resident. Each group was correlated with clinical, pathological, histological and molecular features. Overall survival was tested with SPSS v26.

**Results:** 573 CRC were included in the study. Table 1 summarizes all significantly different variables at univariate analyses. Loose cribriform was seen in 6%, small cribriform glands in 10%, diffuse large cribriform in 9%, and IDCP-like in 8.6%. Overall, loose cribriform CRC showed the same trends as no-cribriform. True cribriform (small cribriform, diffuse large, and IDCP-like) were associated with more left-sided tumors (P=0.049), metastatic diseases (P=0.0001), less MSI-H (P=0.003), and different aneuploidy and fraction genome altered (P=0.003-0.008). Tumors with or without cribriform morphology showed the same grading distribution (P=0.523). Furthermore, T and N staging were not associated with cribriform morphology. Other than MSI-H, they did not harbor any different mutation patterns for typically sequenced genes. Overall survival was significant at Log-rank testing (P=0.037), with loose cribriform morphology showing the same survival trends as non-cribriform. In tumors graded moderately differentiated (Figure 2), unequivocal cribriform was associated with poorer outcomes (P=0.026).

| | No Cribriform (n=391) | Loose Cribriform (n=23) | Small Cribriforming Glands Infiltrating (n=57) | Large Dense Cribriform (n=53) | Large Cribriform IDC-Prostate-Like (n=49) | P |
|---|---|---|---|---|---|---|
| Localisation | 63 (19%) | 2 (10%) | 5 (10%) | 5 (11%) | 6 (13%) | |
| Caecum | 97 (29%) | 4 (19%) | 13 (26%) | 12 (26%) | 4 (9%) | |
| Right Colon | 14 (4%) | 0 (0%) | 2 (4%) | 3 (7%) | 2 (4%) | 0.049 |
| Transverse Colon | 19 (6%) | 1 (5%) | 0 (0%) | 3 (7%) | 1 (2%) | |
| Left Colon | 61 (18%) | 9 (43%) | 10 (20%) | 8 (17%) | 11 (23%) | |
| Sigmoid Colon | 83 (24%) | 5 (24%) | 21 (41%) | 15 (33%) | 23 (49%) | |
| | 3 (1%) | 0 (0%) | 0 (0%) | 0 (0%) | 0 (0%) | |

| | Recto-Sigmoid Rectum | | | | | |
|---|---|---|---|---|---|---|
| Clinical TNM | 13 (4%) | 0 (0%) | 0 (0%) | 0 (0%) | 3 (7%) | |
| T Category | 67 (18%) | 4 (20%) | 8 (15%) | 8 (16%) | 10 (22%) | 0.419 |
| T1 | 252 (67%) | 16 (80%) | 39 (74%) | 34 (68%) | 30 (65%) | |
| T2 | 22 (6%) | 0 (0%) | 5 (9%) | 6 (12%) | 3 (7%) | |
| T3 | 20 (5%) | 0 (0%) | 1 (2%) | 2 (4%) | 0 (0%) | |
| T4a | 225 (60%) | 11 (55%) | 29 (55%) | 24 (50%) | 19 (44%) | 0.792 |
| T4b | 37 (10%) | 3 (15%) | 4 (8%) | 4 (8%) | 6 (14%) | |
| N Category | 49 (13%) | 3 (15%) | 8 (15%) | 8 (17%) | 8 (19%) | |
| N0 | 3 (1%) | 0 (0%) | 0 (0%) | 1 (2%) | 0 (0%) | |
| N1a | 22 (6%) | 2 (10%) | 7 (13%) | 6 (13%) | 3 (7%) | 0.001 |
| N1b | 37 (10%) | 1 (5%) | 5 (9%) | 5 (10%) | 7 (16%) | |
| N1c | 375 (95%) | 22 (96%) | 49 (86%) | 44 (83%) | 43 (88%) | |
| N2a | 13 (3%) | 0 (0%) | 8 (14%) | 7 (13%) | 4 (8%) | |
| N2b | 0 (0%) | 1 (4%) | 0 (0%) | 1 (2%) | 1 (2%) | |
| M Category | 5 (1%) | 0 (0%) | 0 (0%) | 1 (2%) | 1 (2%) | |
| MX | | | | | | |
| M1a | | | | | | |
| M1b | | | | | | |
| M1c | | | | | | |
| Differentiation Grade | 16 (4%) | 2 (9%) | 1 (2%) | 2 (4%) | 1 (2%) | 0.528 |
| Well Diff. (G1) | 287 (73%) | 16 (70%) | 47 (83%) | 41 (77%) | 39 (80%) | |
| Moderately Diff. (G2) | 87 (22%) | 5 (22%) | 7 (12%) | 9 (17%) | 9 (18%) | |
| Poorly Diff. (G3) | 3 (1%) | 0 (0%) | 2 (4%) | 1 (2%) | 0 (0%) | |
| Undifferentiated (G4) | | | | | | |
| MSI-H by the MSI Sensor Score (>10) | 61 (18%) | 0 (0%) | 4 (8.2%) | 2 (5%) | 2 (4%) | 0.003 |
| Median aneuploidy Score (std dev)) | 11.51 (8.29) | 13.04 (1.56) | 14.14 (8.16) | 12.38 (6.85) | 15.86 (6.89) | 0.003 |
| Fraction Genome Altered | 0.23 (0.17) | 0.28 (0.18) | 0.26 (0.17) | 0.28 (0.17) | 0.32 (0.16) | 0.008 |

Figure 1 - 329
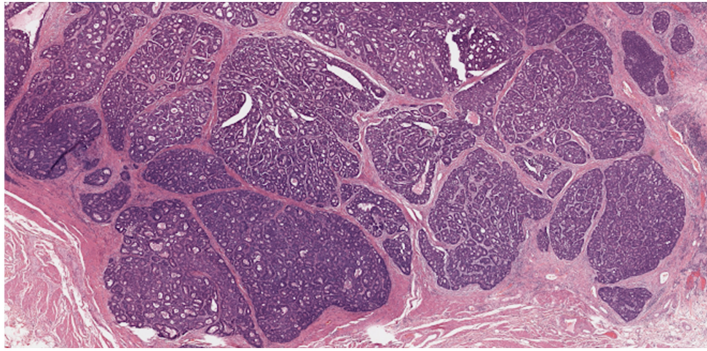


Figure 2 - 329
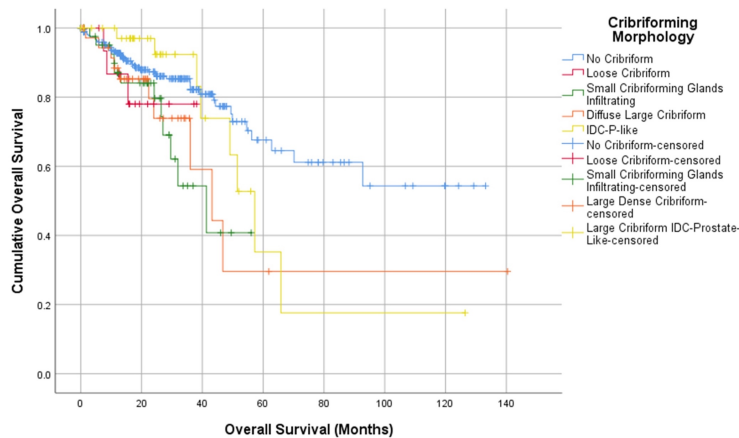


**Conclusions:** Unequivocally cribriform CRC might be associated with poorer outcomes and less microsatellite instability. Validation with our institutional cohort and additional genomic characterization are currently underway.

**330    Hierarchical Clustering of Immune Checkpoint Gene Expression in Colorectal Adenocarcinoma from the TCGA Reveals Discordant Survival Patterns Associated with Over- and Under- Expression**

Philippe Echelard[1], Anne Xuan-Lan Nguyen[2], Vincent Quoc-Huy Trinh[3]
[1]Université de Sherbrooke, Sherbrooke, Canada, [2]McGill University, Montréal, Canada, [3]Vanderbilt University Medical Center, Nashville, TN

**Disclosures:** Philippe Echelard: None; Anne Xuan-Lan Nguyen: None; Vincent Quoc-Huy Trinh: None

**Background:** Immune Checkpoint (IC) inhibitors have a clear therapeutic role in the treatment of colorectal adenocarcinoma (CRC). Still, no obvious biomarker other than MMR and microsatellite status are predictive of response. Studies focusing on PD-L1 are still inconclusive in its ability to predict response to immunotherapy. In this study, we aimed to explore the association between IC gene expression as a whole and clinico-pathological factor in CECRCC from the TCGA dataset.

**Design:** 594 CRC are available from TCGA. Known IC genes were selected from Pubmed-cited publications from 2010-2020. Hierarchical clustering of IC genes Z-scores was performed in Morpheus (Broad Institute) with

complete linkage and Euclidean distance. Immune activation classes were selected by partially supervised clustering. TCGA coded data, pathology reports, and digital diagnostic slides were reassessed by two pathologists, and data was aggregated. All data forms were tested stratified according to IC classes at univariate analyses, which only included tumors in which the invasive front was observed. Overall survival according to classes were also assessed with Kaplan-Meier curves and log-rank testing for all cases. Statistics were performed in SPSS v26.

**Results:** Six clear groups were determined by IC gene expression (Figure 1). Significant clinical variables include tumor location, as right-sided tumors were more often in high IC groups (P=0.037, Table 1). Higher IC groups had larger tumors (P=0.004) and less differentiated (P=0.007). Intratumoral lymphocytes were associated with overexpressed IC groups (P<0.001), while peritumoral lymphocytes were also associated to a lesser degree (P=0.013). The Very High IC activation group contained most of the MMR gene mutated patients from the TCGA, while the High group contained only 1. BRAF was also significantly more mutated in the higher IC groups. At overall survival studies, although not significant when fragmented into 6 different groups, some trends were noted. The best survival was seen in the intermediate IC group, while over- and under-expression of IC genes, as a whole, were associated with poorer outcomes.

| | Class 1: CheckPoint Very High (n=44) | Class 2: CheckPoint High (n=113) | Class 3: CheckPoint Intermediate (n=96) | Class 4: CheckPoint Low (n=60) | Class 5: CheckPoint Very Low (n=83) | Class 6: CheckPoint Very Low with Residual Activation (n=11) | P |
|---|---|---|---|---|---|---|---|
| Localisation | 11 (29%) | 18 (19%) | 17 (19%) | 8 (15%) | 14 (18%) | 0 (0%) | |
| Caecum | 16 (42%) | 31 (32%) | 25 (28%) | 6 (11%) | 15 (19%) | 3 (33%) | 0.037 |
| Right Colon | 1 (3%) | 4 (4%) | 4 (5%) | 2 (4%) | 0 (0%) | 1 (11%) | |
| Transverse Colon | 1 (3%) | 4 (4%) | 4 (5%) | 3 (6%) | 6 (8%) | 0 (0%) | |
| Left Colon | 0 (0%) | 15 (16%) | 16 (18%) | 13 (25%) | 25 (32%) | 3 (33%) | |
| Sigmoid Colon | 9 (24%) | 25 (26%) | 22 (25%) | 20 (38%) | 18 (23%) | 2 (22%) | |
| Recto-Sigmoid | 0 (0%) | 0 (0%) | 0 (0%) | 1 (2%) | 1 (1%) | 0 (0%) | |
| Rectum | | | | | | | |
| Tumor Greatest Dimension in cm (mean and std dev) | 6.79 (2.95) | 5.23 (2.32) | 5.47 (2.10) | 4.77 (1.93) | 5.13 (2.17) | 4.79 (1.93) | 0.004 |
| Differentiation Grade | 0 (0%) | 7 (6%) | 5 (5%) | 1 (2%) | 4 (5%) | 0 (0%) | 0.007 |
| Well Diff. (G1) | 23 (52%) | 89 (79%) | 70 (73%) | 49 (82%) | 65 (77%) | 9 (82%) | |
| Moderately Diff. (G2) | 21 (48%) | 15 (13%) | 19 (20%) | 10 (17%) | 13 (16%) | 2 (18%) | |
| Poorly Diff. (G3) | 0 (0%) | 2 (2%) | 2 (2%) | 0 (0%) | 2 (2%) | 0 (0%) | |
| Undifferentiated (G4) | | | | | | | |
| Intratumoral Lymphocytes | 17 (40%) | 82 (73%) | 74 (77%) | 48 (80%) | 78 (93%) | 8 (73%) | <0.001 |
| None | 8 (19%) | 19 (17%) | 12 (13%) | 6 (10%) | 4 (5) | 3 (27%) | |
| | 18 (42%) | 12 (11%) | 10 (10%) | 6 (10%) | 2 (2%) | 0 (0%) | |

| | | | | | | |
|---|---|---|---|---|---|---|
| Mild | | | | | | |
| Brisk | | | | | | |
| Peritumoral Lymphocytes | 12 (27%) | 24 (21%) | 27 (28%) | 26 (43%) | 34 (41%) | 5 (46%) | 0.013 |
| None | 17 (39%) | 57 (50%) | 40 (42%) | 25 (42%) | 36 (43%) | 6 (55%) | |
| Mild | 15 (34%) | 32 (28%) | 29 (30%) | 9 (15%) | 14 (17%) | 0 (0%) | |
| Brisk | | | | | | | |
| MSI-H Sensor Score (std dev) | 19 (50%) | 15 (15%) | 16 (18%) | 1 (2%) | 4 (5%) | 0 (0%) | <0.001 |
| BRAF alteration | 14 (32%) | 15 (13%) | 9 (9%) | 1 (2%) | 5 (6%) | 0 (0%) | <0.001 |
| MSI genes alteration | 3 (7%) | 1 (1%) | 4 (4%) | 0 (0%) | 1 (1%) | 0 (0%) | 0.110 |
| MLH1 | 3 (7%) | 0 (0%) | 2 (2%) | 0 (0%) | 1 (1% | 0 (0%) | 0.039 |
| MSH2 | 5 (11%) | 0 (0%) | 0 (0%) | 1 (2%) | 0 (0%) | 0 (0%) | <0.001 |
| MSH6 | 2 (5%) | 0 (0%) | 1 (1%) | 0 (0%) | 0 (0%) | 0 (0%) | 0.54 |
| PMS2 | | | | | | | |
| Mean aneuploidy Score (std dev) | 8.67 (9.12) | 12.78 (8.79) | 11.15 (8.60) | 15.23 (6.87) | 13.40 (6.61) | 11.36 (7.63) | 0.001 |
| Mean fraction Genome Altered (std dve) | 0.13 (0.14) | 0.22 (0.16) | 0.22 (0.17) | 0.32 (0.14) | 0.31 (0.16) | 0.24 (0.18) | <0.001 |
| Mean mutation Count | 1233 (1652) | 349 (750) | 440 (873) | 236 (974) | 133 (162) | 70 (28) | <0.001 |

Figure 1 - 330
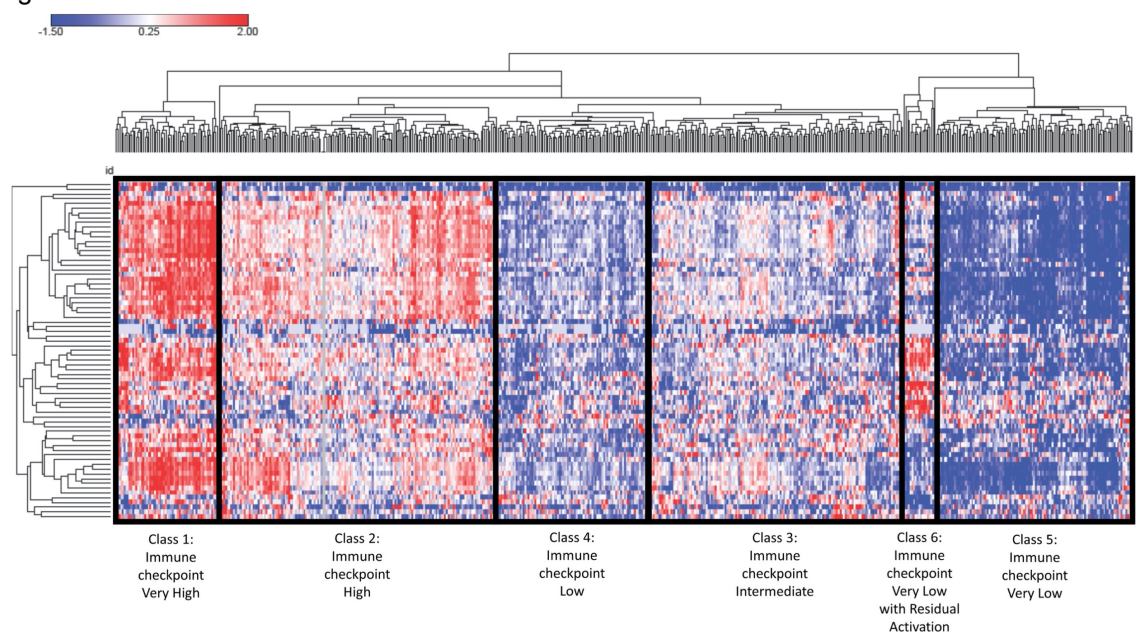
Figure 2 - 330
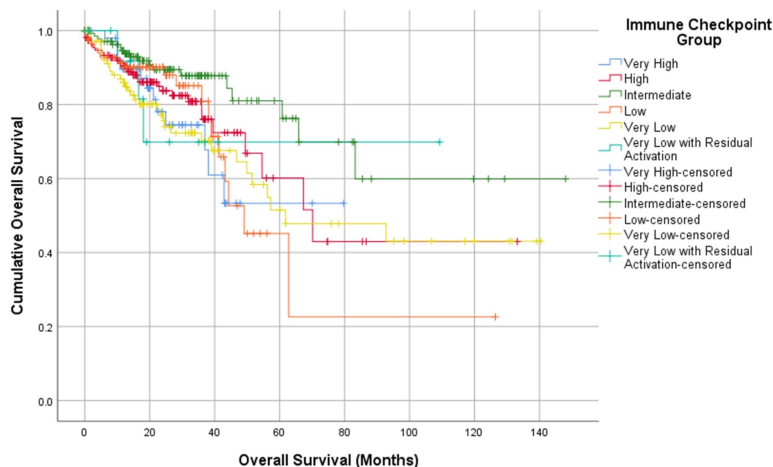


**Conclusions:** Instead of testing each immune checkpoint gene at a time, a global approach to genes with this function reveals interesting particularities in the context of immune checkpoint in CRC. The abnormal expression of these genes in CRC, with opposite ends of the expression spectrum showing worst overall survival, parallels the abnormal role of immune regulation in CRC and warrants further in depth studies.

**331    Severe Fibrosis in Refractory Crohns Disease is Highly Associated with Intense IgG4 Plasma Cell Infiltration**

David Escobar[1], Omar Bushara[2], Guang-Yu Yang[3]
[1]McGaw Medical Center of Northwestern University, Chicago, IL, [2]Feinberg School of Medicine/Northwestern University, Chicago, IL, [3]Northwestern University, Chicago, IL

**Disclosures:** David Escobar: None; Omar Bushara: None; Guang-Yu Yang: None

**Background:** Crohns disease (CD) is a chronic inflammatory bowel disease (IBD) frequently complicated by refractory fibrosis with stricture formation that often requires surgical intervention. Unbalanced wound healing leads to excess fibrogenesis that may not respond to anti-inflammatory therapy. While systemic fibrotic disease has been linked to excessive IgG4-type plasma cells (PC), the contribution of IgG4+ PCs to CD fibrosis is unclear. Recent studies suggest that presence of IgG4+ PCs correlates with higher grade of disease activity, however the pathophysiologic mechanism by which IgG4+ PCs may promote fibrosis in CD remains unknown. In this study, we analyzed the intensity of IgG4+ PCs and its association with severity of fibrosis in refractory CD.

**Design:** Within our pathology database for surgical resections for inflammatory bowel disease, we identified 20 cases of refractory Crohns disease with at least partial colonic resection that demonstrated gross evidence of stricture formation. 25 age- and sex-matched cases of Crohns disease without gross evidence of stricture formation were also identified. H&E slides were inspected and inflammatory activity severity was reported using the simplified Geboes scoring system (J Crohns Colitis. 2017 Mar 1;11(3):305-313). Histologic staining for Masson Trichrome was performed and the degree of fibrosis was measured and quantified using the criteria described in Chiorean et. al (Am J Gastroenterol 2007;102:2541–2550). An immunohistochemical stain for IgG4 was performed on each case and the number of IgG4+ PCs were quantified and averaged for at least 10 high-power fields (HPF). Student's t-test, ANOVA, chi-square, and Fischer's exact tests were calculated, as appropriate.

**Results:** The demographics of the case cohort are shown in the results table. 40 cases (88.9%) showed Geboes score of Grade 2A or higher, and 26 cases (59.1%) were Grade 4, most often due to ulceration and granulation tissue formation. Increased IgG4+ PCs per HPF were associated with increased severity of histologic fibrosis score (Figure 1a, overall p=0.037), regardless of presence or absence of grossly evident stricture formation (Figure 1b, overall p=0.0217). IgG4+ PCs were not significantly associated with extent of active inflammatory disease activity.

| Case Demographics | | |
|---|---|---|
| | | |
| Total Number | 45 | |
| Mean age | 42.8 | |
| Age range | 22-73 | |
| | | |
| Sex | | |
| Female | 23 | 52.3% |
| Male | 21 | 47.7% |
| | | |
| Geboes Score | | |
| Grade 0 | 2 | 4.5% |
| Grade 1 | 2 | 4.5% |
| Grade 2A | 1 | 2.3% |
| Grade 2B | 8 | 18.2% |
| Grade 3 | 5 | 11.4% |
| Grade 4 | 26 | 59.1% |
| | | |
| Gross Stricture | | |
| Present | 20 | 44.4% |
| Absent | 25 | 55.6% |
| | | |
| Stricutre Location | | |
| Small Bowel/ Ileum | 9 | 20.5% |
| Ileocecal valve | 24 | 54.5% |
| Colon | 11 | 25.0% |
| | | |
| Fibrosis Score | | |
| 0 | 7 | 15.9% |
| 1 | 20 | 45.5% |
| 2 | 17 | 38.6% |

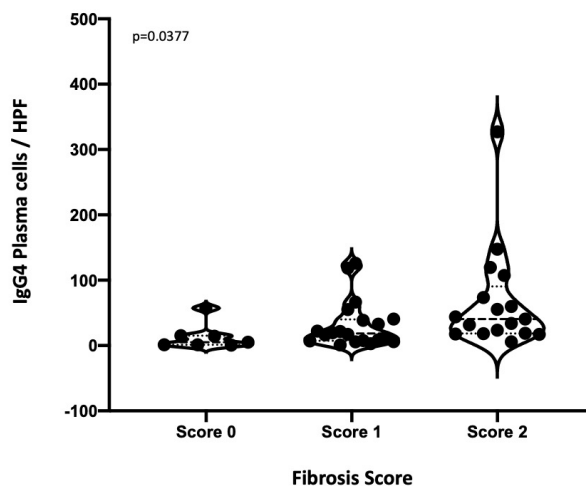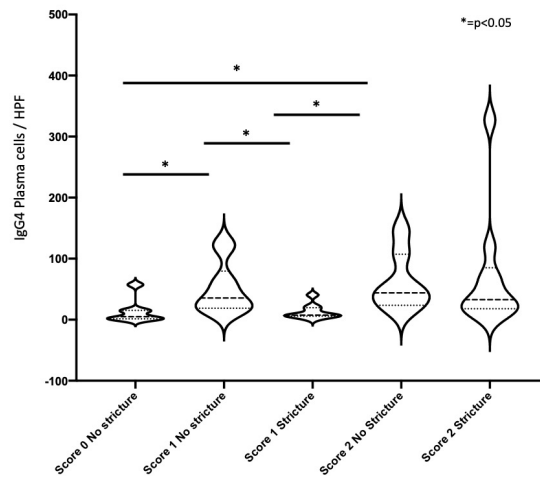**Table 1:** Case cohort demographs

Figure 1 - 331

Figure 2 - 331



**Conclusions:** Increased IgG4+ plasma cell infiltration is significantly associated with severe fibrosis in refractory Crohns disease regardless of inflammatory activity. Our results imply IgG4+ PCs promote fibrogenesis, and underlying biological mechanisms remain a target of future investigation.

## 332 FBXW7 Mutations in Colorectal Carcinoma Lead to Aberrant Localization of Beta-Catenin and Are Not Coincident with CTNNB1 Mutations

David Escobar[1], Leyu Sun[2], Omar Bushara[3], Guang-Yu Yang[2]
[1]McGaw Medical Center of Northwestern University, Chicago, IL, [2]Northwestern University, Chicago, IL, [3]Feinberg School of Medicine/Northwestern University, Chicago, IL

**Disclosures:** David Escobar: None; Leyu Sun: None; Omar Bushara: None; Guang-Yu Yang: None

**Background:** Mutations in the canonical Wnt signaling pathway, including adenomatous polyposis coli (APC) and *CTNNB1/*β-catenin (β-cat) have been well described and are the most common genetic alteration for colorectal carcinoma (CRC), resulting in aberrant nuclear β-cat localization with subsequent signaling pathway activation and uncontrolled proliferation. More recently described, *FBXW7* serves to antagonize the Wnt pathway by promoting β-cat degradation. Mutations that decrease *FBXW7* function allow unopposed β-cat nuclear accumulation. Although *FBXW7* mutations have been described in several cancer types, the contribution of *FBXW7* in CRC remains under-reported. In this study, we analyzed the frequency of *FBXW7* and *CTNNB1* mutations in CRC using a next generation sequencing (NGS) approach and report the association of *FBXW7* mutation with aberrant β-cat localization using an immunohistochemical approach.

**Design:** We searched our pathology database for colorectal adenocarcinoma cases from 2016 to August 2020 that had both microsatellite instability status data available and NGS sequencing performed and identified 80 CRC cases with at least one mutation in either *FBXW7* or *CTNNB1* for this study. The expression of hMLH1, hMSH2, hMSH6, and hPMS2 was reported as intact (stable, MSS) or lost (unstable, MSI). An Ion AmpliSeq second generation sequencing panel was performed using either a 22 gene panel or an expanded 161 gene panel for cases identified after March 2019. Immunohistochemical staining for β-cat and the localization pattern was reported as membranous, cytoplasmic, and/or nuclear. Student's t-test, ANOVA, chi-square, and Fischer's exact tests were calculated, as appropriate.

**Results:** The overall case demographics of the cases cohort is shown in the results table. 69 cases (85.2%) showed mutations in *FBXW7*, which resulted in β-cat cytoplasmic or nuclear localization in 85.3% and 50.0%, respectively. *FBXW7* mutated tumors were significantly more frequently MSS tumors, compared to CTNNB1 (80.9% versus 26.7%, p<0.0001). Mutations at *FBXW7* "hotspots" were associated with high frequencies of β-catenin cytoplasmic or nuclear localization (Figure 1). *CTNNB1* was mutated in 13 cases (16.0%) with aberrant β-cat localization (100% cytoplasmic and 84.6% nuclear). Another unique feature was

that *FBXW7* and *CTNNB1* mutations were generally mutually exclusive events; co-occurrence was observed in only 2 out of 80 cases, one of which had MSI-high/hypermutator phenotype.

| Case Demographics | | |
|---|---|---|
| | | |
| Total Number | 80 | |
| Mean Age | 59.8 | |
| Age Range | 30-90 | |
| Sex | | |
| Male | 41 | 51.3% |
| Female | 42 | 52.5% |
| | | |
| Tumor Location | | |
| Right | 29 | 36.3% |
| Left | 26 | 32.5% |
| Transverse | 4 | 5.0% |
| Rectum | 20 | 25.0% |
| "Unknown" | 4 | 5.0% |
| | | |
| Tumor Stage | | |
| 0 | 3 | 3.8% |
| I | 9 | 11.3% |
| II | 16 | 20.0% |
| III | 28 | 35.0% |
| IV | 20 | 25.0% |
| Unknown | 7 | 8.8% |
| | | |
| Median Tumor size (cm) | 5.072727273 | 5.1 |
| Tumor size Range | 0.2 | 14.5 |
| | | |
| Tumor Grade | | |
| Low/Mod | 55 | 68.8% |
| High | 28 | 35.0% |
| Unknown/Not Resected/Not indicated | 0 | 0.0% |
| | | |
| Lymph Node | | |
| pNX | 19 | 23.8% |
| pN0 | 31 | 38.8% |
| pN1 | 25 | 31.3% |
| pN2 | 8 | 10.0% |
| | | |
| Metastases | | |
| pMX | 64 | 80.0% |
| pM1 | 19 | 23.8% |
| | | |
| Histology Subtypes | | |
| Adenocarcinoma, NOS | 71 | 88.8% |
| Mucinous | 5 | 6.3% |
| Micropapillary | 4 | 5.0% |
| Signet ring | 2 | 2.5% |
| Adenosquamous | 1 | 1.3% |
| | | |
| MSI | | |
| Intact - Stable | 59 | 73.8% |
| Absent - Unstable | 23 | 28.8% |
| Unknown/Not done | 1 | 1.3% |
| | | |
| Genes mutated | | |
| FBXW7 | 68 | 85.0% |
| CTNNB1 | 13 | 16.3% |
| Both | 2 | 2.5% |

Figure 1 - 332

**Beta-catenin localization**
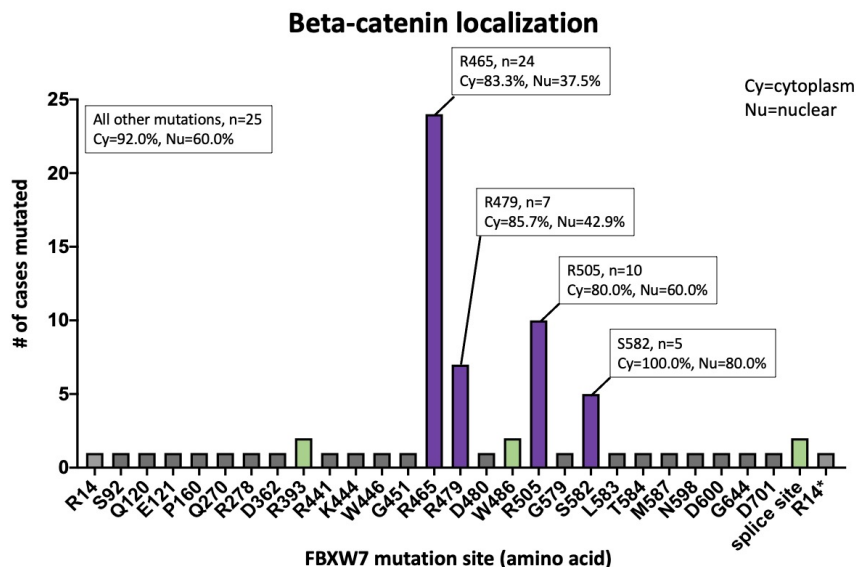


**Conclusions:** Mutations in the Wnt pathway antagonist *FBXW7* in colorectal carcinoma are associated with frequent aberrant β-catenin localization to the cytoplasmic and/or nuclear compartments, indicating the activation of the canonical Wnt pathway. *FBXW7* mutations rarely co-occur with mutations in *CTNNB1*, suggesting a common functional pathway linkage.

**333 Clinicopathologic Characterization of Lichenoid Esophagitis: A Single Institution Experience of 30 Cases**

Mark Ettel[1], Xiaoyan Liao[2]
[1]University of Rochester, Rochester, NY, [2]University of Rochester Medical Center, Rochester, NY

**Disclosures:** Mark Ettel: None; Xiaoyan Liao: None

**Background:** Lichenoid esophagitis (LE) is characterized by lymphocytic inflammatory infiltrates with increased dyskeratotic keratinocytes (Civatte bodies). It can be associated with cutaneous lichen planus (LP) in which case it is best considered LP esophagitis (LPE), while in cases with no evidence of LP it is better characterized as LE pattern (LEP). We aim to compare cases of LPE with LEP to determine clinical implications and associations with other conditions.

**Design:** Esophageal biopsies diagnosed with LE from 2010 to 2020 were identified at our institution, excluding patients with no available clinical history. Statistics were performed using t-test for continuous variables and Fisher's exact test for categorical variables, with significance set at P<0.05.

**Results:** The cohort included 30 patients, 10 females and 7 males, with a mean age of 67 years (range 29-89). Seven (23%) patients had confirmed LPE and 23 (77%) were classified as LEP. There were no significant age or sex differences between LEP and LPE. For both groups, the most common presenting symptoms were dysphagia (n=20, 67%), followed by reflux related symptoms such as pain and heartburn (n=9, 30%). Endoscopically, the most common findings were stricture or narrowing, identified equally in both LPE and LEP (4/7 [57%] vs. 12/23 [52%], NS). Whitish plaques (n=7, 23%) were seen only in patients with LEP, among which 3 cases had biopsy proven Candida. Rings (n=6, 20%) and ulcer/erosion (n=3, 10%) were also noted. Five (17%) cases had normal endoscopic findings. Biopsy sites were distributed equally from proximal to distal esophagus, as well as the gastroesophageal junction. There were no biopsy site differences between LPE and LEP. A variety of underlying conditions were associated with both groups, most commonly gastroesophageal reflux disease (n=8, 27%), diabetes (n=5, 17%), rheumatologic diseases (n=5, 17%), histories of malignancies (n=5,17%), Barrett's post

ablation (n=4,13%), and hypothyroidism (n=4, 13%). One LEP patient had a history of Crohn's disease. Treatments included proton pump inhibitors with or without steroid. Upon follow-up, 2 patients died of other comorbidities.

**Conclusions:** Our study showed that LPE and LEP had remarkable overlap in clinical presentation and endoscopic findings. A variety of underlying conditions were associated with LE. Whitish plaques are a common finding for both LEP and Candidiasis, and thus the latter finding should be considered for work-up of biopsies with LE.

### 334 Mycophenolate Mofetil (MMF) Induced Gastrointestinal Tract Injury: A Single Institutional Experience

Yan Feng[1], Franz Fogt[2], Rifat Mannan[3]
[1]Pennsylvania Hospital, Pennsylvania, PA, [2]Hospital of the University of Pennsylvania, Gladwyne, PA, [3]Perelman School of Medicine at the University of Pennsylvania, Philadelphia, PA

**Disclosures:** Yan Feng: None; Franz Fogt: None; Rifat Mannan: None

**Background:** MMF is an important drug in organ transplantation immune-suppression regimens and known to cause GI mucosal injury. Histologic findings overlap with other causes of acute colitis, importantly acute GVHD. In this study, we sought to analyze the clinicopathologic features of MMF induced GI tract injury.

**Design:** An institutional database was searched for MMF induced GI injury. We retrospectively analyzed clinical, endoscopic, and histologic features from the institutional database over a 4-year period.

**Results:** We identified 27 patients (average age 62.4y, range 35-84; M:F=12:15) on MMF who underwent colonoscopy and biopsy. Detailed results are presented in Table 1. Indications for MMF were solid organ transplants (n=22, 81%), stem cell/bone marrow transplants (n=4, 15%), and Takayasu arteritis (n=1, 4%). Patients presented with watery (n=14, 52%), bloody (n=1, 4%), or chronic non-bloody diarrhea (n=12, 44%). Patients with stem cell/bone marrow transplant had associated GVHD. Those patients had shorter onset of symptoms after transplant than those with solid organ transplants (10.5 months vs. 6.2 years, $p<0.05$), while there was no difference in terms of the microscopic changes ($p>0.05$). In addition, 8 patients (30%) had gastric injuries, 8 (30%) had duodenal injuries, and 6 (22%) had small bowel injuries. Colonoscopy revealed subtle mucosal lesions in 4 patients (15%), while others (85%, 23/27) had normal-appearing mucosa. On histology, colonic biopsies revealed crypt architectural distortion (100%, 27/27, Fig. 1A), reactive epithelial changes (93%, 25/27, Fig. 1B), increased crypt epithelial apoptosis, defined as > 3 per 100 crypts (67%, 18/27, Fig. 2A), increased lamina propria eosinophils (70%, 19/27, Fig. 2A), and microabscesses (with apoptotic debris and eosinophils, 30%, 8/27, Fig. 2B). CMV was identified in 1 patient (4%), while CMV immunohistochemistry was performed in 8 patients.

**Table 1**: Clinicopathologic features of MMF-associated GIT injury:

| Parameter | No. of cases (%) |
|---|---|
| **Sex (F:M)** | 12:15 |
| **MMF indication:** | |
| Solid organ transplant | 22 (81%) |
| SC/BM transplant | 4 (15%) |
| Autoimmune disease | 1 (4%) |
| **Clinical presentation:** | |
| Watery diarrhea | 14 (52%) |
| Bloody diarrhea | 1 (4%) |
| Chronic non-bloody diarrhea | 12 (44%) |
| **Colonoscopy:** | |
| Normal | 23 (85%) |
| Subtle mucosal lesions | 4 (15%) |
| Erosions/ulcerations | 0 (0%) |
| **Histologic findings on colonic biopsies:** | |
| **1. Crypt architectural distortion :** | |

| | |
|---|---|
| Absent | 0 (0%) |
| Mild | 10 (37%) |
| Moderate | 8 (30%) |
| Severe | 9 (33%) |
| **2. Reactive epithelial change:** | |
| Absent | 3 (11%) |
| Mild | 18 (67%) |
| Moderate | 4 (15%) |
| Severe | 2 (7%) |
| **3. Apoptosis (/100 crypts):** | |
| < 3 | 9 (33%) |
| 3-10 | 16 (59%) |
| 11-20 | 1 (4%) |
| >21 | 1 (4%) |
| **4. Eosinophils (/10 HPF):** | |
| < 5 | 8 (30%) |
| 5-20 | 9 (33%) |
| 21-40 | 5 (19%) |
| >41 | 5 (19%) |
| **5. Microabscess:** | |
| Absent | 19 (70%) |
| Present | 8 (30%) |

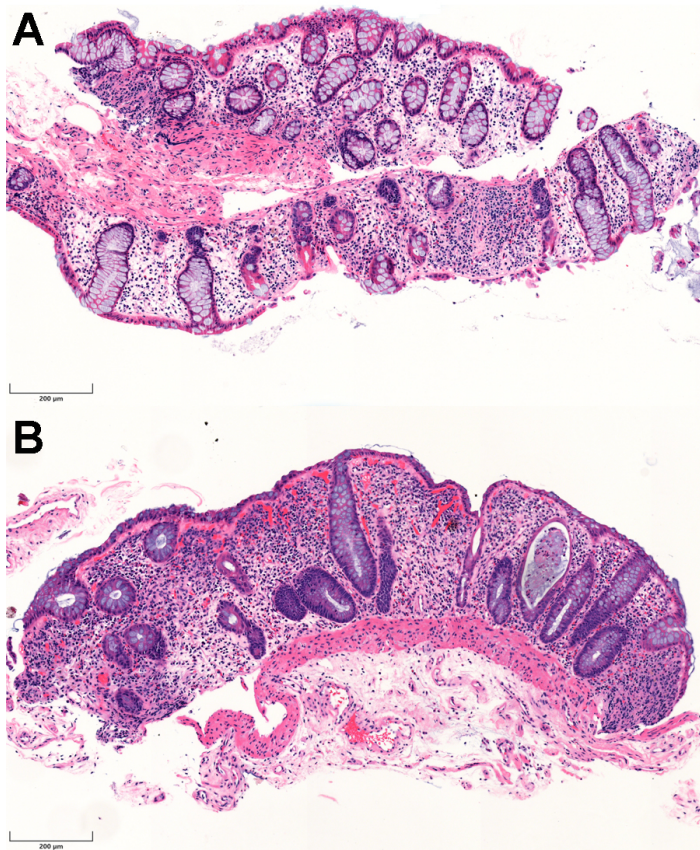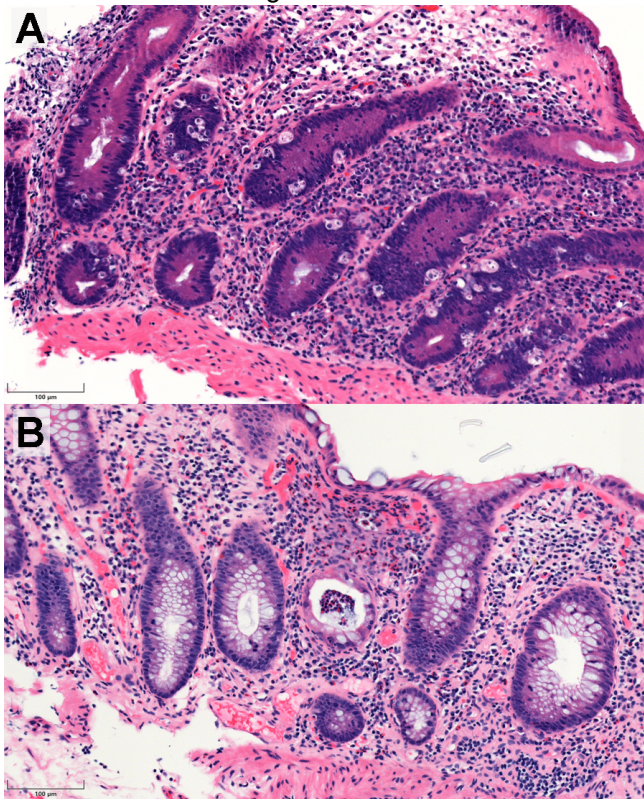SC/BM: Stem cell/Bone marrow

Figure 1 - 334

Figure 2 - 334



**Conclusions:** MMF is an important cause of diarrhea in patients on organ transplantation or autoimmune disease. Colonoscopic findings are often subtle, even when there are obvious microscopic changes. Though increased crypt epithelial apoptosis is historically reported to be a key diagnostic feature of MMF-related colitis, our preliminary data revealed crypt architectural distortion and reactive epithelial change to be more sensitive findings.

**335     HIV Infection and Low CD4 Count are Associated with Faster Progression of HPV-mediated Anal Squamous Intraepithelial Lesions: A Large Clinicopathologic Cohort Study**

Brian Finkelman[1], Sam Weinberg[2], Rebecca Obeng[1], Leyu Sun[3], Jie Liao[3], Guang-Yu Yang[3]
[1]Northwestern University Feinberg School of Medicine, Chicago, IL, [2]McGaw Medical Center of Northwestern University, Chicago, IL, [3]Northwestern University, Chicago, IL

**Disclosures:** Brian Finkelman: None; Sam Weinberg: None; Rebecca Obeng: None; Leyu Sun: None; Jie Liao: None; Guang-Yu Yang: None

**Background:** Anal cancer is common in HIV+ individuals, with an incidence 30 to 80-fold higher than in the general population. HPV infection drives >90% of anal squamous cell carcinoma (SCC), and HIV co-infection may reduce the immune system's ability to clear HPV, leading to higher risk of both anal precursor squamous intraepithelial lesions (SIL) and SCC. However, data on how HIV status and low CD4 affect anal SIL progression at different stages of dysplasia are limited.

**Design:** We collected clinical data on patients with anorectal pathology specimens at our institution from 2010-2019 (5,070 individuals), including laboratory data (81,174 tests) and free text pathology reports (8,987 surgical pathology and 5,797 cytology reports). An algorithm was developed to classify pathology reports as either low-grade SIL (LSIL), high-grade SIL (HSIL), carcinoma in situ (CIS), or SCC, and to exclude SIL outside the anorectum. Age at first SIL diagnosis was compared by HIV status via the t-test. We assessed rate of progression at each stage of anal SIL, by HIV and CD4 status (any CD4 <200 vs all CD4 ≥200), via Cox proportional hazards models, adjusted for race, gender, and age at original SIL diagnosis.

**Results:** Our final cohort had 2,203 individuals with at least one diagnosis of anorectal SIL, who together had 3,428 LSIL, 729 HSIL, 542 CIS, and 172 SCC diagnoses. There were 940 (43%) HIV+ individuals, 39% of whom had at least one CD4 <200. Median follow-up from first LSIL to first SCC was 3.7 years (range 0.01-16.4). Significant findings (Figs 1 and 2) were: 1) mean age at first diagnosis in HIV+ vs HIV- individuals was 44.7 vs 49.7 years for CIS (P<0.001), and 50.2 vs 60.5 years for SCC (P<0.001); 2) HIV+ individuals had faster progression from LSIL to HSIL+ (HR=1.20, P=0.03), from HSIL to CIS+ (HR=1.43, P=0.02), and from CIS to SCC (HR=2.08, P=0.03); and 3) among HIV+ individuals, those with low CD4 had faster progression from HSIL to CIS+ (HR=1.58, P=0.002) and from CIS to SCC (HR=2.54, P=0.01).
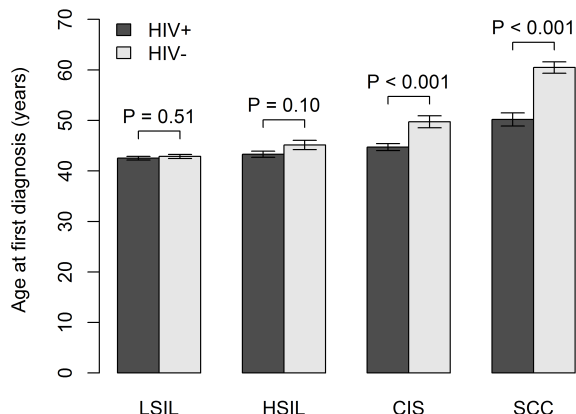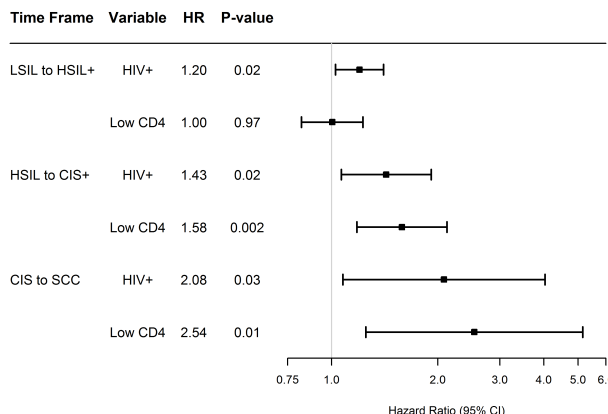
Figure 1 - 335



Figure 2 - 335



**Conclusions:** To our knowledge, this is the largest cohort study to date comparing rates of progression at successive stages of anal SIL by HIV and CD4 status. We found that HIV+ individuals were younger at first CIS and SCC, had faster rates of anal SIL progression at all stages of SIL, and had even faster progression with low CD4 count, with effects appearing stronger with greater dysplasia. Our results provide a strong rationale to further elucidate the biological mechanisms underlying these epidemiologic trends.

**336    Computer Algorithm Learning Process and Initial Mistakes are Similar to Those Expected from Human Students in Evaluation of Colorectal Cancer Tumor Budding**
Eric Freitag[1], Muhammad Khalid Khan Niazi[2], Deborah Knight[1], Metin Gurcan[3], Wendy Frankel[1], Wei Chen[1]
[1]The Ohio State University Wexner Medical Center, Columbus, OH, [2]Wake Forest School of Medicine, Winston-Salem, NC, [3]Center for Biomedical Informatics at Wake Forest University, Winston-Salem, NC

**Disclosures:** Eric Freitag: None; Muhammad Khalid Khan Niazi: None; Deborah Knight: None; Metin Gurcan: None; Wendy Frankel: None; Wei Chen: None

**Background:** Digital image analysis by artificial intelligence is a helpful tool that empowers the pathologist for a more efficient sign out. Tumor budding (TB) has emerged as an adverse prognostic factor for colorectal cancer (CRC); however, manual assessment of TB is time-consuming and subjective. Developing and training a computer algorithm to recognize TB on Hematoxylin & Eosin (H&E) stained slides can be helpful for daily practice, as TB reporting is now recommended on select cases. In this study, we examined the learning curve and initial mistakes of a computer algorithm that automates morphometric analysis of TB in CRC.

**Design:** The development of the computer algorithm consisted of two steps: 1) Identify and differentiate malignant glands from other anatomical structures using two competing conditional Generative Adversarial Networks (cGANs); 2) Identify TB around the resulting borders of malignant glands. The two cGANs were trained in a 4-fold cross-validation of 24 H&E slides of CRC that were manually annotated for tumor and non-tumor regions based on manual registration with respective pan-cytokeratin slides. Furthermore, external testing on a set of 270 high power fields from 91 H&E slides was performed, as we previously reported. After the initial evaluation and refinement of

the results produced by the cGAN model, we utilized DeepLabv3+ to identify malignant glands. All slides were scanned at 40X and were marked by pathologists as the gold standard for comparison.

**Results:** During the initial algorithm development process, the computer mistook several histologic mimickers as tumor cells, including reactive stromal cells, ganglion cells, smooth muscle bundles, vessels, inflammatory cells, necrotic debris, and calcifications (Figures 1 & 2, computer marking = green lines; short arrows = structures mistaken for tumor cells; long arrows = missed tumor cells). Other difficulties the algorithm had were distinguishing carcinoma cells from hyperchromatic crypt bases, adenoma, identifying tumor cells floating in mucin or hidden in perineural spaces (Figure 2, circle), and distinguishing tumor cells from background stroma and inflammation that had similar color characteristics. After corrections by pathologists (Figures 1 & 2, red lines) and engineers, the average precision increased by 9% with a standard deviation of 1.2%.

Figure 1 - 336
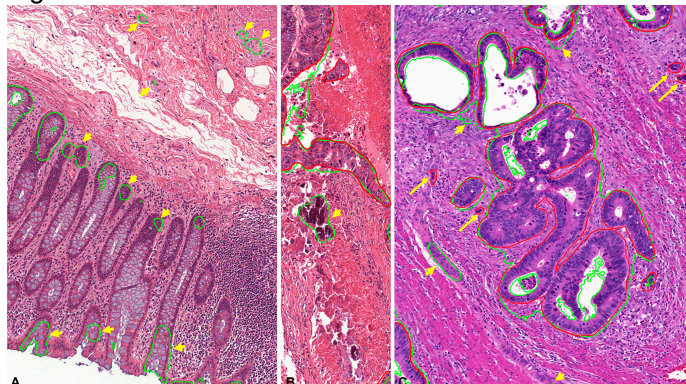


Figure 2 - 336
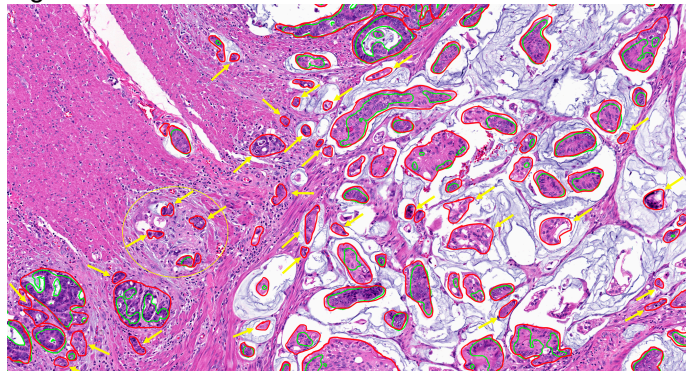


**Conclusions:** To the best of our knowledge, this is the first *de novo* systematic development of a computer algorithm to detect TB from H&E slides of CRC. The computer algorithm was successful in identifying carcinoma and TB, but during the learning process it made mistakes similar to what we would expect from a novice pathology student.

**337 Histologic Features of Diverted Colon in Inflammatory Bowel Disease (IBD) are Distinct from Non-IBD: Reappraisal of Diversion Colitis**

Zhiyan Fu[1], Michel Kmeid[1], Soe Htet Arker[1], Georgi Lukose[1], Edward Lee[2], Hwa Lee[1]
[1]Albany Medical Center, Albany, NY, [2]Albany Medical College, Albany, NY

**Disclosures:** Zhiyan Fu: None; Michel Kmeid: None; Soe Htet Arker: None; Georgi Lukose: None; Edward Lee: None; Hwa Lee: None

**Background:** Diversion colitis (DC) refers to an inflammatory condition involving defunctioned bowel segment isolated from the fecal stream. Histologically, DC is characterized by intramucosal lymphoid aggregates (IMLAs)

with or without variable degree of acute inflammation. Significant histologic overlap between DC and recurrence/progression of IBD poses diagnostic challenges. We aimed to identify histologic features that are common in diverted segments of IBD compared to non-IBD patients, and correlate them with histologic findings in IBD colectomies.

**Design:** Archived slides of resected diverted colon segments from IBD patients (n=79) were reviewed and compared to corresponding prior colectomy specimens (n=52). Resected diverted colon segments from non-IBD patients (n=80) were used as controls. Histologic features including activity, ulcer, architectural distortion, mucosal atrophy, IMLAs, transmural lymphoid aggregates (TMLAs), and transmural inflammation (TMI) were evaluated and graded. Clinical and endoscopic data were collected. Chi square test was performed to compare categorical variables and Mann-Whitney U test to compare continuous variables with significance defined as $p<0.05$.

**Results:** Compared to non-IBD controls, IBD patients were younger (mean age 36.3 vs 57.2 years, $p<0.001$), and more likely to have gastrointestinal symptoms or abnormal endoscopic findings (erythema, friability or nodularity) ($p<0.05$). The duration of diversion was similar (mean 5.5 vs 5.6 months, $p>0.05$) in IBD and control patients. The grades of architectural distortion, mucosal atrophy, TMI, ulcer, IMLAs and TMLAs in diverted segments were significantly higher in IBD compared to controls ($p< 0.001$) [Table 1]. Among these, activity and ulcer in diverted segments were associated with those in colectomies and their distal margins (sections contiguous to diverted segment). IMLAs, TMI and TMLAs in diverted segments correlated with activity, fissuring ulcer and TMI in colectomies, respectively ($p<0.05$).

| Table 1 Clinical presentations and histopathologic evaluation of diverted bowel segments in IBD vs control | | | |
|---|---|---|---|
| | Control, n/N (%) | IBD, n/N (%) | p-value |
| Crohn's disease | | 15/79 (19.0) | |
| Ulcerative colitis | | 63/79 (79.7) | |
| Indeterminate colitis | | 1/79 (1.3) | |
| Diverticulitis | 57/80 (71.3) | | |
| Malignancy/ mass | 10/80 (12.5) | | |
| Other colon perforation (trauma, iatrogenic) | 8/80 (10.0) | | |
| Other (ischemia, obstruction, volvulus) | 5/80 (6.3) | | |
| Age, years, range (mean, median) | 20-90 (57.2, 54.0) | 10-79 (36.3, 35.0) | <0.001[†] |
| Sex, Male | 42/80 (52.5) | 40/79 (50.6) | 0.874 |
| Specimen length, cm, range (mean, median) | 1.5-60.2 (6.8, 5.5) | 3.7-82.2 (13.8, 16.7) | <0.001[†] |
| Duration of diversion, months, range (mean) | 2.5-93.2 (5.6) | 2.5-106.6 (5.5) | 0.625[†] |
| Symptoms during diversion | 7/66 (10.6) | 24/78 (30.8) | 0.004 |
| Endoscopy findings in diverted colon | 5/23 (21.7) | 13/19 (68.4) | 0.004 |
| Architectural Distortion, 1 or 2 | 7/80 (8.8) | 72/77 (93.5) | <0.001 |
| Activity | | | <0.001 |
| 0 | 63/80 (78.8) | 10/79 (12.7) | |
| 1 | 17/80 (21.3) | 15/79 (19.0) | |
| 2 | 0/80 (0.0) | 18/79 (22.8) | |
| 3 | 0/80 (0.0) | 36/79 (45.6) | |
| Mucosal Atrophy | 0/80 (0) | 57/77 (74.0) | <0.001 |
| Ulcer | 0/79 (0) | 35/79 (44.3) | <0.001 |
| Intramucosal Lymphoid Aggregates | | | <0.001 |
| 0 or 1 | 29/80 (36.3) | 9/78 (11.5) | |
| 2 | 44/80 (55.0) | 15/78 (19.2) | |
| 3 or 4 | 7/80 (8.8) | 54/78 (69.2) | |
| Transmural Inflammation, 1 or 2 | 0/80 (0) | 18/77 (23.3) | <0.001 |
| Transmural Lymphoid Aggregates, 1 or 2 | 3/80 (3.8) | 30.79 (38.0) | <0.001 |

Histologic features were graded as follows: architectural distortion (0-2), activity (0-3), mucosal atrophy (0-1),

ulcer (0-1), IMLAs (0-4), TMI (0-2), and TMLAs (0-2). [†] Mann-Whitney U test p-value

**Conclusions:** DC in IBD is clinically, endoscopically, and histologically distinct from that in non-IBD. Activity, ulcer, intramucosal and transmural lymphoid aggregates and transmural inflammation seen in diverted segments in IBD patients may represent underlying IBD component rather than pure DC, given their strong association with histologic features in colectomies that are reflective of disease activity.

**338     MCM6 Expression Correlates with Risk Category and Survival in Gastrointestinal Stromal Tumor**
Mi-Jin Gu, Yeungnam University College of Medicine, Daegu, South Korea

**Disclosures:** Mi-Jin Gu: None

**Background:** Gastrointestinal stromal tumors (GISTs) are the most common mesenchymal neoplasms of the gastrointestinal tract (GIT) with harboring oncogenic mutations in *KIT* (80–85%) and *PDGFRA* (5–7%). GISTs represent a wide variety of disease prognosis, and prediction of malignant potential is assessed by risk stratification based on tumor location, tumor size, mitotic count. Therefore, to search objective and predictive prognostic marker is necessary. Minichromosome maintenance (MCM) proteins complex composed of 6 groups of proteins (MCM 2-7) and are key proteins in the initiation of DNA synthesis and DNA replication. MCM6 expression has been evaluated in various human cancer types and associated with poor prognosis. However, its prognostic role in mesenchymal neoplasm has not been widely evaluated. To the best of our knowledge, this is the first study to evaluate MCM6 protein expression and its prognostic significance in GISTs.

**Design:** A total of 211 GISTs from the stomach (143 cases), small intestine (64 cases), colon and rectum (2 cases), and extragastrointestinal locations were included in this study. The risk of malignant behavior was classified according to the NIH consensus criteria and AFIP criteria, and further reclassified as low, intermediate, or high risk**.** Immunohistochemistry for MCM6 was performed using an automated Benchmark platform. We defined the MCM6 expression when tumor cells showed nuclear staining with or without cytoplasmic reaction more than 10% of total tumor cells.

**Results:** One hundred thirteen male and 98 female patients with a mean age of 57.7 years were included. The median tumor size was 4.92 cm. The 98 cases (46.4%) exhibited high MCM6 expression (Figure 1).  MCM6 expression was significantly correlated with tumor size, mitotic count, tumor necrosis, recurrence/metastasis, AFIP and NIH risk categories. No significant association was observed between high MCM6 expression and sex, tumor cell type, mucosal invasion, and tumor hemorrhage. The Kaplan–Meier curve showed that patients with high MCM6 expression had a significantly worse OS and DFS (both *p*<0.0001) compared to those with low MCM6 expression (Figure 2). In univariate analyses, OS and DFS were found to be shorter in patients with GISTs with tumor necrosis, recurrence/metastasis, NIH risk category, and high MCM6 expression. In multivariate analyses, high MCM6 expression, recurrence/metastasis, and NIH risk category were independent predictors of poorer OS and DFS.

| Variables | Univariate analysis | | Multivariate analysis | |
|---|---|---|---|---|
|  | HR (95% CI) | *p* | HR (95% CI) | *p* |
| Intermediate vs low risk | 4.785 (0.299-76.577) | 0.268 | 3.561 (0.220-57.666) | 0.371 |
| High vs low risk | 56.220 (7.632-414.106) | <0.0001 | 15.235 (1.886-123.038) | 0.011 |
| MCM6 | 12.185 (4.255-34.897) | <0.0001 | 5.034 (1.655-15.312) | 0.004 |
| Necrosis | 8.039 (3.890-16.613) | <0.001 |  |  |
| Recurrence or metastasis | 63.766 (24.161-168.290) | <0.001 | 12,231 (3.692-40.525) | 0.001 |

Figure 1 - 338
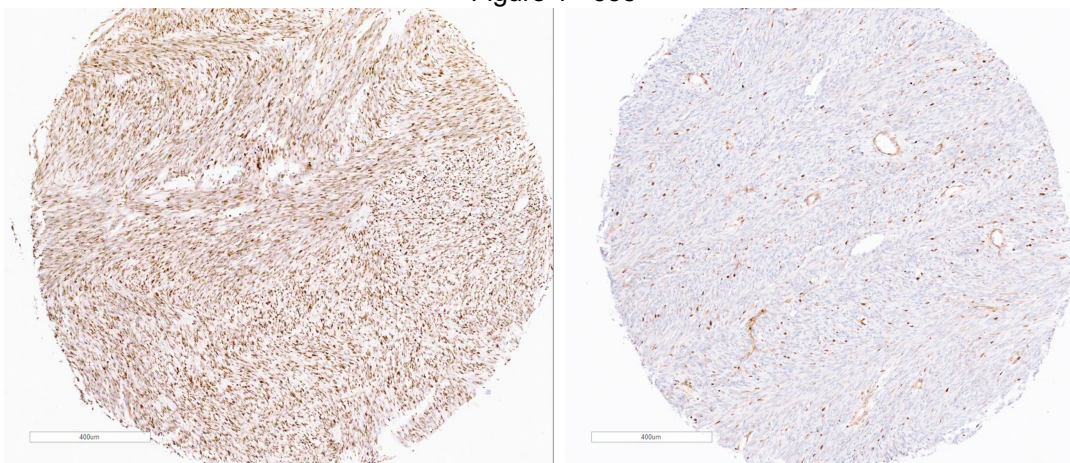
Figure 2 - 338
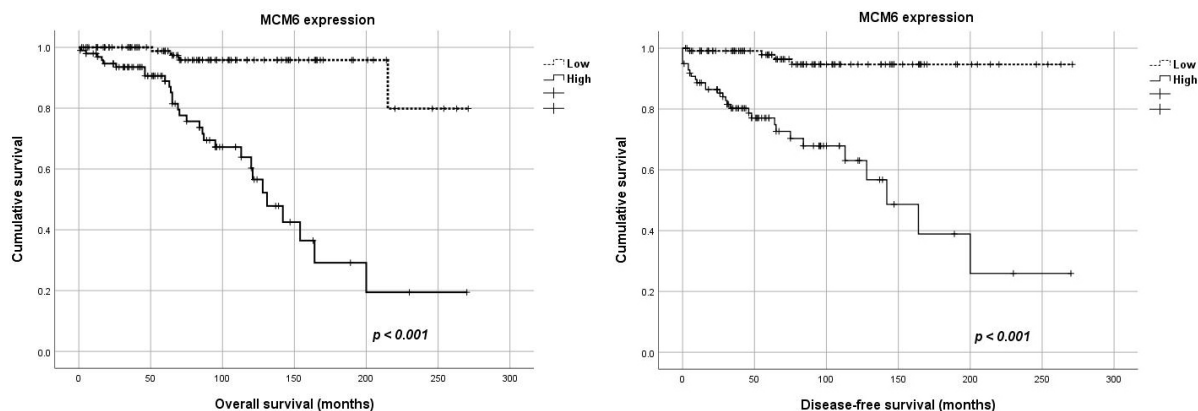


**Conclusions:** In conclusion, our study is the first to assess MCM6 expression and its prognostic value in GISTs. High MCM6 expression was significantly associated with NIH and AFIP risk categories and was an independent adverse prognostic factor. Thus, the assessment of MCM6 expression in patients with GISTs as a routine pathological practice might provide useful information in regard to aggressive behavior.

**339    Malignant Undifferentiated and Rhabdoid Tumors of the Gastroesophageal Junction and Esophagus with SMARCA4 Loss**

Srishti Gupta[1], Stefan Pambuccian[2], Brian Robinson[3], Edward Stelow[4]
[1]University of Virginia, Charlottesville, VA, [2]Loyola University Medical Center, Maywood, IL, [3]Emory University, Atlanta, GA, [4]University of Virginia Health System, Charlottesville, VA

**Disclosures:** Srishti Gupta: None; Stefan Pambuccian: None; Brian Robinson: None; Edward Stelow: None

**Background:** The incidence of esophageal adenocarcinoma is increasing in many parts of the world. Its mutational landscape is complicated and *TP53* is the only gene mutated in more than half of the cases. Approximately 6% of cases have been found to have loss of SMARCA4 expression, although the morphology and ancillary findings of these cases have not been well-described. We present a case series of undifferentiated and rhabdoid esophageal malignancies that were shown to have loss of expression of SMARCA4.

**Design:** Four cases (4/5) of SMARCA4 deficient malignancies of the esophagus or gastrointestinal junction were recognized prospectively during pathologic work-up.  One case (1/5) was identified in a tissue array of 58 cases of esophageal carcinoma.  Immunohistochemistry and in situ hybridization were performed at 3 separate laboratories using standard techniques.  Of note, immunohistochemistry included SMARCA4 (abcam EPR3912 at 1:100 with 30 minute citrate retrieval).

**Results:** Patients' age ranged from 48-79 years; there were 4 men. Three patients were smokers. Diagnosis was made on distal esophageal biopsies in 3 cases, gastroesophageal biopsy in 1 case and an esophageal FNA with cell block in 1 case. One patient had distal metastases at diagnosis.  All 5 cases showed undifferentiated large cells with 4 cases showing rhabdoid cells (Figure 1A). Only one case had intestinal metaplasia, however no cases showed glandular dysplasia. Glandular differentiation was not seen with any of the tumors. An extensive immunohistochemical work-up revealed cases to be immunoreactive with antibodies to keratins (3/5) (Figure 1B), CD34 (2/4), and CD138 (4/5).  All cases showed loss of SMARCA4 (Figure 1C) with intact SMARCB1.

Figure 1 - 339
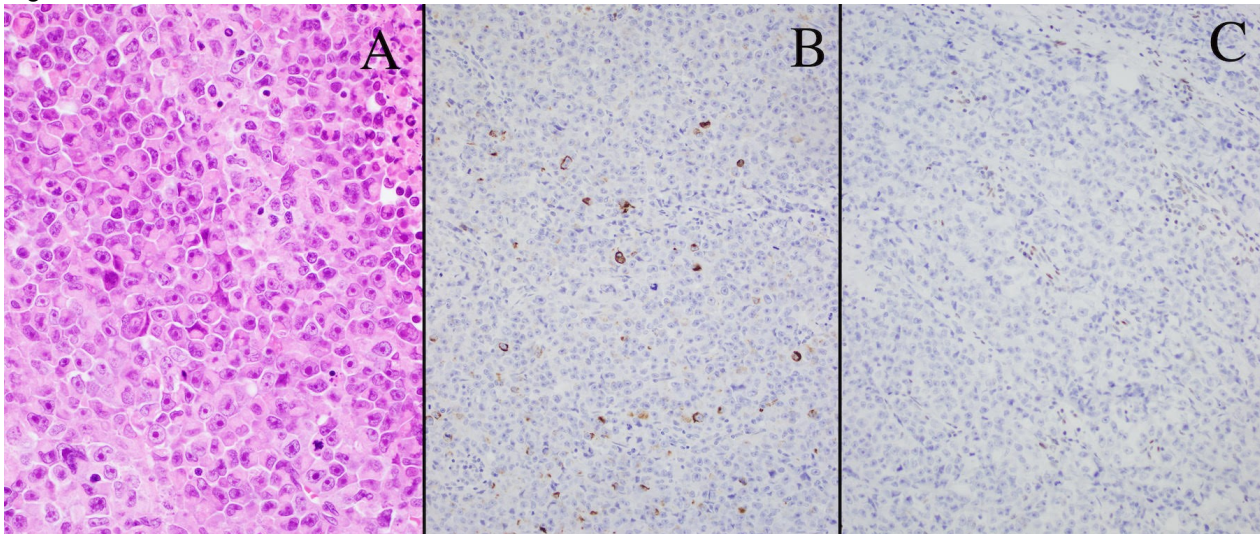


**Conclusions:** Undifferentiated and rhabdoid SMARCA4-deficient esophageal tumors pose diagnostic difficulties. Most cases require an extensive immunohistochemical work-up as both hematolymphoid neoplasms and sarcomas are considered in the differential diagnosis. Pathologists must recognize this as a distinctive morphologic and immunohistochemical phenotype if these tumors are to be correctly classified.

**340    Relationship Between Race, Gastric Injury Patterns, and Intestinal Metaplasia**
Suntrea Hammer[1], James Mitchell[1], Dakota Deutsch[1]
[1]UT Southwestern Medical Center, Dallas, TX

**Disclosures:** Suntrea Hammer: None; James Mitchell: None; Dakota Deutsch: None

**Background:** Longstanding injury to the gastric mucosa can lead to metaplastic changes and potentially dysplasia and carcinoma. Risk factors, such as Helicobacter pylori infection, vary widely in prevalence across the world, as do rates of intestinal metaplasia and gastric carcinoma. While studies in the United States have looked at the risks of gastric injury and intestinal metaplasia, very few have evaluated the risks in minority groups within the country. Our study looks at the association between race, gastric injury patterns, and intestinal metaplasia in a large safety net hospital.

**Design:** A pathology database search for gastric biopsies was performed between January 2011 and December 2011. The first 700 cases were included in this study. Data was collected on patient demographics including age, race, and sex. Pathologic data was collected on gastric mucosal injury pattern, presence of intestinal metaplasia, and absence or presence of H. pylori on Warthin-Starry stain. Patterns of injury were categorized as H. pylori gastritis (HPG), chronic inactive gastritis without H. pylori (CAG), Chronic inactive gastritis (CIG), chemical gastropathy (CG), unremarkable (NSA), or other (O). Student t-test was used to evaluate continuous variables, while the Fisher's exact test was used to calculate categorical variables.

**Results:** The patient population evaluated was diverse, including 20% Caucasian, 6% Asian, 33% African American, 40% Hispanic patients, and 1% other. The average age was 55 yrs and patients were 56% female. HPG was present in 24.4% of all patients biopsied. 12.5% of biopsies contained intestinal metaplasia. Amongst different racial groups, HPG was most common in Asian, Hispanic, and African American patients (p = 0.005, p = 0.0013, and p = 0.0001) when compared to Caucasian patients. CG more common in African American and Hispanic patients (p = 0.0175 and p = 0.0002). Caucasian patients were more likely to have normal gastric biopsies when compared to Asian, African American, and Hispanic patients (p = 0.01, p = 0.0023, p= 0.0002). Rates of intestinal metaplasia varied by race: Asian (9.7%), African American patients (17%), Hispanic (9.7%), and Caucasian (10.6%). When evaluating cases of intestinal metaplasia, background gastric injury patterns included CIG (49.4%),

HPG (18.3%), CAG (11.5%), CG (5%), NSA (1%), and other (9%). The other categories include ulcer, adenocarcinoma, and gastric polyps.

**Conclusions:** Our study highlights the association between race, gastric injury pattern, and intestinal metaplasia. HPG and CG occurred much more frequently in minority patients when compared to Caucasian patients, while CIG showed no statistically significant difference between groups. Intestinal metaplasia is far more common in African American patients than any other group, though it is most frequently associated with CIG, suggesting that race may be a risk factor for metaplasia.

## 341 Prevalence of Chlamydia Proctitis by Immunohistochemistry in Rectal Biopsies of Male Patients

Xin He[1], Sindha Madhav[2], Afsheen Sharifzadeh[1], Michelle Yang[1]
[1]University of Massachusetts Medical School, Worcester, MA, [2]UMass Medical School, UMass Memorial Medical Center, Worcester, MA

**Disclosures:** Xin He: None; Sindha Madhav: None; Afsheen Sharifzadeh: None; Michelle Yang: None

**Background:** Ulcerative proctitis is typically associated with inflammatory bowel disease (IBD). However, in recent years there is an increasing number of proctitis associated with sexually transmitted diseases (STD) especially in men who have sex with men due to chlamydia trachomatis. Patients with chlamydia trachomatis can be largely asymptomatic, and others present as active chronic proctitis with granulation tissue mimicking left-sided IBD. In this study, we aimed to investigate the prevalence of chlamydia proctitis in men who had granulation tissues in rectal biopsy using immunohistochemistry (IHC) assay.

**Design:** A total of 35 patients were identified using keywords "male, rectum, biopsy, granulation" from the electronic pathology records between July 2017 and July 2020, including 33 biopsies and 2 resections. All slides were evaluated by two gastrointestinal (GI) pathologists. Clinical history of STDs, indication for colonoscopy and colonoscopy findings were extracted from the electronic medical record. Chlamydia IHC was performed using a monoclonal antibody (1:100, Progen) validated on formalin fixed paraffin embedded tissue from the index case that was positive for chlamydia by rectal swab RNA test. Positive staining was defined when strong intracytoplasmic or extracellular inclusion bodies visualized under microscopy at 100x magnification.

**Results:** The median age was 57 years old (range: 19 to 88). Two patients had history of STD, including gonorrhea and LGV in index patient and HIV in the other. The indications for colonoscopy were widely variable. The most common endoscopic findings were ulcer and friable mucosa. IHCs were performed at initial diagnosis in 19 cases, including CMV, HSV1/2, adenovirus and spirochetes, which were all negative except for CMV that was positive in 2 cases. Strikingly, chlamydia was positive in 4 of all 35 (11.4%) cases (Figures 1 &2), or in 3 of 33 (9.1%) patients without known STDs. None of the cases had co-infections of tested microorganisms.
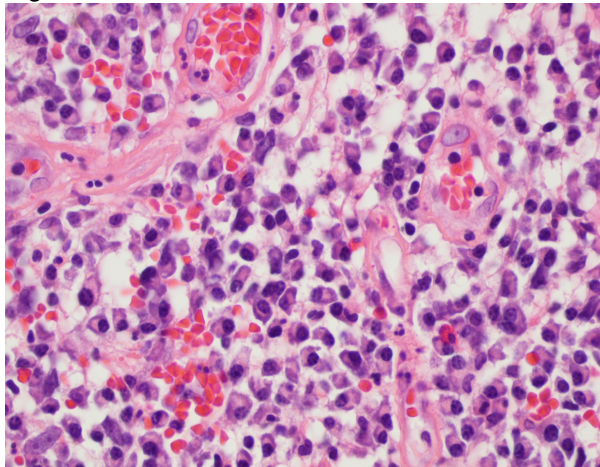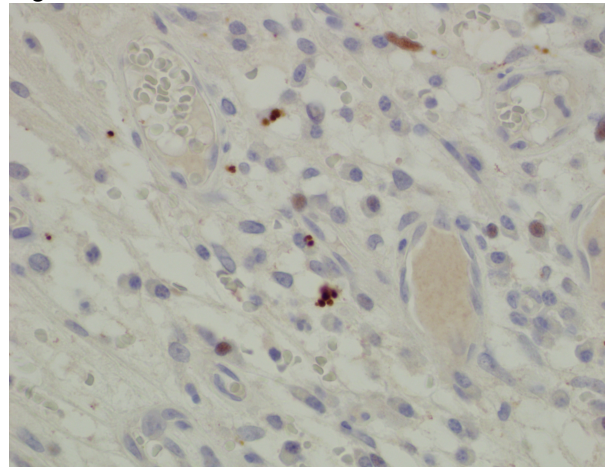
Figure 1 - 341



Figure 2 - 341

**Conclusions:** Our pilot data showed that Chlamydia proctitis is more prevalent than we thought in men with rectal granulation tissue, and Chlamydia IHC in rectal biopsy is a sensitive and reliable method. This data underscores the importance of Chlamydia IHC performed on suspected cases to facilitate early medical intervention in high-risk population.

### 342 Characterization of Colorectal Cancer Immune Microenvironment and Potential Prognostic Biomarkers

Erika Hissong[1], Andrea Sboner[2], Bhavneet Bhinder[2], Rohan Bareja[3], Hiranmayi Ravichandran[4], Jose Jessurun[4], Andre Rendeiro[5], Manish Shah[4], Olivier Elemento[2], Juan Miguel Mosquera[2]
[1]University of Michigan, Ann Arbor, MI, [2]Weill Cornell Medicine, New York, NY, [3]Englander Institute for Precision Medicine, New York, NY, [4]New York-Presbyterian/Weill Cornell Medical Center, New York, NY, [5]Weill Cornell Medical Center, New York, NY

**Disclosures:** Erika Hissong: None; Andrea Sboner: None; Bhavneet Bhinder: None; Rohan Bareja: None; Hiranmayi Ravichandran: None; Jose Jessurun: None; Andre Rendeiro: None; Manish Shah: None; Olivier Elemento: *Stock Ownership*, Volastra Therapeutics; *Stock Ownership*, OneThree Biotech; *Advisory Board Member*, Freenome; Juan Miguel Mosquera: None

**Background:** There is a growing interest in tumor-host interactions, as cancer development and progression may be influenced by the host immune system and tumor microenvironment. Emerging evidence supports that their better understanding will predict response to therapy and likelihood of recurrence. In colorectal carcinoma (CRC), studies highlight the importance of cytotoxic and memory T cell phenotypes in predicting tumor behavior. Recent studies identified the role of dendritic cells in modulating the immune response in CRC, with the ability to obtain immunostimulatory or immunosuppressive function at different stages of development and tumor progression. In fact, data has shown an association with dendritic cell maturation, phenotypic expression, and overall survival in patients with CRC. We sought to evaluate the immune and stromal representation in an outcome cohort of CRC.

**Design:** 41 CRC samples (17 primary and 24 metastatic) from 21 patients underwent RNA-seq and whole-exome sequencing (WES). Immune cell deconvolution of transcriptomes was performed using xCell, a gene signature-based algorithm. We evaluated expression data for 64 immune and stromal cell types; results were associated with WES data, and clinical and pathologic features. To validate our findings, the TCGA CRC cohort (n=477) was also interrogated, and results were correlated with Consensus Molecular Subtypes of CRC.

**Results:** Unsupervised clustering revealed two distinct clusters, C1 with high numbers of activated dendritic cells and Th1, and C2 with increased inactive dendritic cells (Figure 1A). Differences in overall survival probabilities between the two groups was noted in our cohort (p=0.044) (Figure 1B). Relative proportion of inactive vs active dendritic cells in the TCGA cohort was also associated with progression-free survival (Figure 1C). Preliminary immunohistochemical analysis on a subset of cases has confirmed differential expression of dendritic markers CD80 and CD86 in tumors from C1 vs C2 (Figure 2).

Figure 1 - 342



Figure 2 - 342



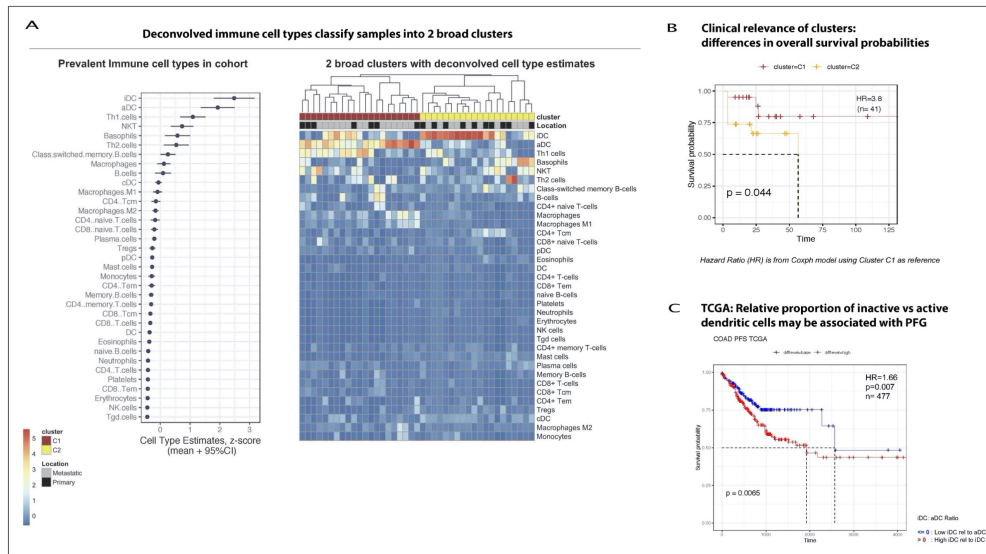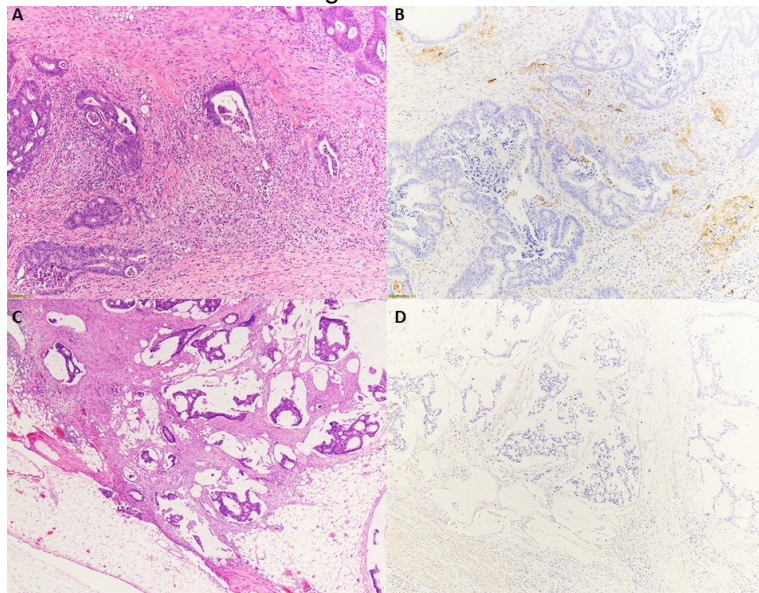**Conclusions:** Our preliminary results support the growing body of evidence that dendritic cells in the tumor microenvironment exist in either an immunostimulatory or immunosuppressive state, and their phenotypic properties may play an important role in the ability of the tumor microenvironment to enhance tumor progression in CRC. Further validation experiments employing Imaging Mass Cytometry are ongoing.

### 343 Colorectal Adenosquamous Carcinoma: A Clinicopathologic Analysis of 32 Cases of a Rare Carcinoma Subtype

Rachel Horton[1], Teri Longacre[2], Daniela Allende[3], Kelsey McHugh[4], Jinru Shia[5], Maria Westerhoff[6], Amitabh Srivastava[7], Wei Chen[8], Jennifer Vazzano[8], Rossana Kazemimood[9], Runjan Chetty[10], Klaudia Nowak[11], Stefano Serra[12], Won-Tak Choi[13], Sanjay Kakar[13], Deyali Chatterjee[14], Hassam Cheema[15], Rifat Mannan[16], Rondell Graham[1], Raul Gonzalez[17]

[1]Mayo Clinic, Rochester, MN, [2]Stanford University, Stanford, CA, [3]Cleveland Clinic, Lerner College of Medicine of Case Western University School of Medicine, Cleveland, OH, [4]Cleveland Clinic, Cleveland, OH, [5]Memorial Sloan Kettering Cancer Center, New York, NY, [6]University of Michigan, Ann Arbor, MI, [7]Brigham and Women's Hospital, Harvard Medical School, Boston, MA, [8]The Ohio State University Wexner Medical Center, Columbus, OH, [9]University of Rochester, Rochester, NY, [10]Royal Sussex County Hospital, Bristol, United Kingdom, [11]Toronto General Hospital, University Health Network, Toronto, Canada, [12]University Health Network, University of Toronto, Toronto, Canada, [13]University of California, San Francisco, San Francisco, CA, [14]Washington University in St. Louis, St. Louis, MO, [15]Barnes-Jewish Hospital/Washington University, MO, [16]Perelman School of Medicine at the University of Pennsylvania, Philadelphia, PA, [17]Beth Israel Deaconess Medical Center, Harvard Medical School, Boston, MA

**Background:** Adenosquamous carcinoma (ASC) is a rare WHO-recognized subtype of colorectal carcinoma. It appears to be aggressive with poor prognosis, though fewer than 100 cases have been reported with detailed pathologic analysis. This study compiled a cohort of colorectal ASC to describe its histologic and molecular aspects using modern parameters.

**Design:** We retrospectively identified 32 cases of colorectal ASC resected at 13 academic medical centers and analyzed available clinical, histologic, and immunohistochemical (IHC) features and prognosis.

**Results:** Clinicopathologic information is summarized in the **Table**. Average patient age at resection was 65 years (range 36-94 years); male:female ratio was 7:9. Most patients were white (23/26, 88%). Common presenting symptoms included abdominal pain (9/27, 33%) and weight loss (7/27, 26%); 6/27 (22%) patients were asymptomatic. Most tumors were in the right colon (20, 63%). Median tumor size was 6.5 cm (range 2.5-12.0 cm). Grossly, tumors appeared ulcerated/fungating (23, 72%) and nearly circumferential (11, 34%). Histologically, squamous features predominated (55% median squamous component; range 10-95%) and were always positive for at least one squamous IHC marker if tested (p40, p63, CK5/6). All cases were moderately (13, 41%) or poorly (19, 59%) differentiated, with lymphovascular (25, 78%) and perineural (16, 50%) invasion common. Most cases had low tumor-infiltrating lymphocytes (23/31, 74%) per International TILS Working Group criteria. Tumor budding was often Bd1 (22, 69%) per International Tumor Budding Consensus Conference criteria. Most cases were pT3 (19, 59%) or pT4 (10, 31%), with nodal metastases in more than half (19, 59%). Twelve cases had distant metastases, usually to the liver. Molecular findings included mismatch repair (MMR) loss in 7/15 (36%), *KRAS* mutation in 3/7 (43%), and *BRAF* mutation in 5/7 (71%). Recurrence was reported in 8/22 cases (36%), with median recurrence-free survival of 9 months. On follow-up, 8/28 (29%) died of disease (median survival 11 months) and another 10/28 (36%) died of unknown or other cause (median survival 6 months); 10 were alive (median follow-up 38 months).

**Table: Clinicopathologic analysis of 32 cases of colorectal adenosquamous carcinoma**

| | |
|---|---|
| **Age (n=32)** | 65 (+/-14.6) |
| Mean (SD) | 66 |
| Median | 36 - 94 |
| Range | |
| **Gender (n=32)** | 14 (44%) |
| Male | 18 (56%) |
| Female | 7:9 |
| M:F | |
| **Race (n=26)** | 23 (88%) |
| White | 1 (4%) |
| Asian | 1 (4%) |
| Black | 1 (4%) |
| Hispanic | |
| **Common Symptoms (n=27)** | 9 (33%) |
| Abdominal Pain | 7 (24%) |
| Weight Loss | 6 (22%) |
| Asymptomatic | 5 (17%) |
| Hematochezia | 5 (19%) |
| Anemia | 4 (15%) |
| Fatigue | 4 (15%) |
| Routine Colonoscopy | |
| **Common Risk Factors (n=26)** | 7 (27%) |
| Smoking | 6 (23%) |
| History of Other Cancers | 6 (23%) |
| Unknown/none | 4 (15%) |
| History of Hypertension | 3 (12%) |
| Coronary Artery Disease | 3 (12%) |
| Obesity | 2 (8%) |
| Alcohol use | 2 (8%) |

| | |
|---|---|
| Hyperlipidemia | 2 (8%) |
| Family History of Colon Cancer | |
| **Gross Description (n=32)** | 23 (72%) |
| Ulcerated/fungating | 11 (34%) |
| Mostly circumferential | 6 (19%) |
| Raised/exophytic | 3 (9%) |
| Partial necrosis | 3 (9%) |
| Polypoid | 2 (6%) |
| Obstructive | |
| **Gross Perforation (n=32)** | 3 (9%) |
| Yes | 29 (91%) |
| No | |
| **Precursor Lesions (n=32)** | 4 (40%) |
| TA | 2 (20%) |
| TVA | 1 (10%) |
| TSA | 1 (10%) |
| VA | 1 (10%) |
| AP | 1 (10%) |
| HP | |
| **Tumor Location (n=32)** | 20 (63%) |
| Right Colon | 6 (19%) |
| Left colon | 6 (19%) |
| Rectum | 12 (38%) |
| **Specifically:** | 4 (13%) |
| Cecum | 3 (9%) |
| Ascending colon | 1 (3%) |
| Hepatic Flexure | 1 (3%) |
| Right colon | 1 (3%) |
| Transverse colon | 3 (9%) |
| Splenic flexure | 1 (3%) |

| | |
|---|---|
| Sigmoid colon | 6 (19%) |
| Rectosigmoid colon | |
| Rectum | |
| **Tumor Size (cm) (n=32)** | 6.4 cm (+/- 2.5 cm) |
| Mean (SD) | 6.5 cm |
| Median | 2.5 – 12 cm |
| Range | |
| **Subtype (n=32)** | 32 (100%) |
| ASC | |
| **Percent Subtype** | 54% (+/- 23%) |
| **Squamous (n=32)** | 55% |
| Mean (SD) | 10-95% |
| Median | 46% (+/- 23%) |
| Range | 45% |
| **Glandular (n=32)** | 5-90% |
| Mean (SD) | |
| Median | |
| Range | |
| **Immunohistochemistry** | 3 (100%) |
| **P40 (n=3)** | 0 |
| (+) | 10 (77%) |
| (-) | 3 (23%) |
| **P63 (n=13)** | 10 (100%) |
| (+) | 0 |
| (-) | |
| **Ck5/6 (n=10)** | |
| (+) | |
| (-) | |
| **Differentiation (n=32)** | 19 (59%) |
| Poor | 13 (41%) |
| Moderate | |

| | |
|---|---|
| **Borders (n=27)** | 19 (70%) |
| Infiltrative | 8 (30%) |
| Pushing Border | |
| **Total LN** | 20.75 |
| Mean | 17 |
| Median | 2-48 |
| Range | |
| **Positive LN** | 3.3 |
| Mean | 1 |
| Median | 0-17 |
| Range | |
| **Tumor Deposits (n=32)** | 5 (16%) |
| Yes | 27 (84%) |
| No | |
| **Small LVI (n=32)** | 22 (69%) |
| Yes | 10 (31%) |
| No | |
| **Large LVI (n=32)** | 11 (34%) |
| Yes | 21 (66%) |
| No | |
| **PNI  (n=32)** | 16 (50%) |
| Yes | 16 (50%) |
| No | |
| **Budding (n=32)** | 22 (69%) |
| Bd1 | 8 (25%) |
| Bd2 | 2 (6%) |
| Bd3 | |
| **Margins (n=32)** | 29 (91%) |
| Negative | 3 (9%) |
| Positive | |
| **TILs (ITWG criteria) (n=31)** | 23 (74%) |
| Low | 3 (10%) |
| Intermediate | 5 (16%) |

| | |
|---|---|
| High | |
| **T (n=32)** | 0 |
| pT1 | 3 (9%) |
| pT2 | 19 (59%) |
| pT3 | 10(31%) |
| pT4 | |
| **N (n=32)** | 13 (41%) |
| pN0 | 9 (28%) |
| pN1 | 10 (31%) |
| pN2 | |
| **M (n=26)** | 14 (54%) |
| pM0 | 12 (46%) |
| pM1 | |
| **Mismatch Repair (n=15)** | 8 (53%) |
| Intact | 7 (36%) |
| Loss | 3 (60%) |
| *KRAS* (n=7) | 4 (40%) |
| (+) | 5 (71%) |
| (-) | 2 (29%) |
| *BRAF* (n=7) | 1 (100%) |
| (+) | |
| (-) | |
| *NRAS* (n=1) | |
| (-) | |
| **Neoadjuvant Treatment (n=28)** | 3(11%) |
| Yes | 25 (89%) |
| No | |
| **Adjuvant Treatment (n=23)** | 14 (61%) |
| Yes | 9 (39%) |
| No | |
| **Last Follow Up Length (months)** | 23.8 (+/- 27.5) |

| | |
|---|---|
| Mean (SD) | 13 |
| Median | 1 – 101 |
| Range | |
| **Recurrence (n=22)** | 8 (36%) |
| Yes | 14 (64%) |
| No | |
| **RFS (mos)** | 13 mos (+/- 14 mos) |
| Mean (SD) | 9 mos |
| Median | 1 – 47 |
| Range | |
| **Recurrence Site (n=12)** | 1 |
| Lymph Nodes | 1 |
| Inguinal | 2 |
| Paracaval | 3 |
| Peritoneum | 2 |
| Liver | 4 |
| Lungs | |
| Other | |
| **Status (n=28)** | 3 (11%) |
| **Alive** | 7 (25%) |
| No Evidence of Disease | 38 mos |
| Other | |
| Median Follow-up | |
| **Deceased** | 8 (29%) |
| Died of Disease | 11  mos |
| Median Survival | 10 (36%) |
| Cause Unknown | 6 mos |
| Median Survival | |
| **Unknown** | 1 (4%) |
| Lost to Follow Up | 2 (7%) |
| Other | |

Abbreviations: ASC: Adenosquamous carcinoma.  TA: Tubular Adenoma. TVA:  Tubulovillous Adenoma. TSA: Traditional serrated adenoma. VA:  Villous adenoma. AP: Adenomatous polyp.  HP:  Hyperplastic polyp. LVI: Lymphovascular invasion.  PNI: Perineural invasion. TIL: Tumor-infiltrating lymphocytes.  ITWG: International TILS Working Group.  LN: Lymph Node.  RFS: Recurrence-free survival. Mos: months.  (+): Positive.  (-): Negative

**Conclusions:** Patients with colorectal ASC may report mild or no symptoms, though the disease usually presents at an advanced stage. Despite high rates of MMR loss and low tumor budding, tumor-infiltrating lymphocytes are generally low, *KRAS* and *BRAF* mutations are common, and it has a high rate of recurrence and poor prognosis.

### 344 Genomic Profile of Carcinomas with Signet-Ring Cell Differentiation

Ghulam Ilyas[1], Peng Wang[1], Ardaman Shergill[1], Kiran Turaga[1], Jeremy Segal[1], John Hart[1], Namrata Setia[1]
[1]University of Chicago, Chicago, IL

**Disclosures:** Ghulam Ilyas: None; Peng Wang: None; Ardaman Shergill: None; Kiran Turaga: None; Jeremy Segal: None; John Hart: None; Namrata Setia: None

**Background:** Signet-ring cell differentiation in carcinomas is associated with an aggressive clinical course and early metastatic disease. Histology-based determination of the primary site is challenging as these tumors are morphologically similar, and may arise from a wide variety of primary sites. Given the advanced clinical stage, tumor sequencing is often performed to guide treatment. The aim of our study was to determine if the tumor genomic profile can be useful in identifying the origin of carcinoma with signet-ring cell differentiation of unknown primary.

**Design:** Carcinomas with signet-ring cell differentiation (Ca-SRC) of the appendix, colorectum, stomach, breast, pancreas, lung, and urinary bladder were identified from the institutional (n=52) and The Cancer Genome Atlas image archives (n=66). The tumor sequencing data was retrieved; only pathogenic/likely pathogenic variants and copy number alterations were included. Two-tailed Fischer's exact test was used to evaluate the data.

**Results:** We identified 118 Ca-SRCs from the appendix (goblet cell carcinomas n=14, 11.9% and non-goblet cell carcinomas n=9, 7.6%), colorectum (n=14, 11.9%), stomach (n=25, 21.2%), breast (n=49, 41.5%), pancreas (n=3, 2.5%), lung (n=3, 2.5%), and urinary bladder (n=1, 0.8%). We observed a significant association between non-goblet cell appendiceal Ca-SRCs and *KRAS* (p=0.0000) and *GNAS* (p=0.0002) mutations, gastric Ca-SRCs and *TP53* (p=0.0000) mutations, breast Ca-SRCs carcinoma and *CDH1* (p=0.0000) and *PIK3CA* (p=0.0000) mutations, and lung Ca-SRCs and *STK11* (p=0.0004) mutations. Microsatellite instability was more frequent in Ca-SRCs from colorectum compared to other sites (p=0.0000). Copy number alterations were less frequent in appendiceal Ca-SRCs (p=0.01) compared to the other sites.

**Conclusions:** Carcinomas with signet-ring cell differentiation of the appendix, colorectum, stomach, breast, and lung have a distinct genomic profile, which can be useful in identifying the origin of a metastatic carcinoma with signet-ring cell differentiation of unknown primary.

### 345 Evaluation of Tumor Regression Systems and Proposal of Simplified Depth of Invasion Scheme as Predictors of Recurrence in Post-Neoadjuvant Esophageal Adenocarcinoma Resection Specimens

Krishna Iyer[1], Iván González[1], Daniel Boffa[2], Ronald Salem[3], Dhanpat Jain[4], Xuchen Zhang[4]
[1]Yale New Haven Hospital, New Haven, CT,  [2]Yale New Haven Healthcare, New Haven, CT, [3]Yale University, New Haven, CT, [4]Yale School of Medicine, New Haven, CT

**Disclosures:** Krishna Iyer: None; Iván González: None; Dhanpat Jain: None; Xuchen Zhang: None

**Background:** Studies have shown that pathological tumor regression is a predictor of recurrence and overall survival in locally advanced esophageal carcinomas (EAC) following neoadjuvant therapy. Pathological tumor regression systems have been proposed, ranging from presence or absence of tumor to 3-4 tier scoring systems based on percentage of residual tumor. However, no regression system has been universally accepted. We sought

to evaluate these different pathological regression systems and  develop a simplified regression scheme as predictors of recurrence in post-neoadjuvant EAC resection specimens.

**Design:** We retrospectively reviewed recurrence and survival data in 126 patients who received neoadjuvant chemotherapy with residual tumor at various pathological stages from 2006-2015. A significant portion of patients clinically presented with stage T2-3 tumor with loco-regional spread. Nineteen patients showed complete response with no microscopically identifiable tumor (Table 1). We compared various regression scoring systems proposed by CAP/NCCN as well as 3 to 4 tier scoring systems proposed by various authors, independently studied in separate cohorts.

**Results:** Our data demonstrated that CAP/NCCN and the 3-tier system proposed by Wu et al. (complete response, 1-50%, and > 50% residual tumor) provided statistically significant differences in recurrence free survival (RFS) analysis, whereas that proposed by Schneider et al. and Barbou et al., using 10% residual tumor cutoff to determine major and minor response to therapy, were not significant.  The 2 tier scoring systems of Barbou et al. and Donington et al. did not provide additional information to further sub-stratify patients. We further demonstrated by using only tumor depth that tumor depth has a stronger significant difference in RFS between groups (p = 0.006). In addition, tumor extending to adventitia had a significantly lower post-neoadjuvant RFS than tumor confined to submucosa and muscularis propria (Figure 1).

| Table-1. Patient and Tumor Characteristics (N = 126) | |
|---|---|
| Gender, n (%) | |
|     Male | 110 (%) |
|     Female | 16 (%) |
| Age, mean ±SD | 63.9 ±10.1 |
| Body mass index, mean ±SD | 25.8 ±5.1 |
| Smoking history, n (%) | |
|    No | 36 (29%) |
|    Yes | 90 (71%) |
| Treatment response, n (%) | |
|    Complete response | 19 (15%) |
|    Near complete response | 29 (23%) |
|    Partial response | 33 (29%) |
|    Poor or no response | 45 36%) |
| Percentage of residual tumor, mean ±SD | 25.9 ±5.1 |
| Lymphovascular invasion, n (%) (n: 107) | |
|     Yes | 36 (34%) |
|     No | 71 (66%) |
| Perineural invasion, n (%) (n: 107) | |
|     Yes | 34 (32%) |
|     No | 73 (68%) |
| Number of involved lymph nodes, mean ±SD | 2 ± 5 |
| Number of lymph nodes evaluated, mean ±SD | 20 ± 10 |
| ypT-stage, n (%) (n: 107) | |
|     ypT1 | 23 (21%) |
|     ypT2 | 24 (22%) |
|     ypT3 | 51 (48%) |
|     ypT4 | 9 (8%) |
| ypN-stage, n (%) | |
|     ypN0 | 74 (59%) |
|     ypN1 | 32 (25%) |
|     ypN2 | 12 (10%) |
|     ypN3 | 8 (6%) |
| ypTNM prognostic group, n (%) | |
|     I | 49 (39%) |
|     II | 31 (25%) |
|     III | 35 (28%) |
|     IV | 11 (9%) |
| Abbreviations: SD - standard deviation. | |
| Percentages might not total 100% due to rounding | |

Figure 1 - 345



**Figure 1: Comparison of Recurrence Free Survival (RFS) using the Proposed Pathological Staging Systems for Post-neoadjuvant Resections**
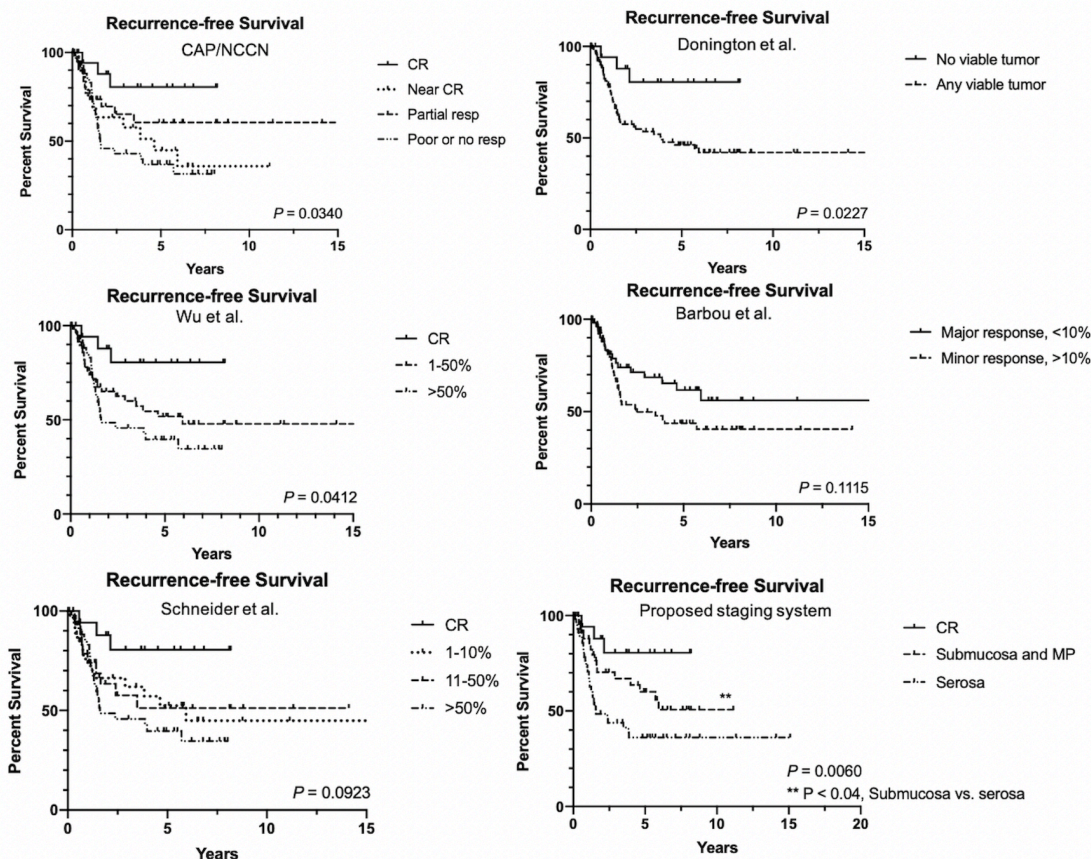
**Conclusions:** Evaluation of tumor depth alone, rather than percentage of residual tumor may be a sufficient prognostic tool in evaluating post-neoadjuvant treated EAC cases.

## 346 PCNA and Ki67 Tumoral Percentages Stratify Risk Recurrence in GIST with High Sensitivity and Specificity

Iyare Izevbaye[1], Gilbert Bigras[2], Benjamin Adam[1], Klaudia Nowak[3], Asifa Amin[4]
[1]University of Alberta, Edmonton, Canada, [2]Cross Cancer Institute, Edmonton, Canada, [3]Toronto General Hospital, University Health Network, Toronto, Canada, [4]University of Alberta Hospital, Edmonton, Canada

**Disclosures:** Iyare Izevbaye: None; Gilbert Bigras: None; Benjamin Adam: None; Klaudia Nowak: None; Asifa Amin: None

**Background:** Schemes for Gastrointestinal stromal tumour (GIST) risk assessment consistently include anatomical site, size, mitotic activity, and variably tumour rupture. Ki67 index and PCNA by immunohistochemistry (IHC) assay are predictive for GIST recurrence. This study evaluates Ki67 and PCNA IHCs via image analysis to assess utility, improve interobserver variability, automation and rapid analysis.

**Design:** Cases and clinical data were obtained from the institution laboratory information system and the cancer registry. Selected cases underwent pathomorphological and risk assessment. PCNA and Ki67 IHC were analyzed by the software QuPath 2.3 to compute percentage of positive nuclei (PPN) of only malignant cells using trained cell classification algorithms applied to whole slide images (WSI). Receiver operating characteristic (ROC) curves

compared PPN with pathologic risk assessment. Kaplan-Meier compared prognostic performance with patient outcome.

**Results:** 56 cases were identified. Survival data was available for 34 cases. Image analysis of Ki67 and PCNA showed increased PPN in high risk (HR) GISTs vs non- high risk (NHR) GISTs. For Ki67, NHR GISTs demonstrated a mean of 2.2% (range 0.7-4.5%) versus 14.0% (range 1.6-46.5%) for HR GISTs (p=0.002), For PCNA, NHR GISTs showed a mean of 13.2% (range 2.7-30.8%) versus 25.9% (range 3.6-83.5%) for HR GISTs (p=0.041).  A combination of the two IHCs (product of PPNs) showed a mean of 32.2 (range 3.2-138.1) for NHR GISTs and 570.0 (range 7.6-3881.5) for HR GISTs (p=0.021).

ROC curves showed that Ki67 alone was the most sensitive (sens 0.905, NPV 0.818). Whereas, combined PCNA and Ki67 PPN was the most specific (spec 0.900, PPV 0.941) The optimal diagnostic cut-offs for PPN, as defined by Youden's J-statistic, were 2.782 for Ki67, 7.606 for PCNA, and 33.013 for Ki67 and PCNA combined. The probability of survival of high PPN cases was compared with low PPN cases by Kaplan-Meier survival curves. All three classes (Ki67 alone, PCNA alone, and combined Ki67 and PCNA) revealed poorer survival outcomes in high PPN in contrast to low PPN (Log-rank test, p<0.0001). Of the high PPN pattern, combined Ki67 and PCNA demonstrated the worst overall survival outcomes. PCNA alone was least predictive of poorer outcome.

| Parameter | | | All GIST cases | GIST cases with outcome data |
|---|---|---|---|---|
| Number of patients | | | 56 | 34 |
| Sex | male | | 31(55%) | 18 (53%) |
| | female | | 25 (45%) | 16 (47%) |
| Age at Diagnosis | Average | | 60.27± 12.86 | 60.21± 12.9 |
| | Median | | 58.5 | 57.5 |
| | Range | | 29 to 89 | 40 to 89 |
| Number of patients alive* | | | NA | 31 (91%) |
| Number of deceased patients* | | | NA | 3 (9%) |
| Number of days of survival postdiagnosis* | Average | | NA | 1020.7 ± 459.0 |
| | Median | | NA | 969.5 |
| | Range | | NA | 348 to 1814 |
| Mutations | CKIT | 9 | 1 (1.8%) | 1 (2.9%) |
| | | 11 | 43 (76.8%) | 27 (79.5%) |
| | | 13 | 1 (1.8%) | 1 (2.9%) |
| | | 17 | 2 (3.6%) | 0 (0%) |
| | PDGFR | 12 | 0 (0%) | 0 (0%) |
| | | 18 | 5 (8.9%) | 3 (8.8%) |
| | None | | 4 (7.1%) | 2 (5.9%) |
| Primary or Recurrence | Primary | | 55 (98%) | 33 (97.1%) |
| | Recurrence | | 1 (1.8%) | 1 (2.9%) |
| | Gastric (G) | | 23 (41.1%) | 17 (50%) |
| | Duodenum (D) | | 3 (5.4%) | 2 (5.9%) |
| | Small bowel(SB) | | 24 (42.9%) | 15 (44.1%) |
| | Rectum (R) | | 3 (5.4%) | 1 (0%) |
| | Metastasis to liver(L) or omentum (O) | | 3 (5.4%) | 0 (0%) |
| Tumour size (cm) | Average | | 9.63 ± 6.6 | 10.57± 5.23 |
| | Median | | 8 | 10.5 |
| | Range | | 1.7 to 38 | 3 to 24.5 |
| Focality | Unifocal | | 52 (92.8%) | 30 (88.2%) |
| | Multifocal | | 4 (7.2%) | 4 (11.8%) |
| Histologic type | Epithelioid | | 5 (8.9%) | 3 (8.8%) |
| | Spindle | | 38 (67.8%) | 21 (61.8%) |
| | Mixed | | 13 (23.3%) | 10 (29.4%) |
| Mitotic rate per 5mm$^2$ | Average | | 10.69 ± 15.7 | 13.35± 18.72 |
| | Median | | 5 | 8 |
| | Range | | 0 to 79 | 0 to 79 |

| | | | |
|---|---|---|---|
| Histologic grade* | G1 | 31 (55.3%) | 17 (50%) |
| | G2 | 24 (42.8%) | 16 (47.1%) |
| Necrosis (%)* | Average | 13.78 ± 15.7 | 16.93± 24.47 |
| | Median | 5 | 16.96 |
| | Range | 0 to 80 | 0 to 80 |
| Risk assessment | Very low (VL) | 3 (5.4%) | 1 (2.9%) |
| | Low (L) | 9 (16.1%) | 2 (5.9%) |
| | Intermediate (I) | 13 (23.2%) | 9 (26.5%) |
| | High (H) | 31 (55.3%) | 22 (64.7%) |
| pT stage | PT1 | 1 (1.8%) | 0 (0%) |
| | PT2 | 11 (19.6%) | 3 (9%) |
| | PT3 | 21 (37.5%) | 12 (35.1%) |
| | PT4 | 21 (37.5%) | 17 (50%) |
| | NA | 2 (3.6%) | 2 (5.9%) |
| pN stage | PN0 | 3 (5.3%) | 1 (2.9%) |
| | PN1 | 2 (3.6%) | 2 (5.9%) |
| | NA | 51 (91.1%) | 31 (91.2%) |
| pM stage | PM1 | 6 (10.7%) | 5 (14.7%) |
| | NA | 50 (89.3%) | 29 (85.3%) |
| ** Count greater than 60 | | | |

Figure 1 - 346



Ki67 IHC: High risk vs. not high risk

AUC: 0.881
95% CI: 0.765-0.997
Accuracy: 0.848
Sensitivity: 0.905
Specificity: 0.750
PPV: 0.864
NPV: 0.818

PCNA IHC: High risk vs. not high risk

AUC: 0.676
95% CI: 0.463-889
Accuracy: 0.774
Sensitivity: 0.905
Specificity: 0.500
PPV: 0.792
NPV: 0.714

Ki67 x PCNA: High risk vs. not high risk

AUC: 0.880
95% CI: 0.756-1.000
Accuracy: 0.833
Sensitivity: 0.800
Specificity: 0.900
PPV: 0.941
NPV: 0.692

Figure 2 - 346



Ki67 immunohistochemistry — Log-rank test, p<0.0001 — Low staining (<35%), High staining (>35%)

PCNA immunohistochemistry — Log-rank test, p<0.0001 — Low staining (<32%), High staining (>32%)

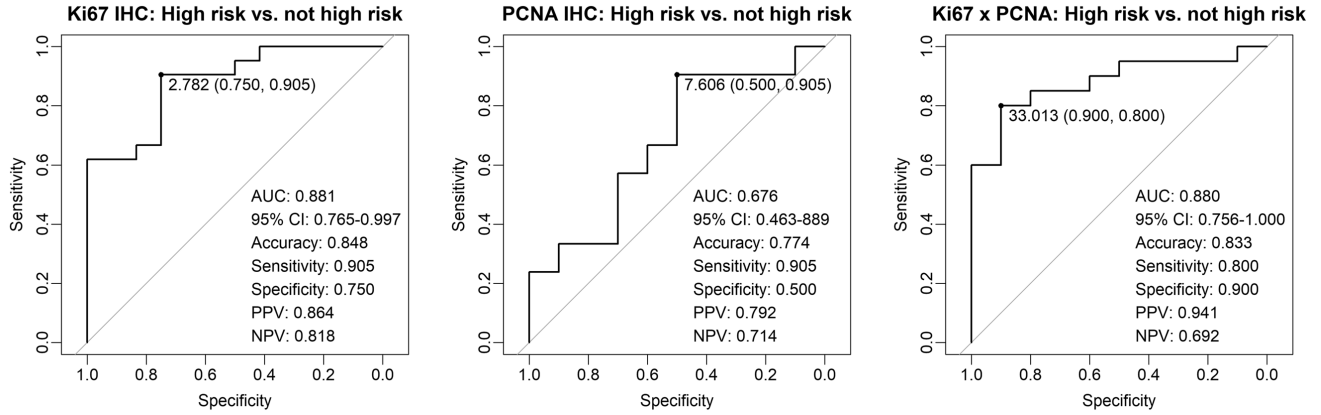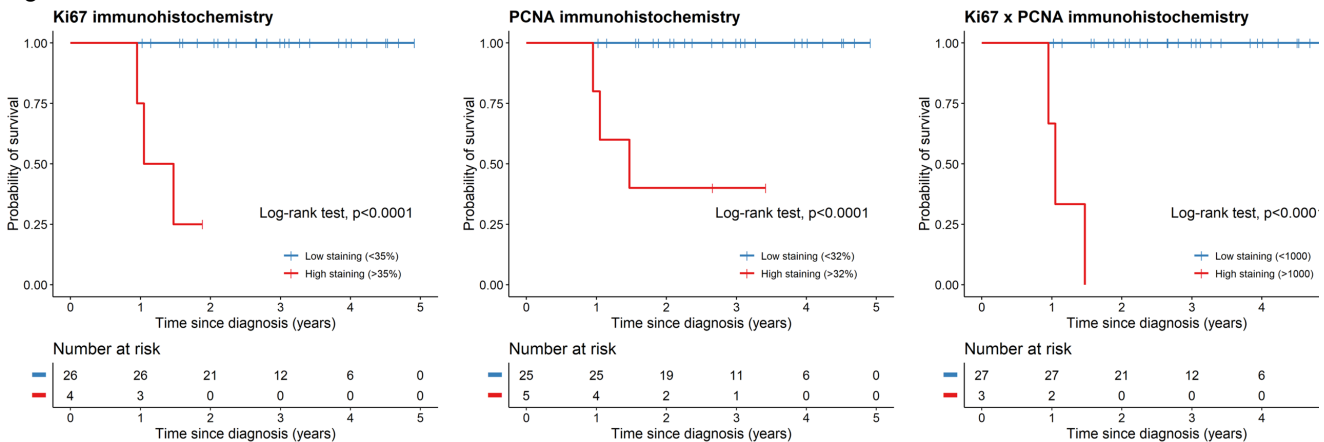Ki67 x PCNA immunohistochemistry — Log-rank test, p<0.0001 — Low staining (<1000), High staining (>1000)

**Conclusions:** PPN assessment of Ki67 and PCNA are predictive of overall survival in GIST tumours and may improve risk assessment of GIST. Image analysis of WSI IHC assays is amenable to automation with improved reproducibility over eye-ball assessment.

**347    Scoring Depth of Invasion of Submucosally Invasive Adenocarcinoma in Esophageal Endoscopic Specimens: How Good are We?**

Dipti Karamchandani[1], Raul Gonzalez[2], Maria Westerhoff[3], Lindsey Westbrook[4], Nicole Panarelli[5], Tonya King[6], Christina Arnold[7]
[1]Penn State Health Milton S. Hershey Medical Center, Hershey, PA, [2]Beth Israel Deaconess Medical Center, Harvard Medical School, Boston, MA, [3]University of Michigan, Ann Arbor, MI, [4]University of Colorado Anschutz Medical Campus, Aurora, CO, [5]Montefiore Medical Center - Moses Division, Bronx, NY, [6]Pennsylvania State University College of Medicine, Hershey, PA, [7]University of Colorado, Aurora, CO

**Disclosures:** Dipti Karamchandani: None; Raul Gonzalez: None; Maria Westerhoff: None; Lindsey Westbrook: None; Nicole Panarelli: None; Tonya King: None; Christina Arnold: None

**Background:** Emerging data support that low-risk, submucosally invasive esophageal adenocarcinomas are cured via endoscopic resection when the following criteria are met: submucosal invasion ≤500 microns (μm), lacking other histologic features predictive of nodal metastasis, and clear margins. Hence, the pathologists' scoring of depth of submucosal invasion may be vital for guiding further management, such as endoscopic follow-up vs. esophagectomy. In this study, we assessed the interobserver agreement in determining the depth of submucosal invasion in esophageal endoscopic specimens.

**Design:** Six subspecialized gastrointestinal (GI) pathologists from 5 academic centers collected and independently reviewed 44 esophageal endoscopic specimens. Seven cases scored as intramucosal carcinoma by 4 or more reviewers were excluded. The remaining 37 cases formed the study group: 28 were scored as submucosal invasion by all reviewers, and 9 were scored as submucosal invasion by 4 or 5 reviewers. The depth of submucosal invasion was measured in μm from the deepest aspect of the muscularis mucosae. Interobserver agreement was assessed by the intraclass correlation coefficient (ICC) and Fleiss's extended kappa statistics.

**Results:** The scoring results for all six reviewers are shown in **Table 1**. The overall ICC among the 6 reviewers in scoring the depth of invasion was *moderate* [0.59, 95% CI 0.45-0.71]; however, this agreement was skewed higher due to an outlying scoring observation that can be seen along the line of agreement in the right corner of graphs (**Figure 1**). When this outlying observation was removed, the ICC was *poor* [0.40, 95% CI 0.26-0.56]. A lack of agreement is seen by the variation around the line of agreement in each plot (**Figure 1**). When the measurements were categorized at 500 μm, 1 case (3%) was scored ≤500 μm and 15 cases (40%) were scored >500 μm by all reviewers. There was disagreement in 21 cases (57%), e.g., a case scored variably as >500 μm and ≤ 500 μm by different reviewers. The overall agreement was only *moderate* [kappa 0.42, 95% CI 0.27-0.58] among the 6 reviewers when measurements were categorized at 500 μm.

**Table 1: Results of scoring of the depth of invasion in esophageal endoscopic resection specimens among the six reviewers**

| Reviewer No.(R) | Cases diagnosed as IMC | No. of cases scored as submucosal invasion ≤ 500 microns | No. of cases scored as submucosal invasion > 500 microns | Total slides reviewed |
|---|---|---|---|---|
| R1 | 0 (0%) | 9 (24%) | 28 (76%) | 37 (100%) |
| R2 | 2 (6%) | 13 (35%) | 22 (59%) | 37 (100%) |
| R3 | 5 (14%) | 10 (27%) | 22 (59%) | 37 (100%) |
| R4 | 3 (8%) | 9 (24%) | 25 (68%) | 37 (100%) |
| R5 | 3 (8%) | 9 (24%) | 25 (68%) | 37 (100%) |
| R6 | 3 (8%) | 1 (3%) | 33 (90%) | 37 (100%) |
| Total reads | 16 | 51 | 155 | 222 |

Figure 1 - 347
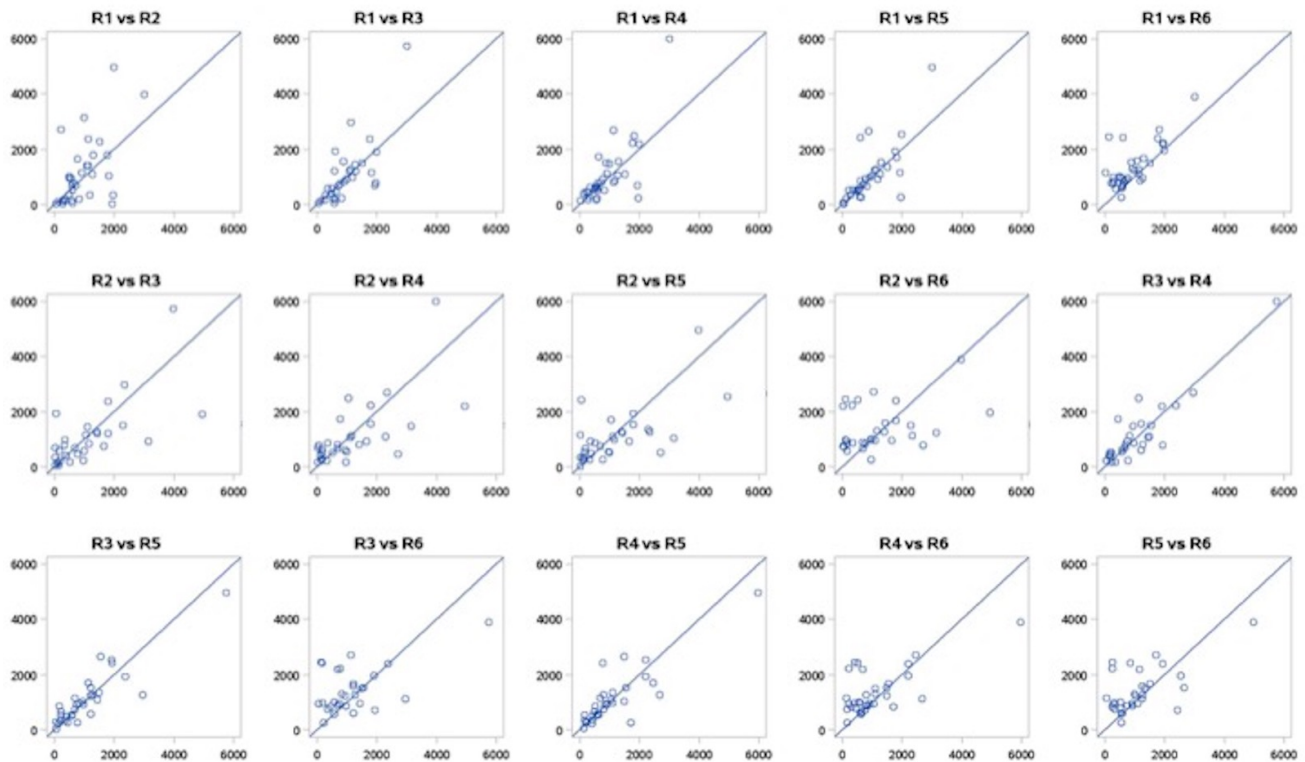


**Conclusions:** Our study shows a lack of agreement among subspecialized GI pathologists in assessing the depth of submucosal invasion in esophagus endoscopic resections. If important management decisions continue to be based upon this parameter, more reproducible and concrete guidelines are needed.

**348 Interobserver Agreement in Assessing Depth of Invasion for Submucosally Invasive Adenocarcinoma in Colonic Endoscopic Resection Specimens**
Dipti Karamchandani[1], Maria Westerhoff[2], Christina Arnold[3], Raul Gonzalez[4], Lindsey Westbrook[5], Tonya King[6], Nicole Panarelli[7]
[1]Penn State Health Milton S. Hershey Medical Center, Hershey, PA, [2]University of Michigan, Ann Arbor, MI, [3]University of Colorado, Aurora, CO, [4]Beth Israel Deaconess Medical Center, Harvard Medical School, Boston, MA, [5]University of Colorado Anschutz Medical Campus, Aurora, CO, [6]Pennsylvania State University College of Medicine, Hershey, PA, [7]Montefiore Medical Center - Moses Division, Bronx, NY

**Disclosures:** Dipti Karamchandani: None; Maria Westerhoff: None; Christina Arnold: None; Raul Gonzalez: None; Lindsey Westbrook: None; Tonya King: None; Nicole Panarelli: None

**Background:** Recent data support that low-risk submucosally invasive colonic adenocarcinomas (i.e., those that lack high-grade morphology or tumor budding and lymphovascular invasion and are resected with clear margins) are considered curable via endoscopic resection, provided that the submucosal depth of invasion is < 1000 microns (µm). Submucosal depth ≥1000 µm is associated with an increased risk of nodal metastases. Hence, the pathologists' assessment of depth of submucosal invasion may guide further management (i.e., surveillance versus

colectomy). This study aimed to assess interobserver concordance among gastrointestinal (GI) pathologists in assessing submucosal depth of invasion in colonic endoscopic resection specimens.

**Design:** Six subspecialized GI pathologists from five academic centers independently reviewed 52 hematoxylin- and eosin-stained slides from endoscopic specimens with submucosally invasive colonic adenocarcinomas. For each slide, each pathologist measured the greatest depth of submucosal invasion in µm, per the recommended guidelines (that is, below the level of recognizable muscularis mucosae or from the ulcer base in cases of ulcerated adenocarcinoma or from the surface of the lesion, when the muscularis mucosae was destroyed or obscured by the tumor). Interobserver agreement was assessed by the intraclass correlation coefficient and Fleiss's extended kappa statistics.

**Results:** The scoring results for all six reviewers are tabulated in **Table 1**. Overall agreement among the 6 reviewers was *poor* [ICC 0.31, 95%CI 0.20-0.45]. Lack of agreement can be seen by the variation around the line of agreement in each plot (**Figure 1**). Eight cases were reported as intramucosal carcinoma by one or two reviewers but as submucosal invasion by remaining reviewers. Twenty cases (38.5%) were scored as > 1000 µm by all six reviewers, while 32 cases (61.5%) showed disagreement when measurements were categorized as < or $\geq$ 1000 microns (i.e., a case scored variably as< 1000 µm and $\geq$ 1000 µm by different reviewers).  The overall agreement was only *slight* [kappa 0.18, 95%CI 0.04-0.31] among the six reviewers when measurements were categorized at 1000 mm.

Table 1: Results of scoring of depth of submucosal invasion in colonic endoscopic specimens among the six reviewers

| Reviewer No.(R) | Cases diagnosed as IMC | No. of cases scored as submucosal invasion< 1000 microns | No. of cases scored as submucosal invasion $\geq$ 1000 microns | Total slides reviewed |
|---|---|---|---|---|
| R1 | 0 (0%) | 11 (21%) | 41 (79%) | 52 (100%) |
| R2 | 0 (0%) | 1 (2%) | 51 (98%) | 52 (100%) |
| R3 | 8 (16%) | 9 (17%) | 35 (67%) | 52 (100%) |
| R4 | 1 (2%) | 22 (42%) | 29 (56%) | 52 (100%) |
| R5 | 0 (0%) | 6 (12%) | 46 (88%) | 52 (100%) |
| R6 | 0 (0%) | 9 (17%) | 43 (83%) | 52 (100%) |
| Total reads | 9 | 58 | 245 | 312 |

Figure 1 - 348
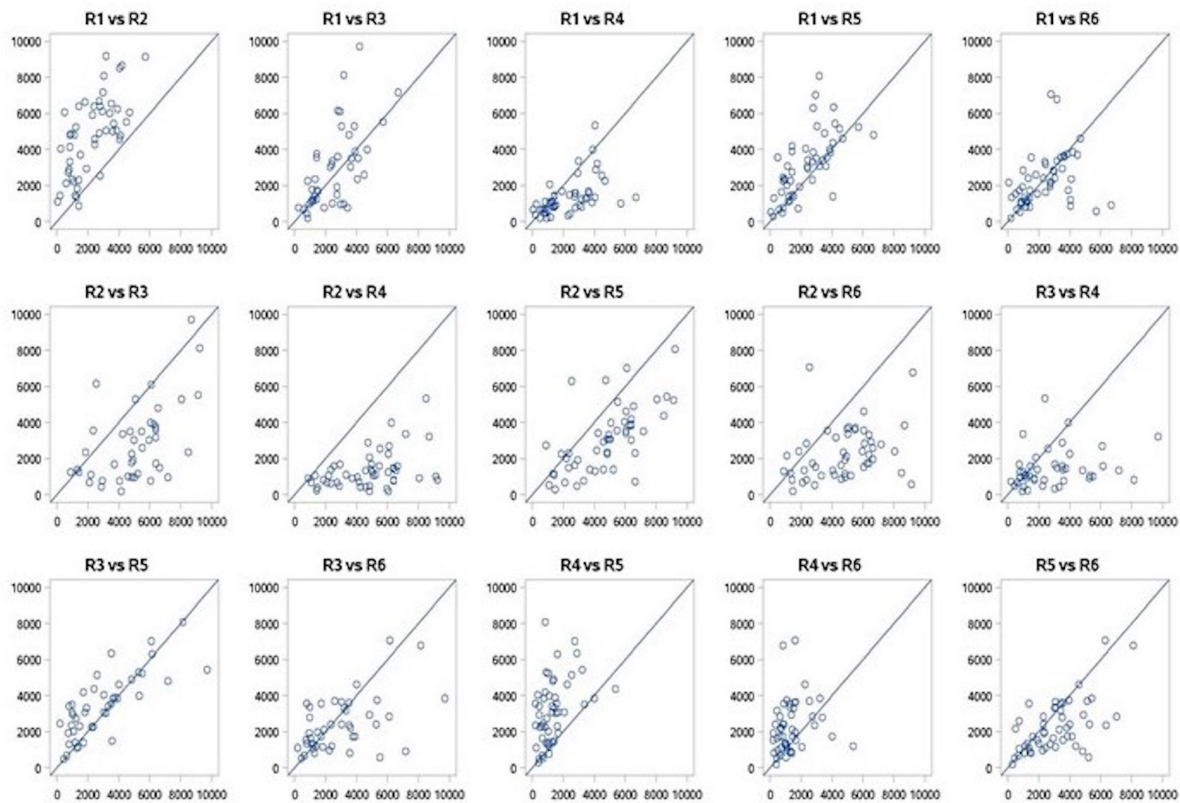


**Conclusions:** Our findings indicate that clearer and more concrete guidelines are needed if clinical colleagues are to base important management decisions on pathologists' estimate of depth of submucosal invasion in the colonic endoscopic resection specimens with submucosally invasive adenocarcinoma.

**349    Appendectomy Specimens During the COVID19 Pandemic: Experience From a Large Hospital System in New York City, an Early Epicenter in the United States**
Binny Khandakar[1], Jihong Sun[2], Stephen Ward[3]
[1]Mount Sinai St. Luke's Roosevelt Hospital, New York, NY, [2]Mount Sinai West, New York, NY, [3]Icahn School of Medicine at Mount Sinai, New York, NY

**Disclosures:** Binny Khandakar: None; Jihong Sun: None; Stephen Ward: None

**Background:** The COVID19 pandemic, declared in March 2020 by the WHO, has impacted patient care in many ways. New York City was one of the early epicenters of the pandemic in the US with the city accounting for more than half of the total COVID19 cases diagnosed in the US to date. To reduce risk of virus transmission, non-urgent surgeries were delayed during this time. Appendectomy for acute appendicitis is one of the most commonly performed surgeries. When appendectomies are delayed, patients are treated with antibiotics before undergoing interval appendectomy, which reveals characteristic findings on histology often with granulomas. Occasionally, alternate and/or incidental diagnoses are found on pathology review of routine appendectomy specimens. We sought to compare the findings in appendectomy specimens before and during the COVID19 pandemic.

**Design:** We reviewed records from appendectomies done 7/1/2017 - 9/30/2020, excluding those submitted as part of colectomies. Cases were divided in 2 groups, pre-COVID (7/1/17 - 2/29/20) and COVID (3/1/20 - 9/30/20). Histopathologic findings were recorded and compared between groups. Chi-square test was applied, $p < 0.05$ considered statistically significant.

**Results:** Total of 2141 appendectomy specimens were included. Acute appendicitis was noted in 89% cases in both pre-COVID and COVID groups, while interval appendicitis was more frequently seen in the COVID group (4% vs. 0.9%) and chronic appendicitis was more frequent in the pre-COVID group (0.8% vs 0 %) [table1]. Diverticula (n=22) were more frequently seen during COVID (2% vs 0.8%), while endometriosis was more frequent pre-COVID (0.7% vs 0%). Incidentally detected neoplasms were seen in 4.7% specimens overall. These include, low grade appendiceal mucinous neoplasm (LAMN; n=53), well-differentiated neuroendocrine tumors (WDNET; all WHO grade 1; n=28), adenocarcinoma (adca; n=5) goblet cell adca (n=7), metastatic adca (n=7). Of the appendicies with incidental tumors, a higher incidence of WDNET and metastatic lesions and lower incidence of LAMN were seen in the COVID group [table2]. Polyps were seen in 1.5% cases (n=32), including, sessile serrated lesion (n=28), tubular adenoma (n=4), and hyperplastic polyp (n=1), with no difference in incidence between groups.

Table 1: Comparative analysis of distribution of cases with histopathologic findings

| Diagnosis | Pre-COVID incidence n (%) | COVID incidence n (%) | Total incidence n (%) |
|---|---|---|---|
| Total | 1767 | 374 | 2141 |
| Normal | 44 (2.5%) | 11 (2.9%) | 55 (2.5%) |
| ***Appendicitis*** | ***1615 (91%)*** | ***359 (95%)*** | ***1973 (92%)*** |
| acute | 1572 (89%) | 334 (89%) | 1906 (89%) |
| chronic * | 14 (0.8%) | 0 | 14 (0.7) |
| interval * | 15 (0.9%) | 16 (4%) | 31 (1.4%) |
| ***Benign findings*** | ***77 (4%)*** | ***20 (5%)*** | ***97 (4.5%)*** |
| Diverticula * | 14 (0.8%) | 8 (2%) | 22 (1%) |
| Endometriosis * | 12 (0.7%) | 0 | 12 (0.6%) |
| Mucocele | 8 (0.5%) | 1 (0.3%) | 9 (0.4%) |
| Fibrous obliteration | 43 (2.5%) | 11 (3%) | 54 (2.5%) |
| ***Polyp*** | ***20 (1%)*** | ***12 (3%)*** | ***32 (1.5%)*** |
| hyperplastic polyp | 1 (0.06%) | 0 | 1 (0.05%) |
| sessile serrated lesion | 17 (1%) | 11 (3%) | 28 (1.3%) |
| tubular adenoma | 3 (0.2%) | 1 (0.3%) | 4 (0.2%) |
| ***Malignancy*** | ***79 (4%)*** | ***21 (6%)*** | ***100 (4.7%)*** |
| LAMN | 47 (3%) | 6 (2%) | 53 (2.5%) |
| WDNET | 19 (1%) | 9 (2%) | 28 (1.3%) |
| GCA | 5 (0.3%) | 2 (0.5%) | 7 (0.3%) |
| Adenocarcinoma | 4 (0.2%) | 1 (0.3%) | 5 (0.3%) |
| Metastatic tumor | 4 (0.2%) | 3 (0.8%) | 7 (0.3%) |

WDNET: well differentiated neuroendocrine tumor; GCA: goblet cell adenocarcinoma; LAMN: low grade appendiceal neoplasm; *p<0.05

Table 2: Incidental Malignancy in Appendix (n=100)

| Tumor Type (n) | Pre-COVID n (%) | COVID n (%) |
|---|---|---|
| Total | 79 | 21 |
| LAMN (53) * | 47 (59%) | 6 (28%) |
| WDNET (28) * | 19 (24%) | 9 (43%) |
| GCA (7) | 5 (6%) | 2 (10%) |
| Adenocarcinoma (5) | 4 (5%) | 1 (4%) |
| Metastatic tumor (7) * | 4 (5%) | 3 (14%) |

*p<0.05

**Conclusions:** The impact of COVID19 pandemic on appendectomy specimen has been noteworthy. Though acute appendicitis remained the most common diagnosis, we showed a >4 fold increase in the incidence of interval appendicitis reflecting the necessary delay of surgery during this time. There were also significant differences in the

distribution of incidental tumors, with a higher proportion of WDNET and metastatic lesions, and fewer LAMN in the COVID group. These findings emphasize the importance of thorough microscopic examination of all appendectomy specimens to identify unexpected conditions which may require further management.

### 350 Gastric Biopsies with Prominent Eosinophils: Associations, Clinical Outcomes and Response to Therapy

Nigar Khurram[1], Dana Balitzer[2], Sanjay Kakar[3]
[1]Hospital of the University of Pennsylvania, Philadelphia, PA, [2]San Francisco VA Health Care System, San Francisco, CA, [3]University of California, San Francisco, San Francisco, CA

**Disclosures:** Nigar Khurram: None; Dana Balitzer: None; Sanjay Kakar: None

**Background:** Increase in eosinophils in gastric biopsies is well known to occur in diverse clinical settings such as atopic disease, peripheral eosinophilia and extra-gastric eosinophilic inflammation. A small number of patients with 'idiopathic eosinophilic gastritis' can show favorable response to steroids. The use of the term "histologic eosinophilic gastritis" (EoG) has been proposed for cases with ≥30 peak eosinophils/HPF in five separate HPF and with no known associated causes of eosinophilia.

**Design:** A retrospective review of cases at our institution was performed to identify gastric biopsy cases with prominent eosinophils (n=103), of which a subset (n=53) fulfilled criteria histologic EoG (n=53). Four patients were excluded for pre-existing clinical conditions (Crohns disease and systemic mastocytosis). Clinical and pathologic data reviews were performed for the remaining patients (n=49), including clinical presentation, type of therapy and documented symptomatic and/or histologic improvement to evaluate clinicopathologic outcomes of cases with a diagnosis of histologic eosinophilic gastritis. Proportions for categorical variables were compared using the Chi-square test, and Fisher exact test when the data were limited. P value < 0 .05 were considered statistically significant.

**Results:** Most patients with idiopathic disease presented with non-specific symptoms of abdominal pain or dyspepsia (n=25, 50%). On clinical follow-up, only one patient was subsequently diagnosed with inflammatory bowel disease, and no definite clinical etiology was identified in the remaining 48 patients. Of the patients with idiopathic disease, 32 patients received therapy with either proton-pump inhibitors (PPIs, n=27) or steroids (n=5), with a documented clinical response to PPIs in 8 patients (30%) and a response to steroids in all 5 patients (100%). Two patients developed relapsing disease characterized by severe abdominal pain dependent on steroid therapy. Patients with steroid responsive disease compared with patients with PPI responsive disease showed no statistical differences in age, gender, history of atopic disease or histologic findings (including presence of chronic gastritis, eosinophilic glandulitis, sheets of eosinophils, presence of eosinophils).

**Conclusions:** The majority of patients with histologic eosinophilic gastritis present with non-specific GI symptoms, with no identifiable clinical etiology of eosinophilia. While a significant proportion of patients improve symptomatically without treatment or with PPIs, a small proportion of patients develop steroid dependent, relapsing idiopathic disease which warrants additional clinical follow-up.

**351  Immune Response Heterogeneity Is Associated with Tumor DNA Methylation Status in Microsatellite-Unstable Colorectal Carcinomas**

Jung Ho Kim[1], Mi-kyoung Seo[2], Ji Ae Lee[1], Seung-Yeon Yoo[1], Nam-Yun Cho[3], Gyeong Hoon Kang[1]
[1]Seoul National University Hospital, Seoul, South Korea, [2]Yonsei University College of Medicine, Seoul, South Korea, [3]Cancer Research Institute, Seoul National University College of Medicine, Seoul, South Korea

**Disclosures:** Jung Ho Kim: None; Seung-Yeon Yoo: None

**Background:** Although most colorectal carcinomas (CRCs) with microsatellite instability-high (MSI-high) are expected to exhibit high immune responses, there is substantial heterogeneity in immune responses between and within MSI-high CRCs. Here, we investigated the association between tumor DNA methylation and differential immune responses in MSI-high CRCs.

**Design:** CpG island methylator phenotype (CIMP) status, LINE-1 methylation levels, and immune microenvironmental features, including tumor-infiltrating T-cells/macrophages, PD-L1 expression, and Crohn-like lymphoid reaction (CLR), were analyzed in 133 MSI-high CRCs. Among the 133 tumors, 28 samples selected were subjected to next-generation sequencing (NGS) analysis to determine tumor mutation burden (TMB), tumor neoantigen burden (TNB), and consensus molecular subtype (CMS).

**Results:** In MSI-high CRCs, CIMP-high significantly correlated with tumor PD-L1 overexpression and high densities of CD8+ T-cells and CD163+ macrophages in both invasive margin and tumor center areas, whereas LINE-1 methylation-low was associated with relatively inactive CLR and low densities of CD4+ T-cells and CD68+ macrophages specifically in the invasive margin area. According to NGS results, there were no significant differences in TMB or TNB between CIMP-high and CIMP-low/negative or between LINE-1 methylation-high and LINE-1 methylation-low subgroups in MSI-high CRCs. CIMP-high/MSI-high CRCs were significantly enriched with CMS1, whereas LINE-1 methylation status was not associated with specific CMS.

**Conclusions:** In MSI-high CRCs, tumor DNA methylation status is linked to intra- and inter-tumoral immune response heterogeneities independent of TMB or TNB status. CIMP-high is associated with a spatially homogeneous increase in tumor-infiltrating cytotoxic T-cells and M2 macrophages, whereas LINE-1 hypomethylation is related to a spatially heterogeneous decrease in tumor-infiltrating helper T-cells and macrophages.

**352  Distribution of Intestinal Metaplasia in Barrett Esophagus**

Tae Kim, Parakrama Chandrasoma[1]
[1]LAC+USC Medical Center

**Disclosures:** Tae Kim: None

**Background:** Barrett esophagus (BE) is defined in the United States by the presence of intestinal metaplasia (IM) in columnar-lined esophagus (CLE). Sensitivity of detecting IM is dependent on sampling and the utilized biopsy protocol. However, the distribution of IM in CLE has not been studied. Knowing the distribution can guide biopsy protocols for the highest yield of IM.

**Design:** 1024 patients underwent endoscopic evaluation for GERD. In patients with CLE, all biopsies were obtained according to the following protocol: 4-quadrant biopsy at intervals of every 1 to 2 cm throughout the CLE. The presence of IM was confirmed histologically, and its distribution within CLE was recorded as proximal, mid-section, distal, diffuse, multifocal, or not otherwise specified. IM in columnar mucosa islands were excluded (n=5). The CLE length and esophageal dysplasia/adenocarcinoma were also noted. Statistical analysis was performed with the Fisher's exact test.

**Results:** 86 out of 1024 patients demonstrated CLE. IM was present in 74 of 86 CLE cases. The most common distribution patterns of IM in CLE were diffuse (45%; 33/74) and proximal (34%; 25/74). The distribution patterns did

not differ significantly between short-segment BE (<3 cm) or long-segment BE (≥3 cm), p=0.64. The distribution pattern did not differ significantly between BE with or without dysplasia/adenocarcinoma, p=0.49.

| Distribution | # Cases | % (only BE, n=74) | | |
|---|---|---|---|---|
| No IM | 945 | | | |
| Diffuse | 33 | 45% | | |
| Proximal | 25 | 34% | | |
| Mid-section | 3 | 4% | | |
| Distal | 3 | 4% | | |
| Multifocal | 4 | 5% | | |
| NOS | 6 | 8% | | |
| | < 3 cm (SSBE) | % | ≥ 3 cm (LSBE) | % |
| Diffuse | 8 | 47% | 25 | 45% |
| Proximal | 6 | 35% | 19 | 35% |
| Mid-section | 0 | 0% | 3 | 5% |
| Distal | 1 | 6% | 2 | 4% |
| Multifocal | 0 | 0% | 4 | 7% |
| NOS | 2 | 12% | 2 | 4% |
| p =0.64 | | | | |
| | No Dys/CA | % | Dys/CA | % |
| Diffuse | 21 | 40% | 12 | 46% |
| Proximal | 19 | 36% | 6 | 23% |
| Mid-section | 2 | 4% | 1 | 4% |
| Distal | 2 | 4% | 1 | 4% |
| Multifocal | 3 | 6% | 1 | 4% |
| NOS | 2 | 4% | 4 | 15% |
| p = 0.49 | | | | |

Key: IM - intestinal metaplasia, NOS – not otherwise specified, BE – Barrett esophagus, SSBE – short segment Barrett esophagus, LSBE – long segment Barrett esophagus, Dys/CA – dysplasia or carcinoma.

**Conclusions:** The distribution of IM in CLE is not random and prefers either a diffuse or proximal pattern. One hypothesis is that intestinal metaplasia arises in a more alkaline environment of the proximal CLE versus the more acidic environment in distal CLE. This distribution does not change throughout the disease progression of BE. Directed sampling of the proximal CLE may improve the sensitivity of detecting IM in CLE.

## 353 Tailgut Cyst (Retrorectal Cystic Hamartoma): A Histopathologic Study with Review of the Literature

Teresa Kim[1], Bita Naini[2]
[1]University of California, Los Angeles, Los Angeles, CA, [2]David Geffen School of Medicine at UCLA, Los Angeles, CA

**Disclosures:** Teresa Kim: None

**Background:** Tailgut cyst is a rare congenital cystic lesion of the retrorectal/presacral space, thought to originate from remnants of the embryonic postanal gut. Our goal in this study was to further characterize the clinicopathologic features of this rare lesion and analyze our findings in conjunction with a review of the literature.

**Design:** We conducted a retrospective analysis of all patients that were histologically diagnosed with a tailgut cyst at our institution over the past 20 years. We performed a detailed histopathologic study and recorded the clinical data.

**Results:** Nine cases were identified, with a slight female predominance (F:M = 2:1) and a mean age of 51 years (range 16-73 years). The patients were commonly symptomatic, and the initial clinical and radiologic impressions were variable (Table 1). In the two asymptomatic patients, cysts were incidentally discovered on radiology. Cysts averaged 5.3 cm (range 1.7-10.9 cm) in size. Two cases were associated with neoplasia arising from the cyst (1 mucinous adenocarcinoma and 1 well-differentiated neuroendocrine tumor). The majority (n=8) were lined by

several epithelial types, including squamous (n=7), transitional (n=2), ciliated columnar (n=4), non-ciliated columnar (n=2), and mucinous (n=5) epithelium. Additional histopathologic findings included inflammation (n=4), necrosis (n=2), calcifications (n=1), and foreign body giant cell reaction (n=2). The presence of smooth muscle in the cyst wall was the most consistent finding (n=9). Of note, one patient underwent a preoperative biopsy, but a definitive diagnosis of tailgut cyst was only made upon complete excision. Mean follow-up was 67.6 months (range 0-228 months), and no patients developed recurrence.

| Characteristics | Number (n=9) |
|---|---|
| **Age (years)** | |
| Mean | 51 |
| Range | 16 – 73 |
| **Sex** | |
| Female | 6 |
| Male | 3 |
| **Clinical Presentation** | |
| Asymptomatic | 2 |
| Symptomatic | 7 |
| Perirectal symptoms related to mass effect | 7 |
| Anorectal signs | 2 |
| **Initial Clinical/Radiologic Impression** | |
| Malignant | 2 |
| Benign | 2 |
| Nonspecific | 5 |
| **Mass size (cm)** | |
| Mean | 5.3 |
| Range | 1.7 – 10.9 |
| **Follow-up (months)** | |
| Mean | 67.6 |
| Range | 0 – 228 |

Table 1. Clinical characteristics of tailgut cysts

**Conclusions:** Tailgut cysts are rare, and a majority present with nonspecific findings in middle-aged adults. A previously reported strong female predominance was not seen in our study, which demonstrated a female to male ratio of only 2:1. The cysts were predominantly lined by multiple types of epithelium, with smooth muscle in the wall. Associated neoplasia (22.2%) was seen at a similar prevalence to that previously reported in the literature. Given the risk of neoplasia, it is important to be aware of this rare diagnosis and include it in the differential diagnosis of cystic lesions of the retrorectal space. Complete excision and histopathologic examination of the entire surgically removed lesions are recommended to prevent recurrence and exclude possible neoplastic transformation.

### 354 Rituximab Induces Lymphocytic Colitis-Pattern Injury (LCPI) Associated With B-Cell Depletion in Endoscopic Biopsies

Michel Kmeid[1], Mahmoud Aldyab[1], Rupinder Brar[1], Hwajeong Lee[1]
[1]Albany Medical Center, Albany, NY

**Disclosures:** Michel Kmeid: None; Mahmoud Aldyab: None; Rupinder Brar: None; Hwajeong Lee: None

**Background:** Rituximab (RTX), a monoclonal antibody directed against the B-cell CD20 antigen, is associated with variable adverse gastrointestinal (GI) events. However, the histologic evidence of this association is limited. We describe the clinical, endoscopic and histologic patterns of injury in patients receiving RTX and correlate them with tissue B-cell depletion.

**Design:** Patients who underwent GI endoscopies while on RTX therapy and/or carrying a diagnosis for which RTX is indicated, were searched (2005-2020; n=992). Electronic medical records were reviewed to identify patients who underwent GI biopsies following treatment with RTX, and the biopsies were reviewed. CD20 and PAX5 immunostains were performed on all biopsies showing inflammatory pathology and normal biopsies that were taken within 1 year from the last RTX infusion. Indication for endoscopy and endoscopic findings were recorded.

Histologic findings were correlated with tissue B-cell depletion (CD20/PAX5 -/-) (Fisher's exact test, significance p<0.05).

**Results:** 93 cases were retrieved. Non-Hodgkin lymphoma was the most common indication for RTX therapy (57%). Biopsy was taken at median 5 months after RTX treatment. 69% of patients had clinical GI symptoms. 36 (39%) biopsies had inflammatory pathology (group A) and 57 (61%) were normal (group B). In group A, common abnormal endoscopic findings were mucosal inflammation (58%) and ulcer (37%). Common histologic abnormalities were active inflammation (50%), intraepithelial lymphocytosis (28%) and ulcer (17%). B-cells were depleted in 12 (33%) of 36 group A biopsies. After excluding biopsies taken >1 year from the last RTX infusion, the frequencies of tissue B-cell depletion were similar between group A (12/26; 46.2%) and group B (15/36; 44.1%)(p>0.05). Also, the frequencies of abnormal histology were not statistically different whether B-cells are depleted or not (p>0.05). In group A with tissue B-cell depletion, causality was confirmed in 2 cases showing LCPI; one with strong temporal association between the pathology and RTX infusion, and the other without confounding factors for LCPI. In the remaining 10 cases, substantial confounding factors precluded the incrimination of RTX as the sole cause for the pathology. **[Figure 1].**

Figure 1 - 354
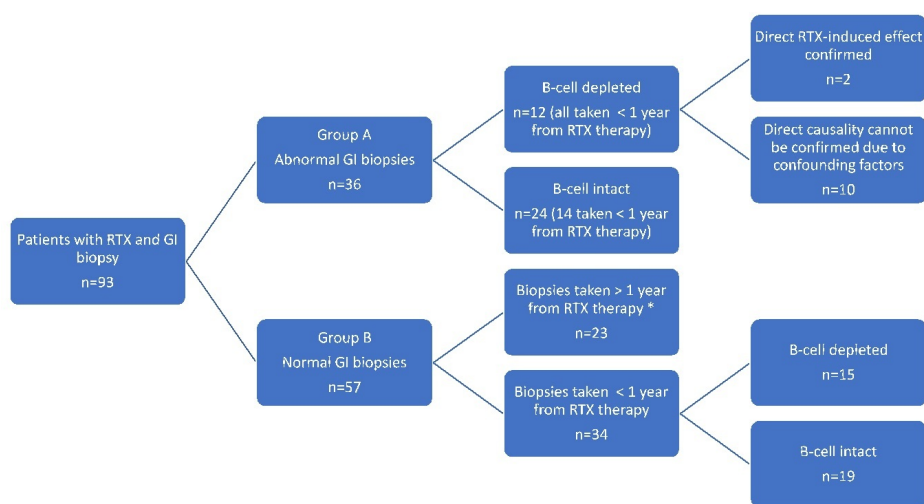


* 2 esophageal biopsies taken < 1 year from RTX therapy were not stained due to insufficient number of lymphocytes for evaluation on H&E.

**Figure 1. Study design and results**

**Conclusions:** In RTX-treated patients, tissue B-cell depletion is not the main cause of inflammatory pathology in GI tract. A minor subset, however, develops histologic evidence of direct RTX-induced effect, notably in the form of LCPI.

**355      Histologic Findings in Mucosa and Muscularis Propria Biopsied Immediately Prior to Peroral Endoscopic Myotomy in Patients with Achalasia**

Enoch Kuo[1], Yaseen Perbtani[2], Kai Wang[1], Peter Draganov[1], Dennis Yang[1], Xiuli Liu[1]
[1]University of Florida, Gainesville, FL, [2]University of Florida College of Medicine, Gainesville, FL

**Disclosures:** Enoch Kuo: None; Kai Wang: None; Dennis Yang: *Consultant*, Boston Scientific; *Consultant*, Lumendi; *Consultant*, Steris; Xiuli Liu: None

**Background:** Peroral endoscopic myotomy (POEM) has been increasingly used to treat achalasia. Previous studies reported high frequency of muscular eosinophilic infiltration in achalasia. Esophageal mucosal changes in achalasia were only studied in esophagectomy specimens. Cardia mucosal changes in achalasia were not reported previously. The aim of this study is to further characterize the esophageal, gastric cardia, and muscularis propria changes in achalasia.

**Design:** This is a prospective study. Patients with clinically and radiographically confirmed achalasia who undergo POEM are enrolled in the study. Mucosal biopsies are taken 1 cm proximal and 1 cm distal to the gastroesophageal junction, and muscularis propria biopsies are taken from the mid esophagus. Tissues are submitted for detailed histological evaluation using H&E stained slides.

**Results:** Eighteen patients (10 male and 8 female, mean age: 60.7 (SD: 13) years) were enrolled in this study. Nine patients had type II achalasia, two type III, one type 1, five esophageal gastric outlet obstruction, and one unspecific type achalasia. The mean duration of achalasia was 79 (range 1-480) months. Ten patients were on proton pump inhibitors. All patients had a dilated esophagus on examination, but none of them showed salmon-colored mucosa endoscopically. Esophageal, gastric cardia, and muscular biopsies were performed in 17, 13, and 17 patients, respectively. Basal hyperplasia, spongiosis, ballooning, and parakeratosis were seen in 92.3%, 100%, 100%, and 76.5% of cases, respectively. Peripapillary lymphocytosis was seen in 58.8% of cases, and active esophagitis was seen in 23.5% of case. Six (35.3%) cases had few intraepithelial eosinophils, but none of them had >15 eosinophils per high power field. Subepithelial inflammation and fibrosis were seen in 33.0% and 41.6% of cases, respectively. Histologic findings in gastric cardia mucosa included carditis (69.2%), H. pylori gastritis (7.6%), and reactive gastropathy (15.4%). One case (7.6%) showed low-grade dysplasia arising from intestinal metaplasia in the cardia. Absence of ganglion cells in the muscular biopsies was noted in 88.2% of cases, and the remaining two showed rare residual ganglion cells with ganglionitis in one case (5.8%). Muscular atrophy and interstitial fibrosis were observed in 52.9% and 82% of cases, respectively. Two cases (11.7%) had eosinophilic inflammation in the muscularis propria and one of them was accompanied by lymphocytic inflammation. **Results are summarized in Table 1.**

Table 1. Esophageal, gastric cardia, and muscular biopsy findings in patients with achalasia undergoing peroral endoscopic myotomy.

| Mucosal biopsy findings | Feature | % |
|---|---|---|
| Esophageal squamous mucosa (N=17) | Basal hyperplasia | 92.3 |
| | Spongiosis | 100 |
| | Ballooning | 100 |
| | Parakeratosis | 76.5 |
| | Periampullary lymphocytosis | 58.8 |
| | Neutrophilic inflammation | 23.5 |
| | Eosinophilic inflammation | 35.3 |
| Gastric cardia mucosa (N=13) | Carditis | 69.2 |
| | H. pylori gastritis | 7.6 |
| | Reactive changes | 15.4 |
| | Intestinal metaplasia | 8 |
| | Low-grade dysplasia | 8 |
| Muscular biopsy findings (N=17) | | |
| | Absence of ganglion cells | 88.2 |
| | Ganglionitis | 5.8 |
| | Muscular atrophy | 52.9 |
| | Interstitial fibrosis | 82 |
| | Eosinophilic inflammation | 11.7 |

**Conclusions:** Muscular biopsies in our study revealed loss of ganglion cells, supporting the view that achalasia is a primary esophageal disease with ganglion cell depletion. Squamous mucosa in achalasia showed changes mimicking reflux and lymphocytic esophagitis, but not eosinophilic esophagitis. Cardia mucosa in achalasia patients often were inflamed and uncommonly showed intestinal metaplasia and glandular dysplasia.

## 356 Cross Sectional Approach of Processing Rectal Cancer Resections Detects Closer Circumferential Margin than the Regular Approach

Whayoung Lee[1], Xiaodong Li[2], Vishal Chandan[3]
[1]UCI Medical Center, Orange, CA, [2]UCI Medical Center, South Pasadena, CA, [3]University of California, Irvine, Orange, CA

**Disclosures:** Whayoung Lee: None; Xiaodong Li: None; Vishal Chandan: None

**Background:** Tumor stage is known to have a profound influence on the overall prognosis of rectal cancer patients. In addition, histologic features such as circumferential margin (CRM), mesorectum intactness (MRI), lymph nodes (LN), perineural invasion (PNI) and lymphovascular invasion (LVI) also influence patient prognosis. It has been suggested, that a cross sectioning approach (CSA) for rectal cancer resections may allow for more accurate evaluation of these histologic features than the conventional regular approach (RA). The aim of this study was to see if there were any significant differences in assessment of these histologic features in rectal cancer resections that were processed using CSA versus RA.

**Design:** CSA included fixing the entire specimen intact (without opening) in formalin for at least 48 hours, followed by cross sectioning the entire specimen at 4mm intervals. RA included routine protocol such as longitudinally opening the fresh specimen, fixing it in formalin for at least 6 hours and taking regular sections from the tumor. The same set of surgeons operated on both groups of cases.

**Results:** 75 primary rectal cancer resections from January 2018 to July 2020 were evaluated, 35 by CSA and 40 by RA. There were no significant differences in pT (p=0.22) and pN (p=0.86) stages between the two groups. CSA detected a significantly closer CRM-clearance than RA (mean 6.1mm vs 12.8mm, p=0.0007). There was no significant difference in the rate of positive CRM (CRM less than or =1mm, 7/35[20%] in CSA vs 6/40[15%] in RA, p=0.57). The greatest-tumor-dimension in CSA cases was also significantly larger than RA (mean 4.5cm vs 2.8cm, p=0.004). There was no difference between the 2 groups in number of total LN-count (mean 23.2 CSA vs 23.1 RA, p=0.95), number of positive LNs (mean 0.6 CSA vs 1.0 RA, p=0.48), MRI (74.2% complete in CSA vs 82.5% complete in RA, p=0.39), distal margin clearance (mean 22.2mm CSA vs 25.5mm RA, p=0.37), LVI (20% vs 20%, p=1.0), PNI (27% vs 25%, p=0.26). Comparable number of cases received preoperative neoadjuvant therapy within both groups, 57.1% in CSA and 65% in RA, respectively (p=0.49) and there was no significant difference in treatment response score (2.4 RCA vs 2.2 RA, p=0.27).

| | Cross Sectional Approach (n=35) | Regular Approach (n=40) | p value |
|---|---|---|---|
| Circumferential/radial margin clearance (mm) | 6.1 | 12.8 | 0.0007 |
| Tumor size (cm) | 4.5 | 2.8 | 0.004 |
| Retrieved # of LNs | 23.2 | 23.1 | 0.95 |
| Positive # LNs | 0.6 | 1.0 | 0.48 |
| Mesorectum Intactness | 26/35 (74.2%) | 33/40 (82.5%) | 0.39 |
| Distal margin clearance (mm) | 22.2 | 25.5 | 0.37 |
| Circumferential/radial margin involvement | 7/35 (20%) | 6/40 (15%) | 0.57 |
| Preoperartive neoadjuvant therapy | 20/35 (57.1%) | 26/40 (65%) | 0.49 |
| Treatment response score | 2.4 | 2.2 | 0.27 |
| LVI | 7/35 (20%) | 8/40 (20%) | 1.0 |
| PNI | 13/35 (27%) | 10/40 (25%) | 0.26 |

**Conclusions:** CSA detected a closer CRM clearance and a larger greatest-tumor-dimension than RA. However, there was no significant difference in rate of positive CRM, total LN-count or number of positive LNs, MRI, LVI and PNI between the two groups.

**357    For HER2 Detection in Metastatic Colorectal Adenocarcinoma: IHC, FISH or Both?**

Whayoung Lee[1], Xiaodong Li[2], Vishal Chandan[3]
[1]UCI Medical Center, Orange, CA, [2]UCI Medical Center, South Pasadena, CA, [3]University of California, Irvine, Orange, CA

**Disclosures:** Whayoung Lee: None; Xiaodong Li: None; Vishal Chandan: None

**Background:** Therapies targeting HER2 are emerging as potential treatments for HER2 positive metastatic colorectal carcinoma (CRC). However, both immunohistochemistry (IHC) and/or FISH HER2 tests are used to determine patient eligibility for this treatment. Many institutions have borrowed their CRC HER2 testing algorithm from breast cancer and use IHC as the first line test for evaluation of HER2 with reflex to FISH only for a subset of 2+ or 3+ cases (PMID: 32773196). The aim of this study is to evaluate the concordance between IHC and FISH HER2 tests and develop a better strategy for HER2 testing in CRC.

**Design:** Simultaneous IHC and FISH testing for HER2 was performed on 38 cases of metastatic CRC. IHC was performed utilizing the FDA approved anti-HER-2 antibody (clone 4B5) and scored according to the HERACLES criteria [PMID: 26449765]. FISH analysis of at least 50 interphase nuclei was performed in two or more independent areas of invasive tumor and a ratio of HER2:CEP17 ≥ 2.0 or HER2/cell >6.0 was considered positive for amplification.

**Results:** Of the 38 cases, the IHC score was 0/1+ (negative) in 31 (81.6%); 2+ (equivocal) in 5 (13.2%); 3+ (positive) in 2 (5.2%) cases. FISH results were negative in 30 (78.9%), indeterminate in 3 (7.9%), and positive in 5 (13.2%) cases. Concordance between IHC and FISH was 92.1.7% (35 out of 38). However, of the 31 IHC negative cases (score 0 or 1), 2 cases were positive by FISH corresponding to a "false negative rate" of 6.5%. Of the 5 cases that were 2+ on IHC, 1 was positive by FISH (20%) while 4 were negative (80%). Both 3+ cases on IHC were positive for FISH. 3 cases that were indeterminate on FISH were negative (1+) on IHC.

**Conclusions:** We found an overall concordance rate between IHC and FISH for HER2 amplification of 92.1% in metastatic CRC. However, 2 cases that were negative on IHC (score 0/1) and 1 case that was equivocal (2+) on IHC, were found to be HER2 positive by FISH, indicating FISH to be more sensitive in detecting HER2 positivity than IHC. The results of our study suggest that both IHC and FISH should be performed concurrently for HER2 evaluation in metastatic CRC, as a subset of patients that are negative or equivocal on IHC may be positive for HER2 by FISH.

**358    Oxyntic Gland Adenoma: A Clinicopathologic Characterization of 11 Cases**

Natalia Liu[1], Hanlin Wang[1]
[1]David Geffen School of Medicine at UCLA, Los Angeles, CA

**Disclosures:** Natalia Liu: None; Hanlin Wang: None

**Background:** Oxyntic gland adenoma is a recently recognized polypoid gastric lesion composed of gland-forming epithelial cells with a predominant chief cell differentiation that resembles oxyntic glands. If submucosal involvement is present, these lesions are classified as gastric adenocarcinoma of fundic gland type. However, its neoplastic potential and clinical behavior are poorly investigated because of its rarity.

**Design:** Pathology databases over the past ten years were searched for cases bearing various related diagnostic terms, such as "adenocarcinoma of the fundic gland type," "adenocarcinoma of chief cell predominant type," "oxyntic gland polyp," and "oxyntic gland adenoma." Hematoxylin and eosin (H&E) stained slides were reviewed to confirm the diagnosis. Clinical follow-up data were obtained by reviewing electronic medical records, which included subsequent endoscopic findings and the general state of health of the patients since the initial diagnosis of oxyntic gland adenoma.

**Results:** A total of 11 patients carrying a diagnosis of oxyntic gland adenoma were identified. These included ten females and one male with a mean age of 76 years (range: 43-85 years). All the polyps were incidental findings in patients who underwent esophagogastroduodenoscopy for gastroesophageal reflux diasese, dysphagia, dyspepsia,

anemia, abdominal pain, or diarrhea. The polyps ranged in size from 0.3 to 1.0 cm (mean 0.48 cm) and were all found in the body or fundus of the stomach. Ten patients had solitary lesions and one had multiple sessile polyps who underwent repeat endoscopy two months later to remove all of the remaining polyps. Histologically, all the lesions were confined to the mucosa. However, none of the specimens showed sufficient submucosal tissue for the evaluation of submucosal involvement. H pylori gastritis was noted in one patient on a random gastric biopsy. The follow-up time ranged from 14 to 87 months (mean: 75.5 months). Except for one patient who died of metastatic breast carcinoma, all patients remained healthy and cancer-free. No additional gastric polyps were identified in six patients who underwent repeat endoscopy 8-49 months after the initial diagnosis.

**Conclusions:** Though only a small number of cases are studied, our data demonstrate an indolent nature of oxyntic gland adenoma. Even with inadequate evaluation of submucosal involvement on polypectomy speciments, the risk of this lesion to progress to invasive adenocarcinoma should be exceedingly low.

### 359 Clinicopathologic Characterization of Primary Appendiceal Invasive Adenocarcinoma

Xiaoqin Liu[1], Irene Chen[1], Xiaoyan Liao[1]
[1]University of Rochester Medical Center, Rochester, NY

**Disclosures:** Xiaoqin Liu: None; Irene Chen: None; Xiaoyan Liao: None

**Background:** Appendiceal invasive adenocarcinoma (APAC) is rare and morphologically resembles its counterpart in colon. The clinicopathologic features are not well understood.

**Design:** A total of 17 cases of APAC diagnosed between 2005 and 2020 were identified at our institution. In addition, 25 cases of goblet cell adenocarcinoma (GCA) and 22 cases of low-grade appendiceal mucinous neoplasm (LAMN), both at advanced tumor stages ($\geq$T3) and diagnosed over the same period of time, were included for comparison.

**Results:** The APCA cohorts included 17 patients, 10 women and 7 men, with a median age of 54 (range: 28-83) years. The tumors consisted of 1 (6%) pT1, 3 (18%) pT2, and 13 (76%) pT3 and above. Lymph node and distant metastasis were present in 5 (30%) patients. Histologically, 11 (65%) APCAs were conventional adenocarcinoma resembling colorectal origin, of which 4 (24%) demonstrated focal (<50%) mucinous features, and 1 showed focal sarcomatoid and signet ring cell features. Six (35%) were mucinous adenocarcinoma ($\geq$50% mucin), of which 1 contained signet-ring cells. All APCAs were associated with mucosal precursor lesions that were classified as tubular adenoma (n=5), tubuovillous adenoma (n=5), villous adenoma (n=2), or LAMN-Tis (n=5). Four cases had mixed mucosal adenoma and LAMN-Tis as precursor lesions. APCA with mucin production (>5% mucin) were more frequently associated with LAMN-Tis or villous adenoma (9/10, 90%), and had higher tumor stages than conventional adenocarcinoma (P<0.05). In contrast, only 2 of 25 GCA demonstrated mucosal precursor lesions (P<0.000). Compared to GCA, APCA had a higher frequency of nuclear $\beta$ catenin expression (10/12 [83%] vs. 7/25 [28%], p<0.01), abnormal p53 expression (7/12 [58%] vs. 3/25 [12%], p<0.01), and SATB2 loss (5/12 [42%] vs. 2/25 [8%], P<0.05). Both GCA and APCA showed similar low frequency of SMAD4 loss and mismatch repair protein deficiency. On follow up, 4 (24%) patients died after a median survival of 20 months. Kaplan-Meier survival analysis revealed a 5-year overall survival rate of 65%. Patients with advanced ($\geq$T3) APCA and GCA had similar overall survival, but worse than patients with LAMN beyond pTis (P<0.05).

**Conclusions:** This case series of APCA, the largest reported so far, demonstrated its association with various precursor lesions and distinct immunohistochemical profiles. Both APCA and GCA had worse survival than LAMN, suggesting the importance of distinguishing from the latter.

**360    Assessment of Prognostic Factors of Solitary Fibrous Tumors Arising from the Gastrointestinal Tract and Liver: A Clinicopathologic Study of 34 Cases**

Xiaoqin Liu[1], Michael-John Beltejar[1], Xiaoyan Liao[1]
[1]University of Rochester Medical Center, Rochester, NY

**Disclosures:** Xiaoqin Liu: None; Michael-John Beltejar: None; Xiaoyan Liao: None

**Background:** Solitary fibrous tumors (SFTs) are mesenchymal neoplasms that predominately arise from the pleura. It is usually indolent but can have malignant potential. SFTs primarily involve the gastrointestinal tract and liver (SFTGIL) are extremely rare, and the clinicopathological features remain largely unclear.

**Design:** A total of 34 SFTGIL, 9 diagnosed at our institution and 25 reported in literature between the years of 2012 and 2020, were included in this study cohort. Three published risk models designed specifically for SFTs [mDemicco, Salas, Pasquali] were evaluated. Statistical analysis was performed by SPSS23. The overall survival (OS) was estimated using the Kaplan–Meier method.

**Results:** As a group, SFTGILs occurred most commonly in males (n = 25, 73.5%), with a median age of 54 years (range 17–80 y) at initial diagnosis. Twenty-five (73.5%) tumors were of gastrointestinal (GI) origin and 9 (26.5%) were of liver origin. The mean tumor size was 14.6 (range: 1.5-36) cm. Microscopically, the tumor cells were generally bland and spindled, organized in a "patternless" growth pattern, admixed with variable amounts of collagen and typical staghorn blood vessels. Immunohistochemically, STAT6, CD34, and Bcl-2 were positive in 10/10 (100%), 32/34 (94%), and 27/29 (93%) tested cases. Thirty-two (94%) patients were managed with resection, while 2 patients had chemotherapy only. Upon follow-up (median: 65 months), 7 of 34 (20.6%) patients developed tumor recurrences or distant metastasis (3 to lungs, 1 to live), of which 3 (8.8%) patients died of disease progression. Comparisons between tumor origins (GI vs. Liver) showed significant sex differences, in that females were predominant (F: 67%) in hepatic SFT while males were predominant (F: 12%) in GI tract SFT (P<0.01). By univariate analysis, female sex, age (>60y), and tumor necrosis were significant prognostic factors associated with adverse outcome (P<0.05). Hepatic SFTs had worse survival than of GI tract SFTs (p<0.01). Among the three risk models, both Salas and mDemicco, but not Pasquali risk scores, were associated with OS (P=0.025 for Salas, 0.043 for mDemicco).

**Conclusions:** Our study showed that hepatic SFTs had distinct clinical features and worse survival than GI tract SFTs. The mDemicco and Salas risk models were reliable risk models for identifying patients with SFTGIL at high risk of recurrence or metastasis, which is important to guide clinical follow-up and management.

**361    Neuroendocrine Differentiation in Anal Basaloid Carcinomas**

Haiyan Lu[1], Daniela Allende[2], John Goldblum[1]
[1]Cleveland Clinic, Cleveland, OH, [2]Cleveland Clinic, Lerner College of Medicine of Case Western University School of Medicine, Cleveland, OH

**Disclosures:** Haiyan Lu: None; Daniela Allende: None; John Goldblum: None

**Background:** The differential diagnosis of basaloid anal carcinomas is challenging and includes basal cell carcinoma of skin (BCC) and basaloid squamous cell carcinoma (BSCC). Morphologic and immunohistochemical characteristics have been previously described and their diagnostic distinction carries therapeutic and prognostic implications. The significance of neuroendocrine differentiation in these tumors remains poorly understood.

**Design:** Cases of anal BCC and BSCC diagnosed during 1992-2020 were retrieved from Cleveland Clinic pathology database. Only cases with blocks or unstained slides available were included for the study 17 BCC and 25 BSCC cases. The cases had a consensus diagnosis integrating histology and immunephenotypic features. Neuroendocrine differentiation was assessed by stains synaptophysin, chromogranin A and Insulinoma-associated 1 (INSM1). Quantitative (1+: < 5%, 2+: 5-25%, 3+: 26-50%, 4+: 51-75%; 5+: 76-100%) and qualitative (weak or strong) interpretation of the stains was compared between the two entities. For the qualitative analysis, weak is defined as finely granular cytoplasmic staining visible at 10x while strong by definition is that granular cytoplasmic staining visible at 4x. The results are presented as N (%). Statistical analysis was performed using Fisher exact test via IBM SPSS Statistics 19. P< 0.05 is considered as statistic significant.

**Results:** 1/17 BCCs weakly expressed synaptophysin (1+) compared with 1/25 BSCCs (4+) (5.9% vs 4.0%; p=0.999; table 1). Chromogranin A expression was seen in 13/16 BCCs (2+ in half of the cases, 3+ in 1 case and 4+ in 4 of them, all of which showed weak staining) while positivity was observed in 2/24 BSCCs (2+, weak) (81.3% vs 8.3%; p=0.001; table 1). INSM1 was not found in any of the BCCs (0/17) while 1 case of BSCC showed weak 4+ staining. (0/17 (0%) vs 1/25 (4.0%), p=0.999; table 1). The unique case of BSCC with neuroendocrine differentiation with immunereactivity to synaptophysin, chromogranin A and INSM1 had plasmacytoid and rhabdoid cytomorphology and was poorly differentiated.

**Table 1. Neuroendocrine profiles of BCCs and BSCCs of the anal region**

| Neuroendocrine markers | BCC (N=17) | BSCC (N=25) | Fisher exact test P value |
|---|---|---|---|
| **Synaptophysin positivity (N, %)** | **1/17 (5.9)** | **1/25 (4.0)** | **0.999** |
| 2+, weak | 1/17(5.9) | - | - |
| 5+, strong | - | 1/25 (4.0) | - |
| **Chromogranin A positivity (N, %)** | **13/16 (81.3)** | **2/24 (8.3)** | **0.001** |
| 2+, weak | 8/16 (50.0) | 2/24 (8.3) | - |
| 3+, weak | 1/16 (6.3) | | |
| 4+, weak | 4/16 (25.0) | - | - |
| **INSM1 positivity (N, %)** | **0/17 (0)** | **2/25 (8.0)** | **0.506** |
| 1+, weak | - | 1/25 (4.0) | |
| 5+, weak | - | 1/25 (4.0) | - |

**Conclusions:** Neuroendocrine differentiation (particularly chromogranin A staining) is more commonly seen in BCCs while it is rarely seen in BSCCs. Chromagranin A positive, when present, supports the diagnosis of BCC rather than BSCC.

**362 Genetic Characterization of Hepatoid Tumors from Different Organs: Context Matters**
Claudio Luchini[1], Rita Lawlor, Concetta Sciammarella[1], Andrea Mafficini[1], Gaetano Paolino[1], Paola Mattiolo[1], Lodewijk Brosens[2], N. Volkan Adsay[3], Liang Cheng[4], Aldo Scarpa[1]
[1]University of Verona, Verona, Italy, [2]University Medical Center Utrecht, Utrecht, Netherlands, [3]Koç University Hospital, Istanbul, Turkey, [4]Indiana University, Indianapolis, IN

**Disclosures:** Claudio Luchini: None; Rita Lawlor: None; Concetta Sciammarella: None; Andrea Mafficini: None; Gaetano Paolino: None; Paola Mattiolo: None; Lodewijk Brosens: None; N. Volkan Adsay: None; Liang Cheng: None; Aldo Scarpa: None

**Background:** Hepatoid tumors (HT) are a rare group of cancers resembling morphologically hepatocellular carcinoma, which arise in different organs other than liver. A comprehensive molecular profile of this group of neoplasms is still lacking.

**Design:** A genetic characterization of 20 HT from different organs was performed using three different multigene next-generation sequencing panels.

**Results:** *TP53* was the only mutated gene occurring in HT of different sites (8/20 cases), while the vast majority of alterations were clustered according to the tissue of origin. The most relevant findings were: i) colorectal HT: microsatellite instability, high tumor mutation burden, mutations in *ARID1A/B* and *KMT2D* genes, and *NCOA4-RET* gene fusion (2/3 cases); ii) gastric HT: *TP53* mutations (2/4); iii) pancreatico-biliary: loss of *CDKN2A* and loss of chromosome 18 (3/5); iv) genital HT: gain of chromosome 12 (3/6); v) lung HT: *STK11* somatic mutations (2/2).

**Conclusions:** The analysis of a heterogeneous cohort of HT from different organs did not reveal a common molecular hallmark that could explain the peculiar hepatoid morphology. Most genetic alterations were clearly clustered by site, highlighting that context matters: the tissue of origin emerged as the most important factor in influencing HT molecular landscape.

**363     Integrated Clinicopathologic and Genomic Analysis to Predict Response to Neoadjuvant Treatment in Esophageal Cancer**

Chih-Ping Mao[1], Lynette Sholl[1], Shih-Chin Wang[2], Alexander Christakis[1], Aaron Dezube[3], Namrata Setia[4], Agoston Agoston[1], Deepa Patil[3], Mark Redston[1], Thomas Abrams[5], Jon Wee[3], Lei Zhao[3]
[1]Brigham and Women's Hospital, Boston, MA, [2]Wyss Institute for Biologically Inspired Engineering, Harvard University, Boston, MA, [3]Brigham and Women's Hospital, Harvard Medical School, Boston, MA, [4]University of Chicago, Chicago, IL, [5]Dana-Farber Cancer Institute, Brigham and Women's Cancer Center, Boston, MA

**Background:** Neoadjuvant chemoradiation (CRT) followed by surgical resection is the standard treatment approach for most patients with locally advanced esophageal cancer. However, benefit from neoadjuvant CRT varies widely among patients, and reliable predictors of treatment response have not been identified. The goal of this study is to identify clinicopathologic features and genetic alterations that correlate with pathologic response to neoadjuvant therapy.

**Design:** In this retrospective study, a total of 10 clinicopathologic parameters (age, gender, histologic type and grade, presence of signet ring cell differentiation in either the tumor biopsy or post-treatment resection specimen, tumor size, location of tumor in the esophagus, pre-treatment clinical T stage (cT) and lymph node status (cN)) were examined in a cohort of 916 patients with esophageal carcinoma who received neoadjuvant CRT followed by esophagogastrectomy. In 224 of these patients, the mutational profiles of selected cancer-related genes (447 genes) were also analyzed. Logistic regression and principal component analysis (PCA) were used to identify clinicopathologic and genomic factors that predict response to therapy (as assessed by pathologic stage on resection).

**Results:** Clinicopathologic characteristics of the study cohort (n=916) are summarized in Table 1. Features that show significant correlation with complete response to neoadjuvant therapy are summarized in Figure 1. Each parameter is assigned a weight based on its relative importance in the logistic regression model (AUC=0.657). For the subset of patients with concurrent molecular analysis (n=224), mutated genes were grouped into six clusters by PCA according to their distribution by post-treatment pathologic stage, as shown in Figure 2a. Although none of the clusters showed significant enrichment in the ypT0 group, we identified a subset of 29 genes (clusters 3 and 4) that were more commonly mutated in patients with stage ypT4 disease than those with earlier stage disease, suggesting that alterations in these genes may be associated with poor response to therapy (Figure 2b).

| **Clinicopathologic characteristics of the entire study cohort and patients with a complete versus incomplete pathologic response.** | | | |
|---|---|---|---|
| | **Entire cohort** | **Complete pathologic response (ypT0N0)** | **Incomplete pathologic response** |
| **Number of patients (%)** | 916 | 243 (26.5%) | 673 (73.5%) |
| **Median age (yrs)** | 64.5 | 64.6 | 63.9 |
| **Male gender (%)** | 751 (81.9%) | 183 (75.3%) | 568 (84.4%) |
| **Histologic type (adenocarcinoma (%) / squamous cell carcinoma (%) / other (%))** | 771 (84.2%) / 131 (14.3%) / 12 (1.3%) | 171 (70.6%) / 62 (25.6%) / 9 (3.7%) | 600 (89.4%) / 68 (10.1%) / 3 (0.45%) |
| **Tumor location (proximal (%) / mid (%) / distal and GE junction (%))** | 12 (1.3%) / 98 (10.7%) / 805 (87.9%) | 5 (2.3%) / 43 (20.2%) / 166 (78.3%) | 7 (1.0%) / 53 (7.9%) / 613 (91.1%) |
| **Pre-treatment cT (T1 (%) / T2 (%) / T3 (%) / T4 (%))** | 22 (2.9%) / 174 (23.4%) / 533 (71.6%) / 15 (2.0%) | 8 (3.9%) / 53 (26.2%) / 139 (68.8%) / 2 (1.0%) | 14 (2.6%) / 120 (22.2%) / 394 (72.8%) / 13 (2.4%) |
| **Pre-treatment cN (N0 (%) / N1 (%) / N2 and above (%))** | 402 (80.4%) / 92 (18.4%) / 6 (1.2%) | 113 (80.1%) / 24 (17.0%) / 4 (2.8%) | 289 (80.5%) / 68 (18.9%) / 2 (0.56%) |

Figure 1 - 363

| Parameter | Parameter estimate | P-value |
|---|---|---|
| Male gender | -0.441 | 0.040 |
| Histologic type - squamous cell carcinoma | 0.876 | 0.0000115 |
| Pretreatment cT  stage | -0.258 | 0.091 |
| Pretreatment cN stage | 0.065 | 0.608 |
| Presence of signet ring differentiation on pathology | -0.963 | 0.00149 |

Figure 2 - 363
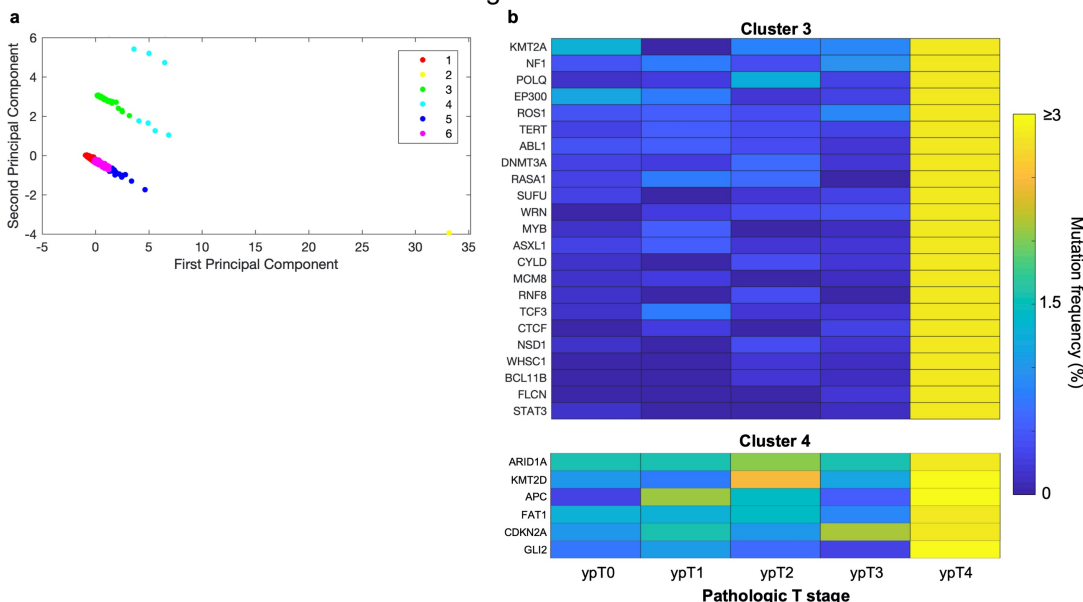


**Conclusions:** This study demonstrates that in patients with esophageal cancer, male gender, high pre-treatment clinical T stage, and presence of signet ring differentiation on histology correlate with poor response to neoadjuvant CRT, whereas squamous cell carcinoma correlates with favorable pathologic response. In addition, we identified a subset of genetic alterations that appears to correlate with poor response to therapy and may serve as prognostic biomarkers and as aids in the identification of patients in whom other therapies are needed.

(The authors would like to acknowledge the DFCI Oncology Data Retrieval System (OncDRS) for the aggregation, management, and delivery of the clinical and operational research data used in this project. The content is solely the responsibility of the authors.)

**364    Distribution of Pathogenic Mutations in Dysplastic Lesions in Patients with Inflammatory Bowel Disease (IBD)**
Haider Mejbel[1], Deepti Dhall[1], Wenjuan Zhang[2], Alexander Mackinnon[1], Chirag Patel[1], Sameer Al Diffalha[1], Goo Lee[3], Eric Vail[2], Kevin Waters[2], Shuko Harada[1]
[1]The University of Alabama at Birmingham, Birmingham, AL, [2]Cedars-Sinai Medical Center, Los Angeles, CA, [3]UAB Hospital, Birmingham, AL

**Disclosures:** Haider Mejbel: None; Deepti Dhall: None; Wenjuan Zhang: None; Alexander Mackinnon: None; Chirag Patel: None; Sameer Al Diffalha: None; Goo Lee: None; Eric Vail: *Speaker*, Thermo Fisher Scientific; Kevin Waters: None; Shuko Harada: None

**Background:** Patients with IBD have increased risk of colorectal carcinoma (CRC). Compared to sporadic adenomas (SA), colitis-associated dysplasia (CAD) has higher risk of progression to carcinoma. In IBD patients, it

is often difficult to distinguish between CAD and SA, particularly when the lesions are polypoid. We recently observed higher tumor mutation burden (TMB) in CAD in comparison to SA in IBD patients. The mutation profile of IBD-associated CRC is reported to be distinct from sporadic CRC. Herein, we studied the molecular signature of CAD compared with SA in IBD patients.

**Design:** Dysplastic lesions were microdissected from twenty-two IBD patients (11 with CAD and 11 with SA). The presence of active chronic colitis in the background mucosa along with the morphologic features of the dysplastic lesion was used to distinguish CAD from SA. Extracted DNA was sequenced with Oncomine Tumor Mutation Load Assay, and sequencing data was analyzed by Ion Reporter 5.6. Nonsynonymous somatic variants downloaded from Ion Reporter was used to calculate the tumor mutational burden (TMB) value of the sample.

**Results:** The median age of both the CAD and SA group was 55, with a nearly equal sex distribution. Ulcerative colitis was the most common IBD type in both groups. Median time for the duration of IBD in CAD and SA was 17 years and 28 years, respectively. All SAs were polypoid whereas CAD had varying endoscopic/gross appearance (n = 9, 82% were polypoid/pseudopolypoid; n= 2, 18% were flat). Associated carcinoma was present in 3 patients (27%) of the CAD group and in 1 patient (9%) of the SA group.

Mutation analysis detected at least one and up to four (mean=1.55) pathogenic mutations in 8 CAD cases (73%) with a median nonsynonymous tumor mutation burden of 6.5 mutations/megabase, among which, *KRAS* and *TSC1* were the most common detected pathogenic mutations (n=2, 20% for each mutation). In SA, there were one and up to two (mean =0.95) pathologic mutations in 7 patients (63%), with a median nonsynonymous tumor mutation burden of 3.0 mutations/megabase, among which, APC was the most detected pathogenic mutation (n=3, 37%). *TP*53 was equally detected in one patient from each group (n=1, 12.5%).

Figure 1 - 364



**# of pathogenic variants in each group**
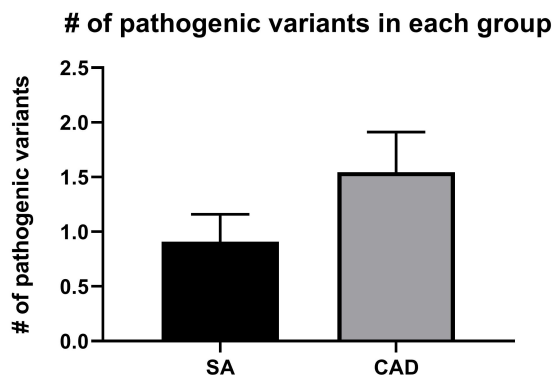
**Conclusions:** Compared to the SA in IBD patients, more frequent pathologic mutations are detected in CAD. This might be explained by tumor microenvironment in CAD, in which, the longstanding inflammation and high level of cytokines likely contribute to tumor development and progression.

**365    Histopathological Evaluation of Sleeve Gastrectomy at a Single Institution: Is it Cost–Effective?**
Charles Middleton[1], Neha Varshney[2]
*[1]University of Mississippi Medical Center, Jackson, MS, [2]University of Mississippi, Jackson, MS*

**Disclosures:** Charles Middleton: None; Neha Varshney: None

**Background:** Amidst the obesity epidemic affecting the United States, sleeve gastrectomies (SG) have become a relatively common bariatric procedure to aid in weight loss. The surgery is essentially a partial gastrectomy and involves the removal of a portion of the stomach. SG are offered to patients who meet the appropriate criteria.

Indications include BMI greater than 40 or between 35 and 40 with concurrent weight-related health issues. The preoperative use of endoscopy is commonly used, yet it is not a standard of care. The current recommendation is for the surgeon to decide on a case-by-case basis. At our institution, routine preoperative endoscopy is not performed. The objective of this study is to assess the utility of histologic evaluation of SG specimens.

**Design:** At our institution, a retrospective analysis of all SG operations performed between the dates of 08-01-2017 and 08-31-2020 was performed. The surgical pathology report for each case was reviewed and the findings were documented along with patient demographics from our electronic medical record. The concomitant CPT code for the procedure was determined. The operating costs associated with the gross prosection of the specimen, resources necessary for histological preparation and processing, and creation of a hematoxylin and eosin stained slide were calculated. The procedural cost was compared to the total integrated cost necessary for histological evaluation of the specimen.

**Results:** A total of 299 patients underwent a SG during the study period. The cohort consisted of 29 males and 270 females ranging in age from 22 to 70 years. Mild chronic gastritis (156) was the most common pathologic finding in these patients, followed by moderate chronic gastritis (11), mild to moderate chronic gastritis (6), and active chronic gastritis (6). Unexpected findings included *Helicobacter pylori* (*H. pylori*, 23), intestinal metaplasia (1), gastrointestinal stromal tumor (GIST, 1), and well-differentiated neuroendocrine tumor (NET, 1). The billing code for sleeve gastrectomy is 88307 and the cost generated is $274 per procedure at our institution. This equates to a substantial financial burden of $81,926 for the complete pathologic analysis of the cases included in our study.

**Conclusions:** The histopathological abnormalities identified from SG specimens are limited. While *H. pylori* gastritis was identified in 7.7% of cases, the overwhelming majority of cases (89.3%) showed no diagnostic pathologic alterations or merely mild chronic gastritis. Incidental GIST and NET were discovered, but no preoperative endoscopy was performed in either case. These findings suggest that the histopathologic diagnosis rendered in roughly 90% of SG cases has no clinical implication. We conclude that the histopathologic evaluation of sleeve gastrectomy specimens is unnecessary in the majority of cases, unless preoperative endoscopy or gross examination reveals any abnormalities.

## 366 Genome Wide Association of Gastroparesis Identifies Novel Disease-Associated Genetic Loci

Mohammad Mohammad[1], Diane Smelser[2], Yi Ding[2], David Carey[3]
[1]Geisinger Commonwealth School of Medicine, Danville, PA, [2]Geisinger Medical Center, Danville, PA, [3]Geisinger Health, Danville, PA

**Disclosures:** Mohammad Mohammad: None; Diane Smelser: None; Yi Ding: None

**Background:** Gastroparesis is a chronic condition characterized by delayed gastric emptying as well as ultrastructural changes of interstitial cells of Cajal (ICC) in the gastric tissue. The etiology remains elusive, with limited treatment options. Gastroparesis affects up to 50% of diabetes mellitus (DM) patients. Our aim is to identify genetic variants associated with this devastating disease, and to assess these variants as diagnostic biomarkers and potential therapeutic targets.

**Design:** Gastroparesis cases were identified from diagnoses recorded in Geisinger electronic health records. Unaffected individuals served as controls. Genotype data was provided through the Geisinger MyCode Community Health Initiative. We ran a genome-wide association study (GWAS) using an additive genetic model, controlling for age, sex and BMI. We also controlled for DM (type-I, type-II) in sub-analyses of the most significant variants.

**Results:** A total of 114,372 eligible participants included 2588 gastroparesis cases. Of these cases, 553 (19%) had type-I DM (OR 5.33, 95% CI: 4.82-5.87), 1492 (53.2%) had type-II DM (OR 3.15, 95% CI: 2.92-3.40), and (28.7%) were idiopathic (p<.0001). Genome-wide significant associations were found for rs2116378, an intronic variant in the *Deleted in Colorectal Cancer (DCC)* gene that encodes the receptor for the axon guidance molecule Netrin (*Net1*) (OR 1.18, 95% CI: 1.12-1.25), and rs9273363, which is upstream of *HLA-DQB1-AS1*, which encodes a long-noncoding RNA that has been implicated in inflammatory disease (OR 1.17, 95% CI:1.09-1.25). When corrected for type-I or type-II DM the association of rs2116378 with gastroparesis remained significant (OR1.18, 95%CI: 1.12-

1.25; and OR 1.15, 95% CI:1.09-1.21), as did that for rs9273363 (OR 1.11, 95% CI:1.04-1.17; and OR 1.14, 95% CI:1.08-1.21).

Figure 1 - 366
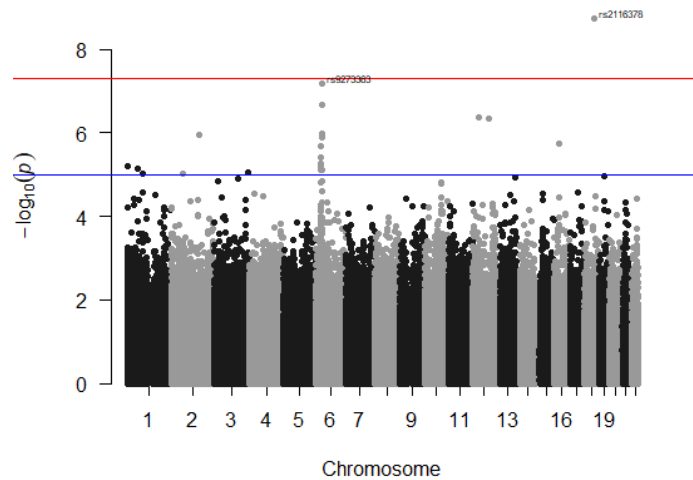


**Conclusions:** To our knowledge this is the first population based GWAS of gastroparesis. We identified two significantly associated genetic loci, which implicate gut dysinnervation and inflammation as possible biological mechanisms.  Ongoing work is extending these findings.

---

**367    Clinicopathologic and DNA Flow Cytometric Analysis of Nonampullary Duodenal Adenomas in Sporadic Versus Familial Adenomatous Polyposis Patients**
Nebil Mohammed[1], Peter Rabinovitch[2], Dongliang Wang[3], Bence Kővári[4], Aras Mattis[1], Gregory Lauwers[5], Won-Tak Choi[1]
[1]University of California, San Francisco, San Francisco, CA, [2]University of Washington, Seattle, WA, [3]SUNY Upstate Medical University, Syracuse, NY, [4]H. Lee Moffitt Cancer Center & Research Institute, Tampa, FL, [5]H. Lee Moffitt Cancer Center & Research Institute, University of South Florida, Tampa, FL

**Disclosures:** Nebil Mohammed: None; Peter Rabinovitch: None; Dongliang Wang: None; Bence Kővári: None; Aras Mattis: None; Gregory Lauwers: None; Won-Tak Choi: None

**Background:** Nonampullary duodenal adenomas (DA) develop sporadically or in the setting of a hereditary syndrome such as FAP. Although they are thought to progress into adenocarcinoma via the adenoma to carcinoma sequence similar to colorectal cancer, limited data suggested that DAs may be biologically dissimilar to colorectal adenomas. Also, the clinicopathologic features of DAs are not extensively studied.

**Design:** Clinicopathologic features of 71 DA patients (34 sporadic and 37 FAP) were analyzed. From the 71 patients, 89 biopsies (47 sporadic and 42 FAP) were evaluated by DNA flow cytometry. Of these, 82 showed low-grade dysplasia (LGD) and 7 high-grade dysplasia (HGD). Twenty-one low-grade adenomas of the ileal pouch (n = 19) and jejunum (n = 2) from 15 FAP patients (41%) were also tested.

**Results:** FAP patients were more likely to be younger (mean: 28 years) and have multifocal disease (92%) than sporadic patients (66 years and 24%, respectively) (p < 0.001). Most DAs presented as a polypoid lesion (87%) in the duodenal bulb or second portion of the duodenum (89%) and showed tubular architecture (65%). The mean size of sporadic DAs (2.4 cm) was larger than that of FAP-related DAs (1.3 cm) (p = 0.005). Sixty-six patients (93%) had LGD, while 5 patients (4 sporadic and 1 FAP) had HGD (p = 0.187). Aneuploidy was detected in only 1 (1%) sporadic DA with HGD, whereas the remaining 109 duodenal, ileal pouch, and jejunal adenomas showed normal

DNA content. Of the 37 FAP patients, 29 (78%) had a history of total proctocolectomy, and 15 (52%) developed low-grade adenomas in the ileal pouch with (n = 2) or without (n = 13) jejunal involvement (versus 0% in sporadic patients, p < 0.001). Only 3 patients (4%) developed adenocarcinoma in the duodenum (n = 2) or ileal pouch (n = 1) within a mean follow-up time of 54 months. Three-, 9-, and 15-year detection rates of adenocarcinoma in FAP patients were 2.7%, 9.7%, and 22.6%, respectively, while all these rates remained at 0% in sporadic patients.

**Conclusions:** Despite having some distinct clinical features, FAP-related DAs appear to share similar molecular features with their sporadic counterpart. Aneuploidy (characteristic of colorectal adenoma) may be an extremely rare or late event in the adenoma to carcinoma sequence in the small intestine. The relatively low incidence rate of nonampullary duodenal adenocarcinoma compared with other sites in the GI tract may be in part explained by the lack of aneuploidy in the adenomatous precursor lesions.

### 368 Progression Risk of Anal Low Grade Squamous Intraepithelial Lesions (LSIL/AIN 1)

Ashley Monsrud[1], Uma Krishnamurti[1], Marina Mosunjac[1]
[1]Emory University, Atlanta, GA

**Disclosures:** Ashley Monsrud: None; Uma Krishnamurti: None; Marina Mosunjac: None

**Background:** The natural history of HPV in the anus is not clearly elucidated. Anal low-grade SIL/AIN 1 carries the potential for progression to HSIL (high grade SIL) or cancer. Studies show that 63% of HIV+ men will progress to HSIL within two years; however, there is no standard follow up recommendation for those patients or histopathology markers that have proven to be successful in detecting this high-risk group of LSIL/AIN1 patients. We propose to investigate the role of p16 in predicting progression risk of anal LSIL in 5 years of follow up with the hypothesis that p16 positive LSIL have a higher risk of progression to HSIL.

**Design:** From August 2013 to December 2014, 324 cases of anal LSIL or condyloma were identified from electronic records. Seventy-three cases had no HSIL diagnosis on the current specimen or previous biopsies. Forty-one of those patients had 108 biopsy parts and had follow up biopsies that were available. H&E slides were reviewed to exclude any cases that would morphologically qualify for HSIL, and p16 stain was done on each biopsy confirmed to be LSIL/AIN 1. p16 positivity was interpreted in concordance with Lower Anogenital Squamous Terminology Standardization Project (LAST) recommendations.

**Results:** There were 37 males, 4 females, and 1 male to female transgender patient. All the patients were HIV positive. The average age of male patients was 38 ± 12.2, and of female patients was 46 ± 5.2. Almost 1/3 (29.3%) of patients with LSIL anal biopsy had positive p16 in one part of the entire biopsy. 15 of 108 (13.9%) biopsy parts showed block positivity for p16. None of these patients progressed to HSIL, with an average follow up 45.8 ± 5.6 months. None of eight patients (19.0%) who progressed to HSIL, showed p16 positivity in their initial LSIL biopsy. Median follow up was 31.5 ± 8.4 months.

**Conclusions:** p16 is not a useful predictive marker of progression to HSIL in patients with anal LSIL. A large proportion of high-risk patients with multiple anal biopsies showed block positivity with p16, and none of those showed progression in follow up. p16 should not be routinely used to evaluate anal LSIL, and LAST recommendations should be closely followed.

### 369 Histologic Findings of Interval Appendectomy Specimens Mimic Crohn Disease and Low Grade Mucinous Appendiceal Neoplasm (LAMIN)

Maria Mostyka[1], Zhengming Chen[2], Rhonda Yantiss[2], Yao-Tseng Chen[3]
[1]New York-Presbyterian/Weill Cornell Medical Center, New York, NY, [2]Weill Cornell Medicine, New York, NY, [3]Weill Cornell Medical College, New York, NY

**Disclosures:** Maria Mostyka: None; Zhengming Chen: None; Rhonda Yantiss: None; Yao-Tseng Chen: None

**Background:** Patients with acute appendicitis are increasingly managed with antibiotic therapy followed by delayed appendectomy because this approach is associated with less morbidity than immediate surgery. The inflammatory

patterns in 22 of such interval appendectomy specimens were reported by Guo and Greenson in 2003, but the topic has not been revisited in the recent literature.

**Design:** We reviewed surgical pathology records to identify interval appendectomy specimens obtained during a 5-year period. All cases were evaluated for the nature and distribution of inflammation (e.g. eosinophils, histiocytes, neutrophils, lymphocytes, granulomas) and associated fibrosis, as well as the presence and type of epithelial and architectural changes, such as goblet cell hyperplasia, diverticula, and extruded mucin. Histologic findings were correlated with clinical history, when available.

**Results:** We examined 124 interval appendectomy specimens. Complete clinical and radiographic information was available for 90 patients, including 56 females and 34 males (mean age: 42 years). Forty-nine (54%) cases were perforated, and 97% of patients were treated with intravenous and oral antibiotics. Percutaneous drains were placed in 32 (36%) cases. Most (52%) appendices contained mural eosinophilic infiltrates. The pattern of inflammation simulated features typical of chronic infections or Crohn disease. These changes were present in 11 (9%) cases and included epithelioid granulomata (n=10) and transmural lymphoid aggregates (n=11). Serosal fibrosis (n=47) was associated with radiographic perforation (p=0.02) and percutaneous drain placement (p=0.04). Goblet cell hyperplasia was present in 14 (11%) cases and, when present in combination with diverticula (n=7, 50%) and/or extravasated mucin (n=6, 43%), simulated the appearance of an appendiceal mucinous neoplasm.

Table 1. Histologic findings in 124 interval appendectomy specimens

| Histologic Findings | Number of cases |
|---|---|
| Inflammatory changes | |
| Eosinophils in wall | 64 (52%) |
| Macrophages in wall | 51 (41%) |
| Neutrophils in wall | 14 (11%) |
| Transmural lymphocytic aggregates | 11 (9%) |
| Granulomatous inflammation | 18 (15%) |
| Epithelioid (Crohn-like) | 10 (8%) |
| Xanthogranulomatous/pulse granuloma | 8 (6%) |
| Giant cells (in granulomas or isolated) | 42 (34%) |
| Epithelial changes | |
| Goblet cell hyperplasia | 14 (11%) |
| Architectural changes | |
| Serosal fibrosis | 47 (38%) |
| Luminal dilatation | 14 (11%) |
| Diverticulum | 15 (12%) |
| Extravasated mucin | 20 (16%) |

Figure 1 - 369
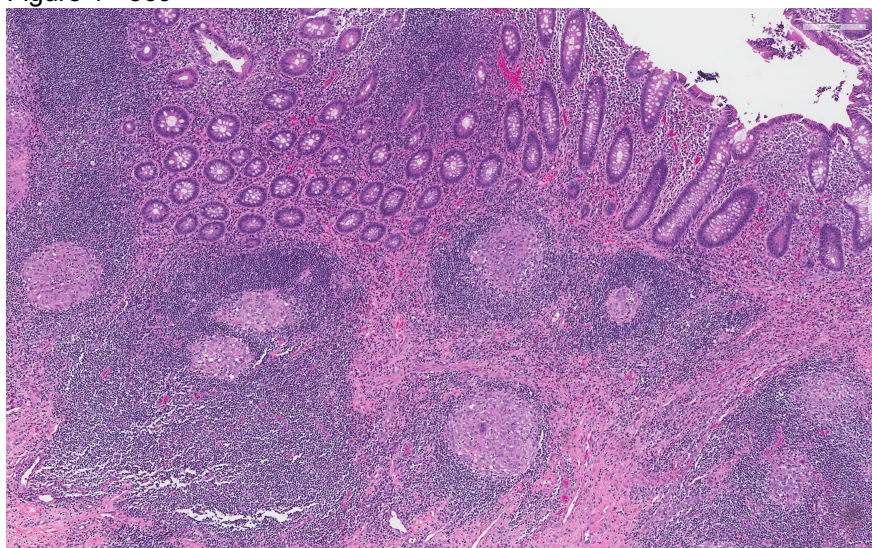
Figure 2 - 369
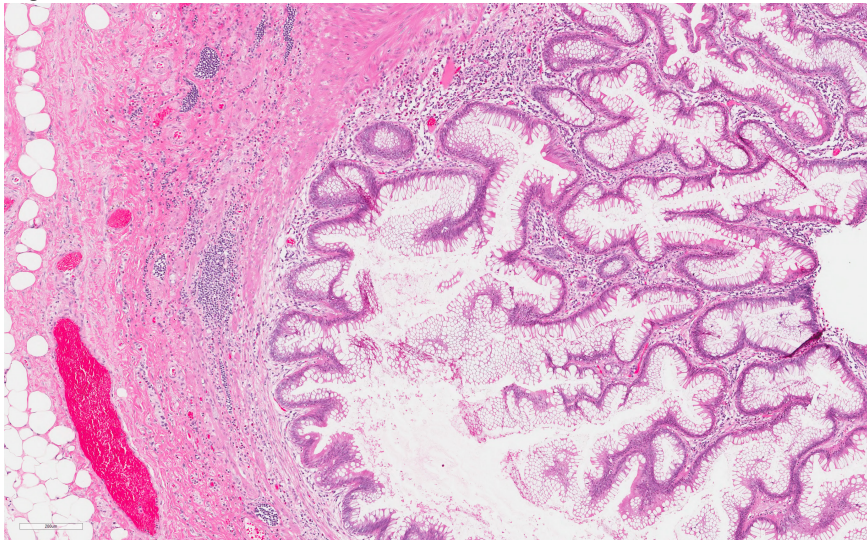


**Conclusions:** As previously described, interval appendectomy specimens can exhibit granulomatous inflammation, transmural lymphoid aggregates, and mural fibrosis that mimic Crohn disease. More importantly, they can also show goblet cell hyperplasia, often associated with diverticula and/or organizing peri-appendiceal mucin, simulating appendiceal mucinous neoplasms. The possibility of a delayed appendectomy should be considered and excluded clinically whenever a diagnosis of appendiceal mucinous neoplasm is entertained.

## 370 Institutional Review of the Diagnostic Utility and Clinical Significance of Deeper levels in Colon Polyps

Smitha Mruthyunjayappa[1], Venkata Dayana[1], Sameer Al Diffalha[1], Goo Lee[2], Deepti Dhall[1], Isam Eltoum[1], Chirag Patel[1]
[1]The University of Alabama at Birmingham, Birmingham, AL, [2]UAB Hospital, Birmingham, AL

**Disclosures:** Smitha Mruthyunjayappa: None; Venkata Dayana: None; Sameer Al Diffalha: None; Goo Lee: None; Deepti Dhall: None; Isam Eltoum: None; Chirag Patel: None

**Background:** Colon polyps (CP) are one of the most frequently encountered specimens in daily pathology practice and deeper levels are often ordered for further diagnostic evaluation. The objective of this study was to investigate the utility of deeper levels in CPs in comparison to the clinical surveillance guidelines.

**Design:** From 9/2019 to 9/2020, our institution received 2924 colon biopsies designated as "colon polyp" on the requisition form.

All of these cases for which additional levels were ordered were retrieved from the histology ordering system. The final diagnosis made after deeper levels were stratified into 3 categories:

The first category (NSHPA) included a final diagnosis of no histopathological abnormality or lymphoid aggregates or surface hyperplastic changes. The second category included deeper levels which revealed a tubular adenoma (TA). The third category included polyps where the levels were ordered to interpret sessile serrated lesion (SSL) vs hyperplastic polyp (HP).

In addition, the count and reported size of the CPs were compared to the latest Post-Colonoscopy surveillance guidelines by U.S. Multi-Society Task Force on Colorectal Cancer (USMSTF).

**Results:** Of the 2924 colon polyp biopsy specimens, only 303 (10%) cases needed additional deeper levels. Of these 303 cases, 158 (52%) were NSHPA; 62 (20.5%) revealed the presence of a TA; and 83 (27.5%) were used to interpret SSL vs HP.

In comparison of the deeper levels ordered which revealed NSHPA (n=158) vs the cases which revealed a TA (n=62) (total n=221), this study shows that only 20.5% of these will reveal a TA on additional deeper levels. Thus, in comparison of all colon polyps received, only 2.1% of all polyps received will require deeper levels to reveal the presence of a TA. Of these 62 cases, 43 were solitary TAs, which would alter the surveillance recommendation from 10 years to 7-10 years. Only 2 cases caused the recommended surveillance guideline to increase from 7-10 to 3-5 year follow up. See table 1

At the estimated cost of $5.82 per H&E slide, the 158 cases which revealed NSHPA x 3 levels would equal an annual cost savings of ~$2,759.

| Changes in Clinical Surveillence based on Deeper levels | | | |
|---|---|---|---|
| N=221 | No Change | From 10 yr to 7-10 yr follow up | From 7-10 yr to 3-5 yr follow up |
| NSHPA | 158 | 0 | 0 |
| TA | 14 | 43 | 2 |

**Conclusions:** Based on our institutional review, deeper levels were ordered on ~10% of all CP cases. Our study shows the significant majority, 71.9%, of CPs where deeper levels are ordered will show no additional changes. Only 28.1% of these CPs where deeper levels were ordered revealed the presence of a TA. In addition, the likely clinical significance of this is minimal as only 2 cases altered the surveillance from 7-10 years to 3-5 years, which would represent 0.06% of all 2924 CPs received. In addition, none of the initial non-diagnostic colon polyps revealed underlying high-grade dysplasia.

Our study shows ordering deeper levels will rarely have significant change on clinical surveillance and reduction in deeper level ordering has cost saving benefits without negatively affecting patient care.

## 371 Genomic Profiling Supports a Hyperplastic Polyp-Traditional Serrated Adenoma-Colorectal Cancer Carcinogenesis Pathway

Grace Neville[1], Danielle Manning[2], Elizabeth Garcia[2], Yonghui Jia[2], Jonathan Nowak[2], Amitabh Srivastava[1]
[1]Brigham and Women's Hospital, Harvard Medical School, Boston, MA, [2]Brigham and Women's Hospital, Boston, MA

**Disclosures:** Grace Neville: None; Danielle Manning: None; Elizabeth Garcia: None; Yonghui Jia: None; Jonathan Nowak: None; Amitabh Srivastava: None

**Background:** Traditional serrated adenomas (TSAs) are widely accepted precursors of colorectal cancer (CRC) while hyperplastic polyps (HPs) are regarded as benign lesions of no malignant potential. However, some TSAs appear to arise on a background of HP. We explored whether such TSAs are clonally related to the background HP and also investigated molecular changes in TSAs as they progress to CRC, with a focus on conventional adenoma-like dysplasia in TSAs.

**Design:** Seventeen TSAs with a component of HP (n=5) or conventional adenoma-like dysplasia (n=5) or foci of HGD/carcinoma (n=7) were identified. Two cases with HGD/carcinoma also had distinct foci of HP. Morphologically discrete regions (n=32) were macrodissected from each polyp and analysed using OncoPanel, a hybrid-capture based next generation sequencing assay targeting 447 genes for multiple alteration types. Genes known to be involved in CRC pathogenesis were selected for further analysis.

**Results:** Seventeen patients were included in the cohort (10 male) with a mean age of 62.41 (+/-10.3) years. 11/17 TSAs were located in rectosigmoid, 2 in descending, 2 in ascending and 1 in transverse colon. Mean polyp size was 1.7cm. All seven paired HP-TSA foci shared a *BRAF* (n=5) or *KRAS* (n=2) mutation, in addition to shared *EML4-ALK* (n=1) and *PTPRK-RSPO3* rearrangements (n=1). Foci of conventional adenoma-like dysplasia were present in six of ten TSAs and in all seven TSAs with HGD/carcinoma and harbored *APC* mutations in 4/6 TSAs and 6/7 HGD/carcinoma cases, respectively. In addition to *APC*, TSAs with HGD/carcinoma also showed

concurrent pathogenic alterations in *TP53*, *SMAD4*, *PTEN* and other genes. In the seven cases with TSA and HGD/carcinoma, *APC* mutations were seen in both components in all cases, in addition to *BRAF* (n=2), *TP53* (n=3) and *KRAS* mutations (n=1). TSA and HP areas were macrodissected in two cases with invasive carcinoma. Both cases showed identical mutations in the CRC and TSA foci. Additionally, one of the two cases showed identical mutations in the HP, TSA and CRC areas while the other showed a *KRAS G12V* mutation in the HP component and a shared *KRAS G12D* mutation in both the TSA and carcinoma foci.

**Conclusions:** Our data provides compelling evidence that TSAs can arise from HPs, which are thus best considered as remote low-risk precursors of colorectal cancer. Furthermore, conventional adenoma-like dysplasia foci in TSAs and in TSAs with HGD/carcinoma harbor *APC* mutations in a high proportion of cases suggesting a morphological and molecular overlap between serrated and conventional pathways in advanced TSAs at risk for malignant transformation.

**372** **Comprehensive Evaluation and Unique Morphologic Features of Nonsteroidal Anti-Inflammatory Drug (NSAID) Enteropathy in the Terminal Ileum**
Jessica Nguyen[1], Sherry Lee[1], Guang-Yu Yang[2]
[1]Northwestern University Feinberg School of Medicine, Chicago, IL, [2]Northwestern University, Chicago, IL

**Disclosures:** Jessica Nguyen: None; Sherry Lee: None; Guang-Yu Yang: None

**Background:** Differentiating long-term NSAID enteropathy from Crohn disease (CD) can be extremely challenging on biopsy. It is important to distinguish between these two entities as management is completely different. In this study, we set out to identify clinical, radiographic, and morphologic characteristics that can help distinguish NSAID enteropathy from CD involving the terminal ileum (TI).

**Design:** A unique cohort of 30 patients diagnosed with long-term NSAID enteropathy and 30 patients diagnosed with CD on TI biopsies was identified through a pathology database search. Clinical, endoscopic, and radiographic findings were assessed for each patient. Comprehensive analysis for histologic features including ulceration/erosion, cryptitis/crypt abscesses, pyloric metaplasia, gland/crypt atrophy, and alteration of goblet cells and Paneth cells was performed. The number of goblet cells and Paneth cells per crypt were scored as normal, increased, or decreased compared to 25 biopsies with morphologic normal terminal ileum.

**Results:** Clinically, seven (23.3%) patients in the NSAID cohort had unremarkable findings on CT abdomen/pelvis around the time of colonoscopy and biopsy. Eighteen (60.0%) patients in the CD cohort had either CT abdomen/pelvis or MR enterography. Moderate to severe CD were found to have bowel wall thickening with fat stranding, prominent surrounding lymph nodes, and luminal distension/narrowing/stricture on imaging while cases of mild CD had unremarkable findings.

Pathologically, >80% of cases in each cohort showed ulceration/erosion and cryptitis/crypt abscesses. The CD cohort had significantly higher degree of lymphoplasmacytic inflammation in the lamina propria compared to the NSAID cohort (90.0% vs 33.3%, p<0.05). In contrast, a significantly higher percentage of the NSAID cohort had gland/crypt atrophy compared to the CD cohort (70.0% vs 16.7%, p<0.05). Notably, 86% (18/21) patients in the NSAID cohort with gland/crypt atrophy had taken an NSAID for more than a year. Paneth cell atrophy was significantly identified in the NSAID cohort (50.0% vs 20.0%, p<0.05). Similar frequencies of pyloric metaplasia, villous blunting, and lamina propria fibrosis were found in both NSAID and CD cohorts.

| Histologic Feature | NSAID enteropathy n = 30 | Crohn ileitis n = 30 |
|---|---|---|
| Ulceration or erosion | 25 (83.3%) | 27 (90.0%) |
| Cryptitis or crypt abscesses | 24 (80.0%) | 29 (96.7%) |
| Lamina propria lymphoplasmacytic inflammation | | |
| 0 (decreased) | 11 (36.7%)* | 0 (0.00%)* |
| 1 (within normal limits) | 9 (30.0%) | 3 (10.0%) |
| 2 (increased) | 10 (33.3%)* | 27 (90.0%)* |
| Granuloma formation | 0 (0.00%) | 3 (10.0%) |
| Pyloric metaplasia | 10 (33.3%) | 12 (40.0%) |
| Gland atrophy | 21 (70.0%)* | 5 (16.7%)* |
| Villous blunting | 8 (26.7%) | 12 (40.0%) |
| Lamina propria fibrosis | 4 (13.3%) | 5 (16.7%) |
| Muscularis mucosa in lamina propria | 9 (30.0%)* | 2 (6.67%)* |
| Goblet cell hyperplasia | 12 (40.0%) | 18 (60.0%) |
| Paneth cell hyperplasia | 0 (0.00%)* | 8 (23.7%)* |
| Paneth cell atrophy | 15 (50.0%)* | 6 (20.0%)* |
| *p<0.05 | | |

Figure 1 - 372
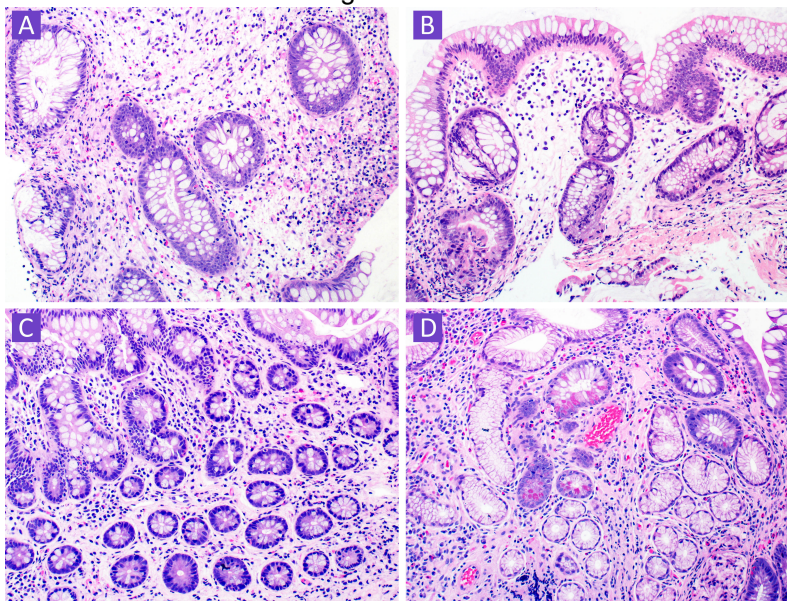


**Figure 1.** Terminal ileum biopsies from NSAID cohort demonstrating gland/crypt atrophy (A, B), Paneth cell atrophy (A, B, C), decreased lamina propria lymphoplasmacytic inflammation (A, B), villous blunting (B), and pyloric metaplasia (D).

**Conclusions:** Along with clinical and radiographic findings, we identified that the combination of gland/crypt/Paneth cell atrophy with decreased lamina propria lymphoplasmacytic inflammation was the significant morphologic alteration to differentiate NSAID enteropathy from CD in TI biopsies.

**373    Nicotinamide N-Methyltransferase (NNMT) Has Prognostic Implications for Microsatellite-Stable Colorectal Adenocarcinoma**

Makiko Ogawa[1], Atsushi Tanaka[1], Kei Namba[1], David Klimstra[1], Jinru Shia[1], Michael Roehrl[1]
[1]Memorial Sloan Kettering Cancer Center, New York, NY

**Disclosures:** Makiko Ogawa: None; Atsushi Tanaka: None; Kei Namba: None; David Klimstra: None; Jinru Shia: None; Michael Roehrl: None

**Background:** We identified nicotinamide N-methyltransferase (NNMT) as a signature marker of colorectal cancer (CRC) using integrated, mass spectrometry-based proteogenomics. The aim of the present study was to validate

the expression of the NNMT protein in an independent cohort of CRCs and to uncover correlations with clinicopathological features.

**Design:** Tissue specimens from 770 CRC cases were obtained and tissue microarrays (TMAs) were constructed. The TMA specimens were stained with NNMT-specific antibodies. IHC slides were evaluated and scored by a semi-quantitative approach (H-score). Categorical variables were compared using Fisher's exact test. Survival analyses were performed using the Kaplan-Meier method and compared by a log-rank test.

**Results:** We evaluated 601 CRC cases with available complete survival follow-up. NNMT is mainly expressed by tumor-associated stromal cells. High NNMT protein expression (H≥110) was observed in 337 cases (56.1%). NNMT positivity correlated significantly with CRCs of stages I or II ($p<0.0001$). High NNMT protein expression was also significantly associated with shorter disease-free (DFS, $p=0.0299$) and overall survival (OS, $p=0.0182$) in early stage microsatellite-stable (MSS) CRC patients. The mean (median) DFS lengths of stage I and II patients with high NNMT vs. low NNMT were 75.3 (64.0) months vs. 82.0 (74.6) months, respectively. No such survival differences were seen for early stage microsatellite-unstable (MSI) CRCs.

**Conclusions:** Stromal NNMT protein overexpression identifies a subset of early stage microsatellite-stable CRCs with poor outcomes and supports a rationale for developing therapies that target the enzyme NNMT in these cancers.

## 374 Correlation of Loss of 5-hydroxymethylcytosine (5-hmC) Expression with Risk of Disease Progression in Smooth Muscle Tumors of the Gastrointestinal Tract

Andrea Olivas[1], Frank Jacobsen[2], Joseph Misdraji[2], Teri Longacre[3], Shyam Raghavan[4], Hanlin Wang[5], Ari Kassardjian[6], Raul Gonzalez[7], Mary Bronner[8], Zachary Dong[8], Marie Robert[9], Iván González[10], Jinru Shia[11], David Klimstra[11], Rhonda Yantiss[12], Shefali Chopra[13], Nicole Panarelli[14], Shaomin Hu[15], Zu-Hua Gao[16], Diana Agostini-Vulaj[17], Deyali Chatterjee[18], Masoumeh Ghayouri[19], Gregory Lauwers[20], Andrew Bellizzi[21], Mojgan Hosseini-Varnamkhasti[22], John Hart[23], Lindsay Alpert[23]

[1]University of Chicago Medical Center, Chicago, IL, [2]Massachusetts General Hospital, Harvard Medical School, Boston, MA, [3]Stanford University, Stanford, CA, [4]University of Virginia School of Medicine, Charlottesville, VA, [5]David Geffen School of Medicine at UCLA, Los Angeles, CA, [6]University of California, Los Angeles, Los Angeles, CA, [7]Beth Israel Deaconess Medical Center, Harvard Medical School, Boston, MA, [8]The University of Utah, Salt Lake City, UT, [9]Yale School of Medicine, New Haven, CT, [10]Yale New Haven Hospital, New Haven, CT, [11]Memorial Sloan Kettering Cancer Center, New York, NY, [12]Weill Cornell Medicine, New York, NY, [13]Keck School of Medicine of USC, Los Angeles, CA, [14]Montefiore Medical Center - Moses Division, Bronx, NY, [15]Cleveland Clinic, Cleveland, OH, [16]McGill University, Montréal, Canada, [17]University of Rochester Medical Center, Rochester, NY, [18]Washington University in St. Louis, St. Louis, MO, [19]H. Lee Moffitt Cancer Center & Research Institute, Tampa, FL, [20]H. Lee Moffitt Cancer Center & Research Institute, University of South Florida, Tampa, FL, [21]University of Iowa Hospitals & Clinics, Iowa City, IA, [22]University of California, San Diego, La Jolla, CA, [23]University of Chicago, Chicago, IL

**Disclosures:** Andrea Olivas: None; Frank Jacobsen: None; Joseph Misdraji: None; Teri Longacre: None; Shyam Raghavan: None; Hanlin Wang: None; Ari Kassardjian: None; Raul Gonzalez: None; Mary Bronner: None; Zachary Dong: None; Marie Robert: None; Iván González: None; Jinru Shia: None; David Klimstra: None; Rhonda Yantiss: None; Shefali Chopra: None; Nicole Panarelli: None; Shaomin Hu: None; Zu-Hua Gao: None; Diana Agostini-Vulaj: None; Deyali Chatterjee: None; Masoumeh Ghayouri: None; Gregory Lauwers: None; Andrew Bellizzi: None; Mojgan Hosseini-Varnamkhasti: None; John Hart: None; Lindsay Alpert: None

**Background:** Prognostic clinicopathologic criteria for intramural smooth muscle tumors of the gastrointestinal (GI) tract have recently been proposed, but the underlying mechanisms leading to aggressive behavior are unknown. Loss of 5-hydroxymethylcytosine (5-hmC), an epigenetic alteration, has been found to correlate with malignant potential in several tumor types and may aid in prognostic assessment of GI tract smooth muscle tumors.

**Design:** 92 GI smooth muscle tumor resection specimens from 18 institutions were included in the study. Patient demographics, follow-up time, and presence of disease progression (local recurrence, metastases, or death) at last follow-up were noted. Tumor characteristics including site, size, and mitotic rate/5 mm$^2$ were recorded. Immunohistochemical (IHC) staining for 5-hmC was performed at one institution on one tumor block from each

specimen; retained staining was defined as nuclear staining present in ≥2/3rds of lesional cells with at least half of the intensity seen in background smooth muscle cells. 5-hmC loss was then correlated with previously published progression-free survival tiers (table 1) and outcome. Statistical significance (p<0.05) was determined using Fisher's exact test.

**Results:** The mean patient age was 54 years (range 21-86 years), with 50 females and 42 males. The 92 tumors were located in the esophagus (n=15, 16%), stomach (n=31, 34%), small bowel (n=24, 26%), and colon/rectum (n=22, 24%). Tumor size ranged from 0.6-29 cm (mean 7.2 cm). Time from initial surgery to last follow-up averaged 71 months (range 6-187 months). 5-hmC loss was detected in 38 specimens (38/92; 41%): 7 (19%) esophageal, 10 (26%) gastric, 8 (21%) small bowel, and 13 (34%) colorectal. When correlated with progression-free survival tiers, 5-hmC loss was seen in 8/53 specimens in tier 1 (15%), 11/16 in tier 2 (69%), and 19/23 in tier 3 (83%) (tier 1 vs tier 2, p=0.0001; tier 1 vs tier 3, p<0.00001; tier 2 vs tier 3, p=0.44). Thirteen of 92 cases (14%) had disease progression, of which 5-hmC loss was seen in 11 (85%) specimens (vs 27/79, or 34% of non-progressive cases; p=0.0013).

**Table 1. Progression-Free Survival Tiers[1]**

|  | Site | Size | Mitotic Rate |
|---|---|---|---|
| Tier 1 | All | ≤10 cm | <3/5 mm$^2$ |
|  | Esophagus | All sizes | All rates |
| (n=53) | Colon/Rectum | >10 cm | <3/5 mm$^2$ |
| Tier 2 | Stomach | >10 cm | <3/5 mm$^2$ |
|  | Stomach | ≤5 cm | ≥3/5 mm$^2$ |
| (n=16) | Stomach | >5 & ≤10 cm | ≥3/5 mm$^2$ |
|  | Small bowel | >10 cm | <3/5 mm$^2$ |
|  | Small bowel | ≤5 cm | ≥3/5 mm$^2$ |
|  | Small bowel | >5 & ≤10 cm | ≥3/5 mm$^2$ |
| Tier 3 | Stomach | >10 cm | ≥3/5 mm$^2$ |
|  | Small bowel | >10 cm | ≥3/5 mm$^2$ |
| (n=23) | Colon/Rectum | All sizes | ≥3/5 mm$^2$ |

Tier 1, no disease progression; Tier 2, disease progression in <50% of cases; Tier 3, disease progression in >50% of cases

[1]Alpert L, et al. Smooth muscle tumors of the gastrointestinal tract: an analysis of prognostic features in 407 cases. *Modern Pathology* 2020; 33: 1410-1419.

**Conclusions:** We demonstrate that loss of 5-hmC by IHC in smooth muscle tumors of the GI tract correlates with risk of disease progression and can be used as an indicator of malignant potential.

**375    Crypt Abscesses, Crypt Distortion, Crypt Rupture, and Paneth Cell Metaplasia Help Distinguish Inflammatory Bowel Disease from Segmental Colitis Associated with Diverticulosis**

Yuho Ono[1], Raul Gonzalez[2]
[1]Beth Israel Deaconess Medical Center, Boston, MA, [2]Beth Israel Deaconess Medical Center, Harvard Medical School, Boston, MA

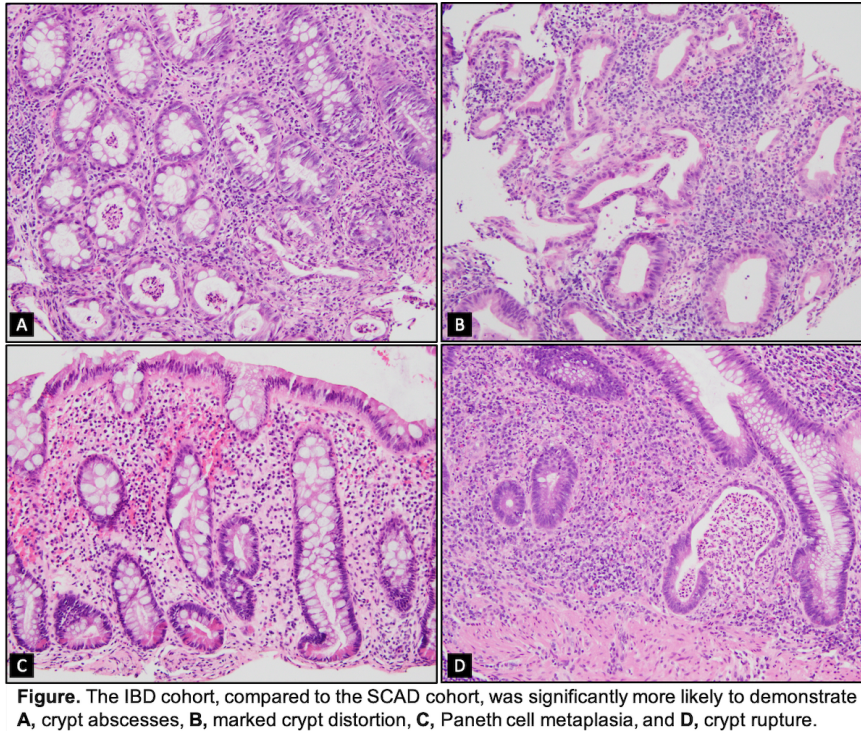**Disclosures:** Yuho Ono: None; Raul Gonzalez: None

**Background:** The histologic differential diagnosis of colitis remains challenging, with etiologies such as infection, drug effect, segmental colitis associated with diverticulosis (SCAD), and inflammatory bowel disease (IBD) causing overlapping microscopic findings. Distinguishing IBD from other colitides is key for patient management. SCAD can histologically resemble IBD colitis, endoscopic correlation of colitis and diverticulosis can be vague, and diverticuli are not always limited to the sigmoid colon. This study aims to examine histologic changes in SCAD and compare them to those in IBD.

**Design:** We retrospectively identified patients with confirmed or highly likely SCAD from 2004 to 2020 at our institution. Inclusion criteria included injured biopsies from a colonic segment involved by diverticulosis, no injury in uninvolved parts of the colon, and no other diagnosis on follow-up that would account for the colitis. All patients with IBD biopsied at our institution in 2019 formed the comparison group. With diagnosis blinded, H&E slides were reviewed for cryptitis, crypt abscesses, lamina propria (LP) neutrophils, erosion/ulceration, LP expansion by mononuclear cells, prominent basal lymphoid aggregates, basal lymphoplasmacytosis, marked crypt distortion, crypt dilation, granulomatous reaction to damaged crypts, increased intraepithelial lymphocytes (>20 lymphocytes/100 enterocytes), mucin depletion, Paneth cell metaplasia, LP smooth muscle wisps, surface hyperplastic change, and crypt rupture. Features between groups were compared, with statistical significance set at $P<0.05$.

**Results:** There were 83 SCAD cases (78% in the sigmoid colon) and 177 IBD cases. Clinical and histologic findings are summarized in the Table. SCAD patients as a whole were significantly older than IBD patients ($P<0.0001$). Most SCAD cases demonstrated cryptitis (71%), LP neutrophils (73%), and LP expansion by mononuclear cells (55%). Compared to the IBD cohort, the SCAD cohort was significantly less likely to demonstrate crypt abscesses (19% vs. 44%, $P=0.00011$), marked crypt distortion (7% vs. 23%, $P=0.0019$), Paneth cell metaplasia (37% vs. 55%, $P=0.0049$), and crypt rupture (1% vs. 10%, $P=0.0096$) (Figure).

| Table. Comparative frequencies of clinicopathologic features in colonic biopsies from SCAD and IBD | | | | | |
|---|---|---|---|---|---|
| | SCAD (n = 83) | | IBD (n = 177) | | P-value |
| Age in years (mean ± standard deviation) | 61 ± 12 | | 46 ± 17 | | <0.0001 |
| Sex | | | | | 0.48 |
|     Male | 35 | 42% | 83 | 47% | |
|     Female | 48 | 58% | 94 | 53% | |
| Histologic features | | | | | |
|     Cryptitis | 59 | 71% | 129 | 73% | 0.76 |
|     Crypt abscesses | 16 | 19% | 78 | 44% | 0.00011 |
|     Lamina propria neutrophils | 61 | 73% | 131 | 74% | 0.93 |
|     Erosion/Ulceration | 17 | 20% | 53 | 30% | 0.11 |
|     Lamina propria expansion by mononuclear cells | 46 | 55% | 116 | 66% | 0.12 |
|     Prominent basal lymphoid aggregates | 30 | 36% | 85 | 48% | 0.072 |
|     Basal lymphoplasmacytosis | 21 | 25% | 49 | 28% | 0.69 |
|     Marked crypt distortion | 6 | 7% | 41 | 23% | 0.0019 |
|     Crypt dilation | 8 | 10% | 25 | 14% | 0.31 |
|     Granulomatous reaction at damaged crypts | 1 | 1% | 1 | 1% | 0.58 |
|     Increase in intraepithelial lymphocytes | 2 | 2% | 4 | 2% | 0.94 |
|     Mucin depletion | 20 | 24% | 61 | 34% | 0.092 |
|     Paneth cell metaplasia* | 30 | 37% | 98 | 55% | 0.0049 |
|     Smooth muscle wisps | 16 | 19% | 41 | 23% | 0.48 |
|     Surface hyperplastic change | 14 | 17% | 25 | 14% | 0.56 |
|     Crypt rupture | 1 | 1% | 18 | 10% | 0.0096 |
| SCAD = segmental colitis associated with diverticulosis; IBD = inflammatory bowel disease | | | | | |
| *n = 82 for SCAD group | | | | | |

Figure 1 - 375



**Figure.** The IBD cohort, compared to the SCAD cohort, was significantly more likely to demonstrate **A,** crypt abscesses, **B,** marked crypt distortion, **C,** Paneth cell metaplasia, and **D,** crypt rupture.

**Conclusions:** SCAD is less likely than IBD to cause crypt abscesses, marked crypt distortion, Paneth cell metaplasia, or crypt rupture. These histologic features, although not entirely specific, may be utilized in distinguishing IBD from SCAD, particularly when clinical context is unclear or not readily available.

**376    Fundic Gland Polyps with Dysplasia: High-Degree of Interobserver Variability with Frequent Overdiagnosis Among Patients with Familial Adenomatous Polyposis**

Christine Orr[1], Debra Beneck[2], Jose Jessurun[2], Lihui Qin[2], Yao-Tseng Chen[3], Rhonda Yantiss[4]
[1]New York-Presbyterian/Weill Cornell Medicine, New York, NY, [2]New York-Presbyterian/Weill Cornell Medical Center, New York, NY, [3]Weill Cornell Medical College, New York, NY, [4]Weill Cornell Medicine, New York, NY

**Disclosures:** Christine Orr: None; Debra Beneck: None; Jose Jessurun: None; Lihui Qin: None; Yao-Tseng Chen: None; Rhonda Yantiss: None

**Background:** Fundic gland polyps (FGPs) arise sporadically and in combination with familial adenomatous polyposis (FAP). They can develop dysplasia, particularly when associated with FAP, but progression to carcinoma is extremely rare in both scenarios. Dysplasia is usually low-grade and of foveolar type. Unfortunately, criteria for foveolar dysplasia have not been well characterized and overlap considerably with reactive epithelial changes. We hypothesize that the diagnosis of dysplasia in FGPs suffers from interobserver variability and is probably influenced by knowledge of the clinical history.

**Design:** All FGPs reviewed at a daily GI pathology consensus conference for possible dysplasia, FGPs with dysplasia, and FGPs arising in the setting of FAP were identified over a 10-year period. From these, we selected 72 FGPs associated with FAP and 34 sporadic polyps. A single slide of each polyp was independently reviewed by 5 senior pathologists, each of whom had $\geq$20 years of experience in gastrointestinal pathology. Pathologists were blinded to the clinical history and asked to classify polyps as negative for dysplasia (score=0) or low-grade dysplasia (score=1). Opinions of all 5 pathologists were collated and each case was assigned a "combined dysplasia score" (CDS) ranging from 0 to 5 (Figure). A score of 0 signified unanimous opinion of negative for dysplasia and a score of 5 signified complete agreement on a diagnosis of low-grade dysplasia.

**Results:** Low-grade dysplasia was originally diagnosed in 41 FAP patients and 26 patients without FAP. Fleiss' kappa showed only moderate agreement for dysplasia scores, [$k$=0.46 (95% CI, 0.40 to 0.52), p<0.005]. Complete consensus was reached in 48 (45%) cases, including 24 with a CDS=0 and 24 with a CDS=5. There was poor interobserver agreement (CDS of 2 or 3) in 28 (26%) cases, including 17 (24%) FAP-related and 11 (32%) sporadic FGPs (Table). All 37 polyps with a CDS of 4 or 5 were originally diagnosed with low-grade dysplasia, in comparison 10 of 41 (24%) polyps with a CDS of 0 or 1 were originally diagnosed with low-grade dysplasia. Over-diagnosis of dysplasia was significantly more frequent than under-diagnosis (p=0.004).

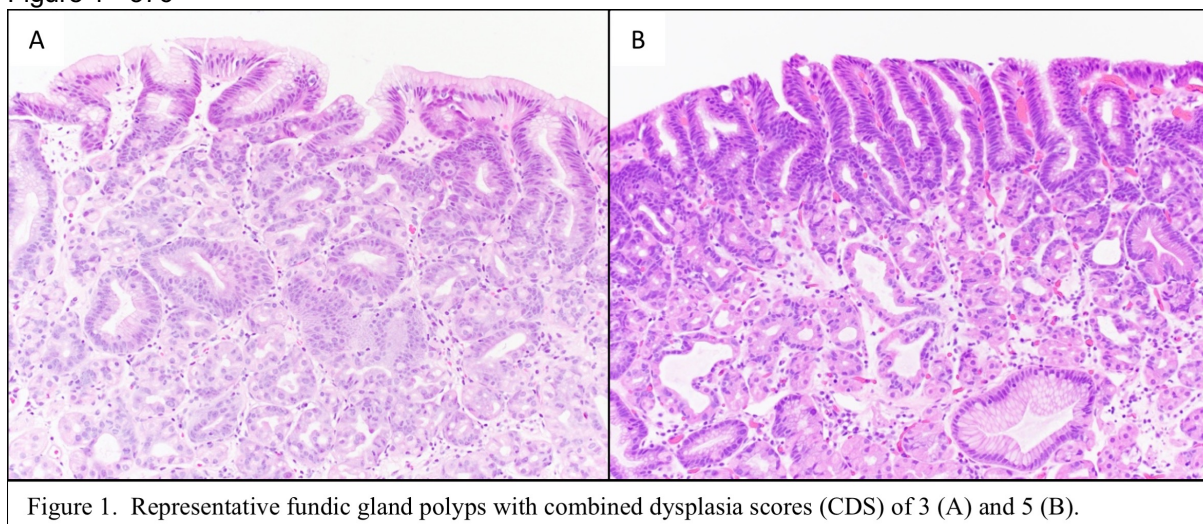| Table 1. Correlation between combine dysplasia score, FAP status, and original diagnosis | | | | | |
|---|---|---|---|---|---|
| **Combined Dysplasia Score** | **Number of Polyps** | **FAP-associated FGP** | | **Sporadic FGP** | |
| | | **Low Grade Dysplasia** | **No Dysplasia** | **Low Grade Dysplasia** | **No Dysplasia** |
| 0 | 24 | 3 | 18 | 0 | 3 |
| 1 | 17 | 5 | 8 | 2 | 2 |
| 2 | 14 | 5 | 3 | 4 | 2 |
| 3 | 14 | 7 | 2 | 3 | 2 |
| 4 | 13 | 8 | 0 | 5 | 0 |
| 5 | 24 | 13 | 0 | 11 | 0 |
| Total | 106 | 41 | 31 | 25 | 9 |

Figure 1 - 376



Figure 1. Representative fundic gland polyps with combined dysplasia scores (CDS) of 3 (A) and 5 (B).

**Conclusions:** There is a high degree of interobserver variability with respect to the diagnosis of dysplasia in FGPs, even amongst senior pathologists. Over-interpretation of mild cytologic abnormalities as dysplasia is more common than a failure to recognize dysplasia. We suspect that the expectation of dysplasia in FGPs from FAP patients coupled with concern for missing dysplasia are important factors that lead to its over-diagnosis. Our findings highlight the benefit of obtaining consensus before diagnosing dysplasia in FGPs, and suggest assessment is ideally performed without clinical history. Although the morphologic features of intestinal-type and high-grade dysplasia are well-known, our results highlight the need to better define criteria for foveolar-type low-grade dysplasia.

**377     Enteroblastoma: Expanding the Spectrum of GLI1-Rearranged Tumors of the Gastrointestinal Tract**

Christine Orr[1], Samantha McNulty[2], Flora Poizat[3], Hussein Alnajar[4], Sun-Joong Kim[5], Feng He[6], Murat Yaylaoglu[2], Kenrry Chiu[7], Yongmei Yin[8], Todd Druley[9], Rhonda Yantiss[6], Lihui Qin[10], Jenny Xiang[6], Jose Jessurun[10], Juan Miguel Mosquera[6]
[1]New York-Presbyterian/Weill Cornell Medicine, New York, NY, [2]ArcherDX, Inc., Boulder, CO, [3]My Institution Is Not Listed, Marseille, France, [4]NorthShore University HealthSystem, Evanston, IL, [5]ArcherDX, Inc., Boulder, MO, [6]Weill Cornell Medicine, New York, NY, [7]Royal Columbian Hospital, University of British Columbia, New Westminster, Canada, [8]New York-Presbyterian/Brooklyn Methodist Hospital, New York, NY, [9]Invitae Corporation, San Francisco, CA, [10]New York-Presbyterian/Weill Cornell Medical Center, New York, NY

**Background:** *GLI1* encodes a transcription factor that targets cell cycle regulators affecting stem cell proliferation. *GLI1* gene fusions were initially reported by Dahlen *et al.* in 2004 in a tumor termed 'pericytoma with a t(7;12) translocation' which resulted in an *ACTB-GLI1* fusion. Subsequently, a *MALAT1-GLI1* fusion was identified in two distinct gastric neoplasms: plexiform fibromyxoma, and gastroblastoma.

**Design:** We studied two distinct tumors from the ileum and duodenum of a 55-year-old male and a 22-year-old female, respectively. Both tumors where located in the submucosa and muscularis propria and showed a biphenotypic morphology with alternating areas of solid uniform small round (ileum and duodenum) and spindled (duodenum) cells, and epithelial cells forming tubules (ileum) or nests (duodenum) (Figure 1). Paraffin embedded tissues from 64 tumor samples which included these tumors and a plexiform fibromyxoma were sequenced using a targeted RNAseq method (a customized version of the Archer® FusionPlex Sarcoma panel) to detect recurrent and/or novel gene fusion events (Table 1).

**Results:** *GLI1* fusions were detected in both intestinal tumors and in the plexiform fibromyxoma (Figure 2). Immunohistochemical analysis of the ileal tumor revealed CD56 expression in both morphologic components and cytokeratins and EMA expression in the epithelial component. The duodenal tumor expressed CD99 in both components, cytokeratins in the epithelial cells; and smooth mucle actin and desmin in the spindled cells.

| Table 1. Diagnosis and anatomic site of 31 of 64 tumors with fusions detected by custom Archer® FusionPlex Sarcoma* | | | |
|---|---|---|---|
| **Diagnosis** | **n** | **Anatomic site(s)** | **Fusion (or gene partner)** |
| Enteroblastoma | 2 | Duodenum, Ileum | GLI1 |
| Plexiform fibromyxoma | 1 | Gastric antrum | GLI1 |
| Inflammatory myofibroblastic tumor | 2 | Uterus | ALK1 |
| Dermatofibrosarcoma protuberans | 2 | Breast, Chest | COL1A1-PDGFβ |
| Desmoplastic small round cell tumor | 2 | Peritoneum | EWS-WT1 |
| Ewing sarcoma | 3 | Soft tissue | EWSR1-FLI1 |
| Myoepithelioma | 1 | Parotid | EWSR1 |
| Spindle cell rhabdomyosarcoma | 1 | Bone | EWSR1-TFCP2 |
| Giant cell tumor of bone | 1 | Bone | FN1-TEK |
| Embryonal rhabdomyosarcoma | 1 | Sinonasal | PAX3-FOXO1 |
| Low grade fibromyxoid sarcoma | 1 | Soft tissue | FUS-CREB3L2 |
| Solitary fibrous tumor | 1 | Nasal | NAB2-STAT6 |
| Mammary analog secretory carcinoma | 1 | Salivary gland | NTRK3-ETV6 |
| Astrocytoma | 1 | Brain | PHIP-ROS1 |
| Pleomorphic adenoma | 3 | Parotid gland | CTNNB1-PLAG1 |

| Synovial sarcoma | 2 | Chest, Soft tissue | SS18-SSX2 |
|---|---|---|---|
| Adenocarcinoma | 1 | Colon | TPM3-NTRK1 |
| Nodular fasciitis | 3 | Chest, Soft tissue | MYH9-USP6 |
| Epithelioid hemangioendothelioma | 2 | Liver | WWTR1-CAMTA1 |

*Orthogonal validation of novel fusions is ongoing including novel gene partners of enteroblastomas and plexiform fibromyxoma, and the rest of the study cohort (total n=64 cases)*
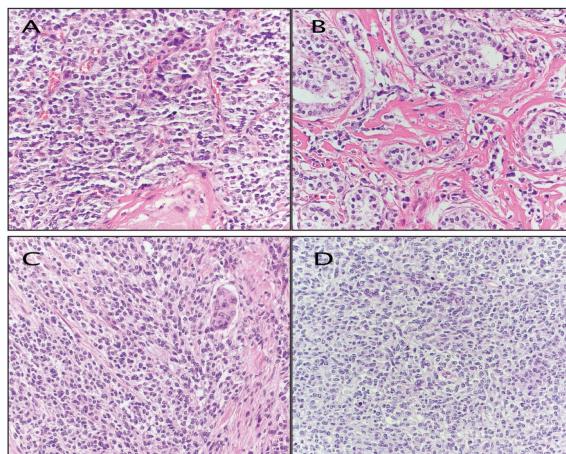
## Figure 1 - 377



**Figure 1.** Representative histologic images of two cases of enteroblastoma, small intestine tumors showing a distinct biphenotypic morphology. **Top.** Ileal tumor in a 55-year-old man with solid and nested areas of small round cells (A) and areas showing tubular formation (B). **Bottom.** Duodenal tumor in a 22-year-old woman with solid and vaguely cord-like areas of small round cells (C) and areas with sheets of epithelioid cells, focally spindled (D). (Original magnification 10x and 20x; H&E stain).
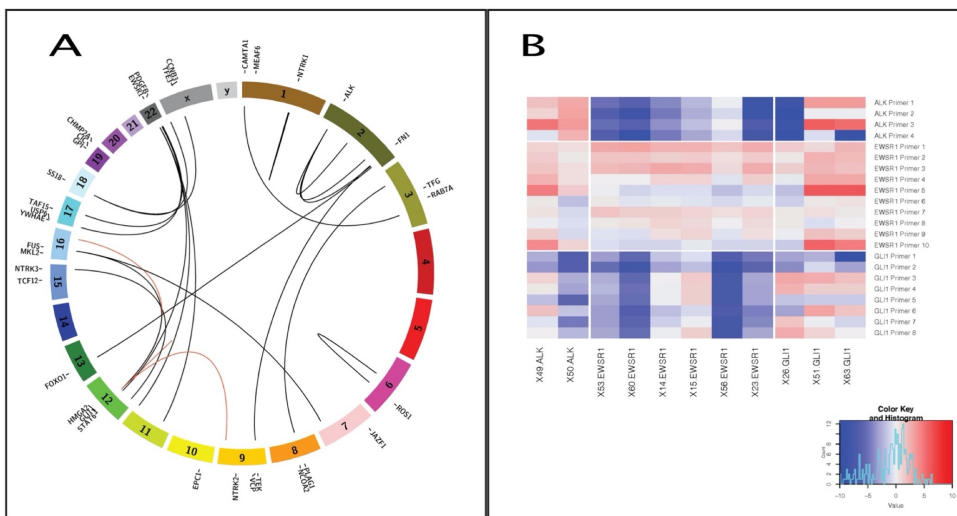
## Figure 2 - 377



**Figure 2. Novel *GLI1* fusions identified in enteroblastoma. A.** Genes targeted for enrichment and sequencing are shown on the outer diameter of the human reference assembly (UCSC hg19). Inner links connect partners involved in gene fusion events. Fusions involving oncogenes were detected in 31 of 64 cases submitted for testing. Fusions involving *GLI1* are highlighted in red. **B.** Normalized expression values were derived from targeted RNAseq (FusionPlex) data, and select cases were plotted to show varied transcription of *ALK, EWSR1*, and *GLI1*. Depicted cases were found to harbor fusions involving these genes as specified in column labels.

**Conclusions:** We describe novel *GLI1* fusions in two biphenotypic neoplasms within the small intestine. Because of the morphological, immunohistochemical and molecular similarities with gastroblastoma, we propose to name this tumor enteroblastoma. Limited follow-up of both cases (16 and 12 months) after surgical resection without additional therapy revealed an indolent biological behavior. Orthogonal validation of novel fusion partners is ongoing.

### 378 Clinicopathologic Characterization of Diffuse Large B-Cell Lymphoma of Gastrointestinal Tract: A Single Institution's Experience

Zenggang Pan[1], Austin McHenry[2], Nana Matsumoto[3], Krishna Iyer[4], Nathan Paulson[1], Dhanpat Jain[1]
[1]Yale School of Medicine, New Haven, CT, [2]Yale University, New Haven, CT, [3]Yale New Haven Hospital, New Haven, CT, [4]Yale New Haven Hospital, New Haven

**Disclosures:** Zenggang Pan: None; Austin McHenry: None; Nana Matsumoto: None; Krishna Iyer: None; Nathan Paulson: None; Dhanpat Jain: None

**Background:** The gastrointestinal (GI) tract is the most common extranodal site for lymphoma, and the most common type is diffuse large B-cell type (DLBCL), which has variable pathogenesis, genetic changes, and clinical behaviors. The goal of the study was to characterize clinicopathological features of GI-DLBCL from a large tertiary care medical center.

**Design:** The pathology archives (2000-2020) at our institution were searched to select all cases of GI-DLBCL. A total of 230 qualified cases were included in this study; the diagnosis of each case was confirmed by necessary immunohistochemical and molecular genetic studies. The major demographic and clinicopathologic features along with follow-up were extracted for all cases and summarized in Table 1.

**Results:** The 230 cases of GI-DLBCL (142 males and 88 females) had a median age of 66 years (range 16-93), including 17 patients with history of organ transplant. The distribution of DLBCL in GI tract is illustrated in Fig 1A; stomach was the most common site of involvement (121/289, 42%; particularly gastric body, 44 cases), followed by small intestine (98/289, 34%; particularly duodenum 33 cases and ileum/terminal ileum 30 cases) and large intestine (64/289, 22%). Sixty-nine of 190 (36%) cases were considered as primary GI-DLBCL, whereas the remaining 121 (64%) represented systemic involvement of GI tract. *Helicobacter Pylori* was detected in 30% (14/46) of gastric DLBCL, and EBV was positive in 25% (18/72) of GI-DLBCL by EBER-ISH.

The GI-DLBCL was mostly of germinal center B-cell (GCB) subtype (99/165; 60%). A dual expression of BCL2 and MYC was detected in 15% (16/109) of cases. *BCL2*, *BCL6*, and *MYC* gene rearrangements were detected in 17/64 (27%), 7/33 (21%), and 29/110 (26%), respectively, including 11% (10/91)
with *MYC* and *BCL2* and/or *BCL6* rearrangements. During a median follow-up of 26 months (range 0-244), approximately 50% (103/207) of patients died, and the median survival for all patients was 71 months (Fig 1B). Compared with systemic disease, primary GI-DLBCL had a significantly better prognosis (median survival 141 months vs. 33 months, *p*<0.001) (Fig. 1C). The median survival for patients with GCB-DLBCL was 117 months, compared to 56 months for non-GCB subtype (*p*=0.04) (Fig. 1D). However, the cases with BCL2/MYC dual expression or *MYC* and *BCL2* and/or *BCL6* rearrangements showed no significantly worse survival, likely related to lower case number in these two groups for analysis.

| Table 1. Clinicopathologic Characteristics of GI-DLBCL | | |
|---|---|---|
| Total Case Number | 230 | |
| Median Age (Years) | 66 (16-93) | |
| Male/Female | 142/88 | |
| HIV-Positive | 5/138 | 3.6% |
| Organ Transplant | 17/230 | 7.4% |
| Primary GI-DLBCL | 69/190 | 36% |
| Bone Marrow Involvement | 13/126 | 10% |
| Clinical Stage | I/II 70, III/IV 139 | |
| Locations *(including cases with multifocal involvement)* | | |
|     Esophagus/GE Junction | 4/2 | |
|     Stomach | 121/289 | 42% |
|     Small Intestine | 98/289 | 34% |

| | | |
|---|---|---|
| Large Intestine | 64/289 | 22% |
| Follow Up (Median, Months) | 26 (0-244; n=222) | |
| Outcome (Deceased) | 103/207 | 50% |
| Overall Survival (Median, Months) | 71 (n=202) | |
| CD20 | 219/224 | 98% |
| BCL2 | 91/151 | 60% |
| BCL6 | 128/158 | 81% |
| CD10 | 75/179 | 42% |
| MUM1 | 73/132 | 55% |
| MYC | 29/82 | 35% |
| H. Pylori | 20/69 | 30% |
| EBER-ISH | 18/72 | 25% |
| GCB Subtype | 99/165 | 60% |
| BCL2/MYC Dual Expression | 16/109 | 15% |
| *BCL2* Rearrangement | 17/64 | 27% |
| *BCL6* Rearrangement | 7/33 | 21% |
| *MYC* Rearrangement | 29/110 | 26% |
| HGBCL, Double- or Triple-Hit | 10/91 | 11% |

Figure 1 - 378
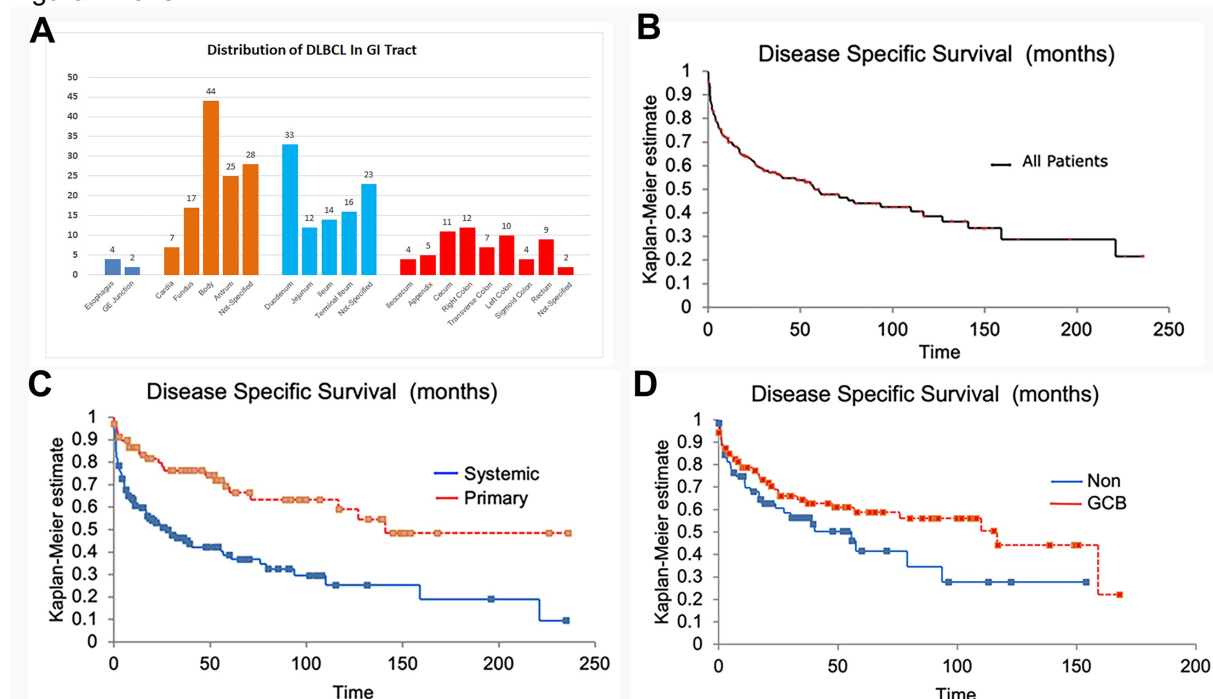


**Conclusions:** GI-DLBCL preferentially involves several subsites of GI tract, including stomach (body) and small intestine (duodenum and ileum) as noted in prior studies. It mostly represents systemic involvement of GI tract, which is associated with a worse prognosis than the primary case.

**379    Assessing the Utility of PDGFRA Immunohistochemistry to Predict PDGFRA Mutations in Gastrointestinal Stromal Tumors**

David Papke[1], Erna Forgo[2], Gregory Charville[2], Jason Hornick[3]
[1]Brigham and Women's Hospital, Boston, MA, [2]Stanford Medicine/Stanford University, Stanford, CA, [3]Brigham and Women's Hospital, Harvard Medical School, Boston, MA

**Disclosures:** David Papke: None; Erna Forgo: None; Gregory Charville: None; Jason Hornick: None

**Background:** Platelet-derived growth factor receptor A (PDGFRA) is a tyrosine kinase receptor that is activated by mutations in 10% of gastrointestinal stromal tumors (GISTs) and 55–70% of inflammatory fibroid polyps (IFPs). *PDGFRA*-mutant GISTs arise in the stomach, show epithelioid morphology and are often KIT-negative by

immunohistochemistry (IHC). SDH-deficient GISTs also arise in the stomach and have epithelioid morphology, and *KIT*-mutant GISTs are sometimes epithelioid. Recently, a novel therapy was approved by the FDA for *PDGFRA*-mutant GISTs, which do not respond to conventional targeted therapies. The purpose of this study was to determine whether PDGFRA IHC could be useful to predict *PDGFRA* mutations for directing targeted therapy.

**Design:** Using a rabbit monoclonal antibody at 1:3K and 1:10K dilutions, IHC was performed on a tissue microarray (TMA) containing 145 GISTs (126 *KIT*-mutant, 17 *PDGFRA*-mutant and 2 SDH-deficient). The positive staining threshold was set to 50% of neoplastic cells at moderate staining intensity. We then evaluated 51 whole sections of GISTs (26 SDH-deficient, 19 *PDGFRA*-mutant, 4 *KIT*-mutant and 2 *NF1*-inactivated) and 127 other gastric tumor types. We pooled whole-section and TMA data to determine sensitivity and specificity of PDGFRA IHC.

**Results:** In the GIST TMA, PDGFRA IHC was 75.0% and 80.5% specific for *PDGFRA*-mutant GISTs at 1:3K and 1:10K dilutions, respectively, and it was 100% sensitive at both. Based on higher specificity, we stained whole-tissue sections at a 1:10K dilution. Combining TMA and whole-tissue section results, PDGFRA IHC was 94.4% sensitive and 80.6% specific for *PDGFRA*-mutant GIST among all GISTs. Restricting analysis to GISTs with an epithelioid component (in the morphologic differential diagnosis of *PDGFRA*-mutant GIST), including 28 SDH-deficient, 1 *NF1*-inactivated and 70 *KIT*-mutant GISTs, the specificity was 83.8%.

PDGFRA IHC was also positive in 15/30 (50%) IFP, 5/9 (56%) synovial sarcomas, 2/8 (25%) plexiform fibromyxomas and 5/10 (50%) inflammatory myofibroblastic tumor. It was negative in poorly differentiated adenocarcinoma (0/20), diffuse large B-cell lymphoma (0/9), schwannoma (0/8), glomus tumor (0/10), gastrointestinal neuroectodermal tumor (0/10), leiomyoma (0/10) and gastroblastoma (0/3).

Figure 1 - 379
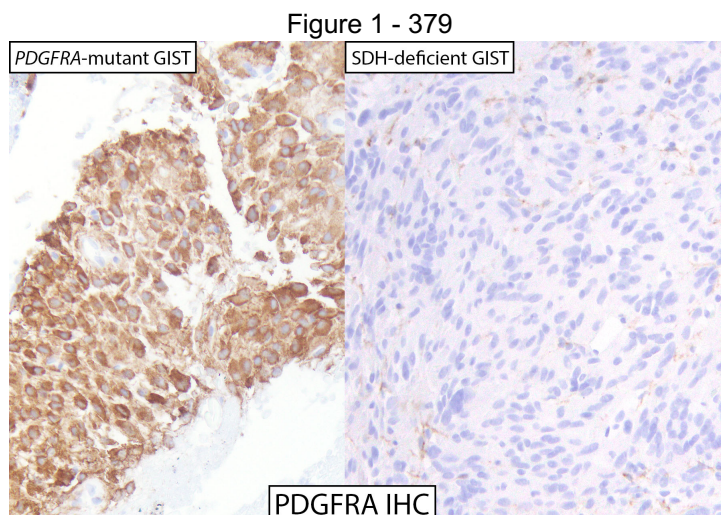


**Conclusions:** PDGFRA IHC is highly sensitive but only moderately specific for *PDGFRA*-mutant GIST among GISTs with an epithelioid component; it is also positive in a subset of IFP and other mesenchymal tumor types. Strong PDGFRA staining in an epithelioid GIST could be useful to triage tumors to *PDGFRA* sequencing for directing targeted therapy.

**380    Value of Examining Routine Hemorrhoidectomy Specimens: Should We Continue?**
Parthavkumar Patel[1], Alan George[1], Julio Poveda[2], Nemencio Ronquillo[1], Jonathan England[3], Clara Milikowski[4], Elizabeth Montgomery[3], Monica Garcia-Buitrago[5]
[1]Jackson Memorial Hospital/University of Miami Hospital, Miami, FL, [2]University of Miami, Miller School of Medicine, Miami, FL, [3]University of Miami Miller School of Medicine, Miami, FL, [4]University of Miami/Jackson Memorial Hospital, Miami, FL, [5]University of Miami Miller School of Medicine/Jackson Health System, Miami, FL

**Background:** Hemorrhoids are a very common anorectal condition due to abnormal dilation and distortion of the anal veins and destructive changes in the supporting connective tissue within the anal cushion. The incidence of unexpected findings in hemorrhoidectomy specimens has been reported to be from 1.42% to 3.38 % . This study aimed to assess the necessity of routine histological examination of frequently clinically undervalued hemorrhoid specimens and evaluate the frequency of unanticipated findings in our high-risk population at a large Southeastern United States urban teaching hospital.

**Design:** We reviewed the Pathology laboratory database of our hospital system from January 2010 to October 2020. We included all cases that were submitted to pathology labeled as hemorrhoids, whether or not hemorrhoids were detected on histologic evaluation. Patients for whom there was a clinical suspicion of malignant or premalignant conditions were excluded from this analysis.

**Results:** Our cohort consisted of material from 537 patients. The male to female ratio was 0.88:1 and a median age of 50 years. Incidental findings were encountered in 7.45% (40) of cases, including low grade squamous intraepithelial lesion (LSIL, 14 cases, 2.61%), high grade squamous intraepithelial lesion (HSIL, 10 cases, 1.86%), acrochordon (7 cases, 1.30%), squamous cell carcinoma (SCC, 3 cases, 0.56%), hyperplastic polyp (4 cases, 0.74%), hidradenoma papilliferum (1 case, 0.19%), epidermal inclusion cyst (1 case, 0.19%) and lichen simplex chronicus (1 case, 0.19%). Thrombosed hemorrhoids were noted in 73 cases (13.59%). The median age of the incidental LSIL, HSIL, and SCC was 39, 43 and 52 years, respectively.

**Conclusions:** The majority of the hemorrhoidal specimens showed expected findings; whereas a subset (5.03%) demonstrated actionable findings (LSIL, HSIL, SCC), a higher figure than previously described in the literature. We attribute this to the high risk population that we serve in our demographic area. Histopathological examination of hemorrhoidectomy specimens resulted in detection of clinically undiagnosed premalignant and malignant conditions that impact patient care and require additional evaluation and treatment, warranting to continue the microscopic evaluation of these specimens.

**381    Diagnostic Challenges in Intra-Abdominal Granulomatous Lesions – Will Multi-Disciplinary Approach be Helpful?**
Rithika Rajendran[1], Febe Suman[1], Pavithra Saai Arun[1], Divya D[1], Swaminathan Rajendiran[1]
[1]Sri Ramachandra Institute of Higher Education and Research, Chennai, India

**Disclosures:** Rithika Rajendran: None; Febe Suman: None; Pavithra Saai Arun: None; Divya D: None; Swaminathan Rajendiran: None

**Background:** Granulomatous lesions in the abdomen are non-specific reactions to a number of etiologies. Distinguishing between tuberculous (TB) and non-TB granulomas is essential for effective patient care but often poses a diagnostic challenge. This study analyses the contribution of clinical, radiological and laboratory parameters to diagnosis.

**Design:** A retrospective review of case records of 109 histologically proven cases of gastrointestinal granulomas (80 TB and 29 non-TB) was done (2017-19). Risk ratios (RR), sensitivity, specificity and likelihood ratios (LR) were calculated to measure the contribution of common clinical, radiological and laboratory parameters to the differential diagnosis. Precision was estimated using binomial confidence intervals. Chi-square test was used to see the association. Either histopathological diagnosis or detection of *M. tuberculosis* was considered the gold standard.

**Results:** The diagnostic challenges in our patient cohort include the wide spectrum of clinical presentations. Ages ranged from 7-74 yrs (mean 39.6) and patients presented with both acute (44.9%) and chronic (55.1%;RR=1.06) symptoms. 2.8% of cases had fever (RR=0.85;p=0.52) and 8.3% had a palpable mass. 17% had a history of TB and 26% had TB sequelae on chest X-ray (p=0.27;RR=1.13). 7.3% were clinically suspected inflammatory bowel disease. The most common finding on imaging was thickening or nodularity (40.4%). The involved sites included luminal (55%), peritoneal (28%), visceral (8%) and mixed (9%) with highest incidence in ileo-cecum and peritoneum (28% each). Mesentric lympadenopathy was present in 24.8% (RR=1.05). Blood counts revealed neutrophilia in 71.4% followed by monocytosis (24.3%). On histopathology, an almost equal number of necrotising (49.5%;p<0.001;RR=1.44) and non-necrotising granulomas (50.5%) were seen and 5 had coexisting neoplasm. Tissue stain for acid fast bacilli (AFB) was positive in 9.5%. *M. tuberculosis* was detected in 11/51 cases (21.57%;

p=0.03) by PCR, gamma interferon assay or sputum for AFB. Fever, radiological diagnosis of TB, necrotising granuloma and presence of AFB were more specific. No single clinical or radiological parameter was both sensitive and specific for the diagnosis of TB (Table 1).

Table 1. Diagnostic performance of clinical, radiological and laboratory parameters for the differential diagnosis of intra-abdominal granulomas

| Characteristic n=109 | Frequency % | TB n=80 | Non-TB n=22 | Sensitivity (95% CI) | Specificity (95% CI) | Positive LR (95% CI) | Negative LR (95% CI) |
|---|---|---|---|---|---|---|---|
| Acute clinical presentation | 40 (44.9) | 29 | 8 | 0.42 (0.30-0.55) | 0.50 (0.25-0.75) | 0.84 (0.48-1.48) | 1.16 (0.68-1.97) |
| Chronic clinical presentation | 49 (55.1) | 40 | 8 | 0.58 (0.45-0.70) | 0.50 (0.25-0.75) | 1.16 (0.68-1.97) | 0.84 (0.48-1.48) |
| Fever | 3 (2.8) | 2 | 1 | 0.02 (0.00-0.09) | 0.95 (0.77-1.00) | 0.55 (0.05-5.79) | 1.02 (0.93-1.13) |
| Neutrophilia | 50 (71.4) | 35 | 10 | 0.66 (0.52-0.78) | 0.17 (0.02-0.48) | 0.79 (0.58-1.09) | 2.04 (0.54-7.63) |
| Monocytosis | 17 (24.3) | 15 | 2 | 0.28 (0.17- 0.42) | 0.83 (0.52-0.98) | 1.70 (0.45-6.46) | 0.86 (0.63-1.17) |
| Radiology diagnosis of TB abdomen | 23 (24.5) | 22 | 1 | 0.32 (0.21- 0.44) | 0.94 (0.73-1.00) | 5.74 (0.83-39.77) | 0.72 (0.59-0.88) |
| Mesentric lympadenopathy | 27 (24.8) | 22 | 5 | 0.28 (0.18- 0.39) | 0.77 (0.55-0.92) | 1.21 (0.52-2.83) | 0.94 (0.72-1.22) |
| AFB positive (tissue stain / microbiology) | 14 (12.8) | 14 | 0 | 0.17 (0.10- 0.28) | 1.00 (0.85-1.00) | - | 0.82 (0.75-0.91) |
| Necrotising granuloma | 54 (49.5) | 48 | 4 | 0.60 (0.48- 0.71) | 0.82 (0.60-0.95) | 3.30 (1.34-8.15) | 0.49 (0.35-0.68) |
| Non-necrotising granuloma | 55 (50.5) | 32 | 18 | 0.40 (0.29- 0.52) | 0.18 (0.05-0.40) | 0.49 (0.35-0.68) | 3.30 (1.34-8.15) |
| TB sequelae on CXR | 19 (26.0) | 17 | 2 | 0.29 (0.18- 0.42) | 0.85 (0.55-0.98) | 1.87 (0.49-7.13) | 0.84 (0.63-1.12) |

TB – Tuberculosis; LR – Likelihood ratio; CI – Confidence interval; AFB – Acid fast bacilli; CXR – Chest X-ray

**Conclusions:** Even in a TB endemic region such as ours, diagnosis of abdominal TB remains a challenge. Histopathology remains the gold standard for diagnosis due to the low sensitivity of clinical and radiological findings and of microbiological sampling.

**382    Aggressive Behavior of Well-Differentiated Neuroendocrine Tumors Arising in the Large Bowel (Excluding Rectum) is Associated with Higher pT-Stage and the Presence of Lymphovascular Invasion**
Ryan Sappenfield[1], Deyali Chatterjee[1]
[1]Washington University in St. Louis, St. Louis, MO

**Disclosures:** Ryan Sappenfield: None; Deyali Chatterjee: None

**Background:** Well-differentiated neuroendocrine tumors arising in the cecum and colon (C-NETs) are relatively rare neoplasms of the lower gastrointestinal tract that typically present with advanced disease and metastasis leading to poor outcomes, in contrast to their rectal counterparts. To our knowledge, no prior studies have systematically evaluated the clinicopathologic characteristics, behavior, and immunohistochemical profile of C-NETs.

**Design:** A retrospective histologic review of all available archival slides of C-NETs excised at our institution was performed and stained for synaptophysin, chromogranin-A, Ki-67, INSM1, CDX2, and SATB2 immunohistochemistry as needed, and if blocks were available. Clinical and follow-up information was obtained from the electronic medical record.

**Results:** A total of 40 C-NETs were included in our cohort, none of which were associated with any adenomatous or other invasive component. The lesions were predominately right-sided with 28 cases (70%) located in the cecum and ascending colon. The mean tumor size was 1.9 cm (range: 0.5 - 8.6 cm). 16 cases (40%) were classified as pT1a, 1 case (2%) as pT1b, 4 cases (10%) as pT2, 14 cases (35%) as pT3, and 5 cases (13%) as pT4. Synaptophysin and INSM1 were reactive in 100% of cases, while chromogranin-A was negative in one case (located in the sigmoid colon). CDX2 and SATB2 were reactive in 82% and 88% of cases, respectively. 73% of cases were classified according to the WHO criteria as grade 1, 23% as grade 2, and 4% as grade 3. The median follow-up time was 76 months (35 cases, range: 4 - 309 months). 20 patients (50%) were identified with lymph node metastasis, all of which showed lymphovascular invasion (LVI) and a tumor stage of pT2 or greater. 13 patients (33%) were identified with distant metastasis with the most common site being the liver (12 of 13 cases, 94%). All cases with distant metastasis showed LVI and 10 cases (77%) showed a pT2 stage or greater. Interestingly, 68% of the WHO grade 1 C-NETs showed involvement of lymph nodes and/or distant metastasis, in contrast to only 50% for WHO grade 2 cases.

**Conclusions:** C-NETs in our fairly large cohort display an aggressive biologic behavior with high rates of lymph node and distant metastasis, which correlate with a tumor stage of pT2 or higher and the presence of LVI, but not with WHO histologic grade. This is also the first systematic study documenting that INSM1 is a highly sensitive neuroendocrine marker in this rare group of neoplasms.

### 383 Utility of Endoscopic Surveillance for Patients with Intestinal Metaplasia of the Stomach at a Tertiary Care Center

Radhika Sekhri[1], Jui Choudhuri[2], Yungtai Lo[1], Nicole Panarelli[3]
[1]Albert Einstein College of Medicine, Montefiore Medical Center, Bronx, NY, [2]Montefiore Medical Center, Bronx, NY, [3]Montefiore Medical Center - Moses Division, Bronx, NY

**Disclosures:** Radhika Sekhri: None; Jui Choudhuri: None; Yungtai Lo: None; Nicole Panarelli: None

**Background:** Recent guidelines advocate for endoscopic surveillance of patients with multifocal gastric intestinal metaplasia (IM, 3 years) or dysplasia [low-grade dysplasia (LGD), 1 year; high-grade dysplasia (HGD), 6 months]. This study assessed the utility of surveillance and the importance of biopsy sampling practices in a large low-risk population with gastric IM or dysplasia.

**Design:** We queried our clinical database for patients diagnosed with gastric IM or dysplasia between January 1, 2009 and December 31, 2010 and analyzed the results of follow-up over the subsequent 10 years. Development of dysplasia or carcinoma and increase in dysplasia grade was considered progression. A subset of patients with similar age and sex distribution who underwent surveillance, but did not progress served as controls. We correlated diagnoses with *H. pylori* status, surveillance intervals, and biopsy sampling practices (Sydney or updated Sydney protocol compliant *vs* not).

**Results:** Stomach biopsy was performed on 18,306 patients during the study interval, and 1,788 had IM. *H. pylori* infection correlated with the presence of IM (p<0.002) and adenocarcinoma (p=0.03). Subsequent biopsies were performed on 495 patients diagnosed with IM during the index biopsy interval. The most advanced lesion was detected by the index procedure in 15 (3%) patients (LGD: n=6; HGD: n=1; adenocarcinoma: n=8). Six (1%) patients with IM progressed (surveillance interval: 1 month-9 years) (see Table). Gastric IM was noted to be focal in 2 (33%) cases. Six (1%) other patients with LGD experienced progression (surveillance interval: 2 months-2 years)

(see Table). Index and surveillance procedures revealing the most advanced lesion were Sydney protocol compliant in 2 (17%) and 1 (8%) cases, respectively for patients who progressed. Gastric IM was focal in 12/20 (60%) controls (surveillance interval: 2 months-5 years).  Index and most recent follow up biopsies were Sydney or updated Sydney protocol compliant in 5 (25%) and 8 cases (40%), respectively.

Table. Features of Patients with Intestinal Metaplasia and Subsequent Neoplastic Progression

| Case | Original Biopsy | | | Final Biopsy | | Time Interval |
|---|---|---|---|---|---|---|
| | Diagnosis | Sydney Compliant | H. pylori status | Diagnosis | Sydney or Updated Compliant | |
| 1 | IM | Yes | Negative | LGD | No | 5 years |
| 2 | IM | No | Positive | Adenocarcinoma | No | 9 years |
| 3 | IM | No | Negative | Adenocarcinoma | No | 2.5 months |
| 4 | IM | No | Negative | Adenocarcinoma | No | 2 months |
| 5 | IM | No | Negative | HGD | No | 1 month |
| 6 | IM | No | Positive | LGD | No | 36 months |
| 7 | LGD | No | Positive | HGD | No | 4 months |
| 8 | LGD | No | Negative | Adenocarcinoma | No | 6 months |
| 9 | LGD | No | Negative | Adenocarcinoma | No | 6 months |
| 10 | LGD | Yes | Negative | HGD | Yes | 7 months |
| 11 | LGD | No | Positive | Adenocarcinoma | No | 24 months |
| 12 | LGD | No | Negative | HGD | No | 2 months |

**Conclusions:** Only 2% of patients followed for IM experienced progression. Most neoplasms (15/27, 56%) were detected by the index biopsy, but a substantial proportion occurred or progressed thereafter (12/27, 44%).  Sydney protocol adherence was low in all groups, and insufficient index sampling may account for the short time to progression in some cases. Our findings support endoscopic surveillance with adequate sampling in patients with multifocal gastric IM and/or dysplasia.

### 384 The Role of the Gastrointestinal Pathologist in the Diagnosis of Cancer Predisposition Syndromes

Namrata Setia[1], Lindsay Alpert[1], Jessica Stoll[2], Christine Drogan[1], Ardaman Shergill[1], Uzma Siddiqui[1], Peng Wang[1], Jeremy Segal[1], Sonia Kupfer[3], John Hart[1]
[1]University of Chicago, Chicago, IL, [2]Tempus Labs, Chicago, IL, [3]University of Chicago Medicine, Chicago, IL

**Disclosures:** Namrata Setia: None; Lindsay Alpert: None; Jessica Stoll: *Employee*, Tempus Labs; Christine Drogan: None; Ardaman Shergill: None; Uzma Siddiqui: None; Peng Wang: None; Jeremy Segal: None; Sonia Kupfer: None; John Hart: None

**Background:** Gastrointestinal polyps and associated tumors may be markers of undiagnosed germline cancer predisposition syndromes. The goal of this study was to identify the clinicopathologic features associated with cancer predisposition syndromes identified in routine sub-specialty GI pathology practice.

**Design:** A total of 221 patients with a recommendation of germline/cancer risk clinical evaluation were identified on review of 33,915 pathology reports, including 28,250 reports from patients with polyps on colonoscopy and 5,665 patients with reported pathogenic germline variants on tumor sequencing. Of the 221 patients, 151 patients had multiple/atypical polyps (polyposis referral group), and 70 had one or more pathogenic/likely pathogenic probable germline variants on next-generation sequencing of GI neoplasms (NGS referral group). Medical records were reviewed to assess the results of germline testing/genetic counselor evaluation, if performed.

**Results:** Fifty-two patients (35.8%) and 22 patients (31.4%) underwent germline testing based on polyposis referral and NGS referral, respectively, and of these patients, 23 (44.2%) and 10 (45.5%) had a confirmed germline mutation or a clinical diagnosis of a cancer predisposition syndrome. Patients ≤50 years of age formed 57.6% of the cohort, including 13 patients in the polyposis referral group and 6 patients in the NGS referral group. Patients over 50 years of age had a history of previous cancer (33.3%), histologically diverse adenomatous and non-

adenomatous polyps (33.3%) and upper GI tract polyps (33.3%) in the polyposis referral group, and synchronous tumors (40%) and non-conventional tumor histology/immunohistochemical profile (60%) in the NGS referral group.

**Conclusions:** GI pathologists can play a critical role in the identification of undiagnosed germline cancer predisposition syndromes by recommending cancer risk evaluation in cases with unusual clinicopathologic features.

### 385 Immunoprofiling Identifies Distinct Populations of Appendiceal Neuroendocrine Tumors

Daniel Shen[1], Amad Awadallah[2], Ozgur Mete[3], Sylvia Asa[1]
[1]Case Western Reserve University/University Hospitals Cleveland Medical Center, Cleveland, OH, [2]University Hospitals Cleveland Medical Center, Cleveland, OH, [3]University Health Network, University of Toronto, Toronto, Canada

**Disclosures:** Daniel Shen: None; Amad Awadallah: None; Ozgur Mete: None; Sylvia Asa: *Advisory Board Member*, Leica Biosystems

**Background:** Appendiceal neuroendocrine tumors (NETs) are common and often are identified as incidental lesions at the time of appendectomy using synaptophysin and chromogranin stains. The guidelines for management are based on tumor size, degree of invasion, and the Ki67 proliferation index. Most small bowel NETs are composed of serotonin-producing EC cells, but there are multiple other neuroendocrine cell types. In the rectum, there are L cell tumors that express glucagon-like peptides (GLPs) and pancreatic polypeptide (PP) that are thought to have a better prognosis than serotonin-producing tumors.   We investigated whether the appendix has distinct neuroendocrine tumor types based on cell type.

**Design:** We collected 48 appendiceal NETs from the archives of our institution and performed immunohistochemistry for serotonin that is expressed by EC cells, and for glucagon (that detects GLPs) and PP that are produced by L cells.

**Results:** Immunohistochemistry identified three types of appendiceal NETs. Among the 48 tumors, 32 (67%) were typical EC cell tumors that stained for serotonin.  12 (25%) had an L cell immunoprofile, expressing GLPs (10/48; 21%) and/or PP (5/48; 10%). A third group of tumors (4/48; 8%) expressed serotonin with GLPs and/or PP.

**Conclusions:** Our study confirms that appendiceal NETs are not a homogeneous tumor population.  There are at least three types of appendiceal NET, including EC cell, L cell and mixed tumors. This information is important for surveillance of patients, as monitoring urinary 5HIAA levels is only appropriate for patients with serotonin-producing tumors, whereas measurement of GLPs and/or PP is more appropriate for patients with L cell tumors. Further analysis will allow us to determine if these different tumor types have different risk of recurrence or metastasis.

### 386 Gastrointestinal Manifestations and Pathology in SARS-CoV-2: Case Series

Sophia Sher[1], Alison Burkett[2], Isam Eltoum[1], Deepti Dhall[1], Chirag Patel[1], Goo Lee[2], Sameer Al Diffalha[1]
[1]The University of Alabama at Birmingham, Birmingham, AL, [2]UAB Hospital, Birmingham, AL

**Disclosures:** Sophia Sher: None; Alison Burkett: None; Isam Eltoum: None; Deepti Dhall: None; Chirag Patel: None; Goo Lee: None; Sameer Al Diffalha: None

**Background:** Initially recognized in December of 2019, the severe acute respiratory syndrome coronavirus 2 (SARS-CoV-2) rapidly emerged as a global pandemic. While the infectious disease predominantly manifests with respiratory symptoms of varying severity following exposure, gastrointestinal complications resulting in significant morbidity and mortality have also been recognized.

**Design:** A thorough review of medical records in conjunction with macroscopic and histopathological findings was performed in four patients, aged 28-46years, with a confirmed positive SARS-CoV-2 RNA on nasal swab.

| Patient Demographics | | | | Laboratory Values | | | | | | Pathologic Findings | |
|---|---|---|---|---|---|---|---|---|---|---|---|
| Age | Sex | Race | Comorbidities | CRP (mg/L) | D-Dimer (ng/mL) | LDH (Units/L) | Lactic Acid (mMol/L) | Troponin I (ng/L) | HgB/Hct | Macroscopic Findings | Microscopic Findings |
| 37 | M | African American | HTN, Obesity (BMI 34.8kg/m²)Insulin Dependent Diabetes Mellitus | 282.6 | 978 | 556 | X | 44 | 11/33 | Ischemic mucosal changes. | Mucosal ulcerations, early microsopic pneumatoiss cystoides intestinalis, fibrin microthrombi, focal serositis. |
| 47 | M | African American | HTN, Obesity (BMI 33.08kg/m²) | 176.3 | 4,064 | X | 4.0 | 39 | 9.9/26 | Ischemic mucosal changes, clots extending into the infrarenal IVC, focal hemorrhage. | Mucosal ulceration, transmural acute and chronic inflammation, cyst formation suggestive of pneumatosis cystoides intestinalis, fibrin thrombi, acute serositis. |
| 40 | M | Caucasian | Obesity (BMI 33.2 kg/m² ) | X | >20,000 | X | 7.1 | 1838 | 15.6/46 | Necrotic, hemorrhagic, and ischemic mucosa/serosa, submucosal thickening. | Transmural hemorrhagic infarction, fibrin thrombi, lamina propria edema, cyst formation suggestive of pneumatosis cystoides intestinalis |
| 28 | M | African American | Diabetes Mellitus | 24.87 | 1,380 | 681 | 10.6 | 98 | 7.3/22 | Ischemic mucosal and serosal changes | Pseudomembrane formation, transmural necrosis, acute serositis |

Figure 1 - 386
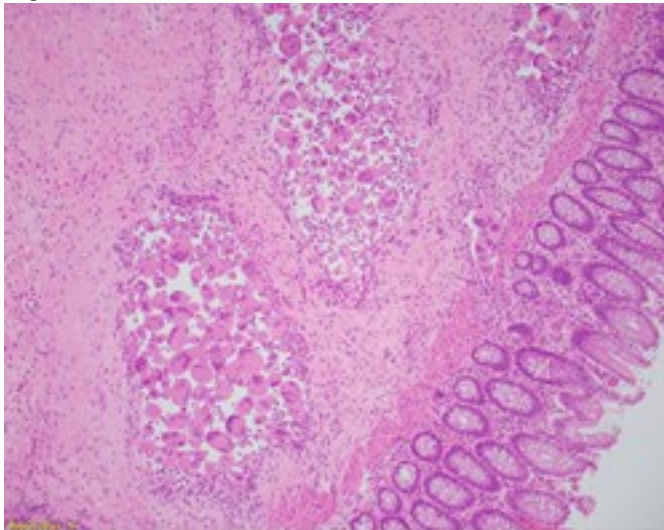


Figure 2 - 386
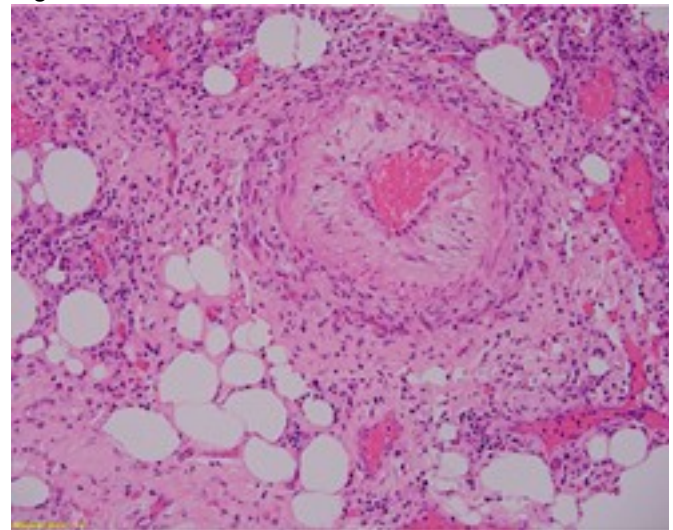


**Conclusions:** In a minority of patients that initially presented with a severe form of pulmonary COVID-19 infection, associated gastrointestinal symptoms were present, and often required surgical intervention for the management of gastrointestinal complications. Histopathological examination of resected GI specimens revealed a spectrum of disease from superficial mucosal ischemic colitis pattern to frank transmural ischemic colitis and associated changes consistent with pneumatosis cystoides intestinalis. These morphological changes suggest viral predilection for the right colon, and may facilitate the potential diagnosis of COVID-19 infection when the etiology of ischemic colitis is unclear.

### 387 Three-Dimensional High-Resolution Imaging of Patient-Derived Esophageal Adenocarcinoma Organoids

Yukiko Shibahara[1], Mathieu Derouet[1], Sangeetha Kalimuthu[2], Gail Darling[3], Jonathan Yeung[4]
[1]University Health Network, University of Toronto, Toronto, Canada, [2]University Health Network, Toronto, Canada, [3]Toronto General Hospital, University of Toronto, Toronto, Canada, [4]Toronto General Hospital, University Health Network, Toronto, Canada

**Disclosures:** Yukiko Shibahara: None; Mathieu Derouet: None

**Background:** Organoids result from the three-dimensional tissue culture of stem cells. When cultured from cancer tissue, cancer organoids arise and have been shown to largely recapitulate the originating tumor. Consequently, patient-derived cancer organoids (PDO) are emerging as an important model for facilitating the identification of personalized treatments. To that end, detailed characterization of each PDO by pathological analysis will be required to identify characteristics and biomarkers which may indicate susceptibility to specific treatments. We have established robust culture of esophageal adenocarcinoma organoids from endoscopic biopsies and demonstrated routine two-dimensional pathological assessment. Given the importance of the 3D structure to organoids, we sought to develop a protocol for high-resolution 3D pathological assessment.

**Design:** We aimed to develop a method for whole-mounting PDO and applying multiplexed immunofluorescent (IF) stains. PDOs were fixed in formalin, but never embedded in paraffin nor sectioned; a protocol using a liquid technique was optimized for this procedure. Distinct panels of frequently studied biomarkers such as CK7, CDX-2, e-cadherin, phalloidin (F-actin) as well as other markers of interest such as CK14, MUC2, MUC6, MIB-1 were generated. Stained slides were imaged using confocal microscopy (Leica SP8). The multiplex IF images were then analyzed using Image J (two dimensional) and Imaris (three dimensional), followed by automated quantification of the biomarkers.

**Results:** We successfully mounted and stained PDO with multiplex IF antibodies. Confocal images were stacked into voxels and reconstructed as digital 3D representations. This revealed novel insights into the 3D organization of organoids; many appear to be toroid rather than spheroid. Multiplex staining was successful and similarly revealed insights into the organization of cellular components; phalloidin (F-actin) preferentially stained the center of the organoid suggesting cellular polarity (Figure 1; E-cadherin, green; phalloidin, red; DAPI, blue). The number/surface area/volume of positive cells and co-localization of biomarkers were facilitated by software.

Figure 1 - 387
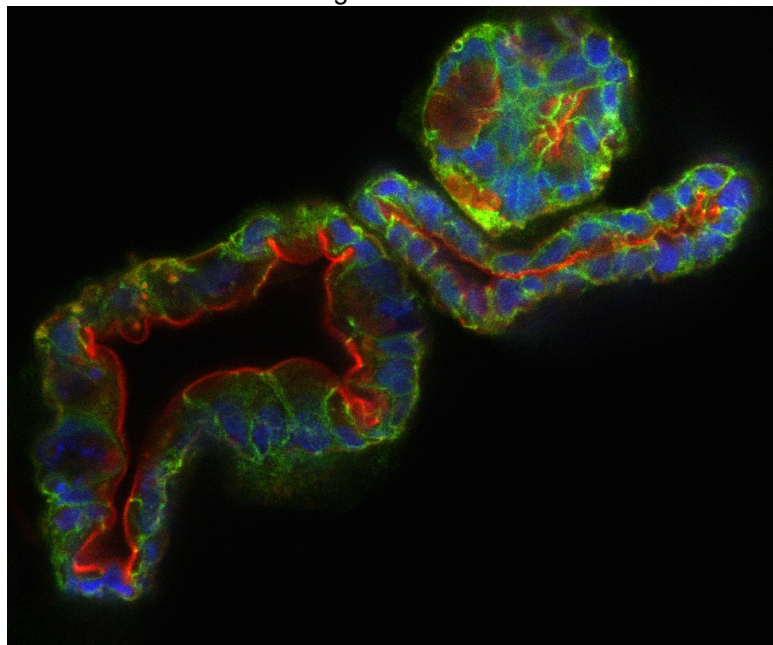
**Conclusions:** Organoid staining has the potential to be adapted for high-throughput screening of individual cancers for personalized therapy. Our process allows for accurate staining of multiple biomarkers on a single slide and the non-sectioned images allow us to study the three-dimensional interactions of multiple expressed proteins. This will also enable the quantitative assessment of biomarkers. We aim to maximize the potential of this protocol using time-lapse and live cell organoid imaging in the future.

### 388 Outcome of Low Grade Appendiceal Mucinous Neoplasm with Aceullar Mucin on the Serosal Surface

Ayesha Siddique[1], Muhammad Akrmah[1], Krishna Patel[1], Muhammad Saad[1], Saverio Ligato[2]
[1]Hartford Hospital, Hartford, CT, [2]Hartford Hospital, Canton, CT

**Disclosures:** Ayesha Siddique: None; Muhammad Akrmah: None; Krishna Patel: None; Muhammad Saad: None

**Background:** Low grade appendiceal mucinous neoplasm (LAMN) of the appendix is a heterogenous disease with challenging therapeutics. There is limited data on prognosis of these lesions and the use of hyperthermic intraperitoneal chemotherapy (HIPEC) in cases of acellular mucin extravasation alone. The aim of this study is to explore outcomes of LAMN specifically in cases of acellular mucin extravasation with or without inflammatory cells.

**Design:** A retrospective study design was used to explore the outcomes in patients with LAMN. A total of 97 patients presenting with LAMN with or without dissemination were studied. Out of these a total of 75 patients had a complete follow-up data and the remaining 22 were excluded from the analysis. Data was collected on age, gender, tumor size, tumor location, perforation of appendix, tumor extension, margin status, satellite tumor nodules, lymphovascular invasion, perineural invasion and TNM staging. We studied metastasis on follow-up including lymph node metastases and pseudomyxoma peritonei as outcomes of these patients.

**Results:** Out of 75 patients, 22 (29.3%) were males and 53 (70.7%) females. The age range was 31-87 years. Twenty-nine(38.7%) patients had a tumor size ≤ 1 cm while 46(61.3%) patients had a tumor size > 1 cm. Twenty-one(28%) patients had the tumor located in the distal tip of the appendix while remaining were seen elsewhere. Twenty-one(28%) patients had a perforated appendix at the time of surgery while others did not. Seven(9.3%) patients had a positive margin of excision while the others had a negative margin. Lymphovascular invasion and perineural invasion was not seen in any of our cases. Forty-one(54.7%) patients were Tis, 11(14.7%) were T3, 14(18.7%) were T4a and 9(12%) were T4b. Lymph node metastases were not observed in any case. Organ metastases were seen in 15 (20%) of the patients at follow-up. Seventeen ( 22.7%) patients presented with pseudomyxoma peritonei on follow-up. Disease extension and mucin extravasation with/without inflammation significantly impacted outcomes with 9.3% patients with acellular mucin extravasation and inflammatory cells presenting with pseudomyxoma peritonei on followup.  (Table 1). Size and margin status in organ confined cases did not have a significant impact on outcome (Table 1).

| Follow-up | Stage (n) | | | | | Acellular mucin extravasation(n) | | | Size(n) | | | Margin Status in organ confined cases(n) | | |
|---|---|---|---|---|---|---|---|---|---|---|---|---|---|---|
| | Tis | T3 | T4a | T4b | P value | With inflammatory cells | Without inflammatory cells | P value | ≤1 cm | >1 cm | P value | Positive | Negative | P value |
| Organ Metastases positive | 0 | 0 | 7 | 8 | <0.001 | 7 | 0 | <0.001 | 6 | 9 | 0.906 | 0 | 0 | - |
| Organ Metastases negative | 41 | 11 | 7 | 1 | | 7 | 11 | | 23 | 37 | | 5 | 47 | |
| Pseudomyxoma peritonei positive | 0 | 1 | 7 | 9 | <0.001 | 7 | 10 | <0.001 | 6 | 11 | 0.745 | 0 | 5 | 0.742 |
| Pseudomyxoma peritonei negative | 41 | 10 | 7 | 0 | | 7 | 1 | | 23 | 35 | | 1 | 46 | |

**Conclusions:** Mucin extravasation without inflammatory cells did not have a worse prognostic outcome while acellular mucin with inflammatory cells revealed metastases and pseudomyxoma peritonei in 9.3% of the patients signifying the importance of reporting inflammatory cells along with mucin extravasation. The use of HIPEC in cases of mucin extravasation with inflammatory cells might help outcomes.

## 389 Gastric Antral Vascular Ectasia (GAVE): A Clinicopathologic and Endoscopic Correlation of 38 Cases

Mohan Sopanahalli Narasimhamurthy[1], Franz Fogt[2], Rifat Mannan[3]
[1]Pennsylvania Hospital of the University of Pennsylvania Health System, Philadelphia, PA, [2]Hospital of the University of Pennsylvania, Gladwyne, PA, [3]Perelman School of Medicine at the University of Pennsylvania, Philadelphia, PA

**Disclosures:** Mohan Sopanahalli Narasimhamurthy: None; Franz Fogt: None; Rifat Mannan: None

**Background:** GAVE accounts for up to 4% of nonvariceal upper GI bleeding. It can be associated with cirrhosis, scleroderma, diabetes mellitus, hypertension, among others. We sought to analyze clinical, endoscopic and histological features of GAVE at our institution.

**Design:** We searched the database and retrospectively analyzed clinical, endoscopic and histologic features of GAVE diagnosed at our institute.

**Results:** Thirty-eight cases (18M and 20F) were identified over a 5-year period. Median age was 60 years (range,19-92). Indications for endoscopy included iron deficiency anemia (29%, 11/38), abdominal pain (21%, 8/38), heartburn (16%, 6/38), screening for varices (10%, 4/38), surveillance for Barrett esophagus (6%, 2/38), and non-specific GI symptoms (19%, 7/38). Associated clinical conditions included: cirrhosis (16%, 6/38), autoimmune disorders (13%, 5/38), chronic kidney disease (11%, 4/38), inflammatory bowel disease (8%, 3/38) and miscellaneous other conditions (52%, 20/38). On endoscopy, GAVE appeared as typical linear striped "watermelon" appearance (26%, 10/38) (Fig1A), diffuse punctate erythema (58%, 22/38) (Fig1C), nodule/polyp (10%, 4/38) (Fig1B,), or unremarkable mucosa (6%, 2/38). The nodular lesions presented on endoscopy as multiple mucosal nodularity (n=3) or as a 1.5 cm solitary sessile polyp (n=1) (Fig1D). In 10 cases (26%) an endoscopic diagnosis of GAVE was entertained. Within the stomach, all lesions were located in antrum. On histology, all cases revealed the characteristic features of GAVE, with intravascular fibrin thrombi, congested ectatic vessels and background fibromuscular proliferation in the lamina propria (Fig 2). Inflammation was minimal, or absent.
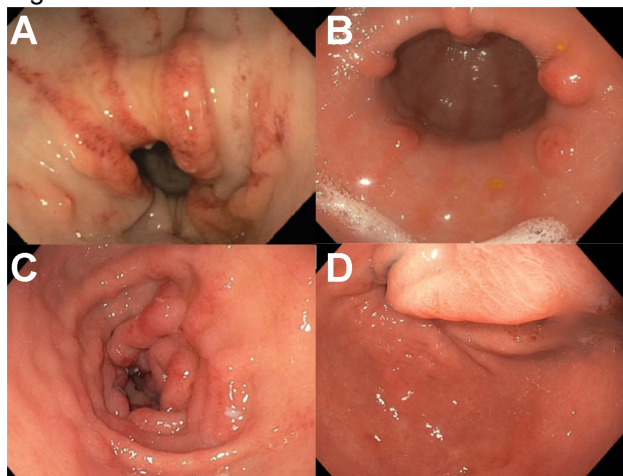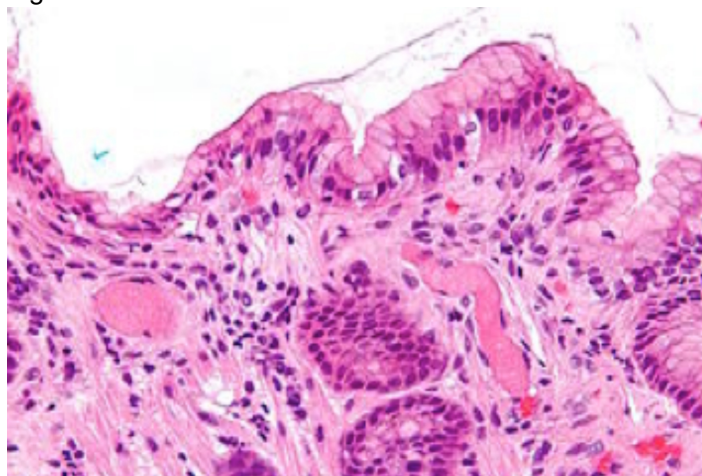
Figure 1 - 389



Figure 2 - 389



**Conclusions:** In our study, GAVE presented with significant endoscopic alterations in the gastric antral mucosa. In addition to the classic linear and diffuse erythematous patterns, we observed an unusual pattern of mucosal nodularity/polyp in our cohort. Histologic diagnosis is important to distinguish from portal hypertensive gastropathy and antral gastritis, as the management is different.

## 390 The Histologic Spectrum of ARB-Induced Gastritis

Tanner Storozuk[1], Ian Brown[2], Stephen Lagana[3], Maria Westerhoff[4], Namrata Setia[5], John Hart[5], Lindsay Alpert[5]
[1]University of Chicago Medical Center, Chicago, IL, [2]Envoi Pathology, Brisbane, Australia, [3]New York-

Presbyterian/Columbia University Medical Center, New York, NY, [4]University of Michigan, Ann Arbor, MI, [5]University of Chicago, Chicago, IL

**Disclosures:** Tanner Storozuk: None; Ian Brown: None; Stephen Lagana: None; Maria Westerhoff: None; Namrata Setia: None; John Hart: None; Lindsay Alpert: None

**Background:** Olmesartan, an angiotensin receptor blocker (ARB) used for hypertension management, causes a sprue-like enteropathy in a subset of patients; other ARBs have also been implicated. Rare cases of gastritis occurring with ARB use have also been reported, but the clinicopathologic features of ARB-induced gastritis have not been closely examined.

**Design:** 15 cases of suspected ARB-induced gastritis were identified from the pathology archives of 4 institutions. H&E slides from gastric biopsies were reviewed by gastrointestinal pathologists at each institution. Clinical data, including endoscopic findings and follow-up information, were collected from the electronic medical records.

**Results:** Fourteen of the patients were female and 1 was male (age range of 48-87 years; mean 70 years). Fourteen patients were taking olmesartan and one was taking telmisartan (duration 6 months to 3+ years). Common symptoms included diarrhea, weight loss, and abdominal pain. Endoscopic findings in the stomach included erythema (n=4), nodularity (n=2), "gastritis" (n=2), and atrophy (n=2). Histologically, a lymphoplasmacytic lamina propria infiltrate was present in all cases, with a significant eosinophilic component in 10 cases. Active inflammation was seen in 11 cases (antrum/body—n=5, antrum only—n=5, and body only—n=1). Nine cases showed intraepithelial lymphocytosis, and 3 cases had patchy subepithelial collagen thickening (1 case had both features). Surface mucin depletion and/or erosion was evident in 12 cases. Four cases demonstrated glandular atrophy in the body. An H. pylori immunostain was performed in 13 cases, including all cases diagnosed as chronic active gastritis, and was negative in all cases. Concurrent duodenal biopsies were obtained in 13 cases: 10 showed villous blunting, intraepithelial lymphocytosis, and/or subepithelial collagen thickening; 1 showed active duodenitis; and 2 showed no abnormalities. Eleven patients had symptomatic improvement after cessation of ARB therapy; follow-up gastric biopsies in 5 of 8 patients showed histologic normalization.

**Conclusions:** We describe the histologic findings seen in ARB-induced gastritis, including chronic active gastritis, prominent eosinophils, intraepithelial lymphocytosis, subepithelial collagen thickening, and surface erosion. Patterns of gastritis with a combination of these features are common. Recognizing the histologic changes associated with ARB-induced gastric injury will allow pathologists to suggest this condition in their reports and can lead to ARB cessation with symptomatic and histologic improvement.

---

**391    Reappraisal of the Utility of Mitosis, Ki67 Index, and SSTR2 Expression in the Differential Diagnosis between Grade 3 Well-differentiated Neuroendocrine Tumor and Poorly Differentiated Neuroendocrine Carcinoma of the Gastrointestinal Tract and Pancreas**

Jacob Sweeney[1], Zhaohai Yang[2]
[1]Hospital of the University of Pennsylvania, Philadelphia, PA, [2]University of Pennsylvania Perelman School of Medicine, Philadelphia, PA

**Disclosures:** Jacob Sweeney: None; Zhaohai Yang: None

**Background:** Distinguishing Grade 3 well-differentiated neuroendocrine tumor (NET G3) from neuroendocrine carcinoma (NEC) can be difficult and requires a constellation of morphologic and immunohistochemical (IHC) features. Some evidence suggests that the somatostatin receptor type 2 (SSTR2) is expressed more frequently in pancreatic NET than NEC. Little is known about SSTR2 expression in luminal gastrointestinal (GI) tract tumors. In this study, we investigated SSTR2 expression in NET G2, NET G3, and NEC from the GI tract and pancreas to assess whether SSTR2 expression, Ki67 index and mitotic count could help distinguish NET G3 from NEC.

**Design:** 29 cases of NET G2, 27 cases of NET G3, and 20 cases of NEC from the GI tract or pancreas were identified. Ki67 index was included in original reports. Mitosis was recounted, and immunostaining for p53, pRb1, and SSTR2 was performed. The percentage of positive SSTR2 staining was quantified by two GI pathologists.   Student's t-test was used to for statistical analysis.  Receiver operating curve (ROC) analysis was performed for mitotic count, Ki67 index, and SSTR2 staining.

**Results:** Mitosis, Ki67 index and SSTR2 staining results in NET G3 and NEC are summarized in Table 1. SSTR2 staining in NET G3 was equivalent to NET G2, and significantly higher than NEC (p<0.0001) in all sites, as well as pancreatic and GI separately. Small cell NEC showed less SSTR2 staining than large cell NEC but without statistical significance (p=0.34). ROC analysis is shown in Figure 1. A mitotic count (cutoff 25/2mm2) yielded the highest area under the curve (AUC) of 0.965, while both Ki67 index (cutoff 65%) and SSTR2 (cutoff 50%) also showed significant AUC (P<0.0001 for all). P53 and RB1 mutation/loss was rarely seen in NET G3 (both GI cases were confirmed by molecular analysis), and was frequent in both GI and pancreatic NEC. There was no statistical difference in the frequency of p53 or RB1 mutations between GI and pancreatic NEC (p>0.25, Fisher exact test).

Table 1. Mitosis, Ki67 index, and expression of SSTR2, P53, and RB in NET G3 and NEC of the digestive system.

| | n | Mitosis/2mm2: Mean (range) | Ki67 index %: mean (range) | SSTR2 %: mean (range) | Abnormal P53 IHC | pRB loss on IHC |
|---|---|---|---|---|---|---|
| All NET G3 | 27 | 14 (1-39) | 30 (13-90) | 80 (10-100) | 1 (3.7%) | 2 (7.4%) |
| All NEC | 20 | 57 (18-150) | 70 (30-94) | 20 (0-90) | 13 (65%) | 8 (40%) |
| GI NET G3 | 11 | 18 (2-39) | 30 (13-90) | 80 (10-100) | 1 (9%) | 1 (9%) |
| GI NEC | 12 | 71 (37-150) | 80 (71-94) | 10 (0-75) | 9 (75%) | 5 (42%) |
| Pancreatic NET G3 | 16 | 12 (1-25) | 30 (21-65) | 90 (10-100) | 0 (0%) | 1 (6.3%) |
| Pancreatic NEC | 8 | 33 (18-43) | 60 (30-80) | 30 (0-90) | 4 (50%) | 3 (38%) |

Figure 1 - 391
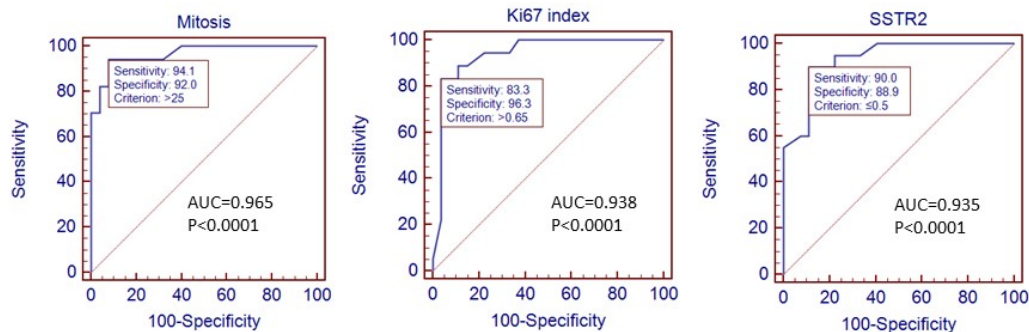


**Conclusions:** Both pancreatic and GI NET G3 showed significantly higher SSTR2 expression than NEC. Mitosis count, Ki67 index and SSTR2 all yielded significant AUC in distinguishing NEG G3 from NEC, with mitosis showing the best sensitivity/specificity. Though P53 and pRb1 mutation/loss are generally considered specific markers for NEC, they can rarely be seen in NET G3.

### 392 Her2 Testing in Colorectal Adenocarcinoma Requires a Tumor Specific Algorithm

Jacob Sweeney[1], Emma Furth[2], Paul Zhang[1]
[1]Hospital of the University of Pennsylvania, Philadelphia, PA, [2]University of Pennsylvania, Philadelphia, PA

**Disclosures:** Jacob Sweeney: None; Emma Furth: None; Paul Zhang: None

**Background:** Colorectal adenocarcinoma (CRC) is a leading cause of cancer-related death for which anti-Her2 therapy may improve outcomes in those CRC with *Her2* amplification. However, in contrast to other malignancies, no standard interpretation guidelines exist for Her2 immunohistochemical staining (IHC) and florescent in situ hybridization (FISH) testing in CRC. As a first step towards developing testing standards, we assessed the concordance of Her2 testing by IHC, FISH, and *ERBB2* gene sequencing retrospectively in cases of CRC.

**Design:** Cases of CRC with Her2 testing performed between 2010 and 2020 were identified. All Her2 testing was performed on formalin fixed paraffin embedded tissue. The PathVysion Her2 dual probe and Pathway (4B5) IHC test were used. *ERBB2* sequencing was performed as a part of a 152 gene next generation sequencing (NGS) panel on an Illumina platform.

**Results:** 49 cases of CRC with Her2 testing were identified. All patients had metastatic disease and underwent chemotherapy; 33 (67%) experienced progression of disease following therapy and 11 (22%) died. IHC was performed in all 49 cases, FISH was performed in 45 (92%) cases, and NGS was performed in 44 (90%) cases; all three methods were used in 39 (80%) cases. 3 cases (6%) showed high levels of *Her2* amplification by FISH (Her2/Cep17>5.0 and Her2/cell>10.0). These cases showed 3+ IHC (10-95% of cells) and *ERBB2* copy number gains by NGS. 3 cases showed lower levels of *Her2* amplification by FISH (Her2/Cep17: 2-3.0 and Her2/cell: 3.37-6.0). These cases showed 0+ IHC and no *ERBB2* copy number gains by NGS. The remaining cases showed Her2/Cep17<2 and Her2/cell<4 by FISH and no *ERBB2* copy number gains. Of these cases, one showed 2+ IHC staining; the remainder were 0+ or 1+.

**Conclusions:** Her2 testing is tumor type specific, and to our knowledge, a CRC specific testing algorithm has not been previously published.  We found that CRC cases with high levels of *Her2* amplification by FISH also showed 3+ IHC and *ERBB2* copy number gains by NGS. In contrast, 3 cases with lower levels of *Her2* amplification by FISH showed 0+ IHC and no copy number gains by NGS. The gastric criteria for FISH testing would consider these 3 cases positive while breast criteria would consider 2 of these cases negative. Testing algorithms which use FISH reflexively following a 2+ IHC staining result would miss these cases. Until the significance of low level *Her2* amplification in CRC becomes clear, our results support the use of both IHC and FISH in all cases.

**393    Uncommon Mucosal Metastases in Endoscopic Colorectal Biopsies: A 20-year Single-Institution Review From 13,564 Specimens**
Suresh Tharmaradinam[1], Selliah Kanthan[2], Dana Diudea[3], Rani Kanthan[2]
*[1]University of Saskatoon, Saskatoon, Canada, [2]University of Saskatchewan, Saskatchewan Health Authority, Saskatoon, Canada, [3]Royal University Hospital, Saskatoon, Canada*

**Disclosures:** Suresh Tharmaradinam: None; Selliah Kanthan: None; Dana Diudea: None; Rani Kanthan: None

**Background:** Colorectal endoscopic biopsies, one of the commonest small biopsy specimens received in general surgical pathology practice has increased exponentially in the past decade with the implementation of screening colonoscopy for the early detection of colorectal cancer.

The aim of this study is to examine the frequency with organ distribution of mucosal metastases as identified in endoscopic colorectal biopsies.

**Design:** We recently identified four endoscopic biopsies with mucosal metastases from the breast, lung, merkel cell and endometrium [Fig1]. This led to a dedicated computerized data search of colon and rectum biopsies for the last 20 years with the diagnosis of colon/rectum and  "breast", "lung", "merkel", "endometrial", "prostate", "ovary", "urothelial", "melanoma", "renal" and "thyroid".  All non-endoscopic biopsies including those obtained at laparoscopy/laparotomy were excluded. Study-selected cases were reviewed together with their original parent malignancy as available in the context of individual clinical history.

**Results:** A total of 13,564 colorectal mucosal biopsies were identified from a general pool of 55,154 colorectal biopsies.  52 cases~0.4% of non-colonic mucosal metastases were identified with the most common primary organ of origin in descending order of frequency being Prostate-17 cases ~33%, Ovary-12 cases~23%, Breast and Urothelial-7 cases each~13%, Lung, Renal  and Endometrial-2 cases each ~4%, Merkel Cell Carcinoma, Malignant Melanoma and Thyroid-1 case each~2%. Thus 14 of these metastases were extrapelvic in origin.  Metastases were overall more common in males-29 cases, than females-23 cases and were found with equal frequency in colonic and rectal biopsies. The average disease interval between the original malignancy and the identification of colorectal mucosal metastases was 7yrs.  Clinicopathological features including indication for endoscopic biopsy are summarized in Table1.

| PRIMARY SITE OF CANCER | MEAN AGE AT PRIMARY DIAGNOSIS | CLINICAL INDICATION FOR ENDOSCOPY | MEAN AGE AT ENDOSCOPIC DIAGNOSIS | CLINICOPATHOLOGICAL CHARACTERISTICS (AWD-Alive with Disease)(DWD- Died with disease) | DISEASE STATUS |
|---|---|---|---|---|---|

| | | | | | |
|---|---|---|---|---|---|
| **Prostate[17]** | 70 | Bleeding PR/Anemia Rectal mass/polyp CT lesion Constipation Weight loss Diarrhea Obstruction | 78 | Grade group 5 [7] Grade group 4 [4] Grade group 3 [2] Grade group 2 [2] | 15 – DWD 2 – AWD |
| **Ovary [12]** | 58 | Ascites, CT Lesion Bleeding PR, FIT + Rectal mass/polyp Elevated CA-125 Ulcer Diarrhea | 59 | Serous adenocarcinoma-high grade [10] Invasive low grade serous carcinoma [1] Poorly differentiated clear cell carcinoma [1] | 10 – DWD 2 – AWD |
| **Breast [7]** | 65 | Rectal Polyp/mass Rectal thickening Malignant ascites Chronic diarrhea, Colonic stricture Obstruction Abnormal PET | 65 | Invasive ductal carcinoma [3] Infiltrating lobular carcinoma [4] | 5 – DWD 2 – AWD |
| **Urothelial [7]** | 70 | Rectal mass/polyp Infiltrative lesion Obstruction Rectal ulcer | 71 | Invasive high grade urothelial ca [7] | 7 – DWD |
| **Lung [2]** | 62 | FIT + Anemia Rectal mass Bleeding PR Fatigue CT Lesion | 73 | Moderately differentiated adenocarcinoma[1] CT based Diagnosis (8.4 x 12.3 mm) RML [1] | 2 – DWD |
| **Endometrial[2]** | 62 | Perforation Query Diverticulitis/ Ca Stricture Intrinsic lesion | 63 | Endometrioid Endometrial Ca [2] | 1 – DWD 1 – AWD |
| **Renal [2]** | 73 | Invading mass | 73 | Clear cell, Renal cell carcinoma (1) Undifferentiated Renal cell Carcinoma [1] | 1 – DWD 1 – AWD |
| **Merkel Cell Carcinoma [1]** | 79 | Colonic mass Melena Abnormal CT | 82 | Merkel cell carcinoma – axillary node 2yrs ago | 1 – DWD |
| **Malignant Melanoma [1]** | 36 | CT suspected lesion | 37 | Lesion forearm -2yrs ago Query Malignant Melanoma | 1 – DWD |
| **Thyroid [1]** | 75 | Rectal Polyps Anemia | 77 | Follicular carcinoma thyroid - gastric and rectal polyps, skin lesions 5-7 years later dedifferentiated Anaplastic carcinoma | 1 – DWD |

Figure 1 - 393
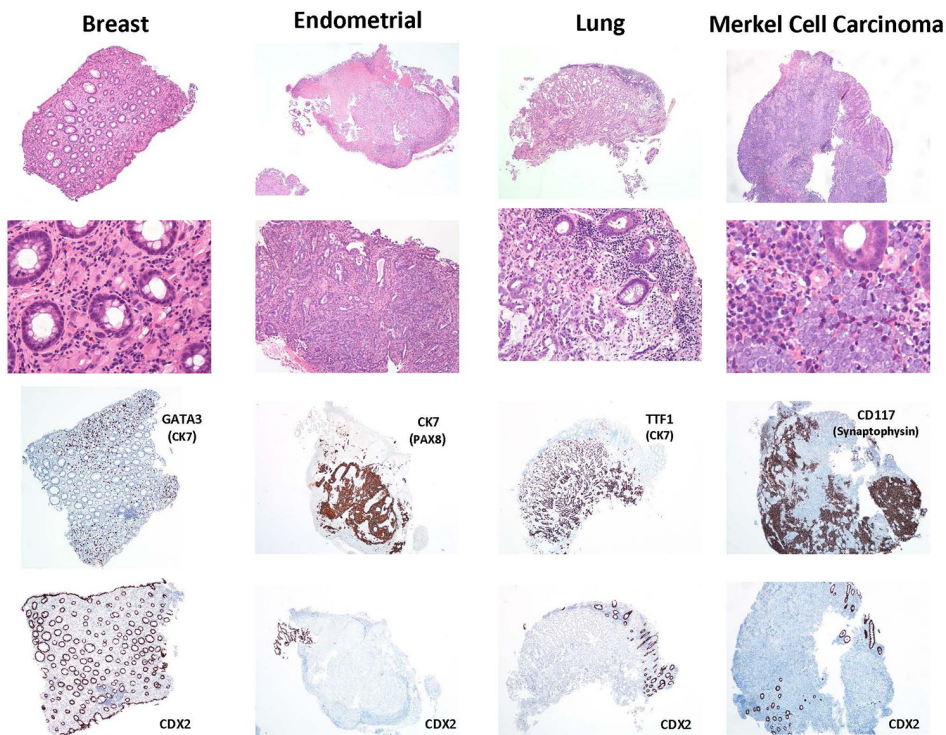


Figure 2 - 393
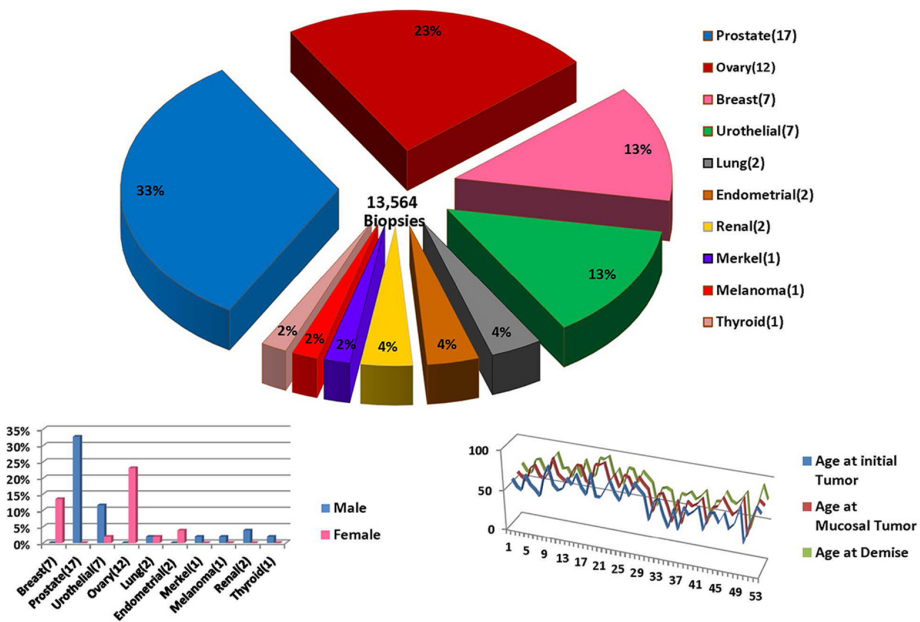


**Conclusions:** Although primary colorectal carcinoma is the commonest malignant diagnosis of endoscopic biopsies, it is important to remember that non-colonic organs, though uncommon, can rarely present as mucosal metastases, often with delayed intervals. Familiarity and awareness of these uncommon metastases is vital for accurate pathological diagnosis which is greatly benefited today with the advent of lineage specific immunohistochemical markers as seen in Fig1. Such precision information is of critical value for judicious triaging of patients in planning their further management.

**394 Prevalence and Clinicopathological Features of Intestinal Perforation Caused by Segmental Muscular Defects in Adults**

Takuji Tsuyuki, Taishi Takahara[1], Akira Satou[1], Toyonori Tsuzuki[1]
[1]Aichi Medical University Hospital, Nagakute, Japan

**Disclosures:** Takuji Tsuyuki: None; Toyonori Tsuzuki: None

**Background:** Segmental muscular defects (SMD) of the intestine can cause intestinal perforation in adults. However, their prevalence and clinicopathological features have not been well-described. This study aimed to determine the prevalence of SMD-associated perforation and characterize its clinicopathological features.

**Design:** We retrospectively examined 109 intestinal perforation cases that underwent surgical resection from January 2009 to December 2019. Cases with intestinal perforation caused by invasion of a malignant tumor or ruptured appendicitis were excluded. SMD was defined as the complete absence of the muscularis propria without extensive inflammation and fibrinous exudation around the perforation.

**Results:** SMD was the second most frequent cause of perforation (26 cases: 24%), the most frequent cause being related to diverticulitis (39 cases: 36%). The most common site was the sigmoid colon (12 cases: 46.2%). The younger group (aged <60 years) exhibited more frequent perforation of the upper segments of the gastrointestinal tract (from the duodenum to descending colon) than the older group did (≥60 years) (p = 0.011). No patients developed recurrence. The most common gross features were well-defined circular or small punched-out lesions, and the histological features were complete absence of the muscularis propria and absence of hemorrhage and necrosis around the area of perforation.

**Conclusions:** The characteristic features of SMD were unique and their prevalence was higher than that which previously reported. The precise recognition of SMD can aid in understanding the cause of perforation and avoiding unnecessary further examinations.

**395 NUTM1-Rearranged Colorectal Sarcoma: Clinicopathologically and Genetically Distinctive Malignant Neoplasm with a Poor Prognosis**

Benjamin Van Treeck[1], Judith Jebastin Thangaiah[1], Jorge Torres-Mora[1], Todd Stevens[2], Christian Rothermundt[3], Matteo Fassan[4], Fotios Loupakis[5], Jason Hornick[6], Andrew Folpe[1]
[1]Mayo Clinic, Rochester, MN, [2]The University of Alabama at Birmingham, Birmingham, AL, [3]Kantonsspital St. Gallen, St. Gallen, Switzerland, [4]University of Padua, Padua, Italy, [5]Istituto Oncologico Veneto IOV - IRCCS, Padua, Italy, [6]Brigham and Women's Hospital, Harvard Medical School, Boston, MA

**Disclosures:** Benjamin Van Treeck: None; Judith Jebastin Thangaiah: None; Jorge Torres-Mora: None; Todd Stevens: None; Christian Rothermundt: None; Matteo Fassan: *Grant or Research Support*, Astellas Pharma; *Grant or Research Support*, QED Therapeutics; *Advisory Board Member*, Astellas Pharma; *Advisory Board Member*, Tesaro; *Consultant*, Diaceutics; Fotios Loupakis: None; Jason Hornick: None; Andrew Folpe: None

**Background:** NUTM1 gene rearrangements were originally identified in NUT carcinoma, an aggressive variant of squamous cell carcinoma. Recently, NUTM1 gene fusions with a variety of partners have been reported in malignancies of diverse location and type. Only 2 NUTM1-rearranged tumors occurring in the gastrointestinal tract have been reported. We present the clinicopathologic features of 4 such tumors, including additional clinicopathologic information on 2 previously reported cases.

**Design:** Following IRB approval, all available material and clinical information from 4 colorectal tumors harboring NUTM1-rearrangements were retrieved.

**Results:** The 4 tumors occurred in 3 females and 1 male, ranging from 38-65 years of age (median 42 yrs). The masses were located in the colon (cecum, descending, sigmoid) and ileocecal valve region and measured 2.5-5 cm in size (median 3.5 cm). Three patients had metastases at presentation or shortly after presentation, to the liver (n=2) and lymph nodes (n=2). Histologically, the lesions arose in the submucosa, were infiltrative into the mucosa and muscularis propria, and grew in fibrosarcoma-like fascicles (figure 1b) with occasional hyalinized to vaguely

osteoid matrix. Cytologically, the cells consisted of a relatively monomorphic proliferation of spindled to epithelioid cells (figure 1a) with focal rhabdoid morphology, hyperchromatic nuclei, and small nucleoli. Mitotic activity was present (range 1-9/ 10 HPF; median 2/ 10HPF); necrosis was absent. The tumors were variably positive for keratins and diffusely positive for NUT (nuclear). Other tested markers were mostly negative. Next-generation sequencing identified MXD4-NUTM1 rearrangement in all cases (MXD4 exon 5; NUTM1 exons 2 or 3). Follow-up showed 1 of 3 patients with metastases at presentation died of disease at 30 months; the other 2 patients were alive with metastatic disease, 7 months and 12 months after diagnosis. The final patient is disease free, 3 months after diagnosis.
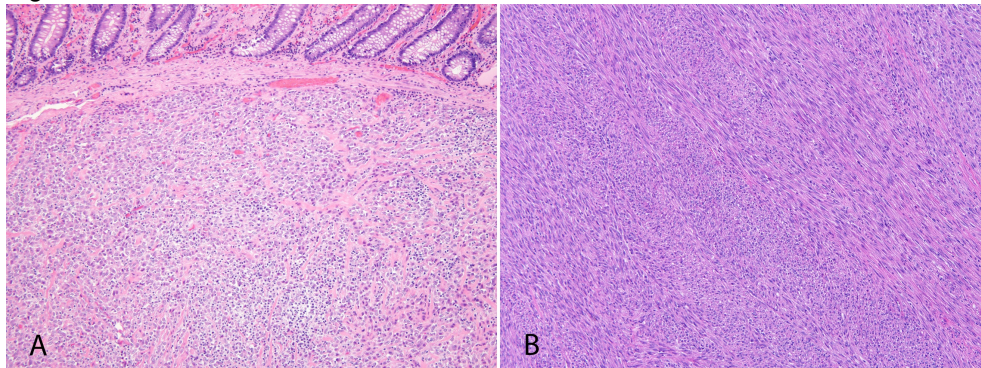
Figure 1 - 395



Figure 2 - 395

**Table 1.** Clinicopathologic Summary of MXD4-NUTM1 Rearranged Neoplasms

| Case | Age (yrs) | Sex | Tumor Site | Tumor size (cm) | Necrosis | Mits/ 10 HPF | Metastases | MXD4 Breakpoint | NUTM1 Breakpoint | Died of Disease | Survival (months) |
|---|---|---|---|---|---|---|---|---|---|---|---|
| 1 | 38 | F | Sigmoid colon | 3.5 | None | 2 | Liver | Exon 5 | Exon 3 | No | 12 |
| 2 | 40 | M | Ileocecal valve | 2.5 | None | 2 | None | Exon 5 | Exon 3 | No | 3 |
| 3 | 65 | F | Cecum | 3.5 | None | <1 | Lymph node and liver | Exon 5 | Exon 2 | Yes | 30 |
| 4 | 44 | F | Descending colon | 5 | None | 9 | Lymph node and liver | Exon 5 | Exon 2 | No | 7 |

**Conclusions:** NUTM1-rearranged gastrointestinal sarcomas usually occur in middle aged females, predominate in the colon, and have an aggressive clinical course despite showing relatively bland morphology. The consistent microscopic, immunohistochemical and molecular genetic features of these very rare lesions suggest they represent a distinct entity within the family of NUTM1-rearranged neoplasia. A NUTM1-rearranged tumor should be considered for any submucosal spindle cell neoplasm of the gastrointestinal tract, in particular those showing monomorphic cytology and keratin expression.

**396    Colonic GVHD versus Mycophenolate Colitis: Reassessment of the Histologic Distinction**
Benjamin Van Treeck[1], Christopher Hartley[1], Katelyn Reed[1], Roger Moreira[1], Catherine Hagen[1]
[1]Mayo Clinic, Rochester, MN

**Disclosures:** Benjamin Van Treeck: None; Christopher Hartley: None; Katelyn Reed: None; Roger Moreira: None; Catherine Hagen: None

**Background:** Colonic graft versus host disease (GVHD) and mycophenolate (MMF) colitis have overlapping histologic features.  A subset of stem cell transplant patients receive MMF as part of their prophylactic immunosuppressive regimen and are therefore at risk of developing both GVHD and MMF toxicity.  Only a few studies have addressed the histologic distinction of these two entities, suggesting eosinophilic inflammation, endocrine cell aggregates, and apoptotic microabcesses as possible distinguishing features.  The aim of this study was to systematically compare cases of colonic GVHD and MMF colitis to identify distinctive histologic features.

**Design:** Cases of colonic GVHD and MMF colitis were retrieved from the pathology archives and histologically assessed for the following:  Lerner grade, presence of neutrophils, apoptotic count (max per 10 contiguous crypts), presence of eosinophilic crypts, apoptotic microabscesses, eosinophilic microabscesses, endocrine cell aggregates, crypt distortion, lamina propria expansion, degree of lamina propria eosinophilia (figure 1), and pyloric gland metaplasia.  Clinical information was collected from chart review.

**Results:** The GVHD group consisted of 30 biopsies from 29 patients (mean age 56 years; M:F 1.4:1) and the MMF group consisted of 15 biopsies from 14 patients (mean age 59.4 years; M:F 1:2.5). Cases of MMF colitis were more likely to have eosinophilic microabscesses (40% vs. 6.7%, p=0.01), increased lamina propria eosinophils (2-3 vs. 0-1, 86.7% vs. 16.7%, p<0.0001, Table 1) and moderate-to-diffuse (>25% of the mucosa) architectural distortion (73.3% vs. 36.7%, p=0.03). Cases of GVHD were more likely to show evidence of Lerner grade 4 disease (26.7% vs. 0%, p=0.04) and higher apoptotic counts (6.5 vs 2.5, p=0.03). Lamina propria expansion and pyloric gland metaplasia were seen in two cases each of MMF colitis and were not seen in any cases of GVHD (13.3% vs. 0%, p=0.11). Endocrine cell aggregates were seen in 4 cases of grade 4 GVHD and not identified in any cases of MMF colitis (13.3% vs. 0%, p=0.28). No significant difference was noted between other histologic variables, including apoptotic microabcesses (27.7% GVHD vs. 20% MMF, p=0.73). On multivariate analysis including lamina propria eosinophils and eosinophilic abscesses, increased lamina propria eosinophils remained a significant predictor of MMF colitis (OR 3.2, 95%CI 1.4-5.0, p=0.001).

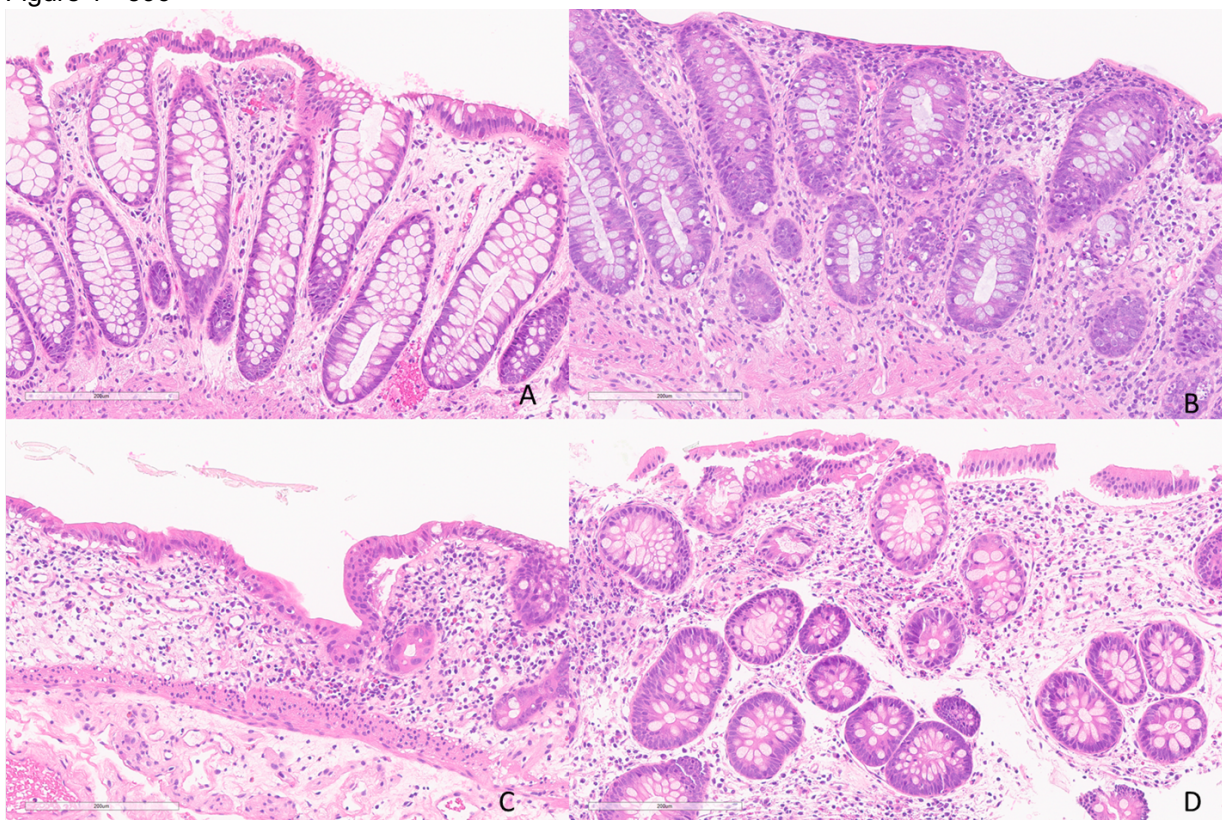| Table 1: Lamina propria eosinophil score in colonic GVHD vs. MMF colitis | | | | |
|---|---|---|---|---|
| | 0 | 1 | 2 | 3 |
| GVHD (n=30) | 6 (20%) | 19 (63.3%) | 3 (10%) | 2 (6.7%) |
| MMF colitis (n=15) | 0 (0%) | 2 (13.3%) | 6 (40%) | 7 (46.7%) |

Figure 1 - 396



Figure 1: Lamina propria eosinophils. Case of GVHD with rare/absent lamina propria eosinophils, grade 0 (A). Case of GVHD with normal number of expected lamina propria eosinophils, grade 1 (B). Case of MMF colitis with mildly increased lamina propria eosinophils, grade 2 (C). Case of MMF colitis with markedly increased lamina propria eosinophils, grade 3 (D).

**Conclusions:** In our cohort, several histologic features were significantly different between colonic GVHD and MMF colitis, with lamina propria eosinophils being the most significant predictor. Other previously reported distinguishing features such as endocrine cell aggregates and apoptotic microabscesses were not significant in our cohort. We will further evaluate the semiquantitative difference in eosinophils with digital image analysis to establish quantitative cutoffs.

**397    Medication Resin/Crystal-Induced Gastrointestinal Injury in Patients with Advanced Chronic Kidney Disease: A Contemporary Clinicopathologic Analysis of 55 Cases**

Linyuan Wang[1], Brian Quigley[2], Alyssa Krasinskas[2], Wei Zheng[2]
[1]Emory University School of Medicine, Atlanta, GA, [2]Emory University, Atlanta, GA

**Disclosures:** Linyuan Wang: None; Brian Quigley: None; Alyssa Krasinskas: None; Wei Zheng: None

**Background:** Medication resins/crystals such as Kayexalate (Kay), Sevelamer (Sev) and Lanthanum carbonate (LC) used in patients with advanced chronic kidney disease (CKD) have been increasingly recognized for their ability to induce gastrointestinal (GI) injury. However, there is little published literature regarding the clinicopathologic features of these injuries.

**Design:** A search was made through our institutional Gastrointestinal Pathology database between 2009 and 2020 for GI specimens with Kay, Sev and LC. Multiple clinicopathologic parameters were analyzed including patient age, sex, status of CKD, dialysis, other relevant medical history, endoscopic impression and clinical outcome.

**Results:** 55 cases (45 biopsies and 10 resections) were identified with 25 (45%) cases of Kay, 23 (42%) cases of Sev, 7 (13%) cases of LC. The patients were 32 males and 23 females with an age range of 19 to 90 years of age. The most common presenting symptoms are GI discomfort or GI bleeding, with occasional acute abdomen. Both Sev and LC were only seen in CKD patients on dialysis, while Kay was seen in both acute kidney injury and/or CKD patients. 6 (11%) cases were associated with pseudopolyps/pseudotumor/lesions endoscopically (Figure 1, 3 cases of Sev, 2 cases of Kay and 1 case of LC). 6 (11%) cases were associated with colon perforation (4 cases of Sev and 2 cases of Kay). Both Kay and Sev had a lower GI predominant distribution pattern (18% in esophagus/stomach and 82% in colon) while LC was seen in upper GI only (63% in stomach and 37% in small intestine). Histologically, mucosal inflammation, ulceration, submucosa hemorrhage and granulation tissue formation were seen in biopsies. Transmural necrosis with ischemic injury was seen in resections.
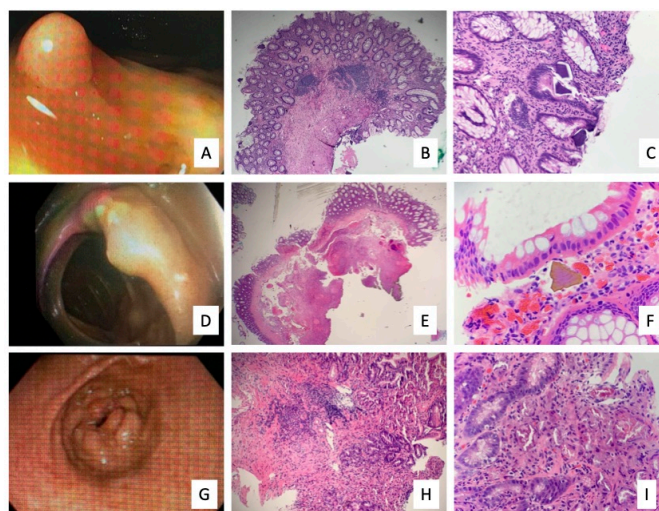
Figure 1 - 397



Figure 1: Resin-Associated Pseudopolyps: A-C: Endoscopic image (A), microscopic image at 4x (B) and at 40x (C) of a kayexalate-induced ascending colon pseudopolyp. D-F: Endoscopic image (D), microscopic image at 4x (E) and at 40x (F) of a sevelamer-induced descending colon pseudopolyp. G-I: Endoscopic image (G), microscopic image at 4x (H) and at 40x (I) of a lanthanum-induced gastric antral pseudopolyp.

**Conclusions:** This is one of the largest clinicopathologic studies on medication resins/crystals-induced GI injury to date. A portion of Kay and Sev-induced GI mucosal injuries were associated with polypoid lesions or mass-forming pseudotumor clinically.  Greater than 10% of Sev and Kay cases developed colonic perforation and caused clinical emergency. Timely recognition of the medication resins/crystals-induced GI injuries in biopsies with clinical correlation is important to avoid serious complications.

398     **Analysis of KRAS Mutational Profiles in the Gastrointestinal Tract Reveals Site-specific Alterations that Can Help Distinguish Pancreatobiliary and Upper Gastrointestinal Primaries**

Linyuan Wang[1], Zaid Mahdi[2], Alyssa Krasinskas[3], Brian Robinson[3]
[1]Emory University School of Medicine, Atlanta, GA, [2]Emory University Hospital, Atlanta, GA, [3]Emory University, Atlanta, GA

**Disclosures:** Linyuan Wang: None; Zaid Mahdi: None; Alyssa Krasinskas: None; Brian Robinson: None

**Background:** Adenocarcinomas (AdCAs) of the luminal gastrointestinal (GI) tract and pancreatobiliary system often show histologic and immunohistochemical (IHC) overlap, making it difficult to delineate the primary site in a metastatic setting. Increasingly, molecular studies are being utilized to delineate tumoral site of origin. Previous studies have shown site-specific missense mutations in the oncogene KRAS could be used in conjunction with IHC to differentiate metastatic pancreatic AdCA from primary lung AdCA. Whether this methodology could be applied to other areas in the GI tract remains unknown. In this study, we examined the KRAS mutational profile in AdCAs across the GI tract and pancreatobiliary system. Secondarily we interrogated the utility of the KRAS mutational profile in differentiating pancreatic AdCA from that of upper GI tract, which often have significant morphologic and IHC overlap.

**Design:** We assessed 3161 KRAS mutations across 6699 cases in 46 separate studies across different sites, including AdCA from the esophagus, stomach, ampulla, biliary system, pancreas, and colon (Figure 1). Factors assessed included frequency of alteration, missense mutational profile, and type of base pair mutation (e.g., transition vs. transversion). We then validated our findings on a smaller local cohort that consisted of 362 cases.

**Results:** GI AdCAs demonstrate regional variation in the frequency of KRAS mutation, with the most frequent KRAS mutation observed in pancreatic AdCA (up to 94.9%), while the frequency is much lower in AdCA from esophagus and stomach (Figure 1). Regional similarity for the type of missense KRAS mutation is also seen, with AdCAs of the foregut (esophagus and stomach) showing a similar profile in amino acid substitution (Figure 2) and AdCAs of the distal biliary system (ampullary and extrahepatic bile duct) showing overlap with the pancreas. G12V mutation is significantly associated with pancreatic primary compared to gastric AdCA with specificity of 95.3% and positive predictive value of 98.7%, while conversely, codon 13 alterations is increased in upper GI primaries with specificity of 98.9% and negative predictive value of 93.6% against pancreatic AdCA. When examining the base pair mutational type, esophageal and gastric AdCAs show an enrichment in transitional mutations while other sites showed an equal distribution (72% and 73% respectively vs 53% at other sites, p < .001). Importantly, examination of our validation cohort revealed similar trends in these findings.

Figure 1 - 398



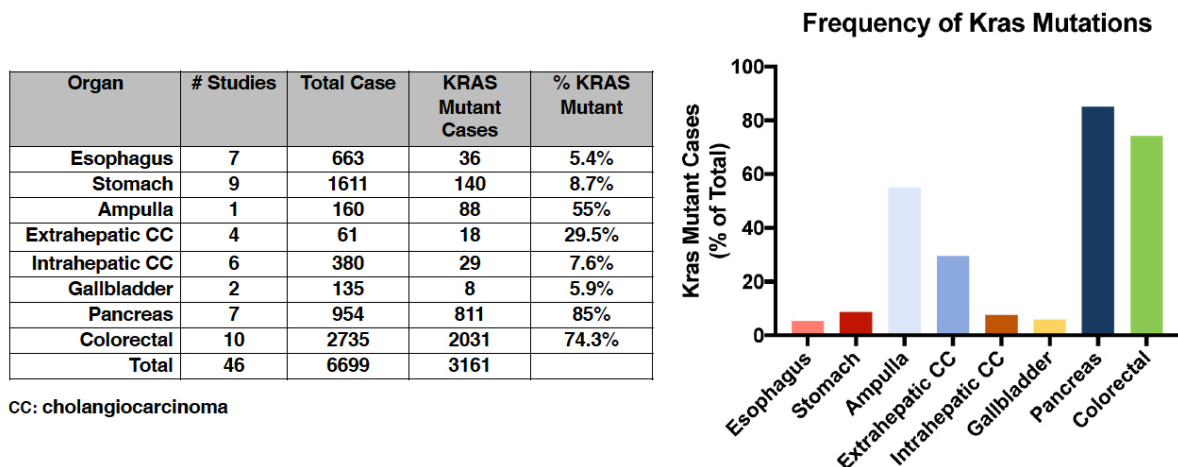| Organ | # Studies | Total Case | KRAS Mutant Cases | % KRAS Mutant |
|---|---|---|---|---|
| **Esophagus** | 7 | 663 | 36 | 5.4% |
| **Stomach** | 9 | 1611 | 140 | 8.7% |
| **Ampulla** | 1 | 160 | 88 | 55% |
| **Extrahepatic CC** | 4 | 61 | 18 | 29.5% |
| **Intrahepatic CC** | 6 | 380 | 29 | 7.6% |
| **Gallbladder** | 2 | 135 | 8 | 5.9% |
| **Pancreas** | 7 | 954 | 811 | 85% |
| **Colorectal** | 10 | 2735 | 2031 | 74.3% |
| **Total** | 46 | 6699 | 3161 | |

**CC: cholangiocarcinoma**

Figure 1: KRAS Mutational Frequency by Gastrointestinal/pancreatobiliary Site.
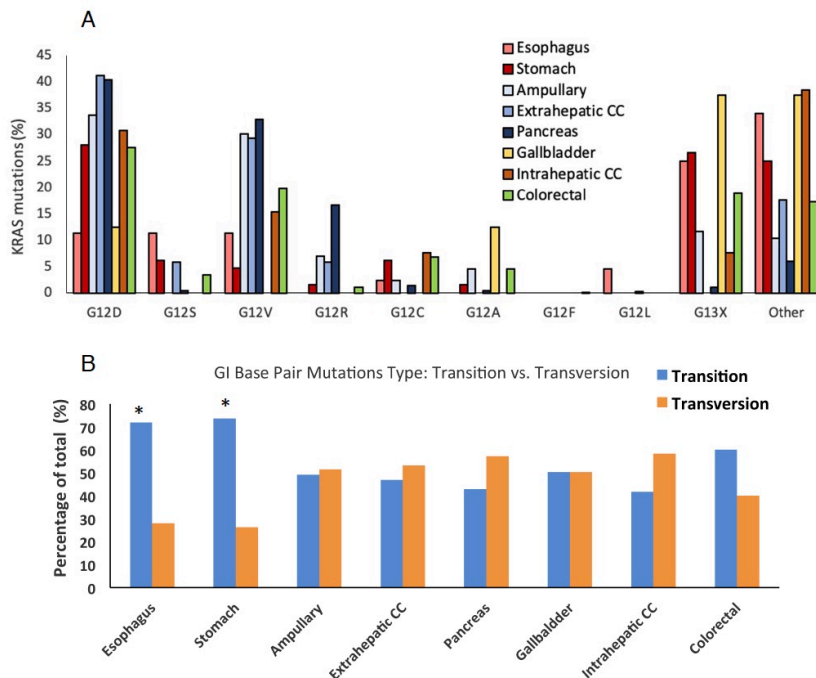
Figure 2 - 398



Figure 2: (A) Type of KRAS mutation reported by site of origin in the gastrointestinal tract and pancreatobiliary system. (B) Percentage of transition and transversion base pair mutational types (* p<0.05 for percentage of transition in esophagus and stomach respectively comparing to other sites).

**Conclusions:** Our findings indicate that in addition to providing theragnostic information, KRAS mutational analysis may prove useful in delineating the site of origin in GI AdCAs with morphologic and immunohistochemical overlap. Moreover, transitional mutations are more frequent in esophageal and gastric AdCAs, reiterating the role of chronic inflammation in the pathogenesis of foregut AdCAs.

**399    Severe Eosinophilic Gastritis May Present as Peptic Ulcer and is Associated with Both Multi-Organ Gastrointestinal Tract Involvement and Peripheral Eosinophilia**

Xintong Wang[1], Yansheng Hao[1], Hansen Lam[1], Huaibin Mabel Ko[2]
[1]Mount Sinai Hospital, New York, NY, [2]Columbia University Irving Medical Center, New York-Presbyterian Hospital, New York, NY

**Disclosures:** Xintong Wang: None; Yansheng Hao: None; Hansen Lam: None; Huaibin Mabel Ko: None

**Background:** Eosinophilic gastritis (EG) is characterized by eosinophilic infiltration of the stomach. In some cases, eosinophilia of the esophagus, small intestine, and colon may also be present. The etiology and presentation of EG is not fully understood. The aim of this study was to assess the clinicopathological spectrum of EG and identify specific features which could aid in the diagnosis.

**Design:** Pathology files were searched for histological eosinophilic gastritis (HEG) from 2017-2019. HEG was defined as marked eosinophilic infiltrates with ≥50 eosinophils per high power field (HPF), with severe HEG defined as >100/HPF. Infectious etiologies (H. pylori, parasites) were excluded. Clinical data were reviewed for endoscopic findings, comorbidities, medication, and peripheral eosinophilia (blood eosinophil count ≥500/mcL). Pathology reports and slides were evaluated for concurrent eosinophilia in the esophagus (EoE, >15 eosinophils/HPF) and intestine (>30 eosinophils/HPF).

**Results:** 35 patients with HEG were identified, (9 children ≤18 years; 26 adults). The average age was 36.7 years (range 1-98 y), and male-to-female ratio was 1.05/1.0 (18 M, 17 F). Of the 35 patients, 22 (62.9%, 15 adults, 7

children) had allergy/atopy and 18 had history of EoE (51.4%, 10 adults, 8 children). Peripheral eosinophilia was documented in 15 patients (55.6%). The most common endoscopic finding was ulceration/erosion (n=10, 41.7%; Figure 1), followed by nodularity (n=7, 29.2%), and erythema (n=4, 16.7%). Four cases had normal endoscopic findings (16.7%). Compared to adult HEG patients, pediatric patients were significantly more likely to be male, 88.9% vs. 38.5% (P= 0.011) and have associated EoE, 88.9% vs. 38.5% (P= 0.011).

In comparison to patients with moderate HEG (eosinophils 50-100/HPF), patients with severe HEG (eosinophils ≥100/HPF; Figure 2) were significantly more likely to have peripheral eosinophilia, 66.7% vs. 16.7% (P=0.034). Fifteen patients (42.9%) had multi-organ GI tract involvement on histology. Concomitant eosinophilia involving the esophagus and duodenum was seen in 14 (50%) and 6 (23.1%) patients, respectively. Two of 6 patients with colonoscopies had colonic eosinophilia. Compared to patients with disease limited to the stomach, patients with multi-organ GI tract involvement were significantly more likely to have severe HEG, 93.3% vs. 65.0% (P=0.049) and ulceration/erosion on histology and/or endoscopy, 73.3% vs. 35.0% (P=0.023).
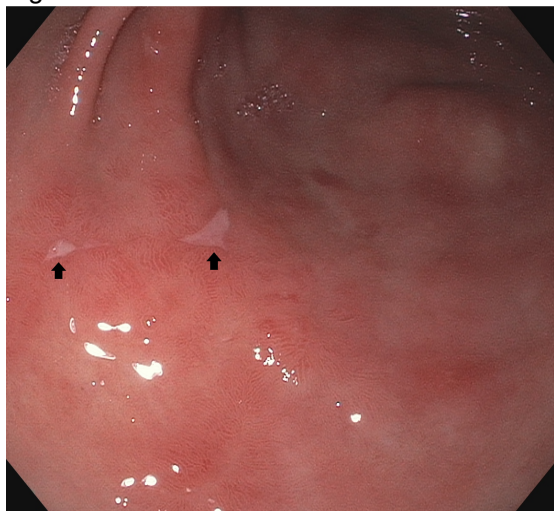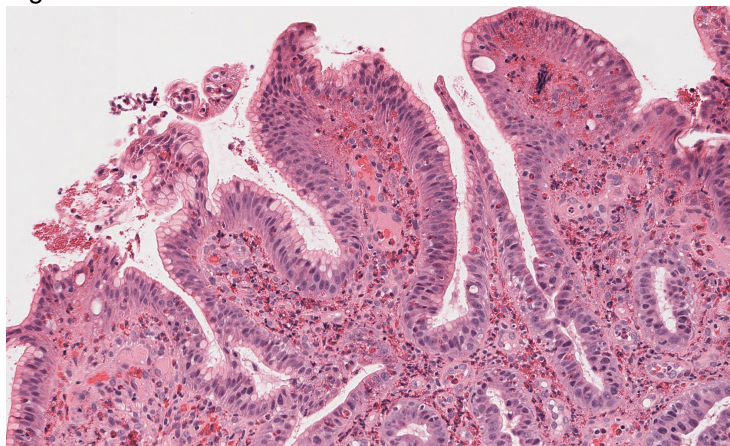
Figure 1 - 399



Figure 2 - 399



**Conclusions:** HEG is commonly associated with allergy in both adults and children and may present with ulcer or nodularity on endoscopy and/or histology. Patients with severe HEG are more likely to have concurrent histologic eosinophilia in other parts of the GI tract and peripheral eosinophilia (≥500/mcL). Male predominance and concomitant EoE are findings associated with pediatric HEG that may not be observed in the adult HEG patient population.

**400    Assessment of Zoom Utility in Grading of Dysplasia in Barrett Esophagus (BE)**
Lindsey Westbrook[1], Michael Arnold[2], Toby Cornish[3], Patrick Henn[1], Jeffrey Kaplan[4], Antonio Galvao Neto[5], Erin Rubin[1], Cassie Xu[3], Christina Arnold[4]
[1]University of Colorado Anschutz Medical Campus, Aurora, CO, [2]Children's Hospital Colorado, Aurora, CO, [3]University of Colorado School of Medicine, Aurora, CO, [4]University of Colorado, Aurora, CO, [5]UCHealth University of Colorado Hospital, Aurora, CO

**Disclosures:** Lindsey Westbrook: None; Michael Arnold: None; Toby Cornish: *Advisory Board Member*, Leica, Inc; Patrick Henn: None; Jeffrey Kaplan: None; Antonio Galvao Neto: None; Erin Rubin: None; Cassie Xu: None; Christina Arnold: None

**Background:** Due to social distancing guidelines during the "severe acute respiratory syndrome coronavirus-2" (SARS-CoV-2) pandemic, the modality of case presentation for our daily consensus conference transitioned from a multi-headed microscope to Zoom, a videoconferencing platform. The purpose of this study was to determine the diagnostic utility of Zoom-based case sharing compared to traditional multi-headed microscope techniques.

**Design:** A search of the pathology laboratory information system for cases containing keywords related to BE from 2017 to 2020 was conducted. This resulted in identification of 10 unique biopsy case parts per dysplasia category (60 total slides): negative for dysplasia (NFD), indefinite for dysplasia (IFD), low-grade dysplasia (LGD), high-grade dysplasia (HGD), intramucosal carcinoma (IMC), and adenocarcinoma (adenoCA). A circled 10x field from each case was shared on Zoom. Then, following a more than two-week washout period, the cases were re-randomized and shared again via the multi-headed microscope. Each scorer recorded their diagnosis, confidence, and time to diagnosis for each case.

**Results:** Intra-observer concordance between Zoom and in person was 66.7% (range 63.3-75.0%) with the highest intra-observer concordance seen in cases where the original diagnosis was LGD or adenoCA, 77.1% and 74.3%, respectively. Although not statistically significant, intra-observer concordance tended to track with years of experience grading dysplasia: resident=63.3%, junior faculty= 66.7%, senior GI faculty=67.33%. The overall concordance with the original diagnosis was similar for Zoom and in person (57.9% vs 55.0%, P=0.444). When compared to the other categories, the diagnostic concordance was significantly higher in NFD and adenoCA cases for both Zoom and in person (P=0.0001 for both modalities). Although not statistically significant, for cases with an original diagnosis of HGD, IMC, and adenocarcinoma, Zoom was more often concordant with the original diagnosis than in person (HGD 67.1% vs. 54.3%, P=0.166; IMC 44.3% vs. 32.9%, P=0.224, adenoCA 78.6% vs. 71.4%, P=0.4353). Self-reported diagnostic confidence was significantly less with Zoom (Zoom=2.92 vs in person=3.07, P=0.0233). Average time to diagnosis was statistically significantly longer for Zoom than in person (Zoom=20.77 seconds vs in person=17.48 seconds, P=0.0001).

**Conclusions:** This study shows that although pathologists may feel less confident when providing BE dysplasia diagnoses via Zoom, it is slightly more effective than in person multi-headed scope review based on slightly higher concordance with the original diagnosis and similar time to diagnosis.

## 401    A Hexaplex PCR Assay Developed for Microsatellite Instability Detection Using Qsep100 DNA Fragment Analyzer

Biao Zhang[1], Hong Gao[2], Jun Yang[1], Lu He[1]
[1]The Affiliated Drum Tower Hospital, Nanjing University Medical School, Nanjing, China, [2]Nanjing Drum Tower Hospital, The Affiliated Hospital of Nanjing University Medical School, Nanjing, China

**Disclosures:** Biao Zhang: None; Lu He: None

**Background:** Microsatellite instability (MSI) is a molecular marker of loss of function of the DNA mismatch repair (MMR) system in various cancers including colorectal cancer. MSI testing has been applied to aid tumor prognosis, predict response to chemotherapeutic drugs and immunotherapy and to screen for lynch syndrome. MSI is generally detected by fluorescence PCR combined with capillary electrophoresis or next generation sequencing (NGS). Both methods either are expensive, time-consuming or laborious.

**Design:** To address these practical needs. We designed a multiplex PCR assay composed of six mononucleotide repeat loci (BAT25, BAT26, NR21, NR24, NR27 and MONO27). In order to distinguish each loci, the amplicons were designed with a length differing from each other by more than 25 bp. DNA was isolated from pairing formalin-fixed paraffin-embedded colorectal cancer and adjacent normal tissues for multiplex PCR reaction. PCR products were separated and analysed on the Qsep100 DNA Fragment Analyzer. And the result was compared with fluorescence-based Bethesda panel performed on ABI 3500Dx to validate its clinical application.

**Results:** Each microsatellite loci was specifically amplified with expected length in a sing-tube multiplex reaction, and all loci could distinguish from each other analysed on the Qsep100 DNA Fragment Analyzer (Figure 1). This panel could accurately assess the MSI status with a high specificity and reproducibility (Figure 2). And the method showed a good concordance with fluorescent dye-based capillary electrophoresis.
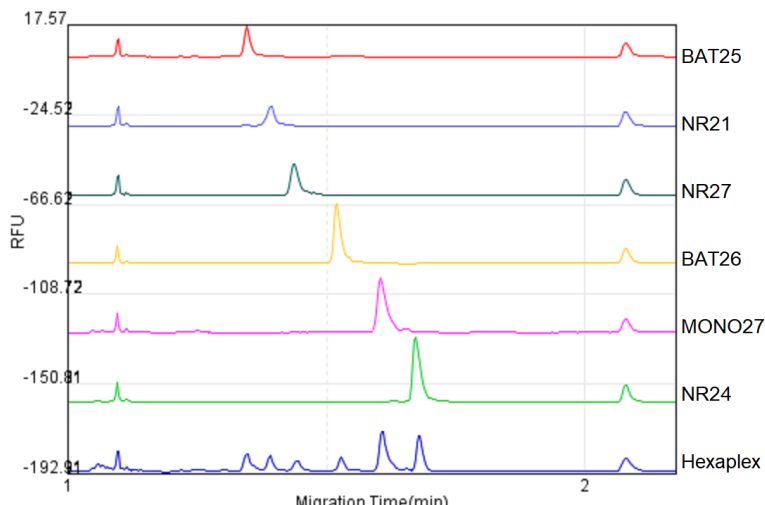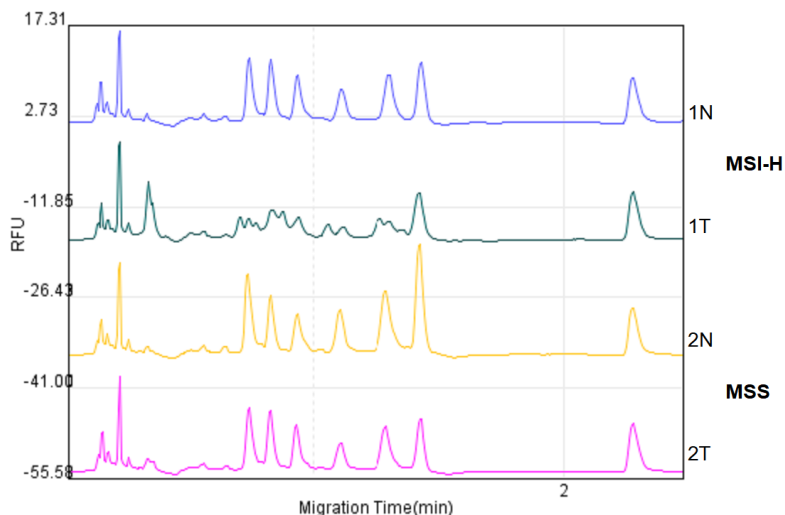
Figure 1 - 401

Figure 1



Figure 2 - 401

Figure 2



**Conclusions:** The hexaplex PCR assay using Qsep100 DNA Fragment Analyzer is feasible for MSI testing. This assay provides a fluorescent dye-free, cost-effective, reliable and reproducible method for MSI diagnosis.

**402   Clinicopathologic and DNA Flow Cytometric Analysis of High-Risk Intestinal Metaplasia in Adjacent Mucosa of Gastric Cancers**

Ruth Zhang[1], Peter Rabinovitch[2], Aras Mattis[1], Gregory Lauwers[3], Won-Tak Choi[1]
[1]University of California, San Francisco, San Francisco, CA, [2]University of Washington, Seattle, WA, [3]H. Lee Moffitt Cancer Center & Research Institute, University of South Florida, Tampa, FL

**Disclosures:** Ruth Zhang: None; Peter Rabinovitch: None; Aras Mattis: None; Gregory Lauwers: None; Won-Tak Choi: None

**Background:** Most gastric cancers (GC) develop via an intestinal metaplasia (IM)-dysplasia-carcinoma pathway. Patients with extensive and/or incomplete IM have been reported to have a higher risk for GC. IM can also display cytoarchitectural atypia limited to the pit epithelium ("gastric pit dysplasia"), and this has been proposed to

represent another morphologic step in the pathogenesis of GC. However, only a very small proportion of IM patients will develop GC, and it remains questionable if IM is a direct precursor to dysplasia or cancer.

**Design:** A cohort of 82 GC patients with IM who underwent gastrectomy were analyzed. DNA flow cytometry was performed on 109 IM samples (including 88 complete IM and 21 incomplete IM) obtained from adjacent mucosa of the 82 GCs.

**Results:** Males (55%) and females (45%) were essentially equally represented with a mean age of 67 years. GC was more common in non-Caucasian patients (68%). Twelve patients (15%) had a family history of GC, and *H. pylori* was present in 28 patients (34%). GC was detected throughout the stomach but most frequently involved antrum (62%). Intestinal-type adenocarcinoma was the most common (70%). Most cases (88%) were either moderately or poorly differentiated. Many cases were deeply invasive (45% pT3 or pT4), and 45% had lymph node metastases. The extent of IM was extensive (i.e., involving corpus) in 63 patients (77%) but limited (i.e., affecting antrum, incisura, or cardia only) in 19 patients (23%). The majority of the patients (n = 66; 80%) had predominantly complete IM, while the remaining 16 patients (20%) showed predominantly incomplete (n = 7) or mixed IM (n = 9). Only 2 (2%) of the 109 IM samples showed aneuploidy, both from 2 minority patients (Asian and Hispanic) with limited complete IM without atypia. The remaining 107 IM samples showed varying degrees of basal gland atypia, but all had normal DNA content.

**Conclusions:** The vast majority of IM cases lack the aneuploidy that is characteristic of gastric dysplasia or cancer. These results suggest that aneuploidy usually occurs after the development of dysplasia rather than at the stage of IM, and the presence of IM alone (regardless of subtype) may not indicate an increased risk for GC. Unless IM patients have other high-risk features (i.e., extensive IM, dysplasia, racial minorities, and/or family history of GC), endoscopic surveillance may not be warranted. IM with basal gland atypia is not uncommon and likely represents metaplastic atypia in most cases.

## 403 PD-L1 Expression and its Clinicopathological Correlation in Esophageal and Gastric Adenocarcinomas: A Single Cancer Center Experience

Yingtao Zhang[1], Kun Jiang[1]
[1]H. Lee Moffitt Cancer Center & Research Institute, Tampa, FL

**Disclosures:** Yingtao Zhang: None; Kun Jiang: None

**Background:** Programmed cell death 1 receptor (PD-1) and its ligand (PD-L1) are immune checkpoint inhibitors found on T cell surfaces. The anti-PD-1/ PD-L1 inhibitors are widely utilized for managing various human cancers. However, few studies have examined PD-L1 expression in esophageal and gastric adenocarcinomas, the most common esophageal and gastric malignancies, in the U.S. The purpose of this study is to assess PD-L1 expression and its association with clinicopathological features in esophageal and gastric adenocarcinoma patients at a NCI-designated comprehensive cancer center.

**Design:** A total of 74 esophageal adenocarcinoma and 52 gastric adenocarcinoma cases were analyzed between 2018 and 2020; cases with prior neoadjuvant management were excluded. PD-L1 combined positive score (CPS) was assessed on formalin-fixed paraffin-embedded tissue using DAKO PD-L1 IHC 22C3 pharmDx Assay. PD-L1 positivity was defined as CPS ≥ 1. The association between PD-L1 expression and clinicopathological parameters including patient age, gender and tumor differentiation was evaluated.

**Results:** PD-L1 was expressed in 80.0% (59/74) of the esophageal adenocarcinoma (Figure 1, 200x) and 63.5% (33/52) of the gastric adenocarcinoma (Figure 2, 200x). Positive PD-L1 CPS ≤10, 10- ≤50 and >50 were denoted in 51.4%, 21.6%, 6.8% of esophageal adenocarcinoma and 48.1%, 15.4%, 0.0% of gastric adenocarcinoma cases, respectively (Table 1). A convincing correlation between PD-L1 levels and the above mentioned clinicopathological variables was not established. However, in esophageal adenocarcinoma patients, PD-L1 expression, which negatively modulates immunity, is more often seen in older patients (>60 years, P=0.11). In gastric cancer patients, PD-L1 expression is more frequently seen with low and moderate grade, instead of high grade adenocarcinomas (P=0.10), suggesting attenuated applicability of immunotherapy for high grade gastric cancers.

**Table 1 Relationships between PD-L1 expression and clinicopathological characteristics in esophageal and gastric adenocarcinoma**

| Esophageal adenocarcinoma | Sample size, n | CPS < 1, n (%) | CPS 1- ≤ 10, n (%) | CPS 10- ≤ 50, n (%) | CPS > 50, n (%) |
|---|---|---|---|---|---|
| Overall | 74 | 15 (20.3%) | 38 (51.4%) | 16 (21.6%) | 5 (6.8%) |
| **Age:** ≤ 60 years | 22 | 7 (31.8%) | 11 (50.0%) | 3 (13.6%) | 1 (4.5%) |
| > 60 years | 52 | 8 (15.4%) | 27 (51.9%) | 13 (25.0%) | 4 (7.7%) |
| **Gender:** Male | 62 | 14 (22.6%) | 32 (51.6%) | 13 (21.0%) | 3 (4.8%) |
| Female | 12 | 1 (8.3%) | 6 (50.0%) | 3 (25.0%) | 2 (16.7%) |
| **Tumor differentiation:** Well differentiated | 1 | 0 (0.0%) | 0 (0.0%) | 1 (100.0%) | 0 (0.0%) |
| Moderately differentiated | 24 | 6 (25.0%) | 12 (50.0%) | 5 (20.8%) | 1 (4.2%) |
| Poorly differentiated | 49 | 9 (18.4%) | 26 (53.1%) | 10 (20.4%) | 4 (8.2%) |

| Gastric adenocarcinoma | Sample size, n | CPS < 1, n (%) | CPS 1- ≤ 10, n (%) | CPS 10- ≤ 50, n (%) | CPS > 50, n (%) |
|---|---|---|---|---|---|
| **Overall** | 52 | 19 (36.5%) | 25 (48.1%) | 8 (15.4%) | 0 (0.0%) |
| **Age:** ≤ 60 years | 19 | 9 (47.3%) | 7 (36.8%) | 3 (15.8%) | 0 (0.0%) |
| > 60 years | 33 | 10 (30.3%) | 18 (54.5%) | 5 (15.2%) | 0 (0.0%) |
| **Gender:** Male | 29 | 10 (34.4%) | 14 (48.3%) | 5 (17.2%) | 0 (0.0%) |
| Female | 23 | 9 (39.1%) | 12 (52.1%) | 2 (8.7%) | 0 (0.0%) |
| **Tumor differentiation:** Well differentiated | 2 | 0 (0.0%) | 1 (50.0%) | 1 (50.0%) | 0 (0.0%) |
| Moderately differentiated | 10 | 2 (20.0%) | 7 (70.0%) | 1 (10.0%) | 0 (0.0%) |
| Poorly differentiated | 40 | 17 (42.5%) | 17 (42.5%) | 6 (15.0%) | 0 (0.0%) |

Figure 1 - 403
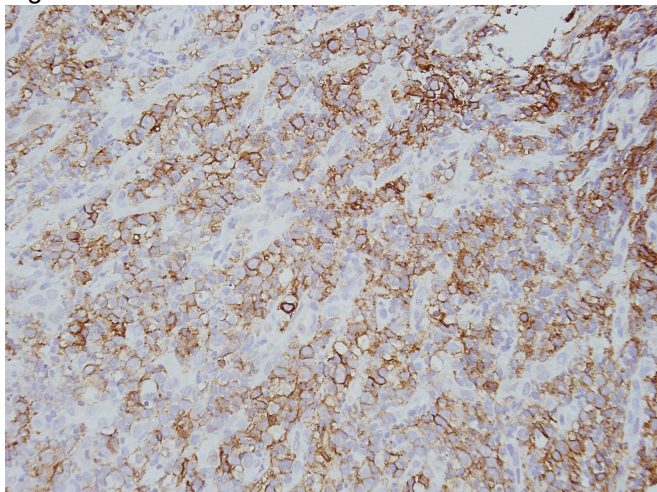


Figure 2 - 403
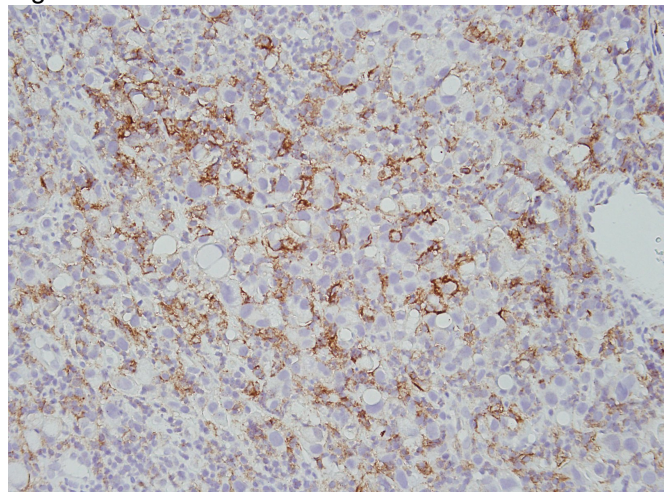
**Conclusions:** Our institutional review suggests a potential correlation between PD-L1 expression and patient age and adenocarcinoma differentiation, as higher percentage of PD-L1 expression was observed in these two categories. Continued investigation with more cases to examine the association between PD-L1 expressions and these parameters in combination with molecular fingerprints such as next generation sequencing and mutation profiles is warranted.

### 404 Histologic Variants of Kaposi Sarcoma in Gastrointestinal Tract

Wei Zheng[1], Rebecca Obeng[2], Borislav Alexiev[3], Shu Kwun Lui[4], Alyssa Krasinskas[1], Rondell Graham[5], Guang-Yu Yang[6], Michelle Reid[4], Yue Xue[2]
[1]Emory University, Atlanta, GA, [2]Northwestern University Feinberg School of Medicine, Chicago, IL, [3]Northwestern Memorial Hospital, Chicago, IL, [4]Emory University Hospital, Atlanta, GA, [5]Mayo Clinic, Rochester, MN, [6]Northwestern University, Chicago, IL

**Disclosures:** Wei Zheng: None; Rebecca Obeng: None; Borislav Alexiev: None; Shu Kwun Lui: None; Alyssa Krasinskas: None; Rondell Graham: None; Guang-Yu Yang: None; Michelle Reid: None; Yue Xue: None

**Background:** Kaposi sarcoma (KS), a low-grade angioproliferative neoplasm derived from lymphatic endothelium, can pose diagnostic challenges for biopsy specimens. Although several histologic variants of cutaneous KS have been described in the literature (1, 2), there is no systematic analysis of the histomorphological spectrum of KS in gastrointestinal (GI) tract. We analyzed GI tract KS variants.

**Design:** Thirty-four GI biopsies/resections diagnosed as KS were retrieved from the authors' pathology database. All had confirmatory immunohistochemistry (IHC) including latent nuclear antigen-1 (HHV8) and CD31.

**Results:** All patients were HIV positive (average age: 36y; M:F = 31:1). In addition to conventional KS (Figure 1a), nine distinct histologic variants were elucidated (Table 1). 1. Lymphangiectatic (n= 15) characterized by large dilated thin-walled lymphatic vessels (Figure 1b). 2. Granulation tissue-like (n= 15) characterized by proliferating fibroblasts-like cells and delicate thin-walled capillaries, infiltrated by inflammatory cells in extracellular loose/hyalinized/fibrotic stroma, often with fibrinopurulent debris (Figure 1c). 3. Mucosal injury/hemorrhage/inflammation (n= 17) composed of acute and/or chronic inflammation in lamina propria (Figure 1d, e). 4. Gastrointestinal stromal tumor (GIST)-like (n= 6), composed of sheets or nodules of spindle/epithelioid cells sometimes with paranuclear vacuoles (Figure 1f). 5. Prolapse-type (n= 4) with spindle cells wrapping around crypts (Figure 1g). 6. Lymphangioma-like (n= 4) composed of irregular, angulated and inter-anastomosing lymphatic channels (Figure 1h). 7. Telangiectatic (n= 1) with intensely congested, ectatic vascular spaces/blood lakes lined by lesional cells (Figure 1i). 8. Pyogenic granuloma-like (n= 1) characterized by lobular arrangement of capillaries within edematous, inflamed stroma often associated with surface ulceration (Figure 1j). 9. Inflammatory myofibroblast tumor (IMT) (n= 2) characterized by spindle cells with inflammatory infiltrate of neutrophils, lymphocytes and plasma cells (Figure 1k, l).

| Variants | Characteristic histopathologic features | Diagnostic Challenges |
|---|---|---|
| Lymphangiectatic (n=15) | Large dilated thin-walled lymphatic vessels | Misdiagnosed as lymphangiectasis |
| Granulation tissue-like (n=15) | Proliferating fibroblasts-like cells and delicate thin-walled capillaries, infiltrated by inflammatory cells in extracellular loose/hyalinized/fibrotic stroma, often with fibrinopurulent debris | Misdiagnosed as granulation tissue/ulcer |
| Mucosal injury/hemorrhage/inflammation (n=17) | Hemorrhage or acute and/or chronic inflammation in lamina propria | Misdiagnosed as nonspecific, mucosal injury due to preparation/procedure artifact or inflammatory process |
| Gastrointestinal stromal tumor (GIST)-like (n= 6) | Sheets or nodules of spindle/epithelioid cells sometimes with paranuclear vacuoles. | Misdiagnosed as GIST |
| Prolapse-type (n= 4) | Smooth muscle-like spindle cells wrapping around crypts | Misdiagnosed as mucosal prolapse-type features |
| Lymphangioma-like (n= 4) | Irregular, angulated and inter-anastomosing lymphatic channels. | Misdiagnosed as lymphangioma |
| Telangiectatic (n= 1) | Intensely congested, ectatic vascular spaces/blood lakes lined by lesional cells | Misdiagnosed as telangiectasia/hemangioma |
| Pyogenic granuloma-like (n= 1) | Lobular arrangement of capillaries within edematous, inflamed stroma often associated with surface ulceration. | Misdiagnosed as pyogenic granuloma/lobular capillary hemangioma |
| Inflammatory myofibroblast tumor (IMT) (n= 2) | Spindle cells with inflammatory infiltrate of neutrophils, lymphocytes and plasma cells. | Misdiagnosed as spindle cell lesions such as IMT, leiomyoma and GIST |

Figure 1 - 404
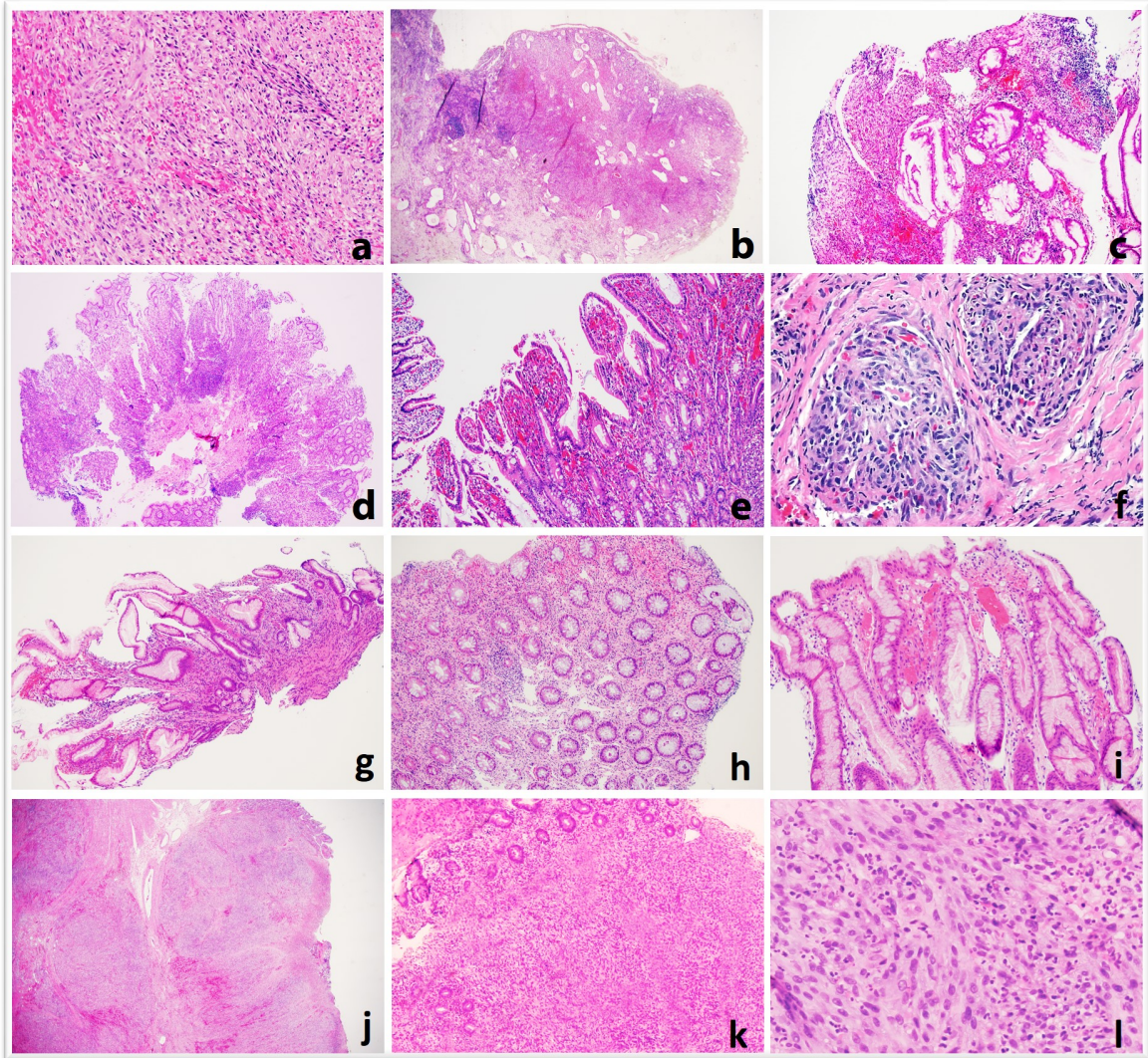


**Conclusions:** In summary, KS exhibits variable histomorphology. Although the prognostic significance of these variants is yet to be determined, the appreciation and recognition of its morphologic diversity should at least prompt an HHV8 IHC in HIV patients, in order to distinguishing these lesions from possible mimickers, particularly in limited biopsies.